Durham University

Durham E-Theses

The origin of bedrock mega-grooves in glaciated terrain

MIHAELA NEWTON

How to cite:

NEWTON, MIHAELA (2022) The origin of bedrock mega-grooves in glaciated terrain. Doctoral thesis, Durham University.

Use policy

The full-text may be used and/or reproduced, and given to third parties in any format or medium, without prior permission or charge, for personal research or study, educational, or not-for-profit purposes provided that:

- a full bibliographic reference is made to the original source
- a https://etheses.durham.ac.uk/id/eprint/14349/ is made to the metadata record in Durham E-Theses
- the full-text is not changed in any way

The full-text must not be sold in any format or medium without the formal permission of the copyright holders.

Please consult the full Durham E-Theses policy for further details.

Academic Support Office, The Palatine Centre, Durham University, Stockton Road, Durham, DH1 3LE
e-mail: e-theses.admin@durham.ac.uk Tel: +44 0191 334 6107
https://etheses.durham.ac.uk

The origin of bedrock mega-grooves in glaciated terrain

Mihaela Newton

Department of Geography
Durham University

A thesis submitted in partial fulfilment of the requirements of the University of Durham for the degree of Doctor of Philosophy

September 2021

Blank page

Abstract

Bedrock mega-grooves (BMGs) are large-scale bedrock corrugations reported from glaciated terrain across the world. They are remarkably straight, and closely parallel with ice-flow direction. BMGs are thought to have formed subglacially, but no consensus exists regarding their typical dimensions, formation or glaciological significance. This thesis aims to improve understanding of BMGs, focussing on their initiation and evolution, and on their relationship to bedrock geology, other subglacial landforms and ice-flow characteristics. The approach is both theoretical, through the compilation of an initial literature review and conceptualisation of several models of BMG initiation, and analytical, involving statistical analysis of morphometric data derived both from a global dataset. The data used in this study has been acquired through remote sensing as well as via fieldwork at selected locations.

Remote sensing measurements show that BMGs have lengths of 224–2269 m, widths of 21–210 m, depths of 2–15 m, elongation ratios of 5:1 to 42:1, and the spacing between adjacent individuals is 35-315 m (n = 1242 and ranges represent the 10^{th}-90^{th} percentiles). The variability in frequency distribution of BMG metrics between the sampled sites is likely due to variability in site geological characteristics, and to differences in palaeoglaciological history. However, all BMGs plot as a single landform population with a unimodal distribution and overlapping value ranges for all metrics, implying that they represent one landform type. BMGs and mega-scale glacial lineations (MSGLs) are similar in shape, but BMGs are on average approximately 4× shorter, 3.5× narrower, 3.5× more closely spaced and 2× deeper than MSGLs. These differences, alongside the essentially different processes inferred to be driving their evolution, support the conclusion that BMGs and MSGLs represent different types of landforms, rather than sitting on a continuum. Despite being sometimes situated in fast-flow onset zones within ice-stream landsystems, it is apparent that BMGs are unlikely to represent a diagnostic landform for ice-streaming. It is more likely that BMGs are a velocity–duration product, which can form beneath slow-flowing ice over long durations or more rapidly in ice-streaming settings. BMG initiation is hypothesised to have occurred either under the control of pre-existing structural features in the bedrock geology or through the agency of large erodents present in pre-Quaternary regolith. Future research could profitably focus on landform dating, modelling experiments, acquisition of empirical evidence to validate hypotheses of BMG initiation, and geophysical methods to explore on-going BMG formation in modern glacial environments.

Contents

List of figures

List of tables

Declaration and statement of copyright

The copyright of this thesis rests with the author.

I confirm that no part of the material presented in this thesis has previously been submitted by me or any other person for a degree in this or any other university. In all cases, where relevant, material from the work of others has been acknowledged.

Mihaela Newton
Department of Geography
Durham University
Initial submission September 2021
Corrected version submitted March 2021

Acknowledgements

Thanks go first to my supervisors Dave Evans, Chris Stokes and Dave Roberts for their professional guidance and support, for their endless patience and unfailing belief in my resources to carry out this research. It has been a blessing and an honour to be part of their team.

This project has been a long journey made possible in the first place by a financial legacy from my beloved grandparents, Rucsanda and Augustin Trelea. Further financial assistance was generously offered by the Department of Geography at Durham University in the form of several Postgraduate Research Grants, which enabled me to attend conferences and research trips organised by the Quaternary Research Association. My fieldwork in Assynt, Scotland, UK was funded through a New Researcher Working Award offered by the Quaternary Research Association. Trevor Faulkner kindly put me in touch with the Grampian Speleological Group who facilitated my stay in their charming hut at Elphin, overlooking those mysterious mega-grooves. Pete Harrison from the Northwest Highlands Geopark proved an invaluable local contact in Assynt, as did Helen O'Keefe and her mother, Ann, from the Elphin Tearooms, who welcomed me every evening upon return from the field. Iain MacFadyen of Langwell Estate and Kim Scobie of Rhidorroch Estate kindly facilitated access to the remote parts of the Ullapool area and offered lifts at short notice. Colleagues and staff from the Department of Geography at Durham University were always helpful despite me being there very rarely. In particular, Chris Orton helped compile several diagrams in Chapter 5. Cristina Balaban has become a precious friend and fellow geomorphologist like no other over the past two years since we first met, always happy to talk, listen and challenge me constructively. Not least, I am grateful for the input of my Viva Voce examiners, Stewart Jamieson and Neil Glasser, especially for their comments which improved Chapter 3 and Chapter 5.

Very special thanks go to my close family. My parents, Rodica and Sorin Trelea, raised me in a spirit of freedom and have always allowed me to follow my aspirations. The only time they did not yield was 30 years ago, when they jointly decided I must start English classes. It was a financial effort to pay for those classes and they sternly did so for several years. Of the many dedicated teachers I have had, Mrs. Corina Moroşan, my Geography teacher, was the one who always brought joy and colour to her classes at a time when life in Romania was neither joyful, nor colourful. My husband, Simon and my delightful daughter, Agnes have been the most tolerant and loving people in my life in the past decade or so, and I thank them for the space they have given me to be a scientist. Simon has also helped digitise Figures 2.10 and 2.15 and copy-edited the manuscript. The fact that they both took up ice skating to allow me to study on Saturdays could translate along the lines: "Look, Mum, there is more fun to ice than glacial geomorphology!". There is no end to feeling the passion…

Mulțumiri

Le mulţumesc în primul rând coordonatorilor mei Dave Evans, Chris Stokes şi Dave Roberts pentru îndrumarea profesională şi sprijinul oferit, pentru răbdarea nemărginită şi credinţa neclintită în resursele mele de a face acest gen de cercetare. A fost o binecuvântare şi o onoare să fac parte din echipa lor.

Acest proiect a constituit o lungă aventură facilitată de la bun început de o moştenire în bani rămasă de la dragii mei bunici, Rucsanda şi Augustin Trelea. Am fost de asemenea sprijinită financiar cu generozitate de Departamentul de Geografie al Universităţii din Durham, prin câteva Granturi de Cercetare Post-Universitară, care au mi-au făcut înlesnit participarea la conferinţe şi la excursii organizate de Asociaţia Cercetătorilor Cuaternari. Munca de teren din Assynt, Scoţia, a fost finanţată prin Grantul pentru Cercetători în Devenire oferit de Asociaţia Cercetătorilor Cuaternari. Trevor Faulkner a fost amabil şi mi-a făcut legătura cu Grupul Grampian de Speologie, care m-au găzduit în coliba lor fermecătoare din Elphin, cu vedere către acele caneluri misterioase. Pete Harrison de la Geoparcul Northwest Highlands mi-a fost un sprijin local de nepreţuit, la fel şi Helen O'Keefe şi mama sa, Ann de la Ceainăria Elphin, care m-au întâmpinat în fiecare seară la întoarcerea de pe teren. Iain MacFadyen de la Moşia Langwell şi Kim Scobie de la Moşia Rhidorroch mi-au facilitat accesul în locurile mai îndepărtate din arealul de studiu şi m-au dus uneori cu maşina. Colegii şi personalul de la Departamentul de Geografie din Durham mi-au fost întotdeauna de ajutor, cu toate că am fost rareori prezentă la departament. Chris Orton m-a sprijinit cu compilarea câtorva diagrame din Capitolul 5. Cristina Balaban mi-a devenit o prietenă apropiată şi o colegă ca nimeni alta în ultimii doi ani de când ne cunoaştem, întotdeauna dispusă să stăm de vorbă, să mă asculte şi să mă ia la întrebări. De asemenea, le sunt recunoscătoare examinatorilor mei, Stewart Jamieson şi Neil Glasser pentru contribuţia lor, în special pentru observaţiile cu care au îmbunătăţit Capitolul 3 şi Capitolul 5.

Cele mai alese mulţumiri le adresez familiei. Părinţii mei, Rodica şi Sorin Trelea, m-au crescut într-un spirit de libertate şi mi-au permis întotdeauna să îmi urmez aspiraţiile. Singura situaţie în care nu au cedat a fost în urmă cu 30 de ani, când amândoi au hotărât că trebuie să încep să studiez engleza. A fost un effort să îmi plătească acele ore şi au făcut-o cu neclintire timp de câţiva ani. Dintre numeroşii profesori dedicaţi, doamna Corina Moroşan, profesoara de geografie, a adus în clasă veselie şi culoare într-o perioadă când viaţa în Romania nu era nici veselă, nici colorată. Soţul meu, Simon şi fiica mea, Agnes au fost cei mai iubitori şi mai toleranţi oameni din viaţa mea în ultimii zece ani, şi le mulţumesc că mi-au acordat spaţiul necesar pentru a face cercetare. Simon mi-a digitizat Figurile 2.10 şi 2.15, şi a făcut corectura textului. Faptul că amândoi s-au apucat de patinaj pentru a-mi permite să studiez sâmbăta s-ar traduce cam aşa: „Iaca, mamă, bucuria gheţii înseamnă mai mult decât geomorfologie glaciară!".

Pasiunea nu cunoaşte margini… [*Translation of the Acknowledgements section into Romanian*]

Chapter 1. Introduction

1.1 Rationale

Bedrock mega-grooves (BMGs) are series of straight troughs eroded in bedrock, typically reported to be 100s to 1000s of metres long and 10s of metres deep, with a consistent parallel conformity with each other and to former ice-flow directions (Smith, 1948; Bradwell et al., 2008; Krabbendam et al., 2016; Eyles et al., 2018; Newton et al., 2018). The alignment of BMGs with other streamlined landforms indicative of former Quaternary ice-flow directions (e.g. striae, drumlins, streamlined ridges), alongside their parallel conformity over very long distances, has prompted most geomorphologists to propose a subglacial origin for their formation (Carney, 1910; Smith, 1948; Funder, 1978; Bradwell, 2005; Bradwell et al., 2008; Eyles, 2012; Bukhari et al., 2021). Over the past one hundred years, approximately 30 sites have been reported from across the world, but overall, BMGs remain among the least studied subglacial landforms, with no consensus over their formation mechanisms and glaciological role. Considering their glacial origin BMGs, formation at the ice–bedrock interface and occurrence within ice stream landsystems, BMGs have the potential to advance understanding of processes operating in subglacial environments and of fast-ice flow feedbacks, which drive ice-sheet evolution (Newton et al., 2018). The importance of BMG research is further highlighted under several aspects.

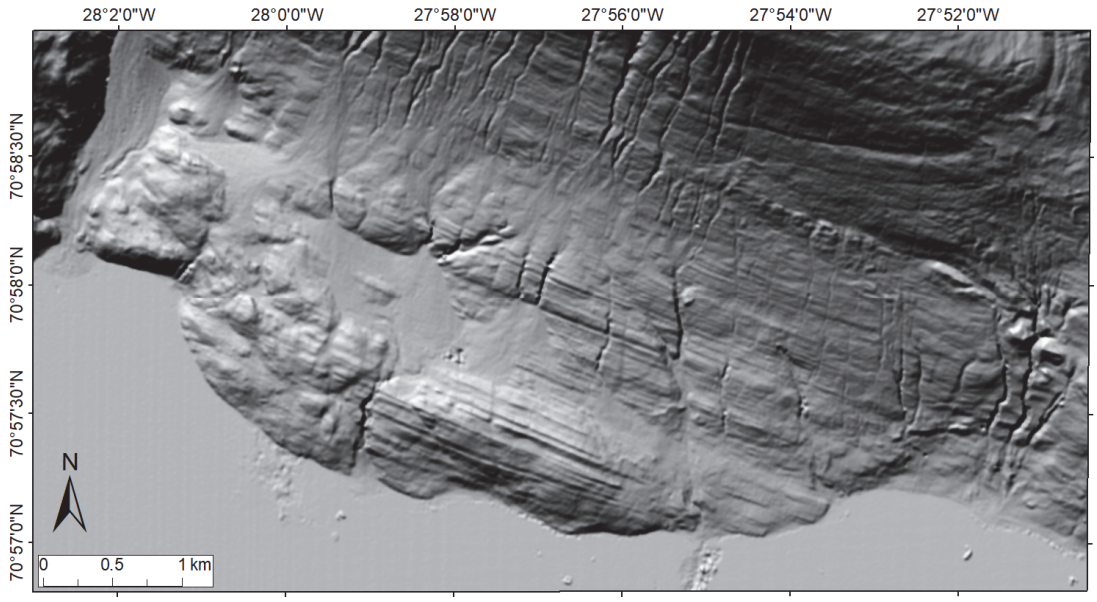

Figure 1.1. Digital elevation model of the grooved terrain at Haarefjord, inner Scoresby Sund, East Greenland. Illumination angle from the north. Arctic DEM provided by the Polar Geospatial Centre under NSF-OPP awards 1043681, 1559691, and 1542736. The ice-flow direction was to the south-east.

Firstly, BMGs can help us better understand processes at the ice–bedrock interface. Beneath warm-based glaciers, where ice is sliding over its substrate, erosion is active through the combined agency of ice, debris and meltwater. Due to their large size and depth, BMGs are ideally positioned to contain erosive agents and thereby focus erosion via a positive feedback mechanism (Boulton, 1974; Eyles et al., 2016; Krabbendam et al., 2016). This is reflected in the preservation of an archive of detailed evidence of subglacial erosion processes in BMGs, such as plucked and abraded surfaces, or smaller grooves including striations, which are sometimes aligned at an angle to the BMGs, indicative of changes in ice flow directions (e.g. Funder, 1978; Munro-Stasiuk et al., 2005; Krabbendam and Bradwell, 2011; Eyles., 2012). Hence, holistically, BMGs should also form an important part of the suite of subglacial landforms of erosion that enable us to understand the interplay between ice sheets and bedrock. One way to deepen the understanding of BMG formation is through morphometric analyses of BMG dimensions. Published studies go into varying levels of detail regarding BMG dimensions, but the results remain site-specific and are rarely derived from systematic measurements of larger samples (Smith, 1948; Gravenor and Meneley, 1958; Heikkinen and Tikkanen, 1989; Bradwell et al., 2008). Systematic measurements that follow consistent protocols and are based on a global landform dataset are needed in the first instance to define the place of the BMGs in the wider hierarchy of streamlined subglacial landforms and to help identify any common features that might give an indication of formation scenarios. This has been undertaken exhaustively for other subglacial landforms of similar magnitude, namely ribbed moraine (Dunlop and Clark, 2006), drumlins (Clark et al., 2009; Ely et al., 2018), mega-scale glacial lineations (MSGLs) (Stokes et al., 2013; Spagnolo et al., 2014), eskers (Storrar et al., 2014) and flutings (Ely et al., 2016).

Secondly, BMGs could give an indication of former ice-flow directions, especially in areas largely devoid of other streamlined landforms, or where younger landforms are superimposed (e.g. eskers, moraines, till sheets, etc.). This is due to their strong potential to survive shifts in ice-flow directions (Finlayson et al., 2014; Krabbendam et al., 2016) which can otherwise reorganise soft-bedded landforms (i.e. MSGLs) into cross-cutting flow sets (Clark, 1993; Dowdeswell et al., 2006; Graham et al., 2009; Ó Cofaigh et al., 2010). BMGs can thus help reconstruct a time-transgressive evolution of ice sheets and contribute to the general understanding of long-term ice-sheet evolution (Boulton and Clark, 1990; Margold et al., 2015).

Thirdly, corrugated terrain with bedrock grooves and ridges contributes to bed roughness. At a small scale, bedrock roughness, in conjunction with subglacial water pressure, determines the degree of ice–bedrock coupling (Falcini et al., 2018). This has direct implications for sliding velocities (Gudlaugsson et al., 2013) and for driving patterns of subglacial erosion through the directing of streaming erodents around bedrock eminences, which enhance the relief and elongation of depressions (Boulton, 1975 and 1979; Eyles, 2012; Eyles et al., 2016). At a large scale, bedrock roughness can be used to develop useful insights into the dynamics and history of ice sheet evolution (Bingham and Siegert, 2009; Jamieson et al., 2014). Due to their size, BMGs could help quantify bed roughness and understand its glaciological role. Significantly, recent studies have highlighted that basal roughness is mirrored in the base of the overriding ice (Le Broque et al., 2013; Jeofry et al., 2018; Drews et al., 2020). BMGs have been shown to correspond to channels in the base of the ice sheet, which are then transferred over the grounding line and further eroded by meltwater on the underside of ice shelves. This scenario may further weaken the ice shelf and increase ice discharge rates in marine-terminating ice streams, and it represents a prime example of how a better understanding of BMG formation and evolution can contribute significantly to understanding ice-sheet flow.

Fourthly, BMGs have been hypothesised to represent the landform signature of the onset zones of palaeo-ice stream landsystems and formed through enhanced erosion induced by fast-flowing ice (Bradwell et al., 2008; Eyles and Putkinen, 2014; Krabbendam et al., 2016; Eyles et al., 2018). There is no strictly defined ice-velocity threshold between slow, ice-sheet flow and ice-streaming. The latter is a corridor of fast-flowing ice characterised by flow velocities at least one order of magnitude higher than those of the surrounding glacier (Stokes and Clark, 2001) and are typically of the order of hundreds of meters per year (e.g. Joughin et al., 2002). The presumed BMG formation under fast-ice flow conditions is difficult to reconcile with BMG occurrence in areas of slower ice-sheet flow (e.g. Smith, 1948; Witkind, 1978) and with evidence from areas of fast-flow onset where streamlined bedrock is the result of long-term subglacial erosion under geological rather than glaciological controls (Roberts et al., 2010). Whereas BMGs remain a conspicuous component of hard-bed landform assemblages in fast-flow onset zones, it is unclear how fast-flowing ice could initiate bedrock grooves in most situations.

Another aspect in need of further investigation is the potential link between BMGs and MSGLs, formed in unconsolidated sediments. BMGs and MSGLs are landforms of similar shape and magnitude, but their dimensions have never been compared because systematic

measurements for BMGs are still lacking. Collectively, these uncertainties raise the question of whether fast-flowing ice is indeed a pre-condition for bedrock groove formation and add to the core questions of BMG research relating to age and scenarios of initiation, for which no overarching theory exists (Newton et al., 2018).

In summary, understanding BMG formation has great potential to advance our knowledge of the subglacial environment in general, and specifically in terms of how processes at the ice–bedrock interface operate. This thesis attempts to unlock this potential by filling gaps in knowledge and clarifying areas of uncertainty regarding how BMGs form and what role they play subglacially, by answering the following research questions:

1. What are typical BMG dimensions?
2. What are the relationships between BMG metrics (e.g. length *versus* width *versus* depth)?
3. What controls BMG formation?
4. How do BMGs compare to MSGLs?
5. Are BMGs formed through ice streaming?
6. How are BMGs initiated?

1.2 Aims and objectives

In order to answer the above research questions, this study aims to characterise the dimensions of BMGs and formulate hypotheses of BMG initiation through fulfilling the following objectives:

1. Critically review existing published studies on BMGs to summarise the state of knowledge and highlight where further research is needed.
2. Map BMGs from key sites across the world and measure their dimensions.
3. Analyse correlations between BMG metrics to better understand groove evolution.
4. Compare the dimensions of BMGs to those of MSGLs.
5. Undertake detailed field observations to constrain the formation of BMGs in an area of hypothesised former ice streaming.
6. Construct conceptual models of BMG initiation.

1.3 Thesis structure and results

The aforementioned objectives are addressed in a series of research papers, which form the body of this thesis. Chapter 2 is a published literature review (Objective 1); Chapter 3 is a morphometric study based on remote sensing techniques (Objectives 2, 3, 4); Chapter 4 is a detailed case study based on fieldwork (Objective 5); Chapter 5 is a conceptual exploration of BMG initiation (Objective 6); and Chapter 6 draws together the conclusions, implications and recommendations for future research.

1.3.1 Chapter 2

Newton, M., Evans, D.J.A., Roberts, D.H. and Stokes, C.R., 2018. Bedrock mega-grooves in glaciated terrain: A review. *Earth-Science Reviews*, *185*, pp. 57-79. https://doi.org/10.1016/j.earscirev.2018.03.007

This paper constitutes a literature review which presents the existing knowledge of BMGs, summarises key findings from individual published sites and highlights areas of consensus as well as differences of opinion regarding BMG formation and their glaciological role. It also classifies BMGs according to their relationship with geological structures and sets out directions for future research. MN wrote the manuscript and prepared all the images and the diagrams. All authors contributed ideas and edited the manuscript throughout the writing period before submission. The manuscript benefited from input from Harold Lovell and an anonymous reviewer before being accepted for publication. At the time of writing, it was decided to use the full name *bedrock mega-groove* instead of the acronym *BMG*, which is used in subsequent chapters.

Several papers with direct implications for the understanding of BMGs have been published since 2018. Thus, Eyles et al. (2018) highlight spatial links between mega-lineated bedrock terrain and ice streaming in a land-terminating palaeo-ice stream landsystem. Bukhari et al. (2021) review key evidence on BMG initiation based on the availability of rubble terrain comprising large-scale boulders of gneissic lithology, which were subsequently used by glacier ice as mega-striators on softer lithologies down-flow. Evans et al. (2021) propose a new model of bedrock grooving applicable to both soft and hard substrates, whereby quasi-rectangular mega-rafts become detached from bedrock along boundary scarps due to pre-existing structural weakness and are then dragged by the ice to form BMGs down-flow.

Some of these findings are incorporated into later chapters, particularly in the conceptual models of BMG initiation in Chapter 5.

1.3.2 Chapter 3

This is a morphometric study based on a global dataset of BMG populations, involving systematic mapping and sampling of BMGs from ten sites across the world. This chapter has been written in a paper format with the intention of it being submitted for publication in the near future. MN did the mapping and sampling in ArcGIS, the statistics and graphics. MN prepared all the figures and wrote the manuscript with ongoing guidance from supervisors. The supporting information pertaining to this chapter is listed in the Appendix. The cross profiles on which groove measurements for depth and width were extracted have been individually labelled and saved in ArcGIS and are available in digital format upon request. The recordings of width and depth for each datapoint were summarised in Excel and are available in Supplementary Material.

1.3.3 Chapter 4

This is a case study based on the BMGs at Ullapool, Scotland, UK. This chapter has been written in a paper format with the intention of it being submitted for publication. The morphometric data for the BMGs were imported from the Excel spreadsheet in Chapter 3, and the measurements for the other landforms were done by MN in ArcMap on the NEXTMap digital terrain model. MN wrote the manuscript, led the fieldwork campaign, drew the maps and undertook measurements and statistical analyses. Supervisors provided feedback on the writing and helped clarify the structure. MN undertook four field excursions into the area in July 2018 and was assisted during one of the trips by D.H. Roberts and by C.R. Stokes.

1.3.4 Chapter 5

This chapter represents a conceptual exploration of different scenarios of BMG initiation, which brings together characteristics of the BMGs with aspects pertaining to structural geology and patterns of long-term pre-glacial weathering. It is written in a paper format with the intention of it being submitted for publication. The ideas in this chapter have developed as a result of ongoing discussions with the supervisory team throughout the duration of this PhD. Chris Orton digitised the drawings in Figures 5.2, 5.5. and 5.8.

1.3.5 Chapter 6

This final chapter presents a summary of the main conclusions of this study, structured to mirror the research questions as they were set out in Section 1.1, and it also highlights suggestions for further research.

1.4 References

Bingham, R.G. and Siegert, M.J., 2009. Quantifying subglacial bed roughness in Antarctica: implications for ice-sheet dynamics and history. *Quaternary Science Reviews*, *28*(3-4), pp.223-236.

Boulton G.S. 1974. Processes and Patterns of Glacial Erosion. In: Coates, D.R. (ed), *Glacial Geomorphology.* University of New York, Binghampton, pp. 41–87.

Boulton, G.S. 1975. Processes and patterns of subglacial sedimentation: a theoretical approach. In Wright A.E and Moseley F. (eds), *Ice ages: ancient and modern* (Vol. 6, pp. 7-42). Seel House Press Liverpool.

Boulton, G.S., 1979. Processes of glacier erosion on different substrata. *Journal of glaciology*, *23*(89), pp.15-38.

Boulton, G.S. and Clark, C.D., 1990. A highly mobile Laurentide ice sheet revealed by satellite images of glacial lineations. *Nature*, *346*(6287), pp.813-817.

Bradwell, T., 2005. Bedrock megagrooves in Assynt, NW Scotland. *Geomorphology*, *65*(3-4), pp.195-204.

Bradwell, T., Stoker, M. and Krabbendam, M., 2008. Megagrooves and streamlined bedrock in NW Scotland: the role of ice streams in landscape evolution. *Geomorphology*, *97*(1-2), pp.135-156.

Bukhari, S., Eyles, N., Sookhan, S., Mulligan, R., Paulen, R., Krabbendam, M. and Putkinen, N., 2021. Regional subglacial quarrying and abrasion below hard-bedded palaeo-ice streams crossing the Shield–Palaeozoic boundary of central Canada: the importance of substrate control. *Boreas 50*(3), pp.781-805.

Carney, F., 1910. Glacial erosion on Kelleys Island, Ohio. *Geological Society of America Bulletin*, *46*, pp.241-283.

Clark, C.D., 1993. Mega-scale glacial lineations and cross-cutting ice-flow landforms. *Earth surface processes and landforms*, *18*(1), pp.1-29.

Clark, C.D., Hughes, A.L., Greenwood, S.L., Spagnolo, M. and Ng, F.S., 2009. Size and shape characteristics of drumlins, derived from a large sample, and associated scaling laws. *Quaternary Science Reviews*, *28*(7-8), pp.677-692.

Dowdeswell, J.A., Ottesen, D. and Rise, L., 2006. Flow switching and large-scale deposition by ice streams draining former ice sheets. *Geology*, *34*(4), pp.313-316.

Drews, R., Schannwell, C., Ehlers, T.A., Gladstone, R., Pattyn, F. and Matsuoka, K., 2020. Atmospheric and oceanographic signatures in the ice shelf channel morphology of Roi Baudouin Ice Shelf, East Antarctica, inferred from radar data. *Journal of Geophysical Research: Earth Surface*, *125*(7), p. e2020JF005587.

Dunlop, P. and Clark, C.D., 2006. The morphological characteristics of ribbed moraine. *Quaternary Science Reviews*, *25*(13-14), pp.1668-1691.

Ely, J.C., Clark, C.D., Spagnolo, M., Stokes, C.R., Greenwood, S.L., Hughes, A.L., Dunlop, P. and Hess, D., 2016. Do subglacial bedforms comprise a size and shape continuum? *Geomorphology*, *257*, pp.108-119.

Ely, J.C., Clark, C.D., Spagnolo, M., Hughes, A.L. and Stokes, C.R., 2018. Using the size and position of drumlins to understand how they grow, interact and evolve. *Earth Surface Processes and Landforms*, *43*(5), pp.1073-1087.

Evans, D.J.A., Phillips, E.R. and Atkinson, N., 2021. Glacitectonic rafts and their role in the generation of Quaternary subglacial bedforms and deposits. *Quaternary Research*, pp.1-35.

Eyles, N., 2012. Rock drumlins and megaflutes of the Niagara Escarpment, Ontario, Canada: a hard bed landform assemblage cut by the Saginaw–Huron Ice Stream. *Quaternary Science Reviews*, *55*, pp.34-49.

Eyles, N. and Putkinen, N., 2014. Glacially-megalineated limestone terrain of Anticosti Island, Gulf of St. Lawrence, Canada; onset zone of the Laurentian Channel ice stream. *Quaternary Science Reviews*, *88*, pp.125-134.

Eyles, N., Putkinen, N., Sookhan, S. and Arbelaez-Moreno, L., 2016. Erosional origin of drumlins and megaridges. *Sedimentary Geology*, *338*, pp.2-23.

Eyles, N., Moreno, L.A. and Sookhan, S., 2018. Ice streams of the Late Wisconsin Cordilleran Ice Sheet in western North America. *Quaternary Science Reviews*, *179*, pp.87-122.

Falcini, F.A., Rippin, D.M., Krabbendam, M. and Selby, K.A., 2018. Quantifying bed roughness beneath contemporary and palaeo-ice streams. *Journal of Glaciology*, *64*(247), pp.822-834.

Finlayson, A., Fabel, D., Bradwell, T. and Sugden, D., 2014. Growth and decay of a marine terminating sector of the last British–Irish Ice Sheet: a geomorphological reconstruction. *Quaternary Science Reviews*, *83*, pp.28-45.

Funder, S., 1978. Glacial flutings in bedrock, an observation in East Greenland. *Bulletin of the Geological Society of Denmark*, *27*, pp.9-13.

Graham, A.G., Larter, R.D., Gohl, K., Dowdeswell, J.A., Hillenbrand, C.D., Smith, J.A., Evans, J., Kuhn, G. and Deen, T., 2010. Flow and retreat of the Late Quaternary Pine Island-Thwaites palaeo-ice stream, West Antarctica. *Journal of Geophysical Research: Earth Surface*, *115*(F3).

Gravenor, C.P. and Meneley, W.A., 1958. Glacial flutings in central and northern Alberta. *American Journal of Science*, *256*(10), pp.715-728.

Gudlaugsson, E., Humbert, A., Winsborrow, M. and Andreassen, K., 2013. Subglacial roughness of the former Barents Sea ice sheet. *Journal of Geophysical Research: Earth Surface*, *118*(4), pp.2546-2556.

Heikkinen, O. and Tikkanen, M., 1989. Drumlins and flutings in Finland: their relationships to ice movement and to each other. *Sedimentary geology*, *62*(2-4), pp.349-355.

Jamieson, S.S., Stokes, C.R., Ross, N., Rippin, D.M., Bingham, R.G., Wilson, D.S., Margold, M. and Bentley, M.J., 2014. The glacial geomorphology of the Antarctic ice sheet bed. *Antarctic Science*, *26*(6), pp.724-741.

Jeofry, H., Ross, N., Le Brocq, A., Graham, A.G., Li, J., Gogineni, P., Morlighem, M., Jordan, T. and Siegert, M.J., 2018. Hard rock landforms generate 130 km ice shelf channels through water focusing in basal corrugations. *Nature communications*, *9*(1), pp.1-9.

Joughin, I., Tulaczyk, S., Bindschadler, R. and Price, S.F., 2002. Changes in West Antarctic ice stream velocities: observation and analysis. *Journal of Geophysical Research: Solid Earth*, *107*(B11), pp.EPM-3.

Krabbendam, M. and Bradwell, T., 2011. Lateral plucking as a mechanism for elongate erosional glacial bedforms: explaining megagrooves in Britain and Canada. *Earth Surface Processes and Landforms*, *36*(10), pp.1335-1349.

Krabbendam, M., Eyles, N., Putkinen, N., Bradwell, T. and Arbelaez-Moreno, L., 2016. Streamlined hard beds formed by palaeo-ice streams: A review. *Sedimentary Geology*, *338*, pp.24-50.

Le Brocq, A.M., Ross, N., Griggs, J.A., Bingham, R.G., Corr, H.F., Ferraccioli, F., Jenkins, A., Jordan, T.A., Payne, A.J., Rippin, D.M. and Siegert, M.J., 2013. Evidence from ice shelves for channelized meltwater flow beneath the Antarctic Ice Sheet. *Nature Geoscience*, *6*(11), pp.945-948.

Margold, M., Stokes, C.R. and Clark, C.D., 2015. Ice streams in the Laurentide Ice Sheet: Identification, characteristics and comparison to modern ice sheets. *Earth-Science Reviews*, *143*, pp.117-146.

Munro-Stasiuk, M.J., Fisher, T.G. and Nitzsche, C.R., 2005. The origin of the western Lake Erie grooves, Ohio: implications for reconstructing the subglacial hydrology of the Great Lakes sector of the Laurentide Ice Sheet. *Quaternary Science Reviews*, *24*(22), pp.2392-2409.

Newton, M., Evans, D.J.A., Roberts, D.H. and Stokes, C.R., 2018. Bedrock mega-grooves in glaciated terrain: A review. *Earth-Science Reviews*, *185*, pp.57-79.

Ó Cofaigh, C., Evans, D.J.A. and Smith, I.R., 2010. Large-scale reorganization and sedimentation of terrestrial ice streams during late Wisconsinan Laurentide Ice Sheet deglaciation. *Bulletin*, *122*(5-6), pp.743-756.

Roberts, D.H., Long, A.J., Davies, B.J., Simpson, M.J. and Schnabel, C., 2010. Ice stream influence on west Greenland ice sheet dynamics during the last glacial maximum. *Journal of Quaternary Science*, *25*(6), pp.850-864.

Smith, H.T.U. 1948. Giant Glacial Grooves in Northwest Canada. *American Journal of Science* 246 (8): 503–14.

Spagnolo, M., Clark, C.D., Ely, J.C., Stokes, C.R., Anderson, J.B., Andreassen, K., Graham, A.G. and King, E.C., 2014. Size, shape and spatial arrangement of mega-scale glacial lineations from a large and diverse dataset. *Earth Surface Processes and Landforms*, *39*(11), pp.1432-1448.

Stokes, C.R. and Clark, C.D., 2001. Palaeo-ice streams. *Quaternary Science Reviews*, *20*(13), pp.1437-1457.

Stokes, C.R., Spagnolo, M., Clark, C.D., Ó Cofaigh, C., Lian, O.B. and Dunstone, R.B., 2013. Formation of mega-scale glacial lineations on the Dubawnt Lake Ice Stream bed: 1. size, shape and spacing from a large remote sensing dataset. *Quaternary Science Reviews*, *77*, pp.190-209.

Storrar, R.D., Stokes, C.R. and Evans, D.J.A., 2014. Morphometry and pattern of a large sample (> 20,000) of Canadian eskers and implications for subglacial drainage beneath ice sheets. *Quaternary Science Reviews*, *105*, pp.1-25.

Witkind, I.J., 1978. Giant glacial grooves at the north end of the Mission Range, northwest Montana. *J. Res. US Geol. Surv*, *6*(4), pp.425-433.

Chapter 2. Bedrock mega-grooves in glaciated terrain: a review

Newton, M., Evans, D.J.A, Roberts, D.H. and Stokes, C.R., 2018. Bedrock mega-grooves in glaciated terrain: A review. *Earth-Science Reviews*, *185*, pp.57-79.

Abstract

Bedrock mega-grooves are assemblages of straight and parallel troughs eroded in bedrock, typically over 1,000 m in length; most sites occur within the limits of the Last Glacial Maximum, both on- and off-shore. In this paper, we review the current understanding of these important yet enigmatic landforms and propose a framework for their future research. Mega-grooves are important to our understanding of ice sheet dynamics, ice–bedrock interactions and bedrock landscape evolution in glaciated areas. The overall straightness of mega-grooves across the landscape, their parallel alignment to palaeo-ice flow direction, and occurrence below the general land-surface level, has led to their unanimous interpretation as landforms of subglacial erosion. Scenarios proposed for mega-groove formation focus on either glacier ice or subglacial meltwater as the principal agent of erosion, yet none offers a comprehensive explanation. At locations where mega-grooves occur along lines of structural geology, their location, formation and morphology were largely controlled by the bedrock characteristics. Where no underlying structural control is apparent, mega-grooves were likely initiated through glacial abrasion, and subsequently modified through a range of erosional processes, potentially involving multiple morphogenetic agencies and feedbacks operating between bedrock topography and basal ice flow. In the absence of absolute dates, morphostratigraphic analyses suggest mega-groove survival through multiple glacial cycles. No specific ice-flow characteristics have been identified as a condition for bedrock grooving, but it has been suggested that some bedrock mega-grooves are related to ice streaming, which deserves further study. An initial analysis of bedrock grooves with seemingly similar morphology at a range of scales hints at a bedrock – groove landform size continuum, which could be a useful framework for exploring process-landform relationships. Future research could usefully focus on quantitative analysis of mega-groove morphology, augmented with detailed field analysis of landform relationships to bedrock structure and lithology, and thereby potentially provide further insight into the age and glaciological significance of these landforms.

Key words: mega-groove; glacial erosion; bedrock geology; landform size continuum; meltwater

2.1 Introduction

Bedrock mega-grooves are series of straight troughs eroded in bedrock, typically over 1,000 m long and up to 10s of metres deep. Mega-grooves display a consistent parallelism throughout their length, without cross-cutting. The essential characteristic of a grooved area is aptly summarised in a pioneering study by Smith (1948: p 507) who noted "the impression thus created is that of ground deeply scored by a giant rake" (Figure 2.1). Over the past hundred years, a number of mega-groove sites have been reported worldwide from areas covered by former Quaternary ice sheets, both onshore (Smith, 1948; Witkind 1978; Wardlaw et al., 1969; Funder, 1978; Heikkinen and Tikkanen, 1989; Bradwell, 2005; Bradwell et al., 2008; Roberts et al., 2010; Krabbendam and Bradwell, 2011; Eyles, 2012; Krabbendam et al., 2016) and offshore (Lowe and Anderson, 2003; Heroy and Anderson, 2005; Bradwell and Stoker, 2015). While most sites are found within the limits of the Last Glacial Maximum (LGM) ice sheets, bedrock mega-grooves of an inferred glacial origin have been reported at some localities lying well outside these limits (Figure 2.2) and used to reconstruct ancient glaciations, such as in the Sahara (Fairbridge, 1974), Australia (Perry and Roberts, 1968) and Argentina (López-Gamundí and Martínez, 2000), as well as in the wider Solar System on Mars (Baker and Milton, 1974, Lucchitta, 1982;). More recently, bedrock mega-grooves have also been inferred from beneath the Greenland ice sheet (Jezek et al., 2011).

The location of mega-grooves and their accordant alignment with other streamlined landforms indicative of former ice-flow direction is usually taken to indicate that they are related to former glaciation. This, together with their parallel conformity and straightness over long distances, has prompted most geomorphologists to propose a subglacial origin for these landforms, traditionally related to quarrying and abrasion (Carney, 1910; Smith, 1948; Zumberge, 1955; Wardlaw, et al., 1969; Witkind, 1978; Goldthwait, 1979; Lowe and Anderson, 2003; Roberts et al., 2010; Krabbendam and Bradwell, 2011; Eyles, 2012; Krabbendam et al., 2016). An alternative school of thought invokes the erosive action of meltwater rather than glacier ice, both on Earth (Baker and Milton, 1974; Tinkler and Stenson, 1992; Shaw, 2002; Bradwell, 2005, Munro-Stasiuk et al., 2009) and Mars (Baker and Milton, 1974). The lack of consensus with respect to the origin of bedrock mega-grooves exists not only between these two schools of thought, (i.e. glacial *versus* glacifluvial), but

also within. For example, advocates of glacial erosion propose various scenarios for mega-groove formation, with specific mechanisms that have included prolonged abrasion over multiple cycles of glaciation (Roberts et al., 2010); lateral plucking under fast-flowing ice (Krabbendam and Bradwell, 2011); and glacial abrasion by fast flowing, debris-rich basal ice (Goldthwait, 1979; Eyles, 2012). Such views are not necessarily conflicting, as they apply to site-specific characteristics related to geology, geomorphology and glacial history. However, few attempts have been made to systematically examine the characteristics of mega-grooves from different settings and assess whether a complex set of conditions and mechanisms could account for their formation, or whether they might be explained by a single mechanism or scenario.

Figure 2.1. Landsat image of mega-grooves in Palaeozoic carbonate bedrock on the western slope of the Franklin Mountains in NT Canada. The mega-grooves formed on the lee side of the ridge relative to palaeo-ice flow direction and represent one of the ten sites described by Smith (1948). The grooves and ridges are straight in planform; their slightly curved appearance towards the top of the Franklin Ridge is given by the 3D-angle of the image. Source of Landsat image - Google Earth © 2016 Google; Image © 2016 DigitalGlobe; #1 on Figure 2.2.

In the last decade, a renewed interest in the analysis of bedrock mega-grooves in a glaciological context has led to the emergence of new research questions, which explore the link between mega-grooves and palaeo-ice streams (e.g. Bradwell et al., 2008; Heroy and Anderson, 2005; Krabbendam and Bradwell, 2011; Eyles, 2012, Krabbendam et al., 2016). The geomorphic signature of ice streams consists of an assemblage of landforms with diagnostic characteristics. In particular, onset zones of fast-flow have bedrock landforms

with high length: width ratios and a convergent flow pattern and are often replaced down-ice by an area of deformed sediment (Stokes and Clark, 1999). Where mega-grooves occur in conjunction with streamlined landforms indicative of fast ice flow, it has been suggested that they belong to the same palaeo-ice stream landsystem for example on the Antarctic continental shelves (Lowe and Anderson, 2003; Wellner et al., 2006), in Scotland (Bradwell et al., 2007; Bradwell and Stoker, 2015), Canada (Eyles, 2012) and also in Norway (Ottesen et al., 2008). At these locations, mega-grooves occur in areas interpreted as the onset zones of fast ice-flow (ice streams), and their formation has been attributed to enhanced and focused glacial erosion assumed to take place in such zones.

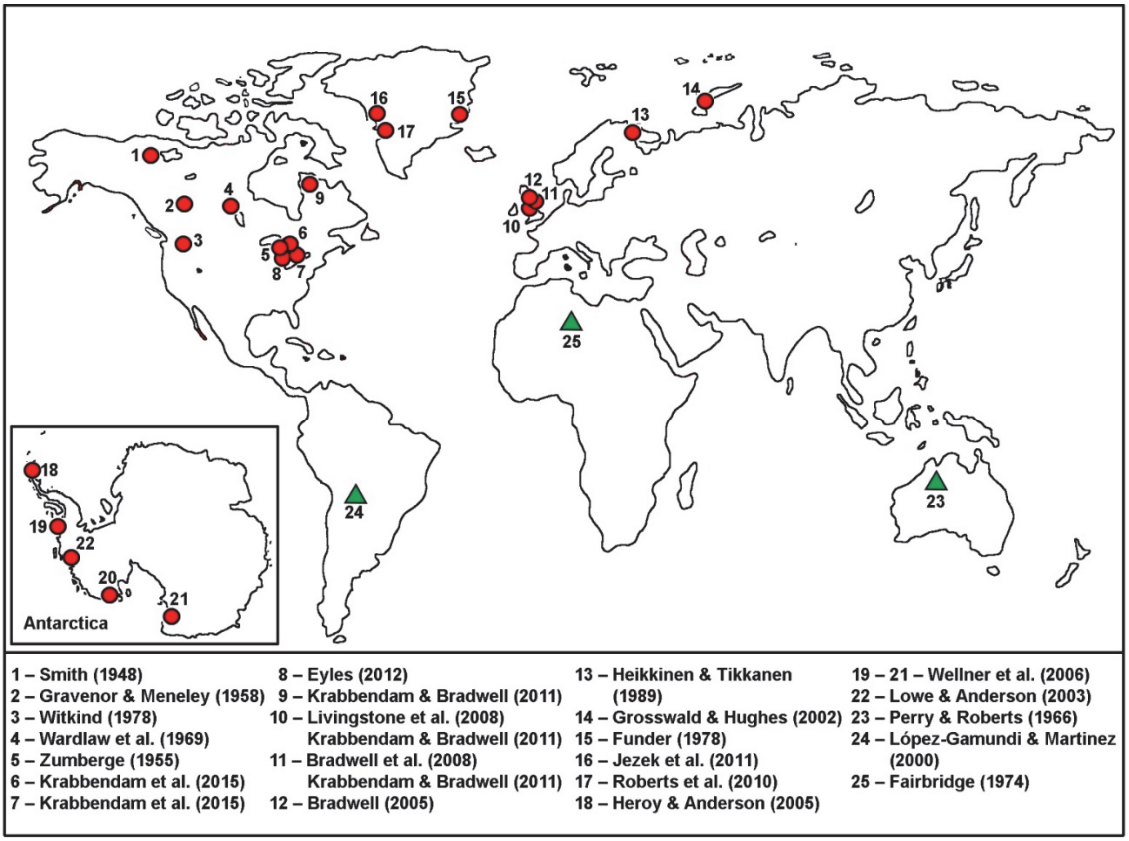

Figure 2.2. Location of bedrock mega-groove sites described in the literature. Circles represent sites within the maximum extent of glaciers during the last, Marine Isotope Stage 2 glaciation, and triangles represent mega-groove sites at locations affected by ancient, pre-Quaternary glaciations.

Addressing the uncertainties relating to mega-groove formation and their glaciological significance would lead to a better understanding of the subglacial environment in terms of spatial variability of subglacial forms and processes, and persistence of bedrock forms beneath ice sheets. This paper presents a systematic review of the existing body of

knowledge on mega-grooves in order to assess the proposed mechanisms of formation and the glacial and geological scenarios in which grooves were likely initiated. First, we review the terminology related to bedrock grooving and provide an historic overview of mega-groove research (Section 2.2). In Section 2.3, we review the physical characteristics of mega-grooves and their relationships to bedrock geology. The mechanisms proposed for mega-groove formation, and possible time frames of development are presented in Section 2.4. In the discussion (Section 2.5) we (i) evaluate the role of geological structure in mega-groove formation, (ii) undertake an initial assessment of mega-grooves in relation to a possible bedrock landform size continuum, and (iii) assess the influence of glaciological conditions on groove formation. Emerging from this critical review, we propose a series of suggestions for future research.

2.2 Terminology and history of research

2.2.1 Terminology

A series of terms have been used over the decades to refer to bedrock corrugations in glaciated terrain, including 'megaflutes', 'flutings', 'fluted terrain' (Gravenor and Meneley, 1958; Funder, 1978, Heikkinen and Tikkanen, 1989), 'giant grooves' (Smith, 1948; Witkind, 1978; Goldthwait, 1979) and 'megagrooves'/'mega-grooves' (Bradwell, 2005; Munro-Stasiuk et al., 2005; Bradwell et al., 2008; Benn and Evans, 2010). Of these, some terms have been used with a wider meaning. For example 'lineations' and 'flutings' can refer to landforms in unconsolidated sediment or unknown substrates and mean either ridges and/or troughs (Baeten et al., 2010). It is important that a specific descriptive terminology be designated for large-scale grooves from glaciated terrain, which occur in bedrock, in order to ensure clarity and unity in scientific communication. It is also important to maintain an awareness of terminology used in the past, in order access references to these landforms in older publications.

Deriving and developing terminology in geomorphology should aim to help differentiate between landforms, particularly those of similar shape and/or process – form regimes. In this respect, bedrock mega-grooves bear morphological similarities with mega-scale glacial lineations (MSGLs: cf. Clark, 1993; King et al., 2009). The latter are typically much longer, generally formed in unconsolidated glacial sediments (cf. Spagnolo et al., 2014), and can exhibit cross-cutting patterns (Clark, 1993; Bradwell et al., 2007; Benn and Evans, 2010). While corrugations in both types of substrate have unequivocally been linked to glaciation, uncertainties regarding their formation and glaciological significance persist. Indeed they

are likely different landforms, with an altogether different morphogenesis, so it is important that differing terminology is used consistently to refer to each type. Because MSGL is a well-established term for highly elongate glacial lineations in unconsolidated sediment (Clark, 1993; Clark et al., 2003; King et al., 2009; Spagnolo et al., 2014), it is preferable to avoid the term 'lineation' when the substrate is bedrock. Whenever the substrate is unclear, the term 'fluting' may be more appropriate, especially as it has been previously employed to describe troughs and ridges collectively in a landscape context (e.g. Gravenor and Meneley, 1958; Lawson, 1976; Funder, 1978; Heikkinen and Tikkanen, 1989) and does not inherently define the nature of the substrate. However, flutings or 'flutes' commonly occur at a much smaller scale than both MSGL and bedrock mega-grooves (Ely et al., 2016).

Ideally, terminology should capture key physical characteristics of landforms in order to be as descriptive and intuitive to envisage as possible. In the case of mega-grooves, one key characteristic is their occurrence in bedrock, and in this respect the word 'groove' is semantically appropriate, as it means a long, narrow cut or depression in hard material (Soanes and Hawker, 2005. However, 'groove' by itself has long been used for general reference to a wide size-range of subglacially-formed troughs in bedrock, (Dahl, 1965; Gjessing, 1965; Flint, 1971). Therefore, a quantifier is required alongside 'groove' when referring to large-scale landforms, in order to render their extraordinary length, which is another key physical characteristic. In older studies, large-scale grooves are referred to as "giant grooves" (e.g. Smith, 1948; Wardlaw et al., 1969; Witkind, 1978; Goldthwait, 1979), and while this expression is still in use (Grosswald and Hughes, 2002), the more morphometrically precise term 'mega-grooves' has gradually replaced it (e.g. Bradwell, 2005).

The term 'megagroove', as explicitly proposed by Bradwell et al. (2008) to refer to large-scale bedrock grooves formed through glaciation, was quickly adopted by the scientific community and has been widely used in the last decade in glacial geomorphology, solely to refer to these landforms (Roberts et al., 2010; Krabbendam and Glasser, 2011; Eyles, 2012; Benn and Evans, 2010; Krabbendam et al., 2016). Although both 'mega' and 'giant' communicate the large size of the grooves, the prefix 'mega' is preferable for the following reasons: i) it can give a technical rather than literary value to the word 'groove'(i.e. 10^6 mm according to the International System of Units), which improves clarity in scientific communication; ii) it allows for classification in the wider range of grooves with similar morphology and instantly conveys the hierarchic place that these landforms occupy in the range, which can be useful in the context of a landform size continuum; iii) unlike 'giant',

'mega' is not a superlative, so it leaves open the nomenclature scale if yet larger grooves are yet to be named (e.g. giga-grooves). The hyphenated version 'mega-groove' is preferred because it maintains a better focus on the semantic value of each component and allows for some flexibility in usage. In conclusion, we regard the term 'mega-groove' as best suited to refer to large-scale bedrock grooves in glaciated terrain, as it conveys concisely and comprehensively the current knowledge of these landforms, while avoiding ambiguity in relation to others.

2.2.2 A brief history of research

The history of mega-groove research spans less than a century, during which time there has been a gradual broadening of the scientific interest related to these landforms. To our knowledge, mega-grooves are first mentioned in land survey reports carried out by Geological Surveys in Canada and the USA (Gilbert, 1873; Bell, 1867). Early papers with a specific focus on mega-grooves are based on observations that were rather incidental to broader geological projects, and the authors implied that the motivation to describe such landforms lay in their unusual nature and rare occurrence. For example, Smith (1948, p 503) explicitly states that his study on mega-grooves in the Northwest Territories (NT), Canada "is based on observations made while serving as a geologist on the Canol Project […]. Ground observations were […] purely incidental to studies of petroleum geology". Notably, Smith's (1948) paper has been the benchmark for later descriptions and interpretations of bedrock mega-grooves, because subsequent studies used it as a basis for morphologic and genetic comparisons (e.g. Zumberge, 1955; Gravenor and Meneley, 1958; Wardlaw et al., 1969; Witkind, 1978; Funder, 1978; Heikkinen and Tikkanen, 1989; Jezek et al., 2011). Mega-groove studies published throughout the 20th century describe the physical characteristics of landforms in detail, in conjunction with their relationship to bedrock geology. Such descriptions are based on data from direct field observations and from aerial photographs, but little is mentioned about the glaciological context (e.g. Smith, 1948; Wardlaw et al., 1969; Funder, 1978).

It was not until the beginning of the 21st century that the glaciological conditions in which mega-grooves formed received considerable attention (Lowe and Anderson, 2003; Wellner et al., 2006; Bradwell et al., 2008). Initially, new sites were reported and analysed with the advent of new survey techniques, such as satellite imagery and digital elevation models onshore (Bradwell et al., 2008; Roberts et al., 2010; Krabbendam and Bradwell, 2011; Eyles, 2012; Krabbendam et al., 2016) and bathymetric surveys offshore (Lowe and Anderson,

2003; Wellner et al., 2006; Eyles, 2012; Bradwell and Stoker, 2015), and geophysical techniques beneath modern ice sheets (Jezek et al., 2011) (Figure 2.3). In addition, some older sites were revisited, and previous interpretations challenged with respect to the agents and processes involved in groove formation (Munro-Stasiuk et al., 2005; Krabbendam and Bradwell, 2011; Eyles, 2012). Most of the more recent studies attempt to explain mega-groove formation in a wider, regional context of ice flow, whether past (Lowe and Anderson, 2003; Wellner et al., 2006; Eyles, 2012; Bradwell and Stoker, 2015) or present (Jezek et al., 2011), and they link groove formation to specific characteristics of ice flow in terms of velocity. It could even be argued that the scientific interest in bedrock mega-grooves has been rekindled recently by their glaciological interpretation as subglacial features formed in the onset zones of -ice streams (Bradwell et al., 2008; Eyles, 2012; Krabbendam et al., 2016). The potential link between ice streams and bedrock mega-grooves has certainly given these enigmatic landforms increased visibility in glacial research at a time when ice streams, ancient and modern, have been receiving more attention (Bamber et al., 2000; Rignot and Kanagaratnam, 2006; Winsborrow et al., 2010; Kleman and Applegate, 2014; Stokes et al., 2016; Eyles et al., 2018; Stokes, 2018).

In summary, the scientific interest in mega-grooves has broadened from the detailed documentation of their physical characteristics, to include their glaciological significance in a wider, regional context of palaeo-ice flow and based largely on remote sensing data. Yet how these landforms were actually initiated and whether or not they are produced by multiple glaciations remain poorly understood.

2.3 Characteristics of mega-grooves

In this section we review the principal physical characteristics of mega-grooves reported in the literature in terms of morphology, morphometry and topographic setting, as well as relationships to bedrock geology. The aim here is to build a database of physical characteristics of mega-grooves, in order to facilitate identification of key physical features and patterns of occurrence. Such data will serve as a basis to test hypotheses of mega-groove formation. Table 2.1 summarises the key data on mega-grooves described in the literature, and their location is mapped on Figure 2.2.

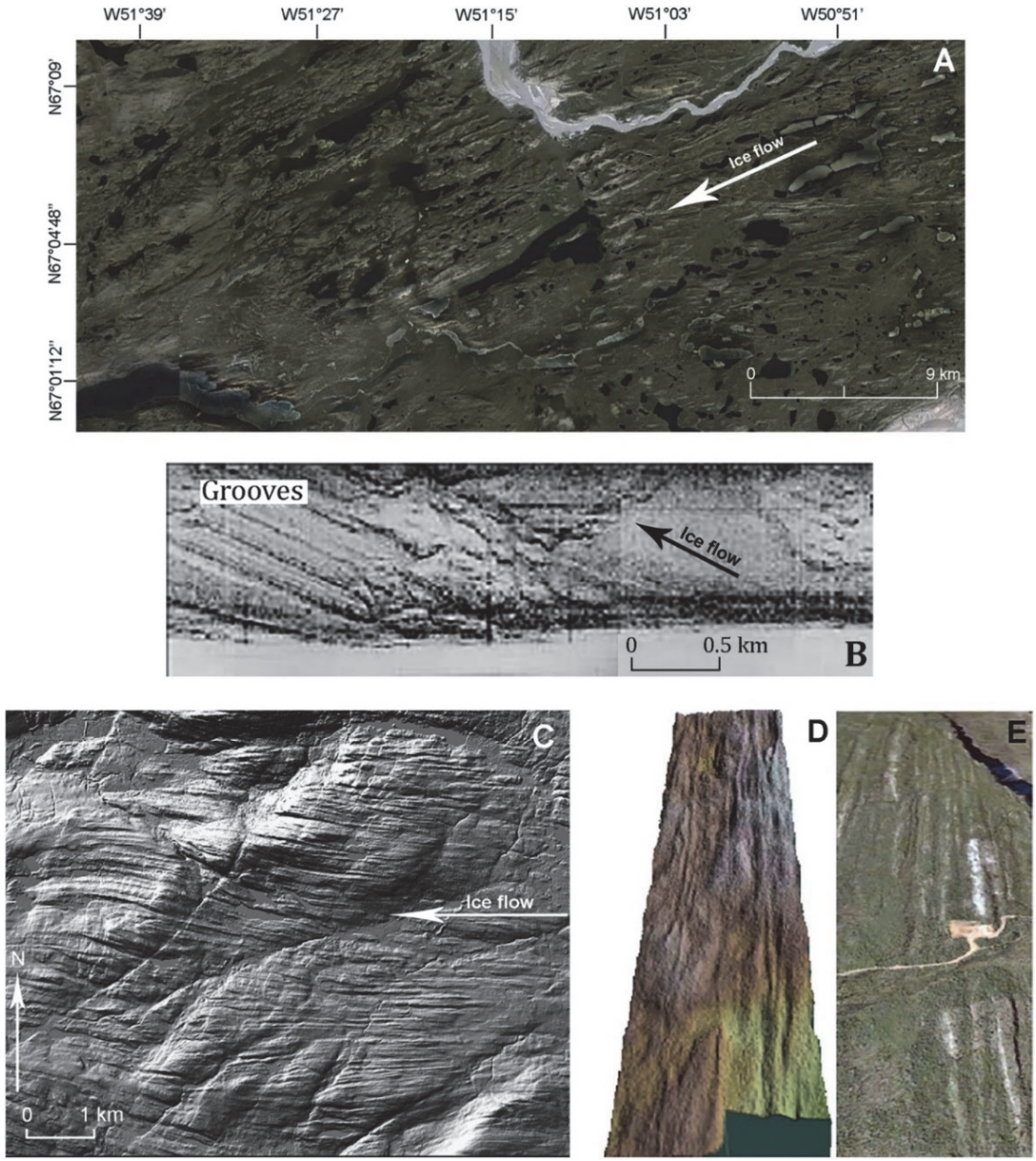

Figure 2.3. Images of mega-grooves obtained through various methods of remote sensing. **A:** Mega-grooves and ridges in west Greenland, ca 100 km north-east of Sisimiut, described by Roberts et al. (2010). The grooves are eroded in gneissic bedrock and the ridges consist of mafic dykes relatively more resistant to erosion. Source of Landsat image - Google Earth © 2015 Google; © 2015 DigitalGlobe; # 17 on Figure 2.2. **B:** Series of straight and parallel mega-grooves at Pine Island Bay, West Antarctica. The image was obtained through a compilation of swath bathymetry data and is modified from Lowe and Anderson (2003). Ice flow was in a NNW direction. Base image reproduced with permission from IGSOC; #22 on Figure 2.2. **C:** Digital surface model (NEXTMap Britain) of large mega-groove field north of Ullapool, Scotland, UK, with 1m resolution in the vertical plane and 2 m in the horizontal plane, illuminated from the north-west. The image is centred on N 57°56'45'' and W 5°02'26''. Image modified from Bradwell et al (2008) and reproduced with permission from Elsevier; #11 on Figure 2.2. **D, E:** Comparison between mega-grooves under the Greenland ice sheet (D), located at approximately N 69°06' and W 48°, and mega-grooves at Norman Wells, NT Canada (E), located at N 65°18' and W 126°42'. The bedrock topography beneath the ice sheet was reconstructed using radar tomography algorithms (Jezek et al., 2011). Close similarity in morphology and size between mega-grooves at the two sites suggests subglacial formation primarily through differential erosion of the bedrock by glacier ice (Jezek et al, 2011). The grooves and ridges measure around 2,000 m in length. Base image modified from Jezek et al. (2011) and reproduced with permission from John Wiley & Sons; (D) corresponds to #16 and (E) to #1 on Figure 2.2.

2.3.1 Morphology and morphometry

Mega-grooves typically occur as series of parallel corrugations in bedrock. In most cases mega-grooves are strikingly rectilinear across the landscape (Figure 2.1) (Smith, 1948; Funder, 1978; Lowe and Anderson, 2003; Bradwell, 2005, 2008; Eyles, 2012), although in some places they can show a slight sinuosity in planform (Zumberge, 1955; Roberts et al., 2010; Krabbendam and Bradwell, 2011; Jezek et al., 2011), or exhibit a broad curve (Smith, 1948). An exceptional case are the mega-grooves described by Witkind (1978), which curve round the northern spur of the Mission Range, Montana, US (Figure 2.4). Witkind (1978) suggests that the overall curvature reflects changes in former regional-ice flow direction in contact with local mountain glaciers, although groove occurrence along bedrock joints is also mentioned at this site. Grooves of similar size tend to maintain their parallelism regardless of whether they are rectilinear, slightly sinuous or crescentic in planform, with the exception of the mega-grooves in Assynt, NW Scotland, which splay out slightly in the palaeo-ice flow direction (Figures 2.5A and B) (Bradwell, 2005).

Mega-grooves usually have an up-and-down long profile, with bedrock knobs and ridges along their floors (Witkind, 1978; Heikkinen and Tikkanen, 1989; Eyles, 2012). In Assynt, NW Scotland, they tend to deepen up-slope, and some terminate abruptly against a steep cliff in the middle of the slope (Bradwell, 2005). The long-profile, as well as the actual depth, have proven difficult to assess at sites where a thick layer of till is present inside the grooves (Witkind, 1978), or if their floor is occupied by lakes (Wardlaw et al., 1969), muskeg, vegetation (Smith, 1948), or peat (Bradwell, 2005). The typical depth is, however, in the range of 10–20 m (Table 2.1). In cross-profile, mega-grooves are typically U-shaped (Witkind, 1978; Funder, 1978; Heikkinen and Tikkanen, 1989; Bradwell, 2005; Eyles, 2012; Krabbendam et al., 2016), although at some localities the cross-profile can vary between V- and U-shaped (Smith, 1948; Bradwell et al., 2008), or parabolic with steep, concave sides (Bradwell et al., 2008) (Figure 2.6).

Mega-grooves are typically 1,000–2,000 m in length. Exceptionally long grooves, of up to 12,000 m, have been reported in the Mackenzie River valley, Northwest Territories, Canada (Smith, 1948), and some that are tens of kilometres have been identified on the Antarctic continental shelf (Wellner et al., 2006). At some locations, mega-grooves are unbroken along their length (Smith, 1948; Funder, 1978; Bradwell, 2005), which contrasts with other sites where either the ridges or the mega-grooves are discontinuous (Krabbendam et al., 2016; Heikkinen and Tikkanen, 1989). Length can also vary widely within the same area. For example, the grooves north of Ullapool in Scotland have been reported to range between

500 and 3,000 m (Bradwell, et al., 2008). In Montana, US, Witkind (1978) noted that a string of two or three grooves joined up longitudinally, thus giving the false impression of extreme length. The width of mega-grooves is typically in the range of 20-200 m and tends to remain constant within the same groove (e.g. Mission Range, Montana; Witkind, 1978), but varies considerably between sites and sometimes within the same site (Table 2.1). Regarding groove spacing (or wavelength), some studies report that mega-grooves are regularly spaced (e.g. at 45 m: Funder, 1978; Bradwell, 2005), or that spacing varies within a certain interval (e.g. 10-20 m, Bradwell et al., 2008), whereas other studies do not report this metric (see also Table 2.1). Gravenor and Meneley (1958) identified two peaks in mega-groove spacing for the five sites they investigated in north-east Alberta, at 90–120 m and 180–215 m, respectively, which occur regardless of the nature of the substrate.

Mega-grooves typically occur in undulating lowland areas with local relief generally below 400–600 m (Smith, 1948; Gravenor and Meneley, 1958; Heikkinen and Tikkanen, 1989; Funder, 1978; Eyles, 2012). They have been reported to occur in all positions on slopes relative to ice-flow direction (e.g. lee, stoss, across-slope), although local trends have been noted. For example, in Ontario, Canada, mega-grooves are present on the slopes tilted to the south-west, which follow the shallow dipping plane of bedrock strata which coincided with regional ice-flow direction (Eyles, 2012). In Finnish Lapland, mega-grooves incise the summits of fjells (local granite hillocks) and fade over intervening lowlands only to re-emerge on the next hill, thereby being traceable over long distances in straight lines over the landscape (Heikkinen and Tikkanen, 1989) (Figure 2.7).

Given the above descriptions of the size and shape, Bradwell et al. (2008) defined mega-grooves as being "large-scale, linear, erosional features with negative topographic expression formed by glaciation, regardless of their genesis". Here, we add to this definition a semi-quantitative reference based on characteristic morphometric values reported in the literature and summarised in Table 2.1. Thus bedrock mega-grooves are:

Series of parallel and closely-spaced bedrock grooves, straight to slightly curvilinear in planform, which occur in glaciated terrain. Typically mega-grooves measure over 1,000 m in length, have length:width ratios between 20:1 and 50:1, and length:depth ratios higher than 100:1.

Although the shape and size of the intervening ridges often mirror those of the grooves (Funder, 1978; Eyles, 2012), we argue that it is mainly the grooves that represent the

geomorphological process of subglacial erosion, whereas the ridges are partial remnants of the initial land surface into which the grooves were incised (c.f. Smith, 1948). There are a few other common features among mega-groove sites that have not been included in the above definition. For example, all sites tend to occur towards the margins rather than the centre of ice sheets (Figure 2.2), and also in areas of relative lowland, close to the base level. While such attributes may have some relevance with regards to mega-groove formation, as yet they are not considered diagnostic features for these landforms.

Table 2.1. Mega-groove characteristics related to basic morphometry, geology and glaciology from sites across the world, extracted from published studies. N/M = not mentioned; LIS = the Laurentide ice sheet; words in bold represent a summary of the text in the cell; the metrics for length, width and relief are average values with maximum values in brackets.

Site & References	Length (m)	Width (m)	Relief (m)	Mega-grooves in relation to			Evidence of glaciation	Hypotheses of formation
				Terrain	Bedrock lithology	Bedrock structure		
Northwest Territories (NT), Canada Smith (1948)	30–1,500 (12,000)	<50	<30	Ten sites (A–J) across the broad and irregular 130 km² lowland bordered by mountains, between the Great Bear Lake and the Mackenzie River; boggy terrain. Grooves: clusters of parallel individuals on tops and stoss sides of slopes; mostly straight, diverge a few degrees (J); broad curvature (C). Ridges: continuous; minor variations in size and shape at crest level; fragmented (B); "en echelon offsets" (G); drumlinised (D). **10 sites in Arctic lowland**	Silurian– Lower Tertiary sedimentary basin. Mega-grooves reach maximum depth in a brecciated limestone, porous to cavernous (lower-Devonian Bear Rock formation) and in Devonian reef limestone, Poorly developed grooves in the harder Devonian and massive Silurian limestone. **Limestone**	Grooves oblique or perpendicular to bedrock strike; parallel to strike (E, F). The cross profile is mostly U-shaped. **Discordant**	Grooved areas close to the margin of Laurentide Ice Sheet (LIS) at its maximum extent; patchy glacial deposits containing erratics; grooves aligned with regional ice flow direction; The Pleistocene glaciation changed the regional drainage pattern; current Mackenzie valley interpreted as a Lateglacial marginal meltwater channel. **Margin of LIS**	Differential glacial erosion controlled by lithology. An estimated 40–80% of the rock layer was removed through erosion from well-developed grooves; model of groove evolution with adjacent grooves merging over time. **Glacial erosion**
Harefjord, East Greenland Funder (1978)	50–2,000	45	1–5	About 50 parallel ridges and grooves on the gently undulating lowland at 50–250 m a.s.l., along the north shore of Harefjord, inner Scoresby Sund; fluted area ca 6 km². The crest of ridges conforms to general topography. Two till ridges, up to 1.5 m high present. **Arctic lowland**	Grooved area confined to an insular outcrop of Røde Ø Conglomerate surrounded by pre-Cambrian metamorphic rocks. Coarse sandstone and conglomerate with gneiss phenoclasts, possibly deposited during a period of faulting activity in the Lower Permian. **Røde Ø Conglomerate**	Grooves cut across beds of sandstone and conglomerate with varying orientations, possibly depositional cones. The ridges have a rounded top and the grooves a U-shaped profile. **Discordant**	Parallel to the Quaternary ice-flow direction. Striations parallel to ridges, also at 20°angle; no cross-striations Thin and patchy till veneer; numerous erratic boulders. Bedrock forms obscured by glacifluvial deposits in the west and north. **Multiple glaciations**	Some lithological control is suggested based on the close association between the flutings and the Røde Ø Conglomerate; possible secondary flow of ice and/or meltwater at glacier sole suggested to account for spacing regularity. **N/M**

Site & References	Length (m)	Width (m)	Relief (m)	Mega-grooves in relation to			Evidence of glaciation	Hypotheses of formation
				Terrain	Bedrock lithology	Bedrock structure		
West Greenland Roberts et al. (2010)	5,000	200	30–50	Ca 100 km northeast of Sisimiut, close to the ice sheet margin. Closely-spaced and elongated bedrock ridges separated by grooves and elongated depressions aligned ENE–WSW. **Arctic lowland**	Precambrian Archean gneissic rocks, heavily foliated and intruded by swarms of ultramafic dykes trending ENE–WSW. The mega-grooves eroded in gneiss; harder dykes form the ridges. **Gneiss and dykes**	The grooves and ridges follow the grain of the land. **Concordant**	Quaternary ice sheets advanced repeatedly over the area, general flow to the west. **Multiple glaciations**	Selective and prolonged abrasion throughout multiple cycles of erosion rather than fast flowing ice. **Glacial abrasion**
North-east Alberta, Canada Gravenor & Meneley (1958)	Several 1,000s	N/M	3– 8	Pure bedrock landforms only north-east of Andrew Lake, other sites contain fluted till. Consistent spacing regularity at 90–120 m and 180–215 m. Flutings occur in various topographic settings. **Spacing regularity**	Precambrian shield rocks in Andrew Lake area. Hard rocks (pegmatite dykes) eroded to the same depth as adjacent softer metasediments across grooved areas. **Canadian shield rocks**	Perpendicular to strike. Groove spacing independent of bedrock characteristics and topographic control. **Discordant**	General flow of regional ice, from the Keewatin ice centre; striae parallel to the grooves. The ridges at Andrew Lake are grade into drumlins, and are similar in size, shape and spacing to till ridges. **Continental glaciation**	Intrinsic properties of ice lead to alternating low- and high-pressure parallel bands at the glacier sole. Groove formed in the high-pressure areas through erosion. Water-logged sediments deposited on top of ridges; assumes pre-existing glacial deposits. **Focused glacial abrasion**
Isle Royale, Michigan, US Zumberge (1955)	2,000–20,000 (65,000)	N/M	N/M	North-east of Lake Superior. Parallel ridges and valleys aligned northeast–southwest. The valley floors are occupied by over 50 lakes at 30–60 m above local base level of Lake Superior. **Lowland**	Lower sequence formed of lava flows intercalated within beds of conglomerate and flow breccia, and upper sequence formed of conglomerate and sandstone. **Intercalated lavas and sedimentary layers**	North flank of the Lake Superior syncline; dips 10–30° to the south-east. Some lava flows are massive, others thin and hexagonally jointed; grooves follow bedrock strike; cross profile asymmetric: shallower slopes along the dipping plane. **Concordant**	The present stepped topography is formed subaerially through fluvial denudation during the Tertiary when Isle Royale was part of the wider Superior Basin drainage system. Assumed multiple glaciations with ice flowing parallel to bedrock strike. **Multiple glaciations**	Quaternary glaciers enhanced Tertiary topography through plucking rather than abrasion, aided by the geological structure with well jointed rocks. Lateral plucking also suggested by Krabbendam and Bradwell (2011). **Lateral plucking**

Site & References	Length (m)	Width (m)	Relief (m)	Mega-grooves in relation to			Evidence of glaciation	Hypotheses of formation
				Terrain	Bedrock lithology	Bedrock structure		
Assynt, NW Scotland, UK Bradwell (2005)	500–1,500 (4,300)	20–30	5–20 (27)	Well defined grooves west of Elphin village; linear, aligned east-west, slightly divergent pattern in planform; discontinuous and less well-defined grooves in adjacent areas. Lowland at ca 300 m a.s.l. surrounded by fragmented highlands. **Lowland**	Cambrian quartzite dipping 7–20° to the east; mega-grooves can be traced across the landscape to the west, in Torridonian sandstone. The longest groove crosses 3 lithologies. Cavernous limestone bedrock to the east. **Quartzite**	Cut across strike; generally unrelated to faults and joints; two grooves follow local fault lines. Long profile: deepen upslope; five end abruptly mid-slope, against steep cliffs; gorge-like aspect. Cross profile: asymmetric; steeper northern slope with signs of plucking; inferred U-shape. **Discordant**	Small-scale erosional features: depressions and undulation surfaces, transverse scours; striae and chatter marks; plucked surfaces; longitudinal channels. Last ice sheet moved from east to west. **Multiple glaciations**	Erosion by subglacial meltwater. Pressurised subglacial jets emerged at the down-glacier end of limestone bedrock and hydrofractured the impermeable but jointed quartzite bedrock. The grooves underwent subsequent fluvial and glacial erosion. **Meltwater erosion**
Ullapool, Scotland Bradwell et al. (2008); Krabbendam and Bradwell, (2011)	500–3,000 (3,500)	50–120 (200)	10–20	Large breach in local watershed; low ground at 300 m a.s.l. flanked by mountains. Area ca 600 km^2. Numerous grooves, closely spaced (100–500 m) and rectilinear; overall convergent pattern; cross all slopes; maximum density on the steeper, north-facing slopes. **Lowland**	Neoproterozoic rocks: coarse and relatively massive Torridonian sandstone (west); Morar metasandstone (east), well bedded and jointed, with thin mica beds. Closely-spaced mega-grooves are more common in sandstone. **Metasandstone**	Where bedrock strike parallels ice flow, grooves have an asymmetric cross profile: steep side cuts across strata ends and shallow side follow bedding plane. Others have a parabolic or a V-shaped profile. **Parallel to strike**	Westwards general ice-flow direction with abundant off-shore evidence for former ice streaming. Grooved area interpreted as onset zone for fast ice flow. Thin and patchy glacial deposits. **Ice streaming**	Focused glacial erosion during the last glaciation in ice-stream onset zone (Bradwell et al, 2008). Krabbendam and Bradwell (2011) propose lateral plucking, whereby the low-pressure cavity forms in the *vertical* lee-side of the rock, so that the loosened block undergoes a rotation around its own vertical axis before complete dislocation. **Lateral plucking**

Site & References	Length (m)	Width (m)	Relief (m)	Mega-grooves in relation to			Evidence of glaciation	Hypotheses of formation
				Terrain	Bedrock lithology	Bedrock structure		
Ungava Peninsula, Canada Krabbendam and Bradwell, (2011)	10,000–40,000	N/M	N/M	Ca 5,000 km^2 of elongated bedrock ridges separated by grooves; closed basins containing lakes. The area was surveyed through remote sensing. **Arctic lowland**	(Meta)sedimentary strata, forming the Cape Smith Belt, include sandstone, carbonates, conglomerate, pelite and semipelite, with igneous intrusions. The strata strike WSW–ENE dip 10–40°north. **(meta)sedimentary and igneous intrusions**	Grooves and ridges follow the strike swings. grooves spacing is 300–700 m dictated by strata thickness. Classic cnoc-and-lochan topography is obvious either side of the Cape Smith Belt, on shield rocks. **Concordant**	Repeated Quaternary glaciations, recorded multiple shifts in the ice flow direction; at some stages the flow paralleled grooves. **Multiple glaciations**	Initiation of ridge-and-groove topography possibly due to pre-glacial differential erosion was further enhanced through lateral plucking (see row above for Ullapool, Scotland). **Lateral plucking**
Kaladar, E Ontario, Canada Krabbendam et al. (2015)	10,000s	300–2,000	10–30	Mega-groove field of 100 km^2 **Lowland close to sea level**	Strongly layered succession of metasedimentary rocks. Well developed in softer and more fractured lithologies. Adjacent tonalite and granite areas are not grooved. **Metasedimentary rocks**	Grooves follow lineaments of bedrock strike. Undetermined shape of cross profile; grooves are partly occupied by lakes and post-glacial debris. **Parallel to strike**	Area occupied by the Laurentide ice sheet, and possibly affected by ice streaming. **Ice sheet and ice streaming**	Differential glacial erosion according to lithology; lateral plucking suggested as the dominant mechanism. **Lateral plucking**
Tyne Gap, England, UK Livingstone et al. (2008); Krabbendam and Bradwell, (2011)	1,000–4,000	N/M	5–20	Topographic breach in the watershed bounded to the north and south by plateau areas, up to 300 m higher. Alternating grooves and ridges spaced 100–400 m. **Watershed lowland**	Carboniferous limestone and mudstone alternates with coal bed; the Whin Sill dolerite intrusion; well developed joints define cuboid rock blocks. **Sedimentary**	The grooves and ridges follow the bedrock lineaments and have an asymmetric cross-profile, flanked by steep slopes to the south, and shallow, bench-like slopes to the north. **Concordant**	Ice flowed eastwards during most of the last, Late Devensian glaciation. Patchy till cover in some grooves. **Regional glaciation**	Initiation of ridge-and-groove topography may be due to pre-glacial differential erosion, and further enhanced through lateral plucking. **Lateral plucking**

Site & References	Length (m)	Width (m)	Relief (m)	Mega-grooves in relation to			Evidence of glaciation	Hypotheses of formation
				Terrain	Bedrock lithology	Bedrock structure		
Lapland, Finland Heikkinen and Tikkanen, (1989)	N/M	5–20 (50)	2–4 (0.5–8)	Area of fairly pronounced relief with relative heights of 100–300 m, south of river Kielajoki. Grooves cut across the fjell summits at 400–600 m a.s.l. and become shallower or disappear over lower ground; extensions of grooves continue in till.	Precambrian bedrock, with various types of gneiss and granite. The grooves are littered with loose blocks removed by postglacial weathering and slope processes.	Cross profile is U-shaped in structureless bedrock and asymmetric in schistose bedrock where grooves parallel strike, uneven long profile, with bedrock knolls and small ridges.	Abundant glacial and glacifluvial deposits (e.g. fluted ridges, Rogen moraines, drumlins and eskers), accounting for shifting direction in ice flow during deglaciation.	Implied glacial erosion for groove formation, especially plucking for the asymmetric grooves. The grooves are inferred to have formed early in the stadial, due to alignment at an angle to that of deglaciation landforms.
				Lowland	**Gneiss and granite**	**Concordant where bedrock structure is obvious**	**Regional glaciation**	**Implies glacial erosion**
Manitoulin Island Ontario Canada Eyles (2012)	>1,000	10s	N/M	Area of intense bedrock erosion with sparse glacial deposits. Bedrock forms: drumlins, mega-grooves and ridges. Numerous striae parallel to long axis of grooves; some post glacial modifications of striae by micro-karst. Mega-grooves continue off-shore.	Best developed on dip slope of the Amabel dolostone, a relatively soft lagoon carbonate rock formation of Palaeozoic age, with bioherms; Mega-grooves flank bedrock ridges containing harder core of fossil remnants at their higher, up-glacier end.	Stacks of Palaeozoic carbonate rocks dipping south-westwards from the periphery of the Canadian Shield. Grooves incise dip planes and are perpendicular to strike. Cross profile: symmetrical, with smooth floors and side-cliffs; long profile: straight or slightly sinuous; elongated and drumlinised ridges.	Multiple continental glaciations with ice flowing to the south-west, from the domed shield area, gradually stripping off the Palaeozoic strata. Saginaw–Huron Ice stream thought to have eroded these forms during the last (Wisconsin) glaciation.	Split flow of sediment-laden basal mini-ice streams around bioherms led to enhanced erosion and groove formation; possible persistence of such landforms through several cycles of glaciation. The author objects to meltwater erosion as the main mechanism of groove formation.
				Lowland	**Limestone with bioherms**	**Perpendicular to strike and parallel to dip**	**Ice streaming**	**Glacial abrasion**
Key Harbour Georgian Bay, Ontario Canada Krabbendam et al. (2016)	10–100s	N/M	1–3	Coastal lowland. Well-developed streamlined bedforms; abundant P-forms and striations; minor post-glacial modification.	Relatively homogeneous granulite gneiss of the Canadian shield.	Fairly structureless with some layering recognisable. U-shaped cross profile. Rounded intervening ridges, many drumlinised.	Integral part of the Huron–Saginaw palaeo-ice stream ladsystem which affected wider area.	Focussed subglacial abrasion along parallel ice flow-lines. Shorter, sinuous channels and other P-forms attributed to meltwater erosion.
				Coastal lowland	**Granulite gneiss**	**Irrespective of structure**	**Ice streaming**	**Glacial abrasion**

Site & References	Length (m)	Width (m)	Relief (m)	Mega-grooves in relation to			Evidence of glaciation	Hypotheses of formation
				Terrain	Bedrock lithology	Bedrock structure		
Interlake, Manitoba, Canada Wardlaw et al. (1969)	1,000–2,000	1–152 (up to a few kms)	12–30	Bedrock partly mantled by till, but the ridge-and-groove topography mirrors bedrock topography. The grooves continue along the lakes' floor. **Lowland**	Silurian and Devonian carbonate rocks: limestone, dolomite and red shale; granitic "islands" north of Lake St. Martin also grooved. Abundant and well-preserved striations indicate little post-glacial chemical weathering. **Carbonate rocks**	In folded strata, the grooves correspond to synclines and the ridges to anticlines. No preferred joint orientation has been found in relation to the grooves. **Concordant to folds**	Grooves aligned north–south parallel to former ice flow direction. Striations parallel to grooves; mega-grooves are cross-cut by smaller grooves. Larger grooves contain smaller grooves and striations. **Regional glaciations**	Glacial origin based on relationship with striae. Authors discuss and reject a number of previously proposed hypotheses of formation. It is suggested that the basins of lakes Winnipeg, Winnipegosis and Manitoba are more mature grooves. **Glacial origin**
Montana, US Witkind (1978)	500–3,000	50–275	10–60	Mega-grooves can be straight or broadly curved, beginning and ending at valley-floor level; some merge lengthwise. Marked contrast between grooved topography in the northern half of the Mission Range and the dendritic pattern, typical of fluvial incision in the southern half. **Local highland**	Slightly metamorphosed fine-grained rocks (argillite, saltire, dolomite and quartzite) belonging to Precambrian Y Belt Supergroup; locally interrupted by thin dykes and diorite sills. Mission Range is a fault block tilted eastwards. **Metamorphic**	Width varies among grooves but remains constant within the same groove; inferred U-shaped cross profile; variable depth. Rock beds dip eastwards and faults disturb rocks in places. Grooves follow neither strike nor dip but reflect some joint control. **Pre-glacial joint control**	Direction of ice flow is uncertain and complex: the Cordilleran glacier likely flowed southwards (straight grooves), the continental glacier flowing northwards and deflected westwards around the spur (curved grooves) **LIS and Cordilleran ice**	Focussed glacial abrasion. Erosion by meltwater under hydrostatic pressure is dismissed, as it fails to explain straightness. Multiple cycles of glacial erosion suggested and groove evolution from an initial stage. **Glacial abrasion**
Pine Island Bay, West Antarctica Lowe and Anderson, (2003)	1,000–5,500	<50–300	20–50	Submerged West Antarctic continental shelf. In places same-magnitude singular bedrock channels cross-cut mega-grooves. Mega-grooves on top of bedrock highs. Size and spacing decreases downstream. **Antarctic continental shelf**	Crystalline bedrock overlain by a 30–450 cm clay deposit with dropstones. **Crystalline**	N/M **N/M**	Onset zone of former ice streaming. Also present are bedrock drumlins and large P-forms, plus a variety of bedrock channels; **Ice streaming**	It is proposed that glacial abrasion formed the mega-grooves where ice was in contact with bedrock, while subglacial meltwater shaped other landforms, indicative of flow separation. **N/M**

2.3.2 Relationships to bedrock geology

Any relationships between mega-grooves and bedrock geology, in terms of lithology and structure, have the potential to explain how the bedrock properties could account for mega-groove formation. Here, published accounts of mega-grooves are reviewed in relation to bedrock geology, and this reveals a clear first-order classification between those that appear to be related to underlying structure and those that do not.

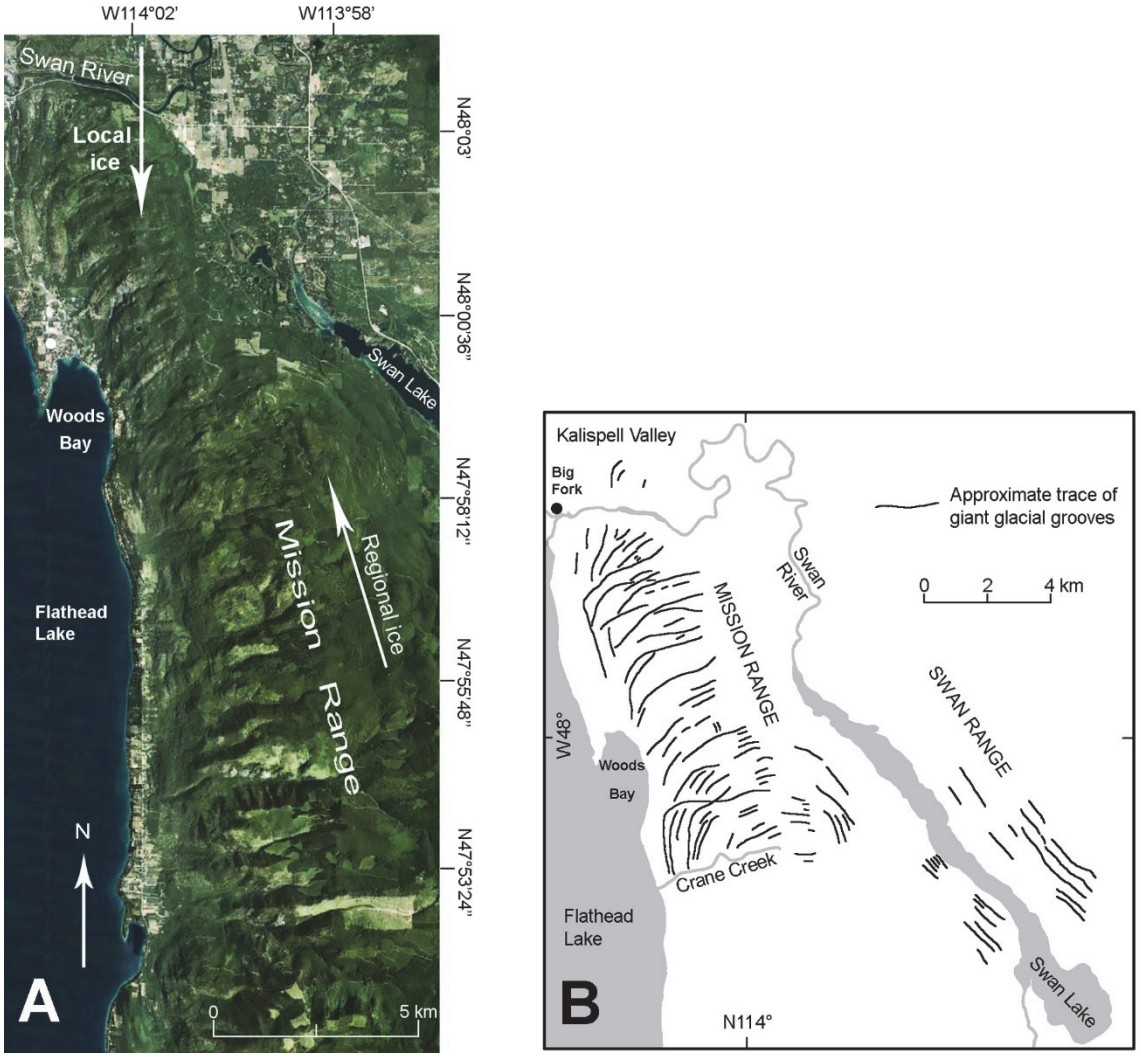

Figure 2.4. A: Crescentic mega-grooves curving round the northern spur of the Mission Range, Montana, US. The grooves immediately south of the Swan River are thought to have been formed by the local, Cordilleran, mountain glacier advancing southwards (Witkind, 1978). Source of satellite image - Google Earth © 2015 Google; #3 on Figure 2.2. **B:** Map modified from Witkind (1978). South of the Crane Creek the overall drainage pattern is described as dendritic, typical of fluvial erosion (Witkind, 1978).

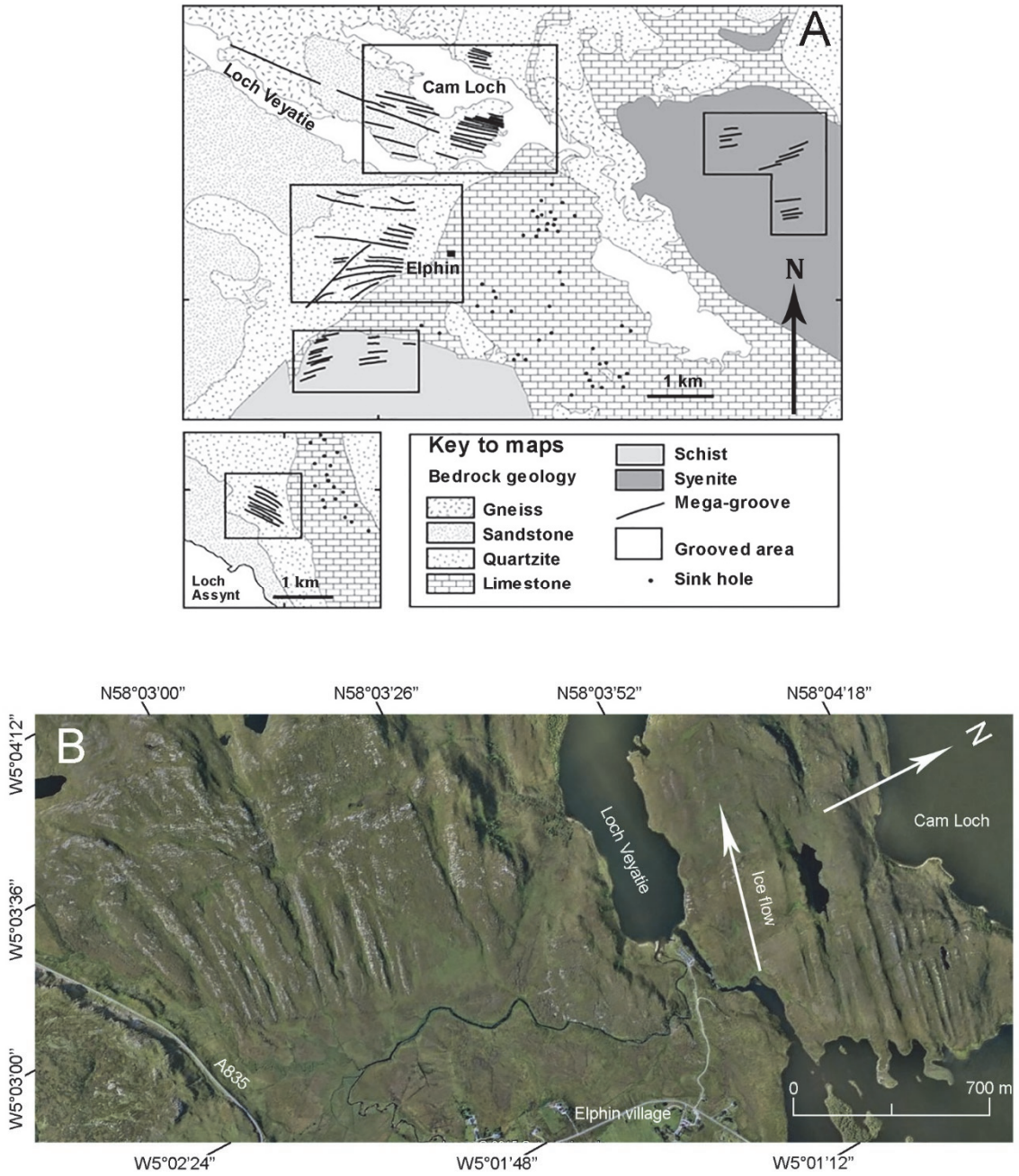

Figure 2.5. Mega-grooves in Assynt, NW Scotland. **A:** mega-grooves in relation to the bedrock lithology showing their preferential occurrence in Cambrian quartzite. Image modified from Bradwell (2005), reproduced with permission from Elsevier. **B:** Satellite image of mega-grooves west and north-west of Elphin village, Assynt, NW Scotland. Note the slightly divergent pattern of the mega-groove south of Loch Veyatie. Source of satellite image - Google Earth © 2015 Google; Image Landsat; image © DigitalGlobe; image © 2015 Getmapping plc; #12 on Figure 2.2.

2.3.2.1 Lithology

Mega-grooves from glaciated terrain have been reported in a variety of lithological settings: carbonate sedimentary rocks (NT Canada – Smith, 1948; Manitoba, Canada – Wardlaw et al., 1969; Georgian Bay, Canada – Eyles, 2012; Novaya Zemlya, Russia – Grosswald and Hughes, 2002), metasedimentary rocks (Ullapool, Scotland – Bradwell et al., 2008; Montana, US –

Witkind, 1978; Ontario, Canada – Krabbendam et al., 2016), conglomerates (East Greenland – Funder, 1978), metamorphic rocks (Assynt, NW Scotland – Bradwell, 2005; West Greenland – Roberts et al., 2010), and also in old and highly metamorphosed shield rocks (Alberta, Canada – Gravenor and Meneley, 1958, Finland – Heikkinen and Tikkanen, 1989; West Antarctica – Lowe and Anderson, 2003; Wellner et al., 2006; Ontario, Canada – Krabbendam et al., 2016). In some places, mega-grooves occur in areas of mixed sedimentary and igneous lithologies (e.g. Isle Royale in Michigan, US – Zumberge, 1955; Tyne Gap, England – Livingstone et al., 2008; Ungava Peninsula, Canada – Krabbendam and Bradwell, 2011). The largest mega-grooves reported occur in the submerged crystalline bedrock of Sulzberger Bay, on the Antarctic continental shelf, where they attain depths of over 100 m and lengths of over 40,000 m (Wellner et al., 2006).

Our review of the literature suggests that the type of bedrock is not a defining factor in mega-groove location, but a direct lithological control over mega-groove formation has been inferred in some cases at a local scale, based on the susceptibility of rocks to erosion. For example, in the Mackenzie River valley, Northwest Territories, Canada, the deepest and widest grooves occur in the Bear Rock formation, a late-Silurian/early-Devonian porous and cavernous brecciated limestone, and in the Devonian reef limestone, whereas harder limestones of roughly the same age have either poorly developed grooves or none (Smith, 1948). On the islands in Georgian Bay, Ontario, the grooves are best-developed in softer, lagoon carbonate facies, in contrast to other carbonate rocks (Figure 2.8A) (Eyles, 2012). In addition, the presence of bioherms, which are hard bedrock mounds more resistant to erosion than the surrounding rock, enabled differential erosion through split flow, as envisaged by Eyles (2012) (Figure 2.8B).

At a number of sites of mixed bedrock lithology, it has been noted that mega-grooves occur exclusively or preferentially on certain rocks. For example, a mega-groove field in East Greenland is strictly confined to areas of Røde Ø Conglomerate (Figure 2.9), which lithologically forms an insular occurrence surrounded by gneissic metamorphic rocks (Funder, 1978). There, the transition between the grooved and non-grooved area is sharp and coincides with the change in lithology, which indicates lithological control over mega-groove formation. Similarly, in Assynt, NW Scotland the grooves are more numerous and better developed in Cambrian quartzite than in adjacent areas to the south and west, underlain by Moine schist and Torridonian sandstone, respectively (Figure 2.5A) (Bradwell, 2005).

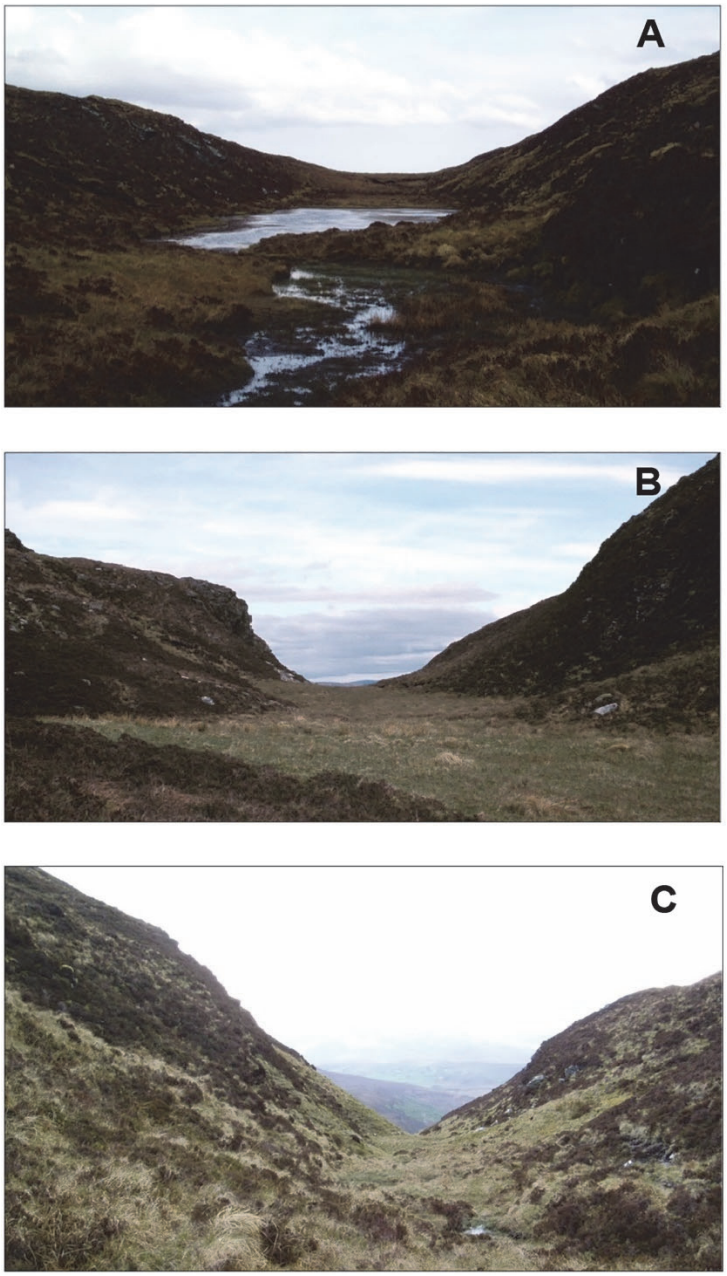

Figure 2.6. Cross profiles of mega-grooves north of Ullapool, Scotland; **A:** parabolic, **B:** U-shaped, **C:** V-shaped. Photographer Maarten Krabbendam (A and C) and Tom Bradwell (B); Images © NERC UK

At the other extreme lie cases in which lithology seems to have been insignificant in mega-groove formation, for example in the Manitoba, Interlake region, Canada, where the granitic bedrock adjacent to the grooved carbonate rocks also bears mega-grooves (Wardlaw et al., 1969). A similar observation has been noted in north-east Alberta, Canada, where mega-grooves cut indiscriminately across lithological boundaries, with hard pegmatite dykes having been 'grooved' to the same depth as adjacent 'softer' metasediments (Gravenor and Meneley, 1958). This shows that erosion rates can be entirely unaffected by the differential resistance of variable and juxtaposed rock types. In west Greenland, on the other hand, the

ridge-and-groove topography is the result of differential erosion between two rock types, whereby the grooves are developed in the metamorphic parent rock and the mafic dyke intrusions stand proud as ridges (Roberts et al., 2010) (Figures 2.3A and 2.10 G).

To summarise, mega-grooves do not occur preferentially on any particular lithology. The degree of influence that bedrock lithology exerts on mega-groove development varies between very high and very low. It is suggested that certain types of rock are more susceptible to glacial erosion than others, but such susceptibility has not been assessed quantitatively.

2.3.2.2 Structure

Studies that analyse the relationship between mega-grooves and bedrock structure often do so in terms of groove alignment relative to the strike and dip, and also to joints and folds. The results fall into two categories: mega-grooves which bear no apparent relationship to any structural lines and cut through structural boundaries (Smith, 1948; Gravenor and Meneley, 1958; Funder, 1978; Bradwell, 2005), and those that follow structural lines (Zumberge, 1955; Bradwell, et al., 2008; Roberts et al., 2010; Krabbendam and Bradwell, 2011; Krabbendam et al., 2016).

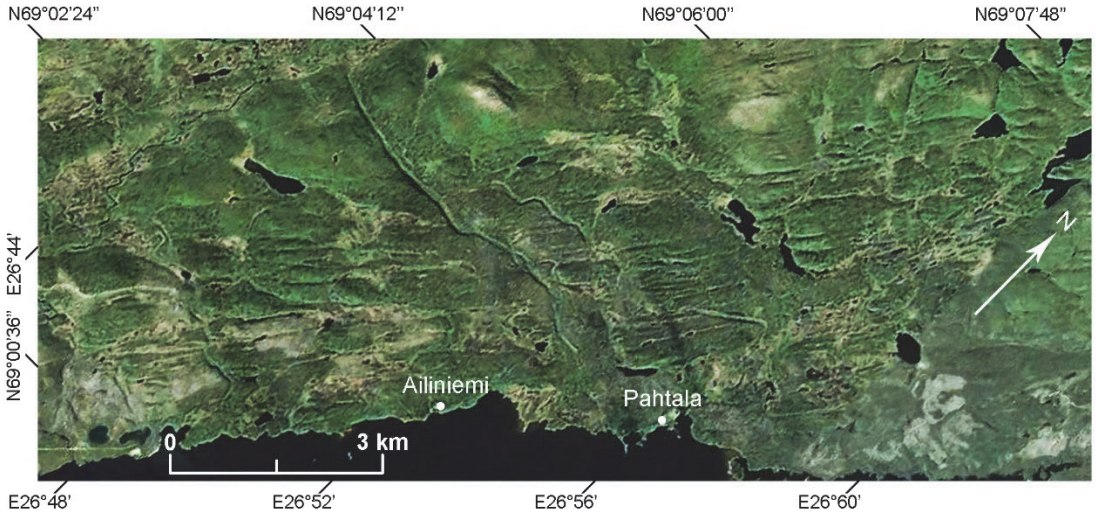

Figure 2.7. Mega-grooves eroded in the Precambrian shield rocks of Finnish Lapland. Note how seemingly discontinuous and quasi-parallel individuals give a general impression of continuity over the landscape (Heikkinen and Tikkanen, 1989). Satellite image from Google Earth © 2015 Google; Image Landsat; © 2015 DigitalGlobe; #13 on Figure 2.2.

Structurally-independent mega-grooves are aligned at an angle to the strike of bedrock strata (Smith, 1948; Gravenor and Meneley, 1958; Funder, 1978; Bradwell, 2005; Eyles, 2012; Krabbendam et al., 2016) and comprise two subgroups: one is formed by mega-grooves in homogenous bedrock (Figure 2.10 A) and the other by mega-grooves which cut through geological boundaries (Figure 2.10 B). The former are confined to single rock formations, with classic examples from Georgian Bay, Ontario, Canada, eroded into Palaeogene carbonate strata (Figure 2.10A) (Eyles, 2012; Krabbendam et al., 2016), and also those in Cambrian quartzite from Elphin, Scotland (Figure 2.5A) (Bradwell, 2005). This subgroup also includes mega-grooves in gneissic rocks, where former structural discontinuities were greatly attenuated through intense metamorphism, thus resulting in a relatively homogenous lithology (Figure 2.11) (Heikkinen and Tikkanen, 1989, Krabbendam et al., 2016). The other subgroup comprises mega-grooves that cross-cut lithological and/or structural boundaries, most typically where two different rock types come into contact, for example west of the Franklin Mountains, Northwest Territories, Canada (Figure 2.1) (Smith, 1948; Krabbendam et al., 2016) and Alberta, Canada (Gravenor and Meneley, 1958). At Elphin, Scotland, the longest groove crosses three consecutive lithologies from east to west, namely Cambrian quartzite, Torridonian sandstone and Lewisian gneiss (Figure 2.5A) (Bradwell, 2005). Structural cross-cutting occurs in lithologically homogenous bedrock at Harefjord, east Greenland, because the dip and strike varies greatly within the grooved area (Funder, 1978) (Figure 2.9).

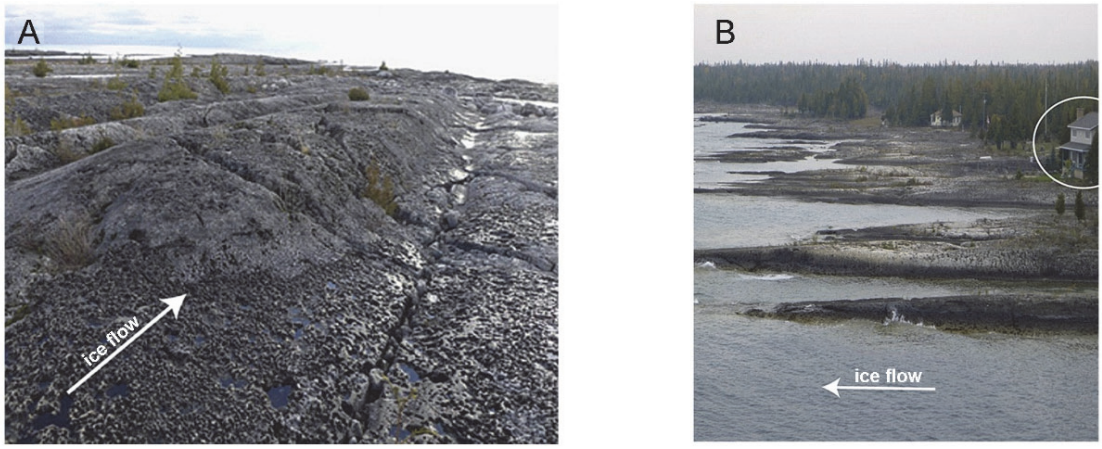

Figure 2.8. A: Bioherm mound more resistant to erosion than the surrounding carbonate bedrock, standing high at the up-glacier end of bedrock ridge, Manitoulin Island, Georgian Bay, Canada. U-shaped Bedrock grooves flank the ridges. **B:** The grooved bedrock topography at the south-eastern end of Manitoulin Island, Georgian Bay, Canada Images (A) and (B) are reprinted from Eyles (2012), with permission from Elsevier; #8 on Figure 2.2.

Among mega-grooves controlled by bedrock structure, they most commonly occur in layered bedrock strata, where the grooves are parallel to strike and palaeo-ice flow direction (Zumberge, 1955; Heikkinen and Tikkanen, 1989; Livingstone et al., 2008; Krabbendam and Bradwell, 2011; Krabbendam et al., 2016). Their cross profile is typically asymmetric, with the steeper side cutting across strata ends, and the shallower side following the dip surface of the bedding plane (Figure 2.10C) (Zumberge, 1955; Heikkinen and Tikkanen, 1989; Krabbendam and Bradwell, 2011). These are suggested to have formed primarily as a result of lateral plucking (Zumberge, 1955; Krabbendam and Bradwell, 2011) (see Section 2.4.1.2). In most cases, this morpho-structural relationship is obvious on remotely-sensed images at sites where the mega-grooves and ridges follow the lineaments of folded or tilted bedrock strata, thus explaining their slightly sinuous aspect (Figure 2.12) (e.g. Zumberge, 1955; Livingstone et al., 2008; Krabbendam and Bradwell, 2011; Krabbendam et al., 2016).

Figure 2.9. Aerial photograph of grooved terrain on the northern shore of Harefjord, inner Scoresby Sund, east Greenland. Note the discordant alignment of mega-grooves to the dip and strike of the bedrock. The thick dashed line (top left) marks the lithological boundary between gneissic bedrock to the west and the Røde Ø conglomerate to the east (Funder, 1978). Note confinement of grooves and ridges to the area of Røde Ø conglomerate. 'A' on the image marks the presence of till flutings, 'B' shows sites with well preserved glacial striations, and the thin dashed/dotted line mark kame terraces (Funder, 1978). Centre of image is at approximately N 70°57'41'' and W 27°56'25''. Image reprinted from Funder (1978), with permission from Danish Geodata Agency. #15 on Figure 2.2.

Structural underpinning in mega-groove location can occur in various other forms. For example, in Manitoba, Canada, in an area of folded carbonate strata, some mega-grooves correspond to synclines, whereas the separating ridges are remnants of anticlines (Figure 2.10D) (Wardlaw et al., 1969). In Assynt, NW Scotland some grooves are reported to occur along fault lines (Figure 2.5A) (Bradwell, 2005), and the mega-grooves in the Mission Range, Montana, US are thought to have formed along pre-existing joints in the bedrock, which directed the action of glacial erosion (Figure 2.10E) (Witkind, 1978).

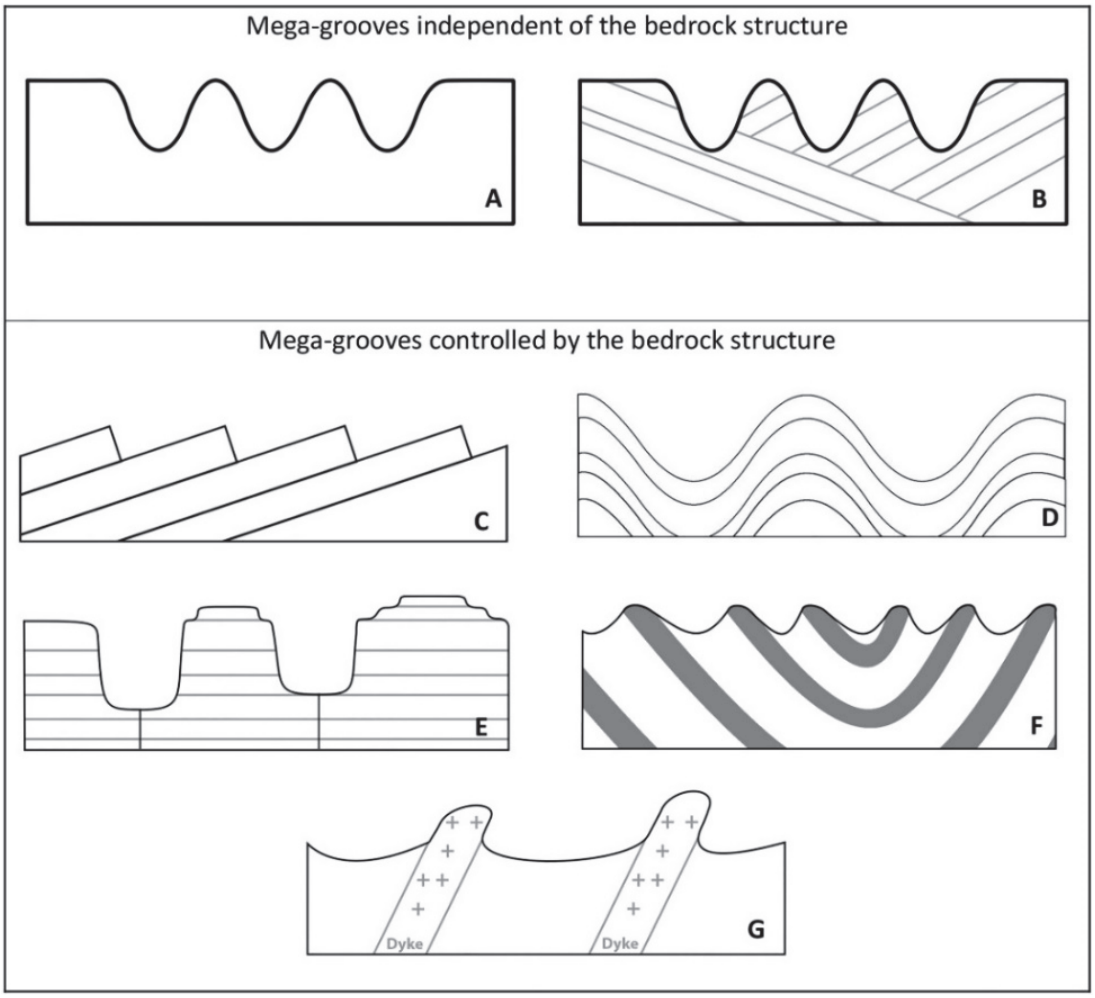

Figure 2.10. Schematic diagrams of different types of bedrock mega-grooves in relation to bedrock structure; ice-flow direction is into the page. A and B illustrate mega-grooves independent of the bedrock structure and C-G illustrate mega-grooves controlled by the bedrock structure. **A:** Mega-grooves in homogeneous rock, unrelated to bedrock structure. Locations: Elphin, Scotland (Bradwell, 2005); NT, Canada – most sites (Smith, 1948); Lapland, Finland – some sites (Heikkinen and Tikkanen, 1989); Kelleys Island (Goldthwait, 1979; Munro-Stasiuk et al, 2005); Ontario, Canada (Eyles, 2012; Krabbendam et al., 2015); **B:** Mega-grooves which cut through lithological and structural lines. No structural control has been reported at these sites. Locations: Elphin, Scotland (Bradwell, 2005); NT, Canada (Smith, 1948); Harefjord, East Greenland (Funder, 1978); Lapland, Finland (Heikkinen and Tikkanen, 1989). **C:** Typical asymmetric profile of mega-grooves which

mould on to the strata ends in areas where ice flow was parallel to the bedrock strike. Locations: Ullapool, Scotland (Bradwell et al., 2008); Northern England (Livingston et al., 2008; Krabbendam and Bradwell, 2011); Isle Royale, Michigan, US (Zumberge, 1955); Cape Smith Belt, Ungava Peninsula, Canada (Krabbendam and Bradwell, 2011); NT, Canada – site E and F (Smith, 1948). **D:** Relatively soft carbonate rocks, where ridges correspond to anticlines and grooves to synclines (Wardlaw et al., 1969). Locations: Interlake Region, Manitoba, Canada (Wardlaw et al., 1969). **E:** Mega-grooves thought to have been formed subglacially along fault lines or joints. Locations: Manitoulin Island and Bruce Peninsula in Georgian Bay, Ontario, Canada (Bell, 1867; Eyles, 2012); Mission Range, Montana, US (Witkind, 1978). **F:** Eroded syncline with mega-grooves corresponding to softer rocks, and ridges to harder rocks. Locations: Kaladar, Ontario, Canada (Krabbendam et al., 2015). **G:** The fluted landscape with grooves and ridges formed through differential erosion throughout prolonged glacial conditions (Roberts et al., 2010). Locations: West Greenland, north-east of Sisimiut (Roberts et al., 2010).

Figure 2.11. Large-scale bedrock grooves and ridges at Key Harbour, Ontario, Canada. The grooves were eroded in highly metamorphosed gneissic bedrock of the Canadian shield and are described in detail by Krabbendam et al. (2015). Source of satellite image - Google Earth © 2016 Google; Image © 2016 DigitalGlobe; #6 on Figure 2.2.

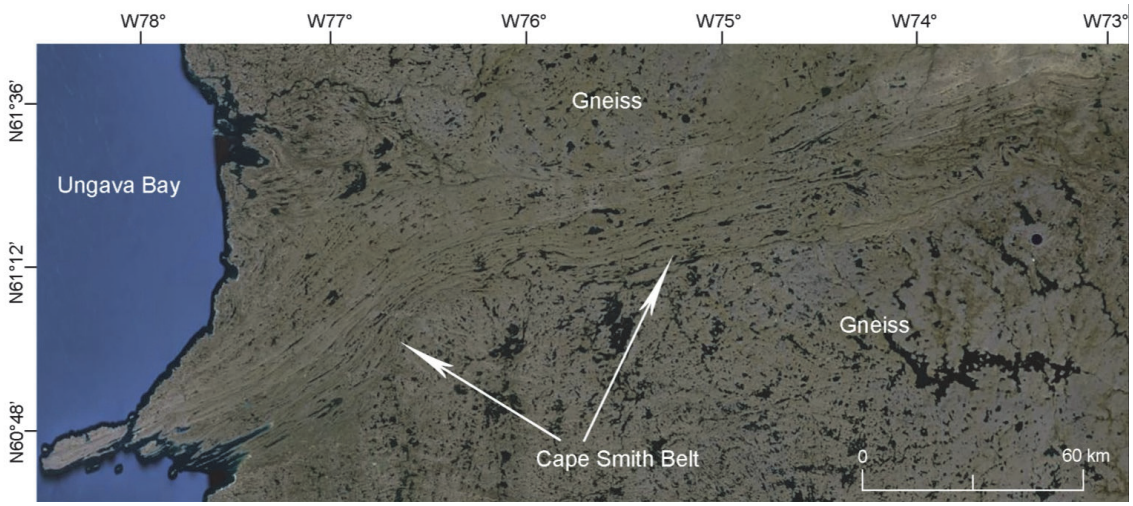

Figure 2.12. Mega-grooves following the SW-NE strike of rock strata in the Cape Smith Belt, Ungava Peninsula, Canada. The area was subjected to multiple glaciations during the Quaternary and the ice flow is inferred to have been on a general west-east direction at least on several occasions (Krabbendam and Bradwell, 2011). Note the contrast between the grooved appearance of the metasedimentary Cape Smith Belt, formed of tilted rock layers of different lithologies, and the cnoc-and-lochan appearance of the gneissic shield, either side of the belt. Source of satellite image Google Earth © 2015 Google; Data SIO, NOAA, U.S. Navy, NGA, GEBCO, Image Landsat; #9 on Figure 2.2.

From the mega-groove sites reported in the literature, we note that around 70% are controlled in some way by the bedrock structure (Table 2.1). Mega-grooves that occur independent of bedrock structure are limited to relatively few clear examples, namely four sites in the Mackenzie River valley, Northwest Territories, Canada (Smith, 1948), Harefjord, East Greenland (Funder, 1978), Assynt, NW Scotland (Bradwell, 2005) and two sites in Ontario, Canada (Eyles, 2012; Krabbendam et al., 2016). At some localities, the relationship with the bedrock structure is less clearly addressed (Gravenor and Meneley, 1958; Wardlaw, et al., 1969; Heikkinen and Tikkanen, 1989) or not even mentioned. This is likely due to difficult direct access to the bedrock in submerged areas (e.g. continental shelves; Lowe and Anderson, 2003; Wellner et al., 2006; Heroy and Anderson, 2005), beneath contemporaneous glaciers (Jezek et al., 2011) or on Mars (Lucchitta, 1982). Sites of structurally-independent mega-grooves may be more numerous than is currently known and lie undiscovered due to lack of visibility in areas highly modified by human activity, buried beneath glacial sediments (see Section 2.5.3), or submerged.

2.4 Mega-groove formation

There is general consensus that mega-grooves are formed beneath ice sheets. This is based on their occurrence in glaciated areas and parallel alignment to ice-flow directions, which can often be inferred from alignment with other subglacial landforms, such as rock drumlins, streamlined ridges (Smith, 1948; Bradwell et al., 2008; Krabbendam et al., 2016; Eyles, 2012), and MSGLs (Lowe and Anderson, 2003). Jezek et al. (2011) found that bedrock mega-grooves beneath the Greenland ice sheet are aligned parallel with the local ice-flow lines, as inferred from measurements at the ice surface (Figures 2.3D and E). It is significant that most sites are found in areas documented to be well within the reconstructed limits of the most recent, Marine Isotope Stage 2 glaciation (Figure 2.2), and which have also been repeatedly glaciated during the Quaternary. Exceptions are sites in Argentina (López-Gamundí and Martínez, 2000), Australia (Perry and Roberts, 1968) and the Sahara (Fairbridge, 1974), where mega-grooves lie well outside the limits of the Quaternary glaciations but within glacial limits attributed to ancient, pre-Quaternary glaciations. At these locations they occur alongside other glacial landforms and are interpreted to have formed at the same time (Perry and Roberts, 1968; Fairbridge, 1974; López-Gamundí and Martínez, 2000).

While there is unanimous agreement that bedrock mega-grooves in glaciated terrain are landforms of subglacial erosion, there is disagreement regarding the agent of erosion. The predominant and traditional idea relates the formation of mega-grooves to direct glacial erosion by ice (Chamberlin, 1888; Carney, 1910; Smith, 1948; Zumberge, 1955; Goldthwait, 1979; Wardlaw, 1969; Boulton, 1974; Witkind, 1978; Lucchitta, 1982; Lowe and Anderson, 2003; Roberts et al., 2010; Krabbendam and Bradwell, 2011; Eyles, 2012; Krabbendam et al., 2016), whereas a more recent and entirely different interpretation claims that erosion of bedrock grooves of various sizes was carried out mainly, if not entirely, by subglacial meltwater (Baker and Milton, 1974; Sharpe and Shaw, 1989; Kor et al., 1991; Tinkler and Stenson, 1992; Shaw, 2002; Bradwell, 2005; Munro-Stasiuk et al., 2005; Munro-Stasiuk et al., 2009).

2.4.1 Glacial erosion

The proponents of a glacial origin for mega-grooves base it on several aspects: i) the morphologic similarity and close association between mega-grooves and smaller grooves, including striations (e.g. Chamberlin, 1888; Carney, 1910; Wardlaw et al., 1969; Boulton,

1974); ii) the parallelism with the direction of ice flow; and iii) the remarkable straightness that mega-grooves maintain over the landscape (Smith, 1948; Eyles, 2012). Smith (1948, p 510) captured the latter aspect when pointing out "the inability of any other known process to produce grooving of the type described, with discordant relations to structural trends and to topographic and drainage features." Some studies mention glacial erosion without suggesting a particular mechanism for groove formation (Gravenor and Meneley, 1958; Funder, 1978; Heikkinen and Tikkanen, 1989; Wardlaw et al., 1969; Jezek et al., 2011). Others refer to positive feedbacks in erosional processes as ice flowed over topographic highs (Heikkinen and Tikkanen, 1989) or in the onset zones of ice streams, where fast ice flow was initiated over the bedrock and enhanced erosion along flow-parallel lines (Bradwell et al., 2008; Krabbendam and Bradwell, 2011; Eyles, 2012; Krabbendam et al., 2016). A few studies discuss scenarios whereby bedrock properties, in conjunction with the glacial conditions, favoured a particular mechanism of glacial erosion (i.e. abrasion *versus* plucking), thus leading to mega-groove initiation (Chamberlin, 1888; Carney, 1910; Smith, 1948; Zumberge, 1955; Witkind, 1978; Roberts et al., 2010; Krabbendam and Bradwell, 2011; Eyles, 2012). Either way, glacial erosion in bedrock takes place through the two essentially distinct mechanisms of abrasion and plucking.

2.4.1.1 Glacial abrasion

Abrasion is performed by rock fragments and debris present at the glacier sole, which incise the bedrock and wear it down as they are being dragged along by the ice (Chamberlin, 1888; Carney 1910; Goldthwait, 1979; Sugden and John, 1976; Boulton, 1974; Iverson, 1990; Rea, 1994). Glacial abrasion is advocated by a number of authors as the principal mechanism for mega-groove formation (e.g. Chamberlin, 1888; Smith, 1948; Boulton, 1974; Goldthwait, 1979; Witkind, 1978; Lowe and Anderson, 2003; Roberts et al., 2010; Eyles, 2012). In studies based on empirical evidence, there is often a strong indication that abrasion was controlled by lithology to a large extent (see Section 3.2.1), either through a generally higher susceptibility of bedrock to erosion, especially the Palaeozoic carbonate rocks around the Canadian shield (Chamberlin, 1888; Carney, 1910; Smith, 1948; Goldthwait, 1979; Eyles, 2012; Eyles and Putkinen, 2014), or through differential erosion in areas of juxtaposed lithologies of different hardness (Roberts et al., 2010). In Georgian Bay, Ontario, Eyles (2012) argued that the prevailing mechanism for groove formation was enhanced abrasion by fast-flowing ice loaded with basal debris, which underwent flow separation around bioherms (see Section 2.3.2.1). This mode of ice flow explains the formation of streamlined bedrock ridges separated by straight and U-shaped grooves (Figure 2.8B). In West

Greenland, the grooves and ridges formed as a result of the two different lithologies experiencing different rates of erosion over time (see Section 2.3.2.1) (Roberts et al., 2010). Goldthwait (1979) inferred abrading glacier ice when he described an erosive agent of enough plasticity to mould itself to the grooves but possessing enough rigidity to grip and hold in place rock particles while moving over considerably long distances. Witkind (1978) proposed glacial abrasion for the formation of the mega-grooves in Montana, US, based on the abundant presence of striated surfaces with highly polished and rounded bedrock knolls.

In order to explain the development of mega-grooves as a series of long, parallel features independent of structural control, some authors advocated the existence of englacial debris banding (Carney, 1910; Smith, 1948; Gravenor and Meneley, 1958; Bradwell et al., 2008). Banding refers to some internal organisation of debris within glacier ice, capable of concentrating the erosive power along parallel lines. This idea was expounded in Carney (1910, p. 644), whereby the grooves on Kelleys Island, Lake Erie, were envisaged as the product of former "localization of tools and a constant supply of them in the basal area of the ice". Bradwell et al. (2008) expressed the same view when referring to the mega-grooves north of Ullapool, Scotland, although a subsequent interpretation of lateral plucking as the main mechanism of groove formation rendered banding unnecessary (Krabbendam and Bradwell, 2011). The regular spacing of mega-grooves prompted Gravenor and Meneley (1958), to suggest that grooving in Alberta, Canada occurred due to some internal organisation of ice flow, rather than to any geological controls, (see Section 2.3.1). Focussed abrasion is proposed by Krabbendam et al., (2016) as the main mechanism of mega-groove formation in a homogenous lithology, based on the likely accumulation of subglacial debris into bedrock troughs, where it enhances the efficiency of glacial erosion and leads to the enlargement of grooves (Figure 2.13A) (see Section 2.5.1.2).

In summary, glacial abrasion has been specifically proposed as the principal mechanism of mega-groove formation in geological settings with uniform lithology, where no structural control is apparent.

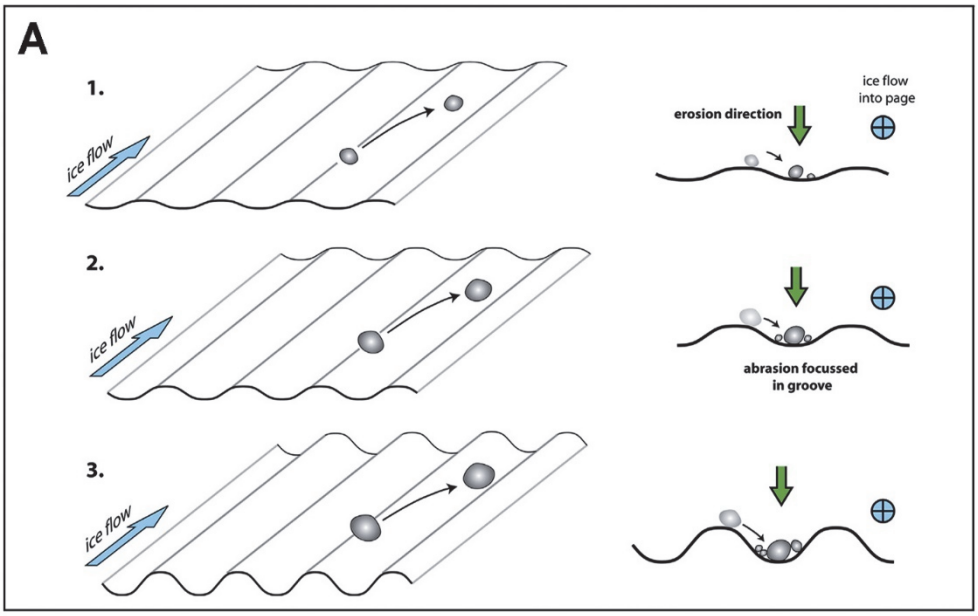
A
1.
ice flow
erosion direction
ice flow
into page
2.
ice flow
abrasion focussed
in groove
3.
ice flow

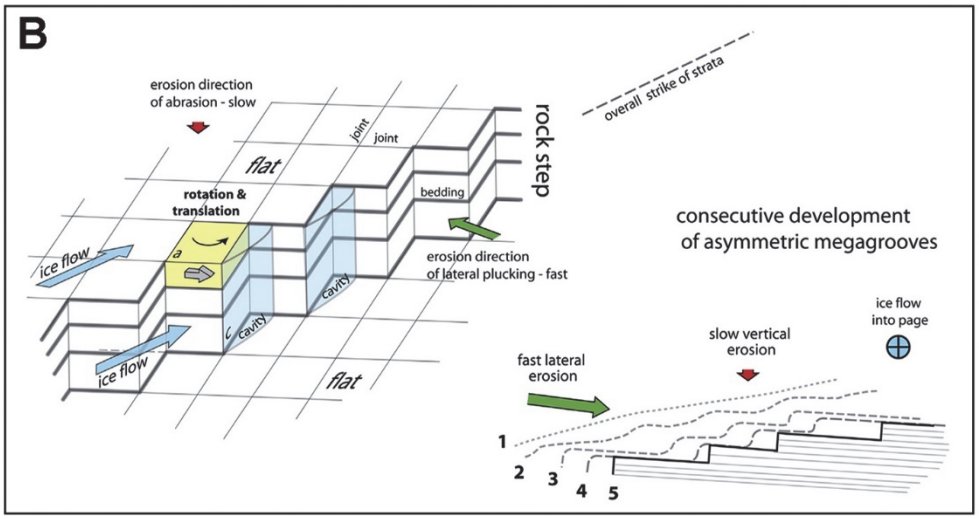
B
erosion direction
of abrasion - slow
flat
joint
joint
rock step
overall strike of strata
rotation &
translation
bedding
ice flow
a
cavity
erosion direction
of lateral plucking - fast
cavity
ice flow
flat
consecutive development
of asymmetric megagrooves
ice flow
into page
slow vertical
erosion
fast lateral
erosion
1
2
3
4
5

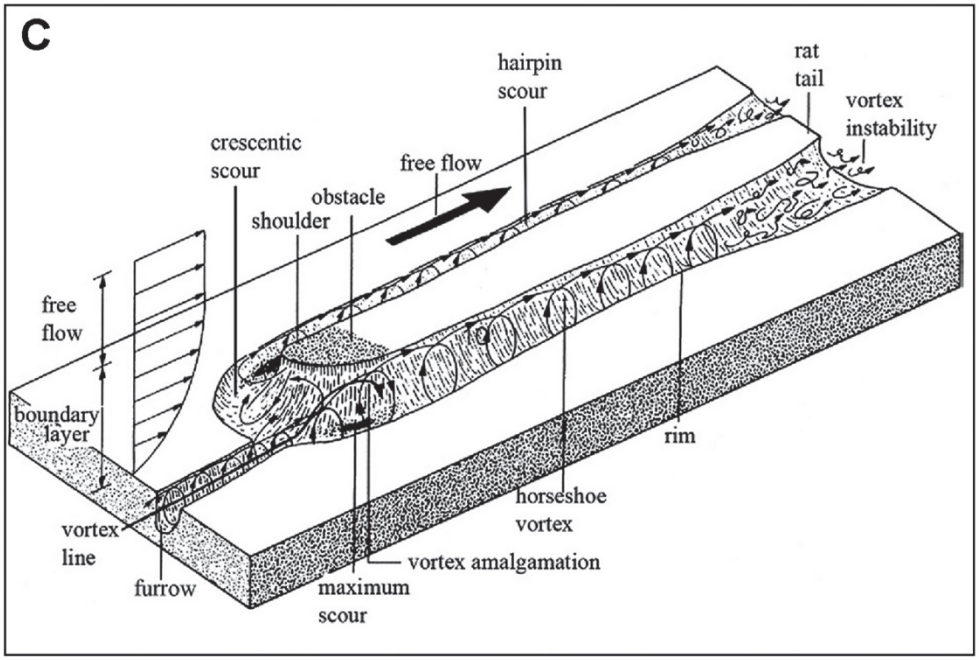
C
hairpin
scour
rat
tail
vortex
instability
crescentic
scour
free flow
obstacle
shoulder
free
flow
boundary
layer
rim
horseshoe
vortex
vortex
line
vortex amalgamation
furrow
maximum
scour

Figure 2.13. Diagram illustrating erosion mechanisms proposed for bedrock groove formation. **A:** Focussed abrasion, whereby subglacial debris tends to accumulate in bedrock troughs and contribute to abrasion, thus enlarging the initial troughs and eventually modifying them into mega-grooves (Boulton, 1974; Krabbendam et al., 2015). **B:** Lateral plucking proposed as the main mechanism of bedrock erosion in tilted layered strata (Zumberge, 1955; Krabbendam et al., 2015). Parts A and B are modified from Krabbendam et al. (2015) with permission from Elsevier. **C:** Meltwater vortex erosion proposed as the main mechanism of groove formation at Kelleys Island (Munro-Stasiuk et al., 2005). Image reproduced from Shaw et al. (2008) with permission from Elsevier.

2.4.1.2 Glacial plucking

Plucking involves the dislocation of rock fragments subglacially, triggered by the development of low-pressure cavities in the lee of bedrock protuberances (Carol, 1947; Gordon, 1991; Rea, 1994). The dislocation takes place along lines of structural weakness, such as joints and bedding planes, thus explaining the presence of a steep vertical surface. Not surprisingly, in areas where glacial plucking was proposed as the main mechanism of groove formation there is a strong relationship between mega-grooves and bedrock structure. Zumberge (1955) argued that glacial plucking, rather than abrasion, was the process that enhanced the pre-glacial stepped topography on Isle Royale, Michigan, USA. He pointed out that the specific geological setting, comprising well-bedded lava flows intercalated within beds of conglomerate and flow breccia, which strike parallel to the palaeo-ice flow, in addition to the presence of vertical hexagonal joints, must have been a favourable setting for plucking. Zumberge (1955) pioneered the idea of lateral plucking, a concept further developed by Krabbendam and Bradwell (2011). The difference between lateral plucking and plucking in its traditional sense is in the attitude of the strata, in that a loosened block has to undergo rotation around its vertical axis in order to be dislocated and removed by the ice, rather than just horizontally translated away from the bedrock (Krabbendam and Bradwell, 2011) (Figure 2.13B).

The resulting mega-grooves typically have an asymmetric cross-profile (Figures 2.10C and 13B) (see Section 2.3.2.2). This mechanism of mega-groove formation has been invoked at several localities, namely Ullapool (Scotland), Ungava Peninsula (Canada) and the Tyne Gap, England (Krabbendam and Bradwell, 2011), the Kaladar area, Canada (Krabbendam et al., 2016), and Isle Royale, Michigan, USA (Zumberge, 1955). With the exception of Ullapool, Scotland, the mega-grooves occur at outcrop scale, and they follow the strike of the bedrock strata, making the structural underpinning obvious even on small-scale satellite images (Figure 2.12). At some sites, the bedrock is of mixed lithology, varying from hard, igneous intrusions to relatively soft sedimentary rocks, like mudstone, which is why a pre-glacial initiation of the current stepped topography was suggested to have formed through

differential subaerial erosion (Zumberge, 1955; Krabbendam and Bradwell, 2011) (see Section 2.5.1.1). The mega-grooves north of Ullapool, Scotland, occur in lithologically-homogeneous and well-jointed metasandstone, and their initiation is attributed to highly effective lateral plucking on the steep, north-facing slopes, where the bedrock has a higher density of joints (Krabbendam and Bradwell, 2011) (see Section 2.3.2.2). According to Smith (1948), the rocks in the Mackenzie basin, Canada, would have been susceptible to different styles of erosion, enabling one mechanism to prevail over the other. Thus, the brecciated and coralline limestone is suggested to have been prone to plucking, while abrasion was probably more effective on the harder Devonian limestone (Smith, 1948). At one locality Smith (1948, p. 509) notes: "an abrupt change in appearance may be observed in passing from one type of rock to another".

In summary, glacial abrasion and plucking have been proposed as the main mechanisms of mega-groove formation, taking into account how the bedrock geology could have influenced each mechanism. Abrasion is often linked to the assumed susceptibility of rocks to this type of erosion, although no geotechnical assessment of what classifies rocks into 'hard' or 'soft' with regards to abrasion has been carried out in the published studies as far as we are aware (see Table 2.1). Plucking is regarded as more effective on jointed bedrock, to allow for rock dislocation. In all cases where lateral plucking is invoked as the main mechanism of groove formation, the grooves occur in layered bedrock strata and ice flow was parallel to the bedrock strike.

2.4.2 Meltwater erosion

Several authors have regarded the large-scale bedrock grooves in Ontario, Canada, as the product of erosion by meltwater released catastrophically in high volumes during subglacial mega-floods (Sharpe and Shaw, 1989; Shaw and Gilbert, 1990; Kor et al., 1991; Tinkler and Stenson, 1992; Shaw, 2002; Munro-Stasiuk et al., 2005; Munro-Stasiuk et al., 2009). The grooves occur in the metamorphic rocks along the south-western margin of the Canadian Shield, as well as in Palaeozoic carbonate bedrock, which borders the shield along its southwestern margin. Most of these bedrock grooves are an order of magnitude smaller than mega-grooves (see Section 2.5.2), including those at Kelleys Island, which is why they have not been included in the mega-groove inventory in Table 2.1. However, we present the discussion regarding a glacifluvial origin for all bedrock grooves that occur in series of straight and parallel individuals because it has implications for the more general problem of bedrock-groove formation (see Section 2.5.2).

The proponents of groove erosion solely by meltwater base their model on the close association of grooves with abundant linear and non-linear P-forms, like cavettos, potholes, schielwannen, mussel gouges and scour marks transverse to former flow direction (Kor et al., 1991; Tinkler and Stenson, 1992; Munro-Stasiuk et al., 2005). Specifically, the scenario proposed for groove-erosion by subglacial meltwater involves fast-moving water vortexes impinging against the bedrock in roughly straight lines and eroding by plucking, abrasion and cavitation within short time frames. The evidence invoked is the presence of sharp-edged rims of some of the grooves through analogy with those commonly occurring in fluvial environments (Kor et al., 1991; Munro-Stasiuk et al., 2005), where they are interpreted as being directly formed through turbulent meltwater flow (Whipple et al., 2011). In addition, elongate bedrock ridges with a higher up-ice end, flanked by grooves, are interpreted as being formed by meltwater erosion through split flow (Figure 2.13C). Indeed, most authors regard P-forms as being formed through a combination of glacial and glacifluvial processes, where meltwater may have played a major morphogenetic role, whether in the form of water-saturated till (Gjessing, 1965; Goldthwait, 1979; Kor et al., 1991) or as a pressurised fluid flowing at the glacier – bedrock interface (Dahl, 1965; Gray, 1981; see also Benn and Evans, 2010 for a brief review). Significantly, Boulton (1974) reported observations that suggest a pure glacial origin for schielwannen formed through split flow of debris-rich ice around bedrock high points, where the normal pressure is higher than that on the surrounding surfaces. These results show that meltwater is not a prerequisite for the formation of P-forms.

Bradwell (2005) interprets the mega-grooves in Assynt, NW Scotland, as Nye channels formed through meltwater erosion in bedrock The grooves are in the form of large parallel furrows eroded in quartzite, aligned east-west, parallel to the flow direction of the former ice sheet. Groove formation through erosion by glacier ice is rejected on the basis that it fails to explain the abrupt termination of some of the grooves in mid-slope. Bradwell (2005) envisaged initial bedrock hydrofracture by meltwater jets released under glaciostatic pressure from the underground cavity system in the carbonate bedrock, present to the east of the grooved area, followed by erosion through known fluvial processes. He attributed other, smaller-scale landforms (e.g. scallops, potholes) to meltwater erosion and assigned the striations in the area to subsequent glacial erosion, during deglaciation or phases of advance.

A glacifluvial origin for mega-grooves has sometimes been dismissed on the basis that it cannot explain the straightness of the grooves (Witkind, 1978; Eyles, 2012). At the same time, the potential effectiveness of subglacial fluids under hydrostatic pressure in eroding sinuous channels is acknowledged by some authors (e.g. Chamberlin, 1888; Witkind, 1978).

In summary, a purely meltwater origin for bedrock mega-grooves, as proposed by a number of authors, refers to large-scale bedrock grooves that occur in close association with P-forms in Ontario, Canada, and also to the mega-grooves in Assynt, NW Scotland. Although there is little consensus, both glacial and glacifluvial proponents often recognise a mixed signature of ice and water erosion in mega-groove morphology, but no quantitative contribution of each agent has yet been established.

2.4.3 Timescales of formation

The chronology of bedrock mega-groove formation is poorly constrained and the few studies that address this aspect (see Table 2.1) base it on landform morphometry and principles of morphostratigraphy, rather than absolute dating techniques. Establishing the chronology of these landforms is important because it offers a time frame for the study of groove formation, with direct implications for establishing rates of erosion and landscape evolution.

Most authors who suggest that mega-grooves formed during multiple glacial cycles advocate glacial erosion for their formation based on the assumption that a long time is required for it to act upon the bedrock in order to produce grooves of such dimensions (Smith, 1948; Gravenor and Meneley, 1958). In West Greenland, Roberts et al. (2010) present a scenario whereby mega-groove formation could have spanned more than one glaciation. The site is close to the present ice sheet margin and comprises bedrock grooves and ridges with uninterrupted continuity over several kilometres (Figure 2.3A); this contrasts with the fragmented ridge topography to the east, which clearly records changes in ice-flow direction. Based on this contrast, Roberts et al. (2010) interpreted the grooves and ridges close to the ice margin as being formed through prolonged glacial erosion as the glacier ice advanced repeatedly over the area in the same direction, likely through multiple glaciations.

In Finnish Lapland, mega-grooves occur alongside, and are aligned sub-parallel to, glacifluvial landforms (i.e. eskers and meltwater channels). The presence of numerous

suites of glacifluvial landforms was interpreted as evidence for frequent changes in ice-flow direction during the latest stages of deglaciation, which led to the conclusion that the mega-grooves were in existence before then, possibly forming earlier in the last glacial cycle (Heikkinen and Tikkanen, 1989).

None of the studies so far provide an absolute age for mega-grooves, but overall results suggest that mega-grooves were in existence before the last glaciation and that they may be much older, possibly spanning more than one glacial cycle.

2.5 Discussion

2.5.1 The influence of geology on bedrock grooving

A clear and useful distinction can be established between geology-controlled *versus* geology-independent mega-grooves (Figure 2.10). Geological control refers here to the bedrock structure that facilitated the formation of some mega-grooves, often in combination with the lithology (Section 2.3.2.2). Where mega-grooves occur in connection to the bedrock structure, their location, morphology and formation are relatively straightforward to explain, whereas structurally-independent mega-grooves remain poorly understood.

2.5.1.1 Mega-grooves controlled by the bedrock structure

Most mega-grooves reported in the literature as being structurally-controlled occur in tilted layered strata and both their location and morphology directly reflect the underlying bedrock structure (see Section 2.3.3.2). The geological underpinning of mega-groove location can also be reflected in the topographic contrast between grooved areas developed in layered rock strata and the non-grooved topography of adjacent areas of a different geology. Classic examples are the groove-bearing belts of meta-sedimentary rocks in Ungava Peninsula, Canada surrounded by areas of Precambrian shield, with a typical non-streamlined, cnoc-and-lochan topography (Figure 2.12) (Krabbendam and Bradwell, 2011; Krabbendam et al., 2016). Morphologically, mega-grooves in layered strata have an asymmetric, stepped cross-profile (Figure 2.10C) (see Section 2.3.2.2), but the tectonic and geological scenarios in which the rocks were formed and tilted can induce variations in the general topography of the grooved terrain, as well as in groove morphology. For example, tilted strata bearing grooves and ridges can be eroded flanks of large synclines and/or subsiding basins, like the Michigan/Lake Superior basin. There, the stepped, groove-and-

ridge topography of Isle Royale (Zumberge, 1955), representing the basin's north-western flank, is matched by similar topography on the opposite side, at Keweenawan Peninsula, on the southern bank of Lake Superior (Halls, 1969). In contrast, at Kaladar, Ontario, the syncline is smaller and the fold tighter. Therefore, the ridges have steeper sides and the lithological symmetry between the two flanks of the syncline is more obvious (Figure 2.10F) (Krabbendam et al., 2016). Large-scale grooves in layered strata occur on the Isle of Mull, Scotland, where the grooves represent the result of differential erosion between stacked lava flows (Figure 2.14) of Palaeogene age (Williamson and Bell, 2012). At this location the grooves formed due to mixed lithological and structural causes. In principle, mega-grooves can occur in any form of layered strata, which may have undergone folding, tilting, overturning, faulting, or other tectonic movement throughout their geological history, before groove formation. Less commonly, mega-grooves have been reported to occur along other lines of structural 'weakness', like faults (Bradwell, 2005) and joints (Witkind, 1978; Eyles, 2012). A well-jointed rock is generally more susceptible to glacial plucking, than a more massive, yet mechanically weaker rock. This is because joints are prone to enhanced weathering due to easier access of water, which contributes to reducing the rock's overall resistance to mechanical stresses.

Figure 2.14. Stacked lava layers in west Mull, Scotland where differential erosion has rendered the topography a terraced aspect. The rocks are of Palaeogene age and a common occurrence on the island (Williamson and Bell, 2012). Note the similarity between the hill profile and the schematic diagram of mega-groves in layered strata from Figure 2.10C. The talus at the slope base is likely post-glacial.

With respect to groove formation, we hypothesise that this is primarily the result of entrainment and transport of pre-existing loosened bedrock, whether in the form of loose debris or Tertiary regolith. A weathering mantle with abundant loose debris would have developed during the Tertiary, and would have been readily available for entraining into, and removal by, glacier ice and meltwater at the onset of early Quaternary glaciations. The mere removal of pre-glacial debris by any denudation agent may have sufficed to uncover a groove-and-ridge topography already present on the underlying bedrock structure, as also suggested by Zumberge (1955) (Figure 2.10 C–G). Indeed, glacial abrasion may not need to be invoked as a prerequisite for groove initiation. Subsequent processes of subglacial erosion almost certainly enhanced the grooves (see also Section 2.5.1.2). Of these, lateral plucking is likely to have been the most efficient (see Section 2.4.1.2), but the role of abrasion could have been more significant than currently thought, because the plucked rock fragments could have further acted as abrasion tools.

In summary, structurally-controlled mega-grooves are likely to be encountered in any geological terrain where glaciers flowed parallel to structural lines, most commonly in tilted, layered rocks. The location of the mega-grooves would have been dictated by the bedrock structure, and their morphology closely controlled by it. The role of glacial erosion was primarily to reveal a pre-existing grooved terrain already partially developed on the backbone of the bedrock geology, rather than to initiate the grooves. The grooves were then subjected to further modification by various erosion mechanisms in subaerial and subglacial environments, most likely through multiple glacial/interglacial cycles.

2.5.1.2 Mega-grooves independent of the bedrock structure

Structurally-independent mega-grooves are unanimously interpreted as landforms of erosion in bedrock, due to their occurrence below the general land surface, which forms a series of accordant surfaces or intervening ridges (Figure 2.10) (Smith, 1948; Heikkinen and Tikkanen, 1989; Bradwell, 2005; Eyles, 2012; see also Section 2.4 and Table 2.1). The full formation of structurally-independent mega-grooves remains difficult to explain. Various mechanisms have been suggested, with a focus on either glacial or glacifluvial erosion (see Sections 2.4.1 and 2.4.2). It is possible that some structural control was inherent in the bedrock layer where the mega-grooves were initiated, which has since then been removed by erosion, while the grooves continued to deepen into the underlying rocks. This would be difficult to prove, but a thorough investigation of the geological history in grooved terrain may at least offer some clues regarding the feasibility of such a scenario.

In the absence of any indication of geological control, we share the view of others (Chamberlin, 1888; Carney, 1910; Smith, 1948; Witkind, 1978; Bradwell et al., 2008; Eyles, 2012) that the main process in the initiation of mega-grooves, was that of abrasion by glacier ice, given their straightness over the landscape and typical U-shaped cross-profile (Figures 2.6A, 2.8A and B, 2.10 A and B) (see Section 2.4.1.1). It is unlikely that straight and parallel grooves of this size could have been initiated in bedrock by fast-flowing water vortexes as implied by the proponents of catastrophic subglacial mega-floods (Sharpe and Shaw, 1989; Shaw and Gilbert, 1990; Kor et al., 1991; Tinkler and Stenson, 1992; Shaw, 2002; Munro-Stasiuk et al., 2009; see also Section 2.4.2). While water vortexes have the ability to erode channels in bedrock (Whipple et al., 2011), they would have had to advance in straight and parallel lines, over long distances and wide areas, in order to erode parallel grooves. The suggested formation of the mega-grooves in Assynt, NW Scotland, as Nye channels may explain certain features (see Section 2.4.2), but it remains difficult to reconcile with the parallelism of the individual grooves. Although Nye channels can form assemblages covering wide areas and could have formed as a result of migration of subglacial drainage routes, their overall pattern is typically dendritic or anastomosing (Sharp et al. 1989; Sugden et al. 1991; Booth and Hallet 1993; Ó Cofaigh 1996). We consider that meltwater erosion more likely modified bedrock grooves *after* they were already initiated, either subglacially or subaerially during deglaciation. Ultimately, the older the landforms, the more numerous the agents and processes that are likely to have modified them (e.g. glacial, glacifluvial and fluvial erosion, chemical dissolution, subaerial weathering, paedogenesis and slope processes during interglacials). It is therefore useful to treat mega-groove formation in two stages, firstly *initiation* followed by *modification*, in order to understand the potential action of different morphogenetic agents and processes (see Section 2.5.2).

A key aspect is that once a bedrock groove is well-enough established (see Section 2.5.2), it is more likely to become self-perpetuating rather than prone to obliteration through subsequent erosion due to positive feedback mechanisms that reinforce ice flow pathways and enhance erosion during successive glaciations. Small-scale bedrock perturbations have been shown to direct basal flow lines at the ice–bedrock interface, regardless of the regional ice-flow direction (Boulton 1974, 1979; Rea et al. 2000; Roberts et al., 2010). Basal sliding along the groove pathway could be enhanced by increased meltwater production, due to increased availability of heat. On an uneven bedrock surface, geothermal heat flow lines are perpendicular to the surface, assuming the thermal conductivity is uniform and isotropic, as would be the case in homogeneous bedrock. Thus, geothermal heat flow lines converge towards the centre of bedrock depressions, (Nobles and Weertman, 1971; Drewry, 1986),

and a higher amount of heat is delivered into the groove relative to the surrounding area (Figure 2.15). This heat is directly proportional to the depth of the groove, so more heat is produced as the groove grows in size. Enhanced basal sliding, combined with the potential that grooves have for concentrating loose, subglacial rock debris released through basal melting (Boulton, 1974; Roberts et al., 2010; Krabbendam et al., 2016) could enhance abrasion and, therefore, landform development.

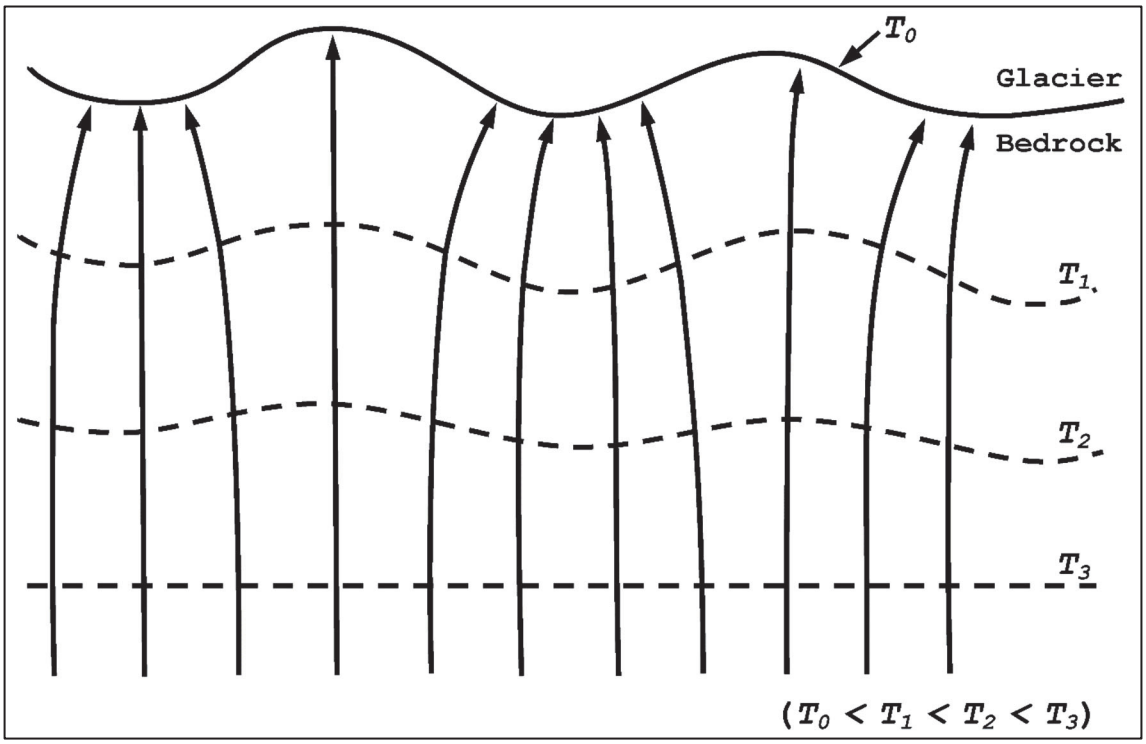

Figure 2.15. Diagram showing the paths of geothermal heat flow intercepting the isotherms (T_0 – T_3) at right angles, thus leading to more heat being delivered into the bedrock depressions than the topographic highs. Image modified from Nobles and Weertman (1972).

Interestingly, no cross-cutting has been reported between mega-grooves, otherwise frequently reported to occur between smaller bedrock grooves (Chamberlin, 1888; Iverson, 1990; Rea, 1994; Rea et al. 2000), which suggests that once a bedrock groove is well enough established, it may be a persistent landform even under ice sheets with shifting flow directions. This idea is strengthened by the presence of striations and other small grooves superimposed on the mega-grooves at an angle (Funder, 1978; Wardlaw et al., 1969; Witkind, 1978), which testify to changing ice-flow directions while mega-grooves were already in existence. Hence, 'average' glacial conditions for mega-groove formation appear to have persisted for much longer than the conditions under which smaller grooves (see Table 2.2) were formed. Similarly, the long axes of roches moutonnées are often a product of prolonged, average basal flow conditions, whereas their striation sets and plucked faces

can display early- and late-stage variability in flow direction in response to ice sheet build-up and decay (Roberts and Long 2005; Lane et al., 2014). This fits in with the notion that basal flow direction during 'average' glacial conditions is predominantly the same during each glacial cycle, and points to long-term evolution of mega-grooves.

In summary, structurally-independent mega-grooves were most likely initiated through glacial abrasion and subsequently modified by geomorphic agents in addition to, or other than, glacier ice. Once initiated, a mega-groove is prone to self perpetuation due to feedbacks operating between the bedrock topography and enhanced basal-ice flow lines, which makes it a persistent landform even beneath ice sheets with shifting flow directions.

2.5.2 A bedrock-groove landform size continuum?

Recent studies have identified a morphology and size continuum of glacial landforms in unconsolidated sediment, confirmed through quantitative analyses (Ely et al., 2016). Fewer studies explore this topic for bedrock grooves (e.g. Chamberlin, 1888; Boulton, 1974). However, the available observations would appear to indicate that discrete grooves with similar morphology, namely U-shaped, straight and elongated grooves, occur at different scales (Chamberlin, 1888; Boulton, 1974; Rea, 1994). Furthermore, Eyles and Putkinen (2014, p 131) recently stated that "morphologically, the bedrock mega-grooves are essentially giant striations". This hints at the possible existence of a bedrock-groove size continuum, which would need to be confirmed before being used as a framework for further exploration of process – form relationships. First, it is important to establish the evidence for the existence of grooves of different sizes, what scale range these sizes span, and the place of mega-grooves in a hierarchy of landforms. As a preliminary exploration, basic morphometric values for bedrock grooves were simply extracted from published studies and are presented in Table 2.2, together with a general description of related grooves in bedrock. It is apparent that studies of bedrock grooves tend to focus on certain size ranges and also that grooves from each size range have specific characteristics. Thus there appear to be four classes of grooves, here referred to with the relevant prefix of micro-/meso-/macro-/mega- (Figure 2.16 and Table 2.2).

Table 2.2. Classification of bedrock grooves according to size, based on data from published studies.

Size range	Length (m)	Width (m)	Depth (m)	Typical occurrence	Hypotheses of formation and references
Micro-grooves (striae) (Figures 2.16 A&B)	0.01–1 Up to 2–3	<0.01	<0.01	Series of straight and parallel individuals on stoss side of other glacial bedforms, and also on flat bedrock.	**Glacial abrasion** :(laboratory and field simulation): Boulton, 1974; Sugden and John, 1976; Iverson, 1990 and 1991; Rea, 1994.
Meso-grooves (medium-scale grooves) (Figures 2.16 C&D)	1–10/20	0.01–1	0.01–1	Within fields of P-forms, occasionally straight, but more often sinuous; sometimes occur in series of parallel individuals.	**Glacial abrasion:** Boulton, 1974; Sugden and John, 1976. **Abrasion by soaked till:** Gjessing, 1965; Gray, 1981. **Meltwater erosion:** Dahl, 1965; Sharpe and Shaw, 1989.
Macro-grooves (furrows) (Figure 2.16E)	10–100s	~10	<10	Straight in planform, but sinuous in detail. Smaller grooves and P-forms abundantly present inside macro-grooves.	**Glacial abrasion:** Chamberlin, 1888, Carney, 2010, Ver Steeg and Yunck, 1935, Goldthwait, 1979. **Meltwater erosion:** Kor et al., 1991; Tinkler and Stenson, 1992; Tinkler, 1993; Munro-Stasiuk et al., 2005.
Mega-grooves (giant grooves) (Figure 2.16F)	100s–over 1000	20–50	>10	Series of straight and parallel individuals and not in conjunction with P-forms, but often cross-cut by striae.	**Glacial erosion:** Smith, 1948; Gravenor and Meneley, 1958; Wardlaw et al., 1969; Witkind, 1978; Lowe and Anderson, 2003; Bradwell, et al., 2008; Roberts et al., 2010; Krabbendam and Bradwell, 2011; Eyles, 2012.

The smallest features are micro-grooves (or striations), which occur as elongated and shallow troughs in bedrock, in series of parallel individuals (Figure 2.16A), typically parallel to ice flow. Cross-cutting is common (Figure 2.16B), attesting to changes in ice- flow direction and they are generally interpreted in the literature as the product of glacial abrasion (e.g. Chamberlin, 1888; Iverson, 1990; Rea, 1994). The grooves of intermediate sizes typically occur in association with P-forms, and a closer analysis of this association reveals that the meso-grooves occur *among* P-forms of similar magnitude (Figures 2.16C-D) (Dahl, 1965; Gjessing, 1965; Gray, 1981), whereas macro-grooves have P-forms present *inside* them (Figure 2.16E). Various scenarios have been proposed to explain the formation of meso- and macro-grooves, ranging from fluvial (Dahl, 1965; Sharpe and Shaw, 1989; Kor et al., 1991) to glacial (Boulton, 1974), and sometimes a combination of the two (Gjessing, 1965; Gray, 1981). Most authors recognise a strong fluvial signal in their formation, based on their slightly sinuous shape in planform, as well as associations with other P-forms The latter are thought to have required turbulent flow, which cannot be attained by ice alone. Mega-grooves, in contrast, have mostly been associated with glacial abrasion (see Section 2.4.1.1). A similar classification can be inferred from that presented by Sugden and John (1976), where streamlined depressions in bedrock are shown to range from striations to grooves, with P-forms present in the mid-range (Figure 2.17).

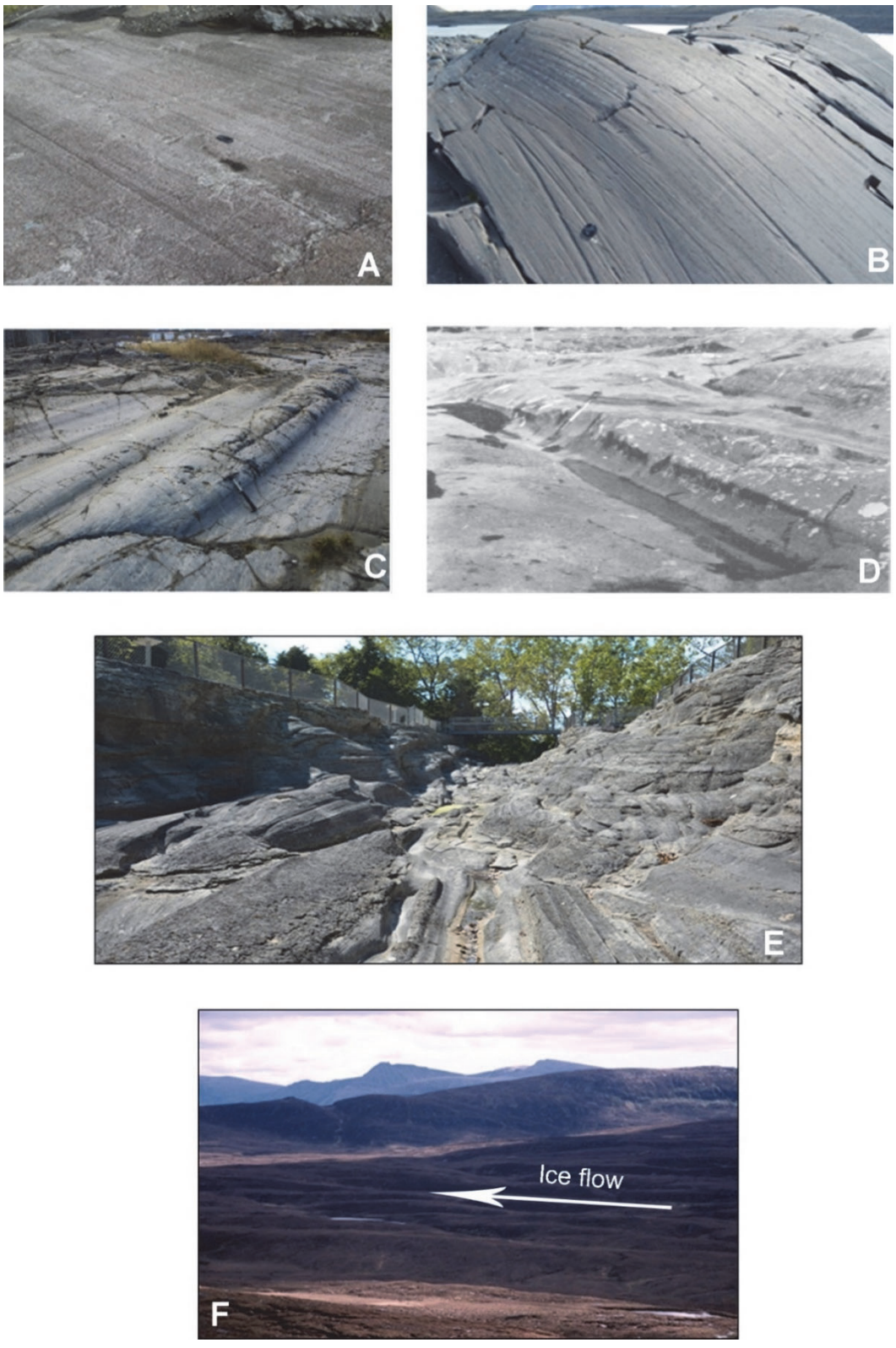

Figure 2.16. Size ranges of bedrock grooves ranging from striations through to mega-grooves. **A:** striated gabbro on the Isle of Skye, Scotland. **B:** striated stoss side of a roche moutonée in Iceland, photo DJA Evans. **C:** meso-grooves in Sudbury, Ontario; image reproduced from Eyles (2006) with permission from Elsevier. **D:** meso-grooves on the Isle of Mull, Scotland; image was reproduced from Gray (1981), image © SJG. **E:** macro-groove in Palaeozoic limestone at Kelleys Island, Michigan, US; image © Bianca Kallenberg. **F:** mega-grooves in Torridonian sandstone, Northwest Highlands, Scotland; author of base image Tom Bradwell, image © BGS – NERC UK, #12 on Figure 2.2.

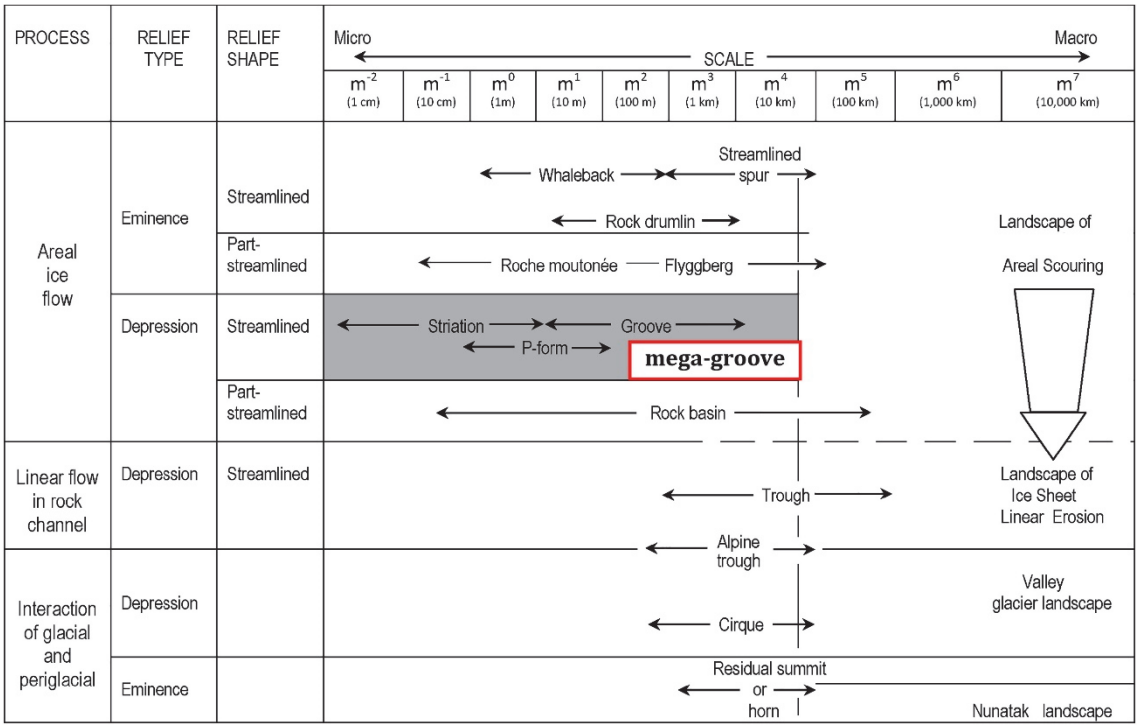

Figure 2.17. Table comprising landforms of glacial erosion, re-drawn from Sugden and John (1976); annotation 'mega-groove' corresponds to bedrock grooves of 100s – 1,000s meters in length. The bedrock grooves highlighted grey span the same size range as those compiled in Table 2.2 from the published literature. Please note the discrepancy in the meaning of 'macro' between Sugden and John (1976), at the top of the table, and this study (see Table 2.2), where macro-grooves refer to grooves in the length-range of 10s – 100s meters. Sugden and John (1976) also mention the prevailing glacial signal in the formation of striations and large-scale grooves, as opposed to meltwater erosion in P-forms.

Table 2.2 is a useful framework to further explore the potential for a bedrock-groove size continuum. It clearly shows that bedrock grooves from glaciated terrain range from the finest and shortest striations to kilometres-long mega-grooves, and that grooves at all scales occur in series of parallel individuals. Further work is now required to test whether the size and shape grade gradually from one type to another and whether length: width ratios exhibit consistency (cf. Ely et al, 2016). If features show a single population of grooves of different shapes and size, which merge together smoothly, this would hint at an overarching formative mechanism, as has recently been reported for ribbed moraines, drumlins and MSGLs (Ely et al., 2016). Alternatively, it may be that there are clear breaks between these different types, which would indicate separate classes and potentially different scenarios of formation. Either way, it is unlikely that mega-grooves have "grown" from millimetre-deep striations, because striations are not deep enough to 'trap' debris and focus erosion. It is equally unlikely, if not impossible under known subglacial conditions, that mega-grooves

could have achieved their current size as a result of bedrock abrasion caused by one large boulder in traction. Most likely, mega-grooves were initiated as small bedrock grooves large enough to sustain their self-perpetuation. In other words, there may be a bedrock - groove size continuum where one end-member is a mega-groove and the other is a groove larger than a striation. The question is then what is the minimum size required of a bedrock groove to trigger the positive feedback mechanisms which lead to self-perpetuation (see Section 2.5.1.2), and is there a critical depth/width/length of a bedrock groove that enables or limits further landform growth? These questions could be approached through modelling experiments of subglacial bedrock erosion at a small scale.

Another fundamental question for understanding the origin of mega-grooves is: how did the initial grooves form? Could a single large boulder in basal traction erode the bedrock efficiently enough as to initiate a mega-groove? So far, most estimates of subglacial bedrock abrasion assume abrading clasts much smaller than boulders (Boulton, 1974; Drewry, 1986; Iverson et al., 2003). A mathematical assessment of bedrock abrasion by large boulders could be used in the first instance to generate a range of scenarios for the initiation of mega-grooves. Such scenarios would imply a ubiquitous presence of large boulders across the landscape at the time of mega-groove initiation, in order to explain typical landform occurrence in series of individuals. The Tertiary weathering mantle could provide an explanation for the availability of boulders. Significantly, on sandstone bedrock areas unaffected by Quaternary glaciations and subjected to millions of years of weathering in a warm climate, large corestone boulders are widely present in the landscape (see Ollier 1984, 1991; Taylor and Eggleton, 2001 for reviews). Ultimately, a reappraisal of the pre-Quaternary geological history combined with fieldwork at key locations (see also Section 2.5.4) could help to assess the potential role of the Tertiary regolith in mega-groove formation. Any mathematical analysis of groove initiation needs to account for specific lithological characteristics responsible for the susceptibility of rocks to abrasion, as well as the relative hardness of the bedrock and the abrading clasts. Laboratory experiments show that high-porosity rocks are more prone to grooving, as whole grains become dislocated due to intergranular cement failure (Lee and Rutter, 2004). Smith's (1948) observation that the deepest mega-grooves occur in highly porous limestone and the most shallow in well-consolidated limestone (see Section 2.3.2.1) could form the starting point for a quantitative exploration of mega-groove initiation through glacial abrasion.

It is intuitive to envisage how, once initiated, a mega-groove is further eroded by different mechanisms and agents (see Section 2.5.1.2). If mechanisms other than glacial abrasion and

plucking are responsible for modifying a groove into a mega-groove, then what are the boundary conditions required by a particular mechanism of erosion to act, and what are the thresholds beyond which others take over? It is apparent from the data presented in Table 2.2 that the geomorphic signature of glacifluvial erosion seems more obvious in grooves in the middle size ranges, (i.e. meso- and macro-grooves), whereas the end members of the range (i.e. striations and mega-grooves) are regarded by most authors as bearing predominantly the signature of erosion by glacial ice (*cf* Sugden and John, 1976). If mega-grooves do lie in a bedrock groove size continuum, then it may be possible to understand their evolution by analysing smaller grooves at different stages, prior to becoming mega-grooves.

In summary, the occurrence of bedrock grooves with seemingly similar shape, spanning a vast range of scales from micro- to mega-grooves, hints at the existence of a landform size continuum, but further morphometric analyses are needed to test this. The ubiquitous presence of large boulders across the landscape prior to glaciation could explain mega-groove initiation through abrasion, and Tertiary weathering mantles are one option for the supply of such tools. The initial grooves were likely further modified by various agents, both glacial and non-glacial to gain their current dimensions. If confirmed, the bedrock-groove landform size continuum would offer a useful framework for exploring process–form relationships, which could help understand groove evolution within a size spectrum.

2.5.3 Glaciological conditions

There are a number of cases where mega-grooves have been mapped as part of larger suites of landforms indicative of ice streaming, based on their spatial association with characteristic features, such as MSGLs and rock drumlins (Lowe and Anderson, 2003; Eyles, 2012; Bradwell and Stoker, 2015). It has been argued that many marine-terminating palaeo-ice stream landsystems comprise large areas of streamlined features, including bedrock mega-grooves. Typically bedrock mega-grooves merge down-stream into long trains of MSGLs that extend to the edge of the continental shelf, where they typically terminate at a large fan of stratified deposits (e.g. Bradwell and Stoker, 2015; Stokes, 2018). General observations regarding the position of mega-grooves in such landsystems, as well as their association with other streamlined bedrock forms that exhibit a convergent pattern, have led to the interpretation that mega-grooves occur in the onset zones of ice streams (Lowe and Anderson, 2003; Wellner et al., 2006; Bradwell et al., 2008; Eyles, 2012; Bradwell and Stoker, 2015; Krabbendam et al., 2016), and are the result of enhanced and focused erosion

at those locations (Bradwell et al., 2008; Krabbendam and Bradwell, 2011; Eyles, 2012; Krabbendam et al., 2016). However, the association between mega-grooves and ice streaming is not obvious at all sites. Mega-grooves at several locations were not initially linked to any particular glaciological conditions or ice-stream landsystem (Smith, 1948; Gravenor and Meneley, 1958; Wardlaw et al., 1969; Funder, 1978; Witkind, 1978; Heikkinen and Tikkanen, 1989). This might be because these studies pre-date the full-recognition of ice streams in the palaeo-record (Stokes and Clark, 2001) which have since then been mapped in much greater detail (e.g. Northwest Territories, Canada – Smith, 1948, Margold et al., 2015a, b). Therefore, there is now scope for a re-appraisal of the glaciological conditions at these sites. However, other mega-groove sites are still not associated with any glacial landsystems (Funder, 1978; Witkind, 1978; Heikkinen and Tikkanen, 1989) or have been shown to occur in ice sheet areas of 'normal' flow conditions (Roberts et al., 2010), so it is difficult to identify any links between groove formation and specific ice-flow velocity at these locations. The mega-grooves in Assynt, NW Scotland, have a divergent pattern in the direction of the palaeo-ice flow (Figure 2.5B), contrary to the typically convergent associated with ice-streaming onset (Stokes and Clark, 1999). This points to the initiation of mega-grooves being unrelated to ice stream onset even though they are located in an area of fast-flow onset (Stoker and Bradwell, 2005). The study of Roberts et al. (2010) in West Greenland shows that it is primarily the differential erosion of contrasting lithologies through prolonged glaciation, rather than fast ice flow, which initiated and maintained the grooved terrain (see Sections 2.4.3 and 2.5.1.2). Thus, overall, the literature points to no specific glaciological conditions (e.g. ice flow velocity, thickness) as a requirement for mega-groove formation. As yet, bedrock mega-grooves cannot be unequivocally associated with fast-ice flow, unlike MSGLs which are now generally regarded as being formed under fast ice-flow conditions (Stokes and Clark, 2002; King et al., 2009).

A further complication with respect to bedrock mega-grooves and ice streams is the existence of mega-lineated areas within palaeo-ice stream landsystems, covered by a discontinuous cover of till, where there is some disagreement regarding the type of substrate in which the grooving occurs. Thus, some areas in Alberta, Canada, have been interpreted as bedrock mega-grooves (Krabbendam et al., 2016), while the Canadian Geological Survey mapped the same lineations as till flutings, or MSGLs, because the till is thicker than 5 m (Paulen and Plouffe, 2009; Fenton et al., 2013; Geological Survey of Canada, 2014). Sometimes the transition in substrate from bedrock to unconsolidated sediment can be difficult to establish. Empirical evidence for flutings composed of mixed bedrock and till (Gravenor and Meneley, 1958; Atkinson et al., 2014) show that bedrock can be present at,

or close to, the surface within MSGLs. Indeed, it is possible that MSGLs overlie fluted bedrock, especially where the till cover is relatively thin, which implies that the underlying bedrock is grooved. This could mean that areas of grooved bedrock are much more extensive than currently documented. Another possibility is that the stoss end of MSGLs could contain bedrock bumps similar to crag-and-tails, with 'tails' buried under till. On the one hand, the bedrock – till interplay in fluted terrain makes it challenging to establish the actual spatial extent of the grooved bedrock. On the other hand, such complex terrains likely contain information related to landforms that could help decode a potentially diachronous geomorphic signature of palaeo-ice stream activity.

2.5.4 Further research

Future research into the origin of bedrock mega-grooves could fruitfully address several key aspects of their formation.

First, a rigorous reappraisal of geological detail would be instrumental in the search for any geological controls on mega-groove initiation. This would involve an assessment of structural geology and lithological characteristics in detail, as well as an attempt to reconstruct the characteristics of the Tertiary regolith mantle. The latter could help infer lithological characteristics that were present at the time of mega-groove initiation and potentially relevant to glacial abrasion.

Second, detailed geomorphic mapping of mega-grooves followed by morphometric analyses are necessary to enable quantitative approaches to process – form relationships. Quantifying landform distribution and dimensions has led to some important progress in our understanding of other subglacial bedforms (Clark et al., 2009; Ely et al., 2016), and this type of analysis could be extended across all bedrock-groove size ranges (Table 2.2) in order to establish whether a morphology and size continuum exists.

Third, empirical data from key locations is needed to assess groove evolution and efficiency of various erosion mechanisms. Particularly promising are localities where mega-grooves cut through structural and lithological boundaries, and where the groove profile is reported to change as a result (e.g. Smith, 1948; Bradwell, 2005). Comparative observations at these sites and Schmidt hammer tests could give an indication of how different rock types lend themselves to erosion and which erosion mechanism is likely to be most efficient. Other key points are the termini of mega-grooves, which could offer clues as to whether and how

bedrock grooves increase in length. At locations where mega-grooves merge into MSGLs, field survey using ground-penetration radar could help gain an understanding of how such transitions occur and help establish the role of mega-grooves in the context of ice streaming.

Fourth, numerical modelling could be used to test scenarios of groove formation and help gain insight into boundary conditions for rates of erosion. Cosmogenic nuclide dating could help constrain differential erosion between the groove base and the adjacent ridge (Briner and Swanson, 1998; Young et al., 2016). Not least, the increasing amount of data retrieved from modern subglacial environments is likely to help refine our understanding of processes at the ice – bedrock interface and thus support research into the origin of mega-grooves.

2.6 Conclusions

Bedrock mega-grooves are series of predominantly straight, long and parallel troughs in bedrock that occur in terrain formerly or currently occupied by ice sheets. In this paper, we review the literature pertaining to these landforms in order to assess our current understanding, identify aspects which require further investigation, and propose a general framework for further research. Historically, mega-groove research spans less than a century, in which the focus has widened from understanding groove formation based on empirical observations, to landform interpretation in a wider, regional context of palaeo-ice flow and, potentially, ice streaming. Generally, mega-grooves measure >1,000 m in length, have length:width ratios between 20:1 and 50:1, and length:depth ratios >100:1. They typically occur in lowlands, towards the periphery of the most recent mid-latitude ice sheets, both on- and off-shore, but have also been reported beneath modern ice sheets (Jezek et al., 2011).

There is a clear distinction between mega-grooves controlled by the bedrock structure and those independent of it. Structurally-controlled mega-grooves represent around 70% of all reported sites and occur in areas where palaeo-ice flow was parallel to lines of structural geology. The most common examples are those in layered tilted rocks, where the grooves are parallel to strike, and where their location, formation and morphology are directly explained by the underpinning bedrock structure. Mega-grooves independent of bedrock structure are unrelated to the orientation of bedrock dip and strike, often cut through geological boundaries, and their location and formation remain as yet unexplained. At present there is no consensus with regards to the formation of structurally-independent

mega-grooves, but most site-specific case studies strongly suggest that they are subglacial landforms initiated through glacial erosion. Other factors have been identified that may have been important at different stages in mega-groove formation, namely the pre-glacial relief, the presence of Tertiary regolith, the presence of meltwater at the glacier – bedrock interface, ice-flow conditions, ice – bedrock feedback mechanisms, subaerial processes, and time. The age of mega-grooves is poorly constrained, but they have likely survived through multiple cycles of glaciation. At several locations, mega-grooves have been mapped and interpreted as onset zones of fast ice-flow in palaeo-ice stream landsystems, and their formation attributed to presumed high rates of basal ice velocity and erosion. However, the exact relationship between ice stream flow and bedrock erosion is currently insufficiently understood for firm conclusions to be drawn regarding ice streaming and mega-groove formation.

Bedrock grooves with similar morphology, ranging in length from millimetres to kilometres have been identified from published studies, where they tend to be treated in the context of their specific size range and of which four classes emerge in the literature. It is possible that mega-grooves belong to a landform size continuum, and this would offer a context for process – form relationships and feedbacks to be explored and help understand groove evolution from small to large. It is suggested that the next steps in mega-groove research focus on:

i) detailed mapping of key physical features to enable morphometric analyses. These are necessary to derive a quantitative definition for mega-grooves, to test the existence of a bedrock groove size continuum and to constrain numerical modelling experiments;

ii) scrutiny of the current bedrock geology at a small scale, as well as an attempt to reconstruct the Tertiary regolith, in order to investigate any geological controls on groove formation;

iii) field survey through geomorphological mapping, sediment analyses and geophysical techniques at key locations, to assess the likelihood of different erosional processes in mega-groove formation and to explore the link between ice-flow velocity and mega-grooves;

iv) numerical modelling to test scenarios of groove initiation and help gain insight into boundary conditions for rates of erosion, alongside the application of absolute dating techniques.

Collectively, the data gathered from these lines of investigation should help address current uncertainties regarding mega-groove formation and advance overall understanding of these landforms and their glaciological significance.

2.7 Acknowledgements

The authors would like to thank Dr Harold Lovell and an anonymous reviewer for constructive comments, and Professor Ian Candy, the editor, for handling the manuscript. Simon Newton offered technical support with Adobe Photoshop, the software used to produce the figures, and helped draw the images in Figures 2.10 and 2.15.

2.8 References

Atkinson, N., Utting, D.J., Pawley, S.M., 2014. Glacial landforms of Alberta, Canada. Alberta Energy Regulator, AER/AGS Map 604 (Scale 1:1 000 000).

Baeten, N.J., Forwick, M., Vogt, Vorren, T.O., 2010. Late Weichselian and Holocene sedimentary environments and glacial activity in Billefjorden, Svalbard. *Geol. Soc. Lond., Spec. Publ. 344* (1), pp. 207–223.

Baker, V.R., Milton, D.J., 1974. Erosion by catastrophic floods on Mars and earth. *Icarus 23* (1), pp. 27–41.

Bamber, J.L., Vaughan, D.G., Joughin, I., 2000. Widespread complex flow in the interior of the Antarctic ice sheet. *Science 287* (5456), pp. 1248-1250.

Bell R., 1867. Geology of Manitoulin Island. In: *Report on Progress, Geological Survey of Canada* 1863-6. Ottawa.

Benn, D.I. and Evans D.J.A., 2010. *Glaciers and Glaciation*. Second edition. Routledge, London.

Booth, D.B. and Hallet B., 1993. Channel networks carved by subglacial water: observations and reconstruction in the eastern Puget Lowland of Washington. *GSA Bulletin 105*, pp. 671-682.

Boulton, G.S., 1974. Processes and Patterns of Glacial Erosion. In: Coates, D.R. (ed), *Glacial Geomorphology.* University of New York, Binghampton, pp. 41–87.

Boulton, G.S., 1979. Processes of glacier erosion on different substrata. *Journal of Glaciology 23*, pp. 15-38.

Bradwell, T., 2005. Bedrock Megagrooves in Assynt, NW Scotland. *Geomorphology, 65* (3-4), pp. 195–204.

Bradwell, T., Stoker, M.S., 2015. Submarine Sediment and Landform Record of a Palaeo-Ice Stream within the British–Irish Ice Sheet. *Boreas 44* (2), pp. 255–76.

Bradwell, T., Stoker, M.S., Larter, R.D., 2007. Geomorphological Signature and Flow Dynamics of The Minch Palaeo-Ice Stream, NW Scotland. *Journal of Quaternary Science, 22*(6), pp. 609-617.

Bradwell, T., Stoker, M.S. and Krabbendam, M., 2008. Megagrooves and streamlined bedrock in NW Scotland: the role of ice streams in landscape evolution. *Geomorphology*, *97*(1-2), pp.135-156.

Briner, J.P. and Swanson, T.W., 1998. Using inherited cosmogenic 36Cl to constrain glacial erosion rates of the Cordilleran ice sheet. *Geology*, *26*(1), pp.3-6.

Carney, F., 1910. Glacial erosion on Kelleys Island, Ohio. *Geological. Society of America Bulletin*, *46*, pp.241-283.

Carol, H., 1947. The formation of roches moutonnées. *Journal of Glaciology*, *1*(2), pp.57-59.

Chamberlin, T.C., 1888. The Rock-Scorings of the Great Ice Invasions. *US Geological Survey, 7th Annual Report*, pp. 155–254.

Clark, C.D., 1993. Mega-scale glacial lineations and cross-cutting ice-flow landforms. *Earth surface processes and landforms*, *18*(1), pp.1-29.

Clark, C.D., Hughes, A.L., Greenwood, S.L., Spagnolo, M. and Ng, F.S., 2009. Size and shape characteristics of drumlins, derived from a large sample, and associated scaling laws. *Quaternary Science Reviews*, *28*(7-8), pp.677-692.

Clark, C.D., Tulaczyk, S.M., Stokes, C.R. and Canals, M., 2003. A groove-ploughing theory for the production of mega-scale glacial lineations, and implications for ice-stream mechanics. *Journal of Glaciology*, *49*(165), pp.240-256.

Dahl, R., 1965. Plastically sculptured detail forms on rock surfaces in northern Nordland, Norway. *Geografiska Annaler, 47*(2), pp.83-140.

Drewry, D.J., 1986. *Glacial geologic processes*. E. Arnold, London.

Ely, J.C., Clark, C.D., Spagnolo, M., Stokes, C.R., Greenwood, S.L., Hughes, A.L., Dunlop, P. and Hess, D., 2016. Do subglacial bedforms comprise a size and shape continuum?. *Geomorphology*, *257*, pp.108-119.

Eyles, N., 2006. The role of meltwater in glacial processes. *Sedimentary Geology*, *190*(1-4), pp.257-268.

Eyles, N., 2012. Rock drumlins and megaflutes of the Niagara Escarpment, Ontario, Canada: a hard bed landform assemblage cut by the Saginaw–Huron Ice Stream. *Quaternary Science Reviews*, *55*, pp.34-49.

Eyles, N. and Putkinen, N., 2014. Glacially-megalineated limestone terrain of Anticosti Island, Gulf of St. Lawrence, Canada; onset zone of the Laurentian Channel ice stream. *Quaternary Science Reviews*, *88*, pp.125-134.

Eyles, N., Moreno, L.A. and Sookhan, S., 2018. Ice streams of the Late Wisconsin Cordilleran Ice Sheet in western North America. *Quaternary Science Reviews*, *179*, pp.87-122.

Fairbridge, R.W., 1982. Glacial grooves and periglacial features in the Saharan Ordovician. In Coates, D.R. (Ed) *Glacial Geomorphology*, pp. 315-327. Springer, Dordrecht.

Fenton, M.M., Waters, E.J., Pawley, S.M., Atkinson, N., Utting, D.J. and Mckay, K., 2013. Surficial geology of Alberta. Alberta Energy Regulator, AER/AGS Map 601, scale 1: 1 000 000.

Flint RF. 1971. Glacial and Quaternary Geology. Wiley, New York.

Funder, S., 1978. Glacial flutings in bedrock, an observation in East Greenland. *Bulletin of the Geological Society of Denmark*, *27*, pp.9-13.

Geological Survey of Canada, 2014. Surficial geology of Canada; Geological Survey of Canada, Canadian Geoscience Map 195(preliminary, Surficial Data Model v. 2.0 conversion of Map 1880A), scale 1:5 000 000.

Gilbert, G.K., 1873. Surface geology of the Maumee Valley. *Ohio Geological Survey*, *1*, pp.535-556.

Gjessing, J., 1965. On 'Plastic Scouring'and 'Subglacial Erosion. *Norsk Geografisk Tidsskrift* 20 (1-2), pp.1-37

Goldthwait, R.P., 1979. Giant grooves made by concentrated basal ice streams. *Journal of Glaciology*, *23*(89), pp.297-307.

Gordon, J.E., 1981. Ice-scoured topography and its relationships to bedrock structure and ice movement in parts of northern Scotland and West Greenland. *Geografiska Annaler: Series A, Physical Geography*, *63*(1-2), pp.55-65.

Gravenor, C.P. and Meneley, W.A., 1958. Glacial flutings in central and northern Alberta. *American Journal of Science*, *256*(10), pp.715-728.

Grosswald, M.G. and Hughes, T.J., 2002. The Russian component of an Arctic ice sheet during the Last Glacial Maximum. *Quaternary Science Reviews*, *21*(1-3), pp.121-146.

Halls, H.C., 1969. Compressional wave velocities of Keweenawan rock specimens from the Lake Superior region. *Canadian Journal of Earth Sciences*, *6*(4), pp.555-568.

Heikkinen, O. and Tikkanen, M., 1989. Drumlins and flutings in Finland: their relationships to ice movement and to each other. *Sedimentary geology*, *62*(2-4), pp.349-355.

Heroy, D.C. and Anderson, J.B., 2005. Ice-sheet extent of the Antarctic Peninsula region during the Last Glacial Maximum (LGM)—Insights from glacial geomorphology. *Geological Society of America Bulletin*, *117*(11-12), pp.1497-1512.

Iverson, N.R., 1990. Laboratory simulations of glacial abrasion: comparison with theory. *Journal of Glaciology*, *36*(124), pp.304-314.

Iverson, N.R., 1991. Morphology of glacial striae: implications for abrasion of glacier beds and fault surfaces. *Geological Society of America Bulletin*, *103*(10), pp.1308-1316.

Iverson, N.R., Cohen, D., Hooyer, T.S., Fischer, U.H., Jackson, M., Moore, P.L., Lappegard, G. and Kohler, J., 2003. Effects of basal debris on glacier flow. *Science*, *301*(5629), pp.81-84.

Jezek, K., Wu, X., Gogineni, P., Rodríguez, E., Freeman, A., Rodriguez-Morales, F. and Clark, C.D., 2011. Radar images of the bed of the Greenland Ice Sheet. *Geophysical Research Letters*, *38*(1) L01501.

King, E.C., Hindmarsh, R.C. and Stokes, C.R., 2009. Formation of mega-scale glacial lineations observed beneath a West Antarctic ice stream. *Nature Geoscience*, *2*(8), pp.585-588.

Kleman, J. and Applegate, P.J., 2014. Durations and propagation patterns of ice sheet instability events. *Quaternary Science Reviews*, *92*, pp.32-39.

Kor, P.S.G., Shaw, J. and Sharpe, D.R., 1991. Erosion of bedrock by subglacial meltwater, Georgian Bay, Ontario: a regional view. *Canadian Journal of Earth Sciences*, *28*(4), pp.623-642.

Krabbendam, M. and Bradwell, T., 2011. Lateral plucking as a mechanism for elongate erosional glacial bedforms: explaining megagrooves in Britain and Canada. *Earth Surface Processes and Landforms*, *36*(10), pp.1335-1349.

Krabbendam, M. and Bradwell, T., 2014. Quaternary evolution of glaciated gneiss terrains: pre-glacial weathering vs. glacial erosion. *Quaternary Science Reviews*, *95*, pp.20-42.

Krabbendam, M., Eyles, N., Putkinen, N., Bradwell, T. and Arbelaez-Moreno, L., 2016. Streamlined hard beds formed by palaeo-ice streams: A review. *Sedimentary Geology*, *338*, pp.24-50.

Krabbendam, M. and Glasser, N.F., 2011. Glacial erosion and bedrock properties in NW Scotland: abrasion and plucking, hardness and joint spacing. *Geomorphology*, *130*(3-4), pp.374-383.

Krabbendam, M., Eyles, N., Putkinen, N., Bradwell, T. and Arbelaez-Moreno, L., 2016. Streamlined hard beds formed by palaeo-ice streams: A review. *Sedimentary Geology*, *338*, pp.24-50.

Lane, T.P., Roberts, D.H., Rea, B.R., Ó Cofaigh, C., Vieli, A. and Rodés, A., 2014. Controls upon the Last Glacial maximum deglaciation of the northern Uummannaq ice stream system, West Greenland. *Quaternary Science Reviews*, *92*, pp.324-344.

Lawson, D.E., 1976. Observations on flutings at Spencer glacier, Alaska. *Arctic and Alpine Research*, *8*(3), pp.289-296.

Lee, A.G.G. and Rutter, E.H., 2004. Experimental rock-on-rock frictional wear: Application to subglacial abrasion. *Journal of Geophysical Research: Solid Earth*, *B09202*, pp.1-11.

Livingstone, S.J., Ó Cofaigh, C. and Evans, D.J.A., 2008. Glacial geomorphology of the central sector of the last British-Irish Ice Sheet. *Journal of Maps*, *4*(1), pp.358-377.

López-Gamundí, O. and Martínez, M., 2000. Evidence of glacial abrasion in the Calingasta–Uspallata and western Paganzo basins, mid-Carboniferous of western Argentina. *Palaeogeography, Palaeoclimatology, Palaeoecology*, *159*(1-2), pp.145-165.

Lowe, A.L. and Anderson, J.B., 2003. Evidence for abundant subglacial meltwater beneath the paleo-ice sheet in Pine Island Bay, Antarctica. *Journal of Glaciology*, *49*(164), pp.125-138.

Lucchitta, B.K., 1982. Ice sculpture in the Martian outflow channels. *Journal of Geophysical Research: Solid Earth*, *87*(B12), pp.9951-9973.

Margold, M., Stokes, C.R., Clark, C.D. and Kleman, J., 2015a. Ice streams in the Laurentide Ice Sheet: a new mapping inventory. *Journal of Maps*, *11*(3), pp.380-395.

Margold, M., Stokes, C.R. and Clark, C.D., 2015b. Ice streams in the Laurentide Ice Sheet: Identification, characteristics and comparison to modern ice sheets. *Earth-Science Reviews*, *143*, pp.117-146.

Munro-Stasiuk, M.J., Fisher, T.G. and Nitzsche, C.R., 2005. The origin of the western Lake Erie grooves, Ohio: implications for reconstructing the subglacial hydrology of the Great Lakes sector of the Laurentide Ice Sheet. *Quaternary Science Reviews*, *24*(22), pp.2392-2409.

Munro-Stasiuk, M.J., Shaw, J., Sjogren, D.B., Brennand, T.A., Fisher, T.G., David, R., Sharpe, P.S.K. and Claire, L., 2009. The morphology and sedimentology of landforms created by subglacial megafloods. In Burr, D. M., Carling, P. A., and Baker, V. R. (Eds.): *Megaflooding on Earth and Mars*, pp.78-103.

Nobles, L.H. and Weertman, J., 1971. Influence of irregularities of the bed of an ice sheet on deposition rate of till. In Goldthwait R.P. (ed): *Till, a symposium*, pp. 117-126. Columbus: Ohio State Univ. Press.

Ó Cofaigh, C., 1996. Tunnel valley genesis. *Progress in physical geography*, *20*(1), pp.1-19.

Ollier, C.D., 1984. *Weathering*. Second edition. Longman, London, 270pp.

Ollier, C.D., 1991. *Ancient Landforms*. Belhaven Press, London, 233pp.

Ottesen, D., Stokes, C.R., Rise, L. and Olsen, L., 2008. Ice-sheet dynamics and ice streaming along the coastal parts of northern Norway. *Quaternary Science Reviews*, *27*(9-10), pp.922-940.

Paulen, R.C. and Plouffe, A., 2009. Surficial geology of the Cameron Hills area. (NTS 84N/NW). Energy Resources Conservation Board, ERCB/AGS Map420, Geological Survey of Canada, Open File 6104, scale 1:100 00.

Perry, W.J. and Roberts, H.G., 1968. Late Precambrian glaciated pavements in the Kimberley region, Western Australia. *Journal of the Geological Society of Australia*, *15*(1), pp.51-56.

Rea, B,R., 1994. Plucking and Abrasion beneath Temperate Plateau Icefields. Unpublished PhD thesis, Queen's University, Belfast, UK.

Rea, B.R., Evans, D.J.A., Dixon, T.S. and Whalley, W.B., 2000. Contemporaneous, localized, basal ice-flow variations: implications for bedrock erosion and the origin of p-forms. *Journal of Glaciology*, *46*(154), pp.470-476.

Rignot E and Kanagaratnam P. 2006 Changes in the velocity structure of the Greenland Ice Sheet. *Science* 311.5763: 986-990.

Roberts D.H. and Long A.J., 2005. Streamlined bedrock terrain and fast ice flow, Jakobshavns Isbrae, West Greenland: implications for ice stream and ice sheet dynamics. *Boreas*, *34*(1), pp.25-42.

Roberts, D.H., Long, A.J., Davies, B.J., Simpson, M.J. and Schnabel, C., 2010. Ice stream influence on west Greenland ice sheet dynamics during the last glacial maximum. *Journal of Quaternary Science*, *25*(6), pp.850-864.

Sharp, M.J., Gemmell, J.C. and Tison, J-L., 1989. Structure and stability of the former subglacial drainage system of the Glacier de Tsanfleuron, Switzerland. *Earth Surface Processes and Landforms*, *14*(2), pp.119-134.

Sharpe, D.R. and Shaw, J., 1989. Erosion of bedrock by subglacial meltwater, Cantley, Quebec. *Geological Society of America Bulletin*, *101*(8), pp.1011-1020.

Shaw, J., 2002. The meltwater hypothesis for subglacial bedforms. *Quaternary International*, *90*(1), pp.5-22.

Shaw, J. and Gilbert, R., 1990. Evidence for large-scale subglacial meltwater flood events in southern Ontario and northern New York State. *Geology*, *18*(12), pp.1169-1172.

Shaw, J., Pugin, A. and Young, R.R., 2008. A meltwater origin for Antarctic shelf bedforms with special attention to megalineations. *Geomorphology*, *102*(3-4), pp.364-375.

Smith, H.T.U., 1948. Giant glacial grooves in northwest Canada. *American Journal of Science*, *246*(8), pp.503-514.

Soanes, C., and Hawker, S. (eds). 2005. *Compact Oxford English Dictionary of Current English*. 3rd ed. Oxford University Press.

Spagnolo, M., Clark, C.D., Ely, J.C., Stokes, C.R., Anderson, J.B., Andreassen, K., Graham, A.G. and King, E.C., 2014. Size, shape and spatial arrangement of mega-scale glacial lineations from a large and diverse dataset. *Earth Surface Processes and Landforms*, *39*(11), pp.1432-1448.

Stokes, C.R., 2018. Geomorphology under ice streams: moving from form to process. *Earth Surface Processes and Landforms*, *43*(1), pp.85-123.

Stokes, C.R. and Clark, C.D., 1999. Geomorphological criteria for identifying Pleistocene ice streams. *Annals of glaciology*, *28*, pp.67-74.

Stokes, C.R. and Clark, C.D., 2001. Palaeo-ice streams. *Quaternary Science Reviews*, *20*(13), pp.1437-1457.

Stokes, C.R. and Clark, C.D., 2002. Are long subglacial bedforms indicative of fast ice flow? *Boreas*, *31*(3), pp.239-249.

Stokes, C.R., Margold, M., Clark, C.D. and Tarasov, L., 2016. Ice stream activity scaled to ice sheet volume during Laurentide Ice Sheet deglaciation. *Nature*, *530*(7590), pp.322-326.

Sugden, D.E. and John, B.S., 1976. *Glaciers and landscape: a geomorphological approach*. London, Edward Arnold.

Sugden, D.E., Denton, G.H. and Marchant, D.R., 1991. Subglacial meltwater channel systems and ice sheet overriding, Asgard Range, Antarctica. *Geografiska Annaler: Series A, Physical Geography*, *73*(2), pp.109-121.

Taylor, G. and Eggleton, R.A., 2001. *Regolith geology and geomorphology*. John Wiley & Sons, Chichester.

Thornbury, W.D., 1969. *Principles of Geomorphology*. John Willey & Sons, Chichester, 594 pp.

Tinkler, K.J., 1993. Fluvially sculpted rock bedforms in Twenty Mile Creek, Niagara Peninsula, Ontario. *Canadian Journal of Earth Sciences*, *30*(5), pp.945-953.

Tinkler, K. and Stenson, R., 1992. Sculpted bedrock forms along the Niagara escarpment, Niagara Peninsula, Ontario. *Géographie physique et Quaternaire*, *46*(2), pp.195-207.

Ver Steeg, K. and Yunck, G., 1935. Geography and Geology of Kelley's Island. *The Ohio Journal of Science 35* (6), pp.421-433.

Wardlaw, N.C., Stauffer, M.R. and Hoque, M., 1969. Striations, giant grooves, and superposed drag folds, Interlake area, Manitoba. *Canadian Journal of Earth Sciences*, *6*(4), pp.577-593.

Wellner, J.S., Heroy, D.C. and Anderson, J.B., 2006. The death mask of the Antarctic ice sheet: comparison of glacial geomorphic features across the continental shelf. *Geomorphology*, *75*(1-2), pp.157-171.

Whipple, K.X., Hancock, G.S. and Anderson, R.S., 2000. River incision into bedrock: Mechanics and relative efficacy of plucking, abrasion, and cavitation. *Geological Society of America Bulletin*, *112*(3), pp.490-503.

Williamson, I.T. and Bell, B.R., 2012. The Staffa Lava Formation: graben-related volcanism, associated sedimentation and landscape character during the early development of the Palaeogene Mull Lava Field, NW Scotland. *Scottish Journal of Geology*, *48*(1), pp.1-46.

Winsborrow, M.C., Clark, C.D. and Stokes, C.R., 2010. What controls the location of ice streams? *Earth-Science Reviews*, *103*(1-2), pp.45-59.

Witkind, I.J., 1978. Giant glacial grooves at the north end of the Mission Range, northwest Montana. *J. Res. US Geol. Surv*, *6*(4), pp.425-433.

Young, N.E., Briner, J.P., Maurer, J. and Schaefer, J.M., 2016. 10Be measurements in bedrock constrain erosion beneath the Greenland Ice Sheet margin. *Geophysical Research Letters*, *43*(22), pp.11-708.

Zumberge, J.H., 1955. Glacial erosion in tilted rock layers. *The Journal of Geology*, *63*(2), pp.149-158.

Chapter 3. Bedrock mega-grooves (BMGs) in glaciated terrain: morphometric analyses from a global dataset

Abstract

Bedrock mega-grooves (BMGs) are subglacial landforms of erosion present in previously glaciated terrain, in a variety of geological and glaciological settings across the world. Despite a significant number of reports describing BMGs published throughout the last hundred years, no systematic measuring of these landforms has been undertaken. This is a necessary step towards exploring the formation of these landforms and has been successfully applied to other subglacial landforms of similar magnitude (e.g. mega-scale glacial lineations (MSGLs) and drumlins). In this study, BMGs from ten locations across the world are systematically mapped, sampled and measured. Based on the 10th–90th percentile of the aggregated global population (n = 1242), BMGs have lengths of 224–2269 m, widths of 21–210 m, depths of 5–15 m, elongation ratios of 5:1–41:1, and the spacing between adjacent grooves is 35-315 m. Frequency distributions for all metrics are unimodal, strongly suggesting that BMGs form a single landform population, which strengthens their position as a geomorphic entity in its own right within the suite of subglacial landforms. The variability of the metrics and their correlations between and within sites most likely reflect site-specific geological characteristics. At sites where fast ice flow appears to have been the main control factor, the BMGs attain the largest size and lowest elongation ratios, whereas BMGs formed under a primary geological control occupy smaller size ranges and have higher elongation ratios. Morphometrically, BMGs and MSGLs plot as different populations, with BMGs being on average 4× shorter, 3.5× narrower, 3.5× more closely spaced and about 2× deeper. It is suggested that future research focuses on numerical modelling experiments to test rates of erosion in different bedrock substrate under varying glaciological conditions, and on adding to the body of existing field-derived empirical observations, which remains key to validating geological controls over BMG formation and assessing the efficiency of erosion mechanisms.

3.1 Introduction

The aim of this paper is to provide the first quantification of the size, shape and spacing of BMGs across a range of locations, in order better understand the characteristics and origin

of these enigmatic landforms. BMGs are assemblages of straight grooves eroded in bedrock, typically several hundred meters long, which occur within the limits of Late Quaternary ice sheets and are aligned parallel with the palaeo-ice flow direction, often in conjunction with other subglacial landforms (Smith, 1948; Gravenor and Meneley, 1958; Funder, 1978; Witkind, 1978; Heikkinen and Tikkanen,1989; Bradwell, 2005; Bradwell et al., 2008; Eyles, 2012; Lowe and Anderson, 2003; Krabbendam et al., 2016; Newton et al., 2018). Based on these observations, BMGs have been unanimously interpreted as having formed subglacially, primarily through glacial erosion in bedrock (Smith, 1948; Gravenor and Meneley, 1958; Funder, 1978; Witkind, 1978; Heikkinen and Tikkanen,1989; Bradwell, 2005; Bradwell et al., 2008; Jezek et al., 2011; Eyles, 2012; Krabbendam et al., 2016; Newton et al., 2018). The subglacial origin of BMGs has raised awareness of the potential that these landforms hold for unravelling geomorphic processes at the ice–bedrock interface, as well as possible links to (palaeo) ice flow conditions, especially to ice-streaming (Bradwell et al., 2008; Eyles, 2012; Krabbendam et al., 2016).

Two questions have been at the core of BMG research for the past few decades (Newton et al., 2018): i) what is the mechanism of BMG formation, and ii) what information do they provide about the palaeoglaciological setting? Regarding the first question, many authors have explored scenarios of groove formation in an effort to explain their large dimensions and ubiquitous parallel conformity, based mainly on bedrock susceptibility to subglacial erosion either directly by glacier ice (Smith, 1948; Gravenor and Meneley, 1958; Funder, 1978; Heikkinen and Tikkanen, 1989; Bradwell, 2005; Krabbendam and Bradwell, 2011; Eyles, 2012) or by meltwater (Sharpe and Shaw, 1989; Shaw, 2002; Bradwell 2005). Thus, it has been noted that certain lithologies (e.g. limestone, sandstone, conglomerate, gneiss) have favoured groove formation primarily through glacial abrasion (Smith, 1948; Funder, 1978; Heikkinen and Tikkanen, 1989; Eyles, 2012), whereas the BMGs present in densely jointed meta-sedimentary bedrock owe their formation mainly to glacial plucking (Zumberge, 1955; Krabbendam and Bradwell, 2011). These observations are valuable, but they remain mostly qualitative and site-specific, and can only be extrapolated in as much as similar lithological conditions occur elsewhere (e.g. Krabbendam and Bradwell, 2011; Krabbendam et al., 2016). A quantitative approach based on BMG metrics, which up until now has been missing, would enable groove analysis at a global scale, across sites of different lithologies, which could reveal common features and thus lead to more generalised conclusions and overarching hypotheses.

Regarding the second question, some recent studies advocate that BMGs at several sites formed in onset zones of fast-flowing ice (palaeo-ice streams), through focussed bedrock erosion enhanced by high ice-flow velocities in conjunction with meltwater erosion (Lowe and Anderson, 2003; Bradwell et al., 2008; Eyles, 2012; Smith et al., 2012; Krabbendam et al., 2016; Eyles et al., 2018). This idea is based on the occurrence of some BMGs within palaeo-ice stream landsystems, in close spatial association with other elongate subglacial landforms, such as MSGLs and bedrock drumlins (Bradwell et al., 2008; Lowe and Anderson, 2003; Eyles, 2012; Krabbendam et al., 2016). However, some doubt has been expressed regarding fast-ice flow as a precondition for BMG formation (Newton et al., 2018; see also Section 4.5.3 in Chapter 4), given groove occurrence in areas not known to have been affected by ice streaming (e.g. Funder, 1978), or where the evidence for ice streaming is equivocal (e.g. Brown, 2012). Additionally, some BMGs appear to owe their development to long-term glacial erosion controlled by the bedrock geology despite being situated within palaeo-ice stream landsystems (e.g. Roberts et al., 2010). Further insight into the role that fast-ice flow plays in BMG formation could be gained through morphometric comparisons between BMGs and other large-scale subglacial landforms of similar shape (e.g. MSGLs) within and across ice-stream landsystems, as well as between BMGs from areas affected by ice streaming and those from areas of normal ice-sheet flow.

Elsewhere in glacial geomorphology, quantitative analyses of landform metrics have led to important advances in the understanding of streamlined subglacial landforms such as ribbed moraine (Dunlop and Clark, 2006), drumlins (Clark et al., 2009; Ely et al., 2018) MSGLs (Stokes et al., 2013; Spagnolo et al., 2014), eskers (Storrar et al., 2014) and flutings (Ely et al., 2016). Specifically, the availability of morphometric data derived from systematic measurements of large landform populations has enabled statistical analysis of pattern distributions and comparisons within and between groups of landform populations (Hillier et al., 2013; Hillier et al., 2016). The results have been used to test formation hypotheses (Stokes et al., 2013; Spagnolo et al., 2014), endorsed the previously proposed close connections with ice streaming (Clark, 1993), and enabled a deeper exploration into landform continua (Stokes et al., 2013; Ely et al., 2016). Large samples of empirical data on subglacial landform metrics have also been used to test numerical models of landform formation (e.g. Dunlop et al., 2008; Livingstone et al., 2015).

Despite BMGs generally being recognised as a distinctive landform category in the wider range of subglacial bedforms, their dimensions have never been quantitatively established using systematic mapping and sampling from a global dataset. Studies spanning over 100

years of research (Table 3.1) report mean values for landform metrics extracted from various sites and following different protocols (see Section 3.3.3), which has invariably produced inconsistent results across sites and cannot form a suitable basis for global quantitative analysis. Few site-specific studies have undertaken measurements systematically (e.g. Gravenor and Meneley, 1958) or on large enough population samples for the results to be statistically robust. In general, quantification remains scarce in the published literature and, in contrast to other subglacial landforms, no study has yet characterised the morphometry of BMGs. Older BMG studies have often been incidental to other projects, and the authors aimed to signal the presence of these unusual landforms while also providing some general information on their dimensions (e.g. Smith, 1948; Funder, 1978; see Table 2.1 in Chapter 1; Newton et al., 2018).

In conclusion, specific measurement protocols need to be applied systematically to produce sufficient data for robust quantitative analyses (Chandler et al., 2018). Here we presentaim to fill this gap by presenting a database of BMG metrics of comparable complexity and magnitude to that existing for MSGLs (Spagnolo et al., 2014), and use these data to analyse the morphometry and distribution of BMGs. Specifically, we aim to: i) constrain the dimensions of BMGs; ii) highlight and explain distribution patterns, particularly in relation to bedrock lithology; iii) compare BMGs to MSGLs and use the results to further explore links with ice streaming; and iv) gain a deeper insight into possible overarching conditions for BMG formation.

3.2 Study areas

3.2.1 Site selection

BMGs are relatively scarce compared to other subglacial landforms, with only about 20–25 reported sites worldwide (Newton et al., 2018; Table 3.1). Of these, ten sites were selected for the purposes of this study (Figure 3.1) in order to balance the time incurred for sampling with the aim of producing a sizeable and representative dataset. The availability of suitable imagery to measure the BMGs was also an important consideration and precluded the sampling of several sites. Although many sites may go unreported, a conservative estimate is that 35%–40 % of the global population has been sampled in this study. The sites were selected according to the four criteria described in the following paragraphs, and a detailed description of the selected sites is presented in Section 3.2.2.

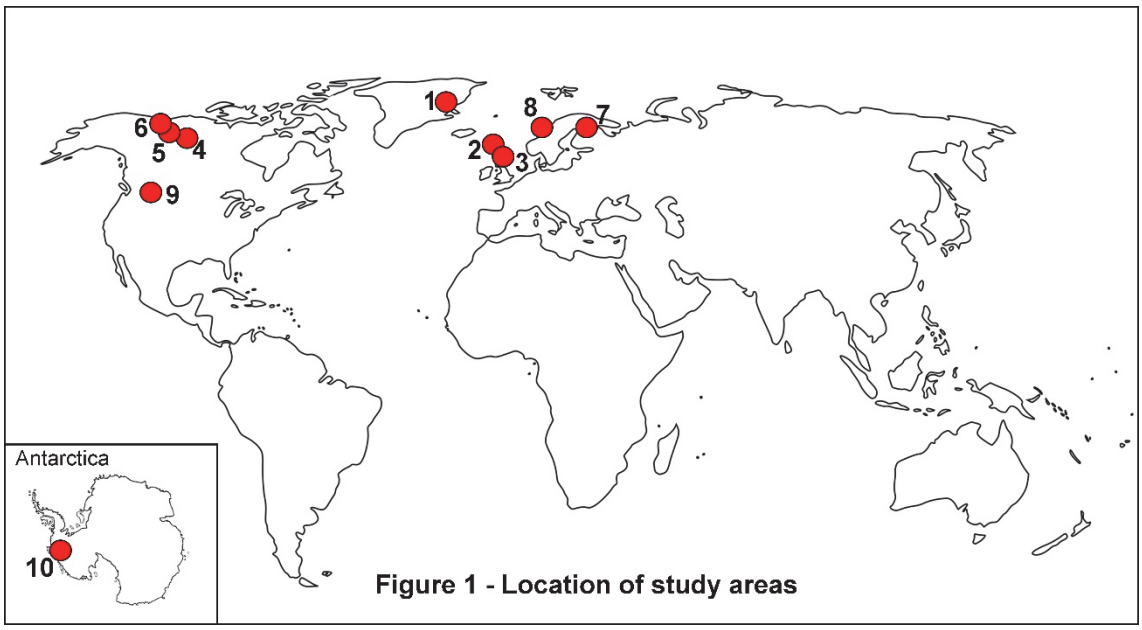

Figure 3.1. Location of study areas. 1 – Haarefjord; 2 – Elphin; 3 – Ullapool; 4 – Franklin; 5 – Hanna; 6 – Beavertail; 7 – Iivaara; 8 – Vikna; 9 – Hazelton; 10 – Pine Island. The study areas are referred to by their site ID. More details about the exact location and physical characteristics of each site are presented in Table 3.2. The site numbering follows the order in which the sites were mapped and sampled, which is reflected throughout the structure of this chapter (e.g. Figure 1 in the Appendix).

First, an assessment of the substrate was carried out to ensure that the mega-grooves occurred in bedrock rather than in unconsolidated glacigenic deposits. This was to avoid confusion between BMGs and MSGLs, considering their sometimes-similar appearance on remotely sensed imagery (Krabbendam et al., 2016). The substrate assessments for the onshore sites were based on information from geological maps of solid bedrock combined with that from maps of superficial deposits, in conjunction with published empirical evidence from BMG studies, where available (e.g. see Sections 3.2.2.1 and 3.2.2.4) and with fieldwork results from sites at Elphin and Ullapool, Scotland, UK (see also Chapter 4). At Vikna and Pine Island, which are situated offshore, the solid bedrock substrate was inferred through geophysical investigations (e.g. Lowe and Anderson, 2003; see Section 3.2.2.8 and 3.2.2.10). The aim was to cover a variety of lithologies to allow for tentative correlations between groove metrics and bedrock characteristics. Overall, the study areas are devoid of unconsolidated glacigenic sediment and, where this does occur, it is patchy and thinly draped over the bedrock topography, thus preserving the shape of the bedrock topography underneath.

Table 3.1. Summary of basic morphometric values for mega-grooves and their relationship with the bedrock geology, reported in the literature from sites across the world. The figures for length, width, depth and lateral spacing are average values in meters, with maximum values given in parentheses. Sites 1–8 have been mapped and sampled in the present study. The table was modified and updated from Newton et al. (2018) (see Table 2.1 in Chapter 2).

No	References	Location	Length (m)	Width (m)	Depth (m)	Lateral spacing (m)	Bedrock lithology	Relationship to structure
1	Funder (1978)	Haarefjord, East Greenland	50–2,000	-	1–5	45	Coarse sandstone and conglomerate	Independent
2	Bradwell (2005)	Elphin, Assynt, NW Scotland, UK	500–1,500 (4,300)	20–30	5–20 (27)	-	Quartzite	Independent
3	Bradwell et al. (2008) Krabbendam and Bradwell, (2011)	Ullapool, Assynt, NW Scotland, UK	500–3,000 (3,500)	50–120 (200)	10–20	100–500	Metasandstone	Controlled
4	Smith (1948)	Franklin Mountains (locality A), NT, Canada	30–1,500 (12,000)	>90	<30	-	Soft and porous limestone, sandstone	Independent
5	Smith (1948)	Hanna River (locality J), NT, Canada	Ca 1,600	>45	<30	-	Sandstone	Independent
6	Smith (1948)	Localities B–H	30 – 1,500	<50	<30	-	Limestone, sandstone	Independent
7	Sutinen et al. (2010)	Kuusamo, Finland	W/L = 1:15–1:35	-	-	Igneous (syenite) intrusion	Independent	
8	Lowe and Anderson, (2003)	Pine Island Bay, West Antarctica	1,000–5,500	<50–300	20–50	-	Crystalline bedrock	Likely independent
9	Krabbendam et al. (2016)	Hazelton, British Columbia, Canada	500 – 1,000	-	-	-	-	Independent
10	Roberts et al. (2010)	West Greenland	5,000	200	30–50	-	Gneiss and dykes	Controlled
11	Gravenor and Meneley (1958)	Multiple sites, NE Alberta, Canada	Several 1,000s	-	3–8	90–120 180–215	Precambrian shield rocks	Independent
12	Zumberge (1955) Krabbendam and Bradwell, (2011)	Isle Royale, Michigan, US	2,000–20,000 (65,000)	-	-	400–800	Lavas and sedimentary layers	Controlled
13	Krabbendam and Bradwell, (2011)	Ungava Peninsula, Canada	10,000–40,000	-	-	300–700	(Meta)sedimentary and igneous intrusions	Controlled
14	Krabbendam et al. (2016)	Kaladar, E Ontario, Canada	10,000s	300–2,000	10–30	300–2,000	Metasedimentary rocks	Controlled
15	Livingstone et al. (2008). Krabbendam and Bradwell (2011)	Tyne Gap, England, UK	1,000–4,000	-	5–20	100–400	Limestone and mudstone	Controlled
16	Heikkinen and Tikkanen, (1989)	Lapland, Finland	-	5–20 (50)	2–4 (0.5–8)	-	Gneiss and granite	Independent
17	Eyles (2012)	Manitoulin Island Ontario Canada	>1,000	10s		-	Limestone	Independent
18	Krabbendam et al. (2016)	Key Harbour Ontario, Canada	10–100s	-	1–3	2–10	Granulite gneiss	Independent
19	Wardlaw et al. (1969)	Interlake, Manitoba – Canada	1,000–2,000	1–152 (1000s)	12–30	-	Carbonate rocks: limestone, dolomite and shale;	Controlled
20	Witkind (1978)	Montana, US	500–3,000	50–275	10–60	-	Metamorphosed fine-grained rocks	Independent

Second, the local and regional glacial history of the selected sites had to be well documented to enable assessment of groove alignment with independent indicators of palaeo-ice flow direction, as well as their subglacial origin. This assessment was particularly relevant at Vikna and Beavertail, where the BMGs have not been previously described in any published literature (to the author's knowledge). Reconstructions of former ice-flow direction at these sites were based on the presence of other streamlined landforms, such as drumlins, crag-and-tails, MSGLs in conjunction with BMGs (e.g. Smith, 1948; Ottesen et al, 2002).

The third site selection criterion was ease of access to remotely sensed imagery of adequate resolution for topographic measurements. In this respect, aerial imagery for onshore sites is more widely available and in open-access format. Additionally, the resolution is higher than that for offshore sites and the substrate is usually known in more detail. Therefore, eight out of the ten chosen sites are situated on-shore (Figure 3.1 and Table 3.2).

In summary, the study areas comprise a representative collection of BMGs that are geographically widespread and occur in a variety of geological settings, both on- and off-shore.

Table 3.2. Summary of general information of the ten BMG sites analysed in this study, with regards to location, source aerial imagery, and bedrock lithology. For more detailed information please refer to Section 3.2.2. Abbreviations: a.s.l. = above sea level; b.s.l. = below sea level; BC = British Columbia; Mts = mountains; NT = Northwest Territories; NLSF = National Land Survey of Finland; NHS = Norwegian Hydrographic Service; Rng = range. Throughout the paper the sites are referred to by their ID name (first column).

Site ID	Location	Position	Latitude	Longitude	Elevation range (m)	Area km²	Data type - provider	Horizontal gridding	Vertical accuracy	Bedrock lithology	Structure control	Ice streaming
Haarefjord	East Greenland, Scoresby Sund	onshore	70°57′45″ N	27°56′ W	0–305 a.s.l.	31.2	DigiGlobe satellites – ArcticDEM	2 m	<1 m	Conglomerate	No	Not known
Elphin	West of Elphin in Scotland, UK	onshore	58° 3′30″ N	5°3′ W	140–295 a.s.l.	2.3	Airborne Radar (IFSAR – NextMAP	5 m	1	Quartzite	Yes	Yes
Ullapool	North-east of Ullapool in Scotland, UK	onshore	57°56′ N	5°2′ W	220–430 a.s.l.	44.9	Airborne Radar (IFSAR) – NextMAP	5 m	1	Metasandstone	Yes	Yes
Franklin	Franklin Mts, NT Canada	onshore	65°7′ N	124°49′ W	130–340 a.s.l.	119	DigiGlobe satellites – ArcticDEM	2 m	<1 m	Limestone, sandstone, shale	No	Possible
Hanna	Hanna River, Sans Sault Rapids, NT Canada	onshore	65°40′42″ N	128°28′ W	150–360 a.s.l.	4.2	DigiGlobe satellites – ArcticDEM	2 m	<1 m	Sandstone	Not known	Not known
Beavertail	Beavertail Range NT Canada	onshore	65°52′ N	128°48′ W	130–260 a.s.l.	2.7	DigiGlobe satellites – ArcticDEM	2 m	<1 m	Sandstone	Not known	Not known
Iivaara	Kuusamo, Eastern Finland	onshore	65°47′56″ N	29°41′51″ E	320–450 a.s.l.	2	Laser scanning – NLSF	2 m	<0.5 m	Syenite	No	Yes
Vikna	Trøndelag Platform, West Norway	offshore	64°57′ N	10°23′ E	180–235 b.s.l.	43	Multibeam swath bathymetry – NHS	50 m	4-6 m	Likely sedimentary	No	Yes
Hazelton	West of New Hazelton, BC Canada	onshore	55°16′17 N	127°50′45″ W	1300–1530 a.s.l.	2	Satellite – Google Earth Pro	-	-	Sandstone	No	Yes
Pine Island	Pine Island Bay, West Antarctica	offshore	74°2′ S	106°10′10’ W	1250–950 b.s.l.	140	Multibeam swath bathymetry – GeoMapApp	35 m	Not known	Crystalline	No	Yes

3.2.2 Site descriptions

This section presents a brief description of each study area, focussing on relationships between BMGs and bedrock geology as well as the general structural and lithological characteristics of the bedrock. A summary of all site descriptions is presented in Table 3.2. Each site description is accompanied by an aerial image of the BMGs in their wider topographic context, and a combined geomorphological and geological map with focus on major lithology units and structural lines. For each site, the sampled grooves and the exact locations of sampling points are shown in Figure 1 in the Appendix. Each map title represents the site ID as used throughout the paper (see also Table 3.2). The arrows indicate the direction of regional palaeo-ice flow.

3.2.2.1 Haarefjord

The BMGs at Haarefjord occur in a lowland area sloping gently in a NNE–SSW direction from 350 m down to sea level, at an angle of 10–15° (Figure 3.2A). The Røde Ø conglomerate, in which the mega-grooves occur, forms an insular outcrop surrounded by Precambrian gneissic bedrock to the west (Figure 3.2B) and approximately 4 km east of the grooved terrain (Sørensen, 1970; Henriksen, 1983). The Røde Ø conglomerate typically consists of coarse sandstone and conglomerate with gneiss phenoclasts (Figure 3.2C), derived through erosion following faulting activity related to the Caledonian orogeny (Collinson, 1972) and deposited during the middle-late Permian (Stemmerick and Piasecki, 2004). The conglomerate beds show varying orientations with a low-angle dip (Figures 3.2B and C), possibly reflecting different cones of deposition (Funder, 1978), and it is generally massive or poorly jointed (Figure 3.2C). The grooves and ridges are aligned irrespective of the bedrock structure, but parallel to the palaeo-ice flow direction (Figure 3.2B) and have been interpreted as being the result of glacial erosion (Funder, 1978).

Superficial deposits are present within the grooved terrain. In the west, the fluviatile sediments obscure the BMGs, as suggested by the presence of grooved bedrock protruding through the sediment cover (Figure 3.2B). To the south-east, the area of undifferentiated sediment (Henriksen, 1983) also obscures the bedrock grooves and ridges, as suggested by the gradual fading of the groove/ridge profiles (Figure 3.2A). The unconsolidated sediments there are likely glacifluvial, as suggested by the presence of clustered sinuous ridges and mounds 50–350 m long and 1–8 m in amplitude, indicative of eskers (Figure 3.2B). To the north, the bedrock has several incisions 350–650 m long and 3–5 m deep which cross-cut the grooves and ridges. No horizontal displacement is apparent on the digital elevation model (DEM) imagery, and many ridges match on both sides of the incisions. However, the grooves have been mapped as continuous lines only where there is a clear landform continuation across a bedrock incision (Figure 3.2B).

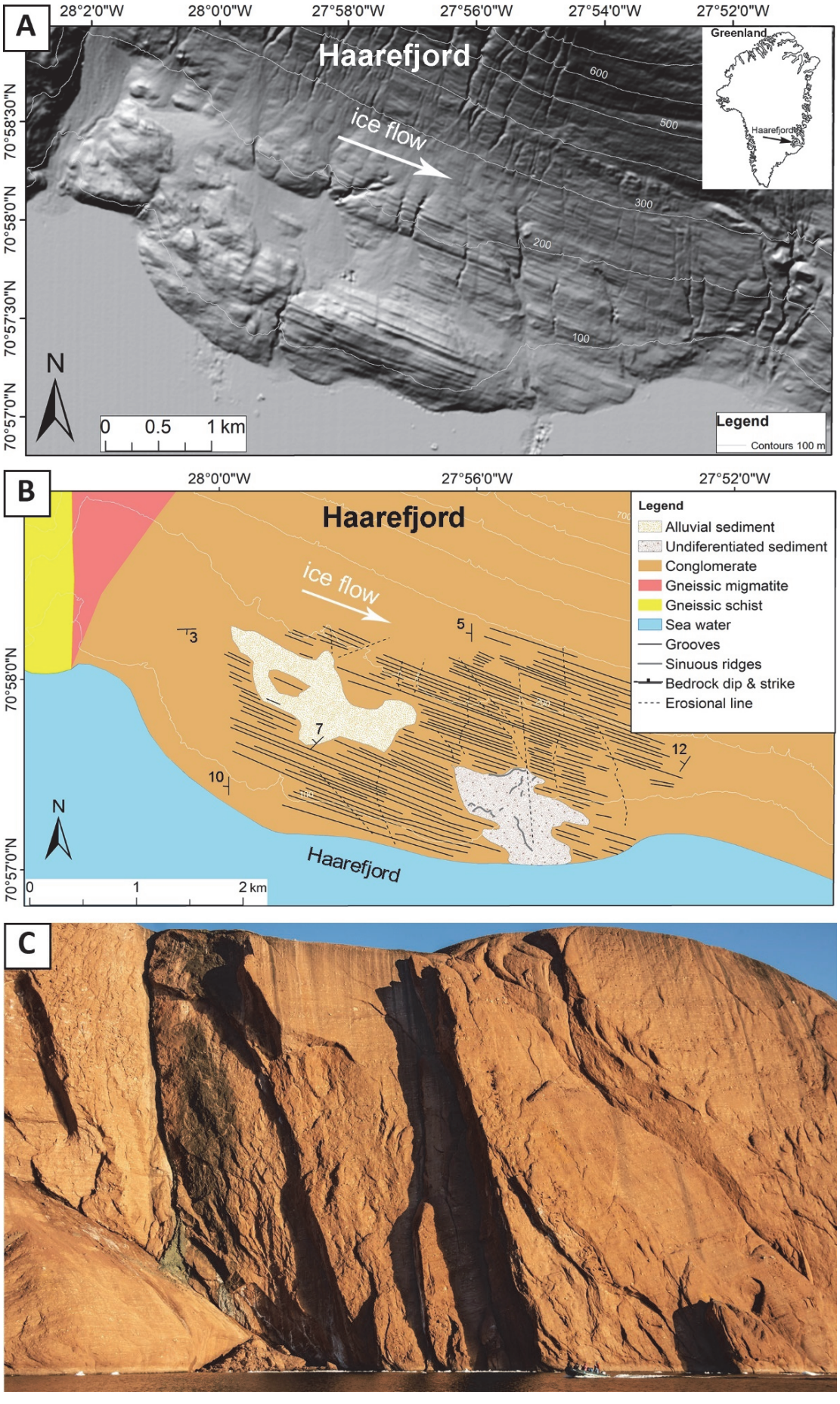
A
28°2'0"W
28°0'0"W
27°58'0"W
27°56'0"W
27°54'0"W
27°52'0"W
70°58'30"N
70°58'0"N
70°57'30"N
70°57'0"N
Haarefjord
ice flow
600
500
300
200
100
Greenland
Haarefjord
N
0 0.5 1 km
Legend
Contours 100 m
B
28°0'0"W
27°56'0"W
27°52'0"W
70°58'0"N
70°57'0"N
Haarefjord
ice flow
3
5
7
10
12
N
0 1 2 km
Legend
Alluvial sediment
Undiferentiated sediment
Conglomerate
Gneissic migmatite
Gneissic schist
Sea water
Grooves
Sinuous ridges
Bedrock dip & strike
Erosional line
C

Figure 3.2. A: Digital elevation model of the grooved terrain at Haarefjord, inner Scoresby Sund, East Greenland. Illumination angle from the north. Inset shows location of study area in eastern Greenland. Outline of inset map © PatternUniverse.com. Arctic DEM provided by the Polar Geospatial Centre under NSF-OPP awards 1043681, 1559691, and 1542736. **B:** Schematic map of bedrock and surficial geology compiled from Henriksen (1983) and the Geological Map of Greenland 1: 500,000 (2014). **C:** Outcrop of Røde Ø conglomerate at Haarefjord. Note the massive appearance of the rock with layers of clasts aligned at different angles, and the lack of jointed beds. Photo courtesy Terry Allen © allenfotowild.com.

3.2.2.2 Elphin

The Elphin grooves occur in a topographically lowland area, and trend upslope relative to the palaeo-ice flow direction (Figure 3.3A). The bedrock consists of well-bedded quartzite with a hardness of R = 61 (Krabbendam and Bradwell, 2011). Initial deposition was as horizontal beds of fine-grained sediment in a shallow marine environment during the Cambrian, and the beds subsequently tilted with a dip of 12–19 ° to the south-east and metamorphosed into quartzite (Peach et al., 1907) (Figure 3.3B). The mega-grooves are eroded into a pre-existing surface as suggested by the matching height of the intervening ridges (Figure 3.3C) and are aligned slightly obliquely to the bedrock strike (Bradwell, 2005) (Figure 3.3A).

There is widespread evidence of glacial abrasion in the form of polished rock surfaces with shallow striations less than 2 mm deep and well-rounded strata edges (Figure 3.4A), as well as vestiges of meltwater erosion (Figure 3.4B) and chattermarks (see also Bradwell, 2005). However, by far the largest volume of bedrock removed subglacially was through plucking, considering the relatively large size of plucked rocks and the abundant evidence of plucking across the grooved area (Figures 3.4C and D). Block dislocation though plucking was enabled by the three-dimensional joint system present in the bedrock, namely one nearly-horizontally defined by the bedding planes, and two nearly-vertical joint systems striking sub-perpendicular to each other (see also Krabbendam and Bradwell, 2011). The plucked blocks measure on average 10 × 15 × 30 cm (Figure 3.4D). The Elphin site represents an example of where glacial erosion was controlled by the geological structure, despite the landforms being aligned obliquely to the bedrock strike or to any other major structure.

Glaciologically, the grooved terrain at Elphin has been hypothesised as an area of fast-flow onset, along the flow corridor of a tributary glacier to the Minch Ice Stream, which drained

the north-west sector of the British Ice Sheet during the last glacial cycle (Stoker and Bradwell, 2005; Bradwell et al., 2007).

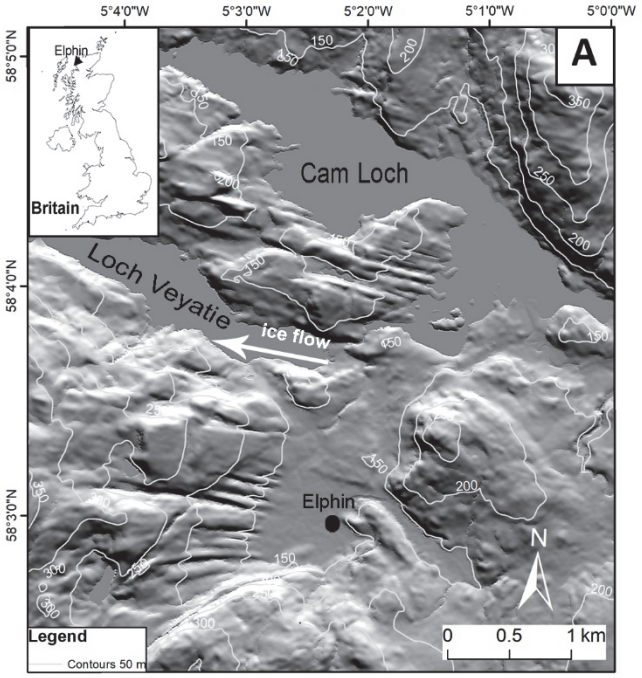
A
5°4'0"W
5°3'0"W
5°2'0"W
5°1'0"W
5°0'0"W
58°50'N
58°40'N
58°30'N
Elphin
Britain
Cam Loch
Loch Veyatie
ice flow
Elphin
N
0 0.5 1 km
Legend
Contours 50 m

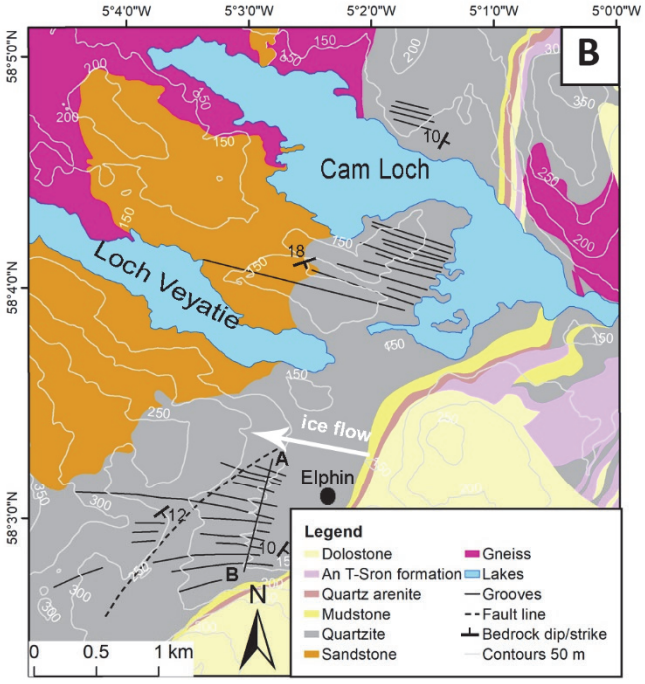
B
5°4'0"W
5°3'0"W
5°2'0"W
5°1'0"W
5°0'0"W
58°50'N
58°40'N
58°30'N
Cam Loch
Loch Veyatie
ice flow
Elphin
A
B
N
0 0.5 1 km
Legend
Dolostone
An T-Sron formation
Quartz arenite
Mudstone
Quartzite
Sandstone
Gneiss
Lakes
Grooves
Fault line
Bedrock dip/strike
Contours 50 m

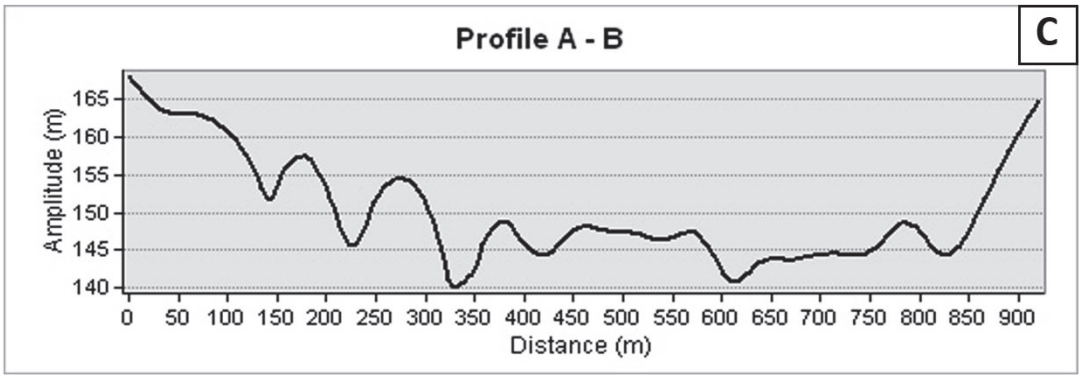
C
Profile A - B
Amplitude (m)
165
160
155
150
145
140
0 50 100 150 200 250 300 350 400 450 500 550 600 650 700 750 800 850 900
Distance (m)

Figure 3.3. A: Hill-shaded relief NEXTMap digital terrain model showing the grooved terrain west of Elphin village in Assynt, the Northwest Highlands of Scotland, UK. Illumination angle at 45° from the north. Inset shows the site location in Northwest Scotland, UK; outline of inset map © vemaps.com. Base image © NERC BGS UK. **B:** Schematic geology map showing the mega-grooves occurrence in quartz, sub-parallel to the palaeo-ice flow direction. Map modified from digital version (DigMapGB_50, 2016, https://digimap.edina.ac.uk/webhelp/digimapsupport/about_1.htm). The bedrock dip and strike was manually transferred here from the geological map Sheet 101 Ullapool bedrock (British Geological Survey, 2008). A–B represents the profile transect in Figure 3.3C. **C:** topographic profile across the grooved terrain. The A–B transect location is marked in Figure 3.3B.

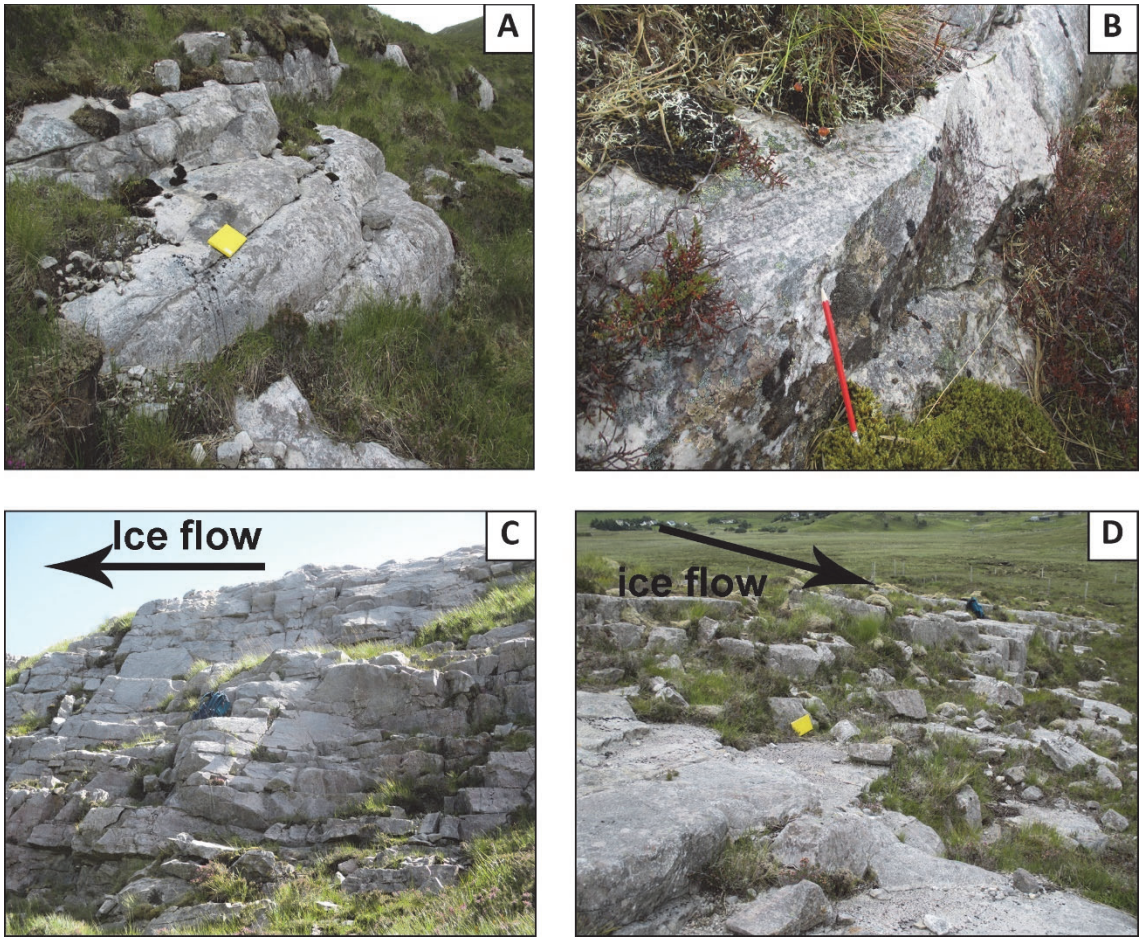

Figure 3.4. A: abraded strata edges close to the groove floor. **B:** Small-scale evidence of meltwater erosion in the form of shallow cavities with sharp edges. **C:** plucked bedrock in the groove's flank. Note the densely jointed bedrock which enabled block dislocation through plucking. **D:** plucked debris in a groove flank. Yellow notebook measures 10 × 20 cm.

3.2.2.3 Ullapool

The BMGs at Ullapool cover an area of around 60 km^2 (Figure 3.5A) and occur in metasandstone, which comprises mainly psammitic rocks (Figure 3.5B). The rocks were initially deposited as sandstone in the Proterozoic, in a fluviatile environment (Krabbendam et al., 2008) and subsequently subjected to low-grade metamorphism during the Caledonian orogenesis, which led to pervasive recrystallisation, bed thinning, and the development of strong mica foliation (Fettes et al., 1985). The overall rock hardness is R = 52, the bed thickness is 10–20 cm, the rocks are cleaved along the bedding planes and the bedrock is well jointed (Krabbendam and Bradwell, 2011).

The BMGs were first described by Bradwell et al. (2008) who proposed that they were initiated through focused glacial abrasion under fast-ice flow conditions, because the grooved terrain is situated in a zone of fast-flow onset and at the up-ice end of the Ullapool tributary, which fed into the Minch Ice Stream (Stoker and Bradwell, 2005; Bradwell et al., 2007). The BMGs were subsequently modified by lateral plucking (Krabbendam and Bradwell, 2011). The evidence for plucking is ubiquitous across the area, especially along the upper part of the ridges (Figure 3.6A). Block dislocation through plucking was enabled by the existence of a 3-dimensional system of joints present in the bedrock, namely one along the bedding planes and foliation, dipping to the south-east at shallow angles of 12–19°, and two defined by sub-vertical joint systems (J1 and J2 in Figure 3.6B) (see also Krabbendam and Bradwell, 2011 and Section 4.4.2.1 in Chapter 4).

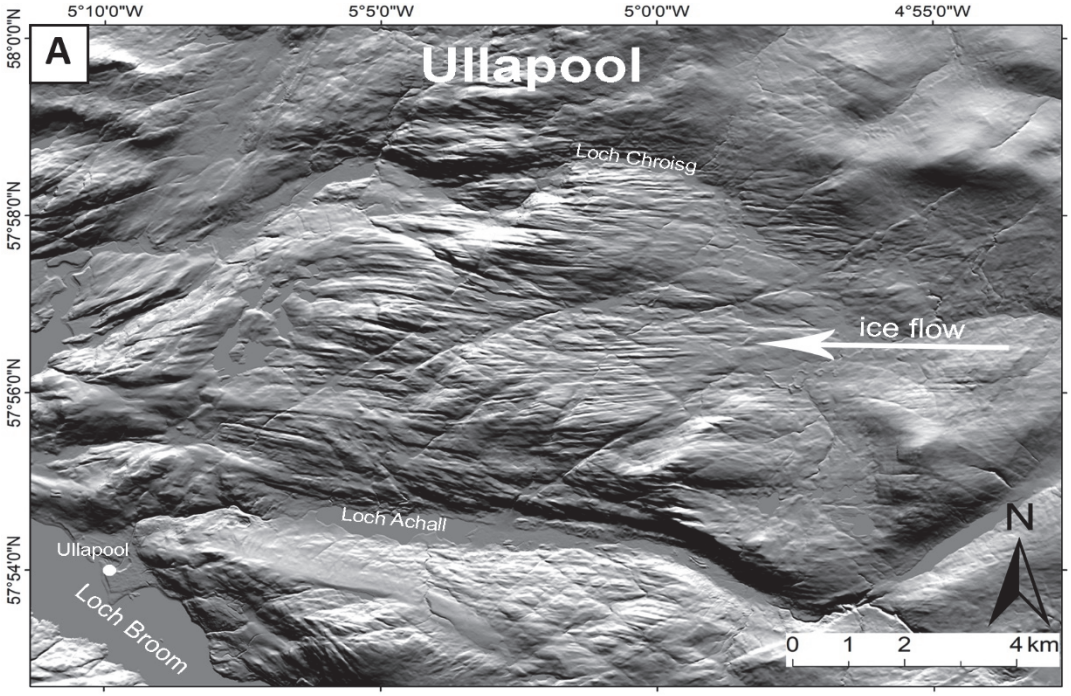
A
Ullapool
Loch Chroisg
ice flow
Loch Achall
Ullapool
Loch Broom
N
0 1 2 4 km
5°10'0"W
5°5'0"W
5°0'0"W
4°55'0"W
58°0'0"N
57°58'0"N
57°56'0"N
57°54'0"N

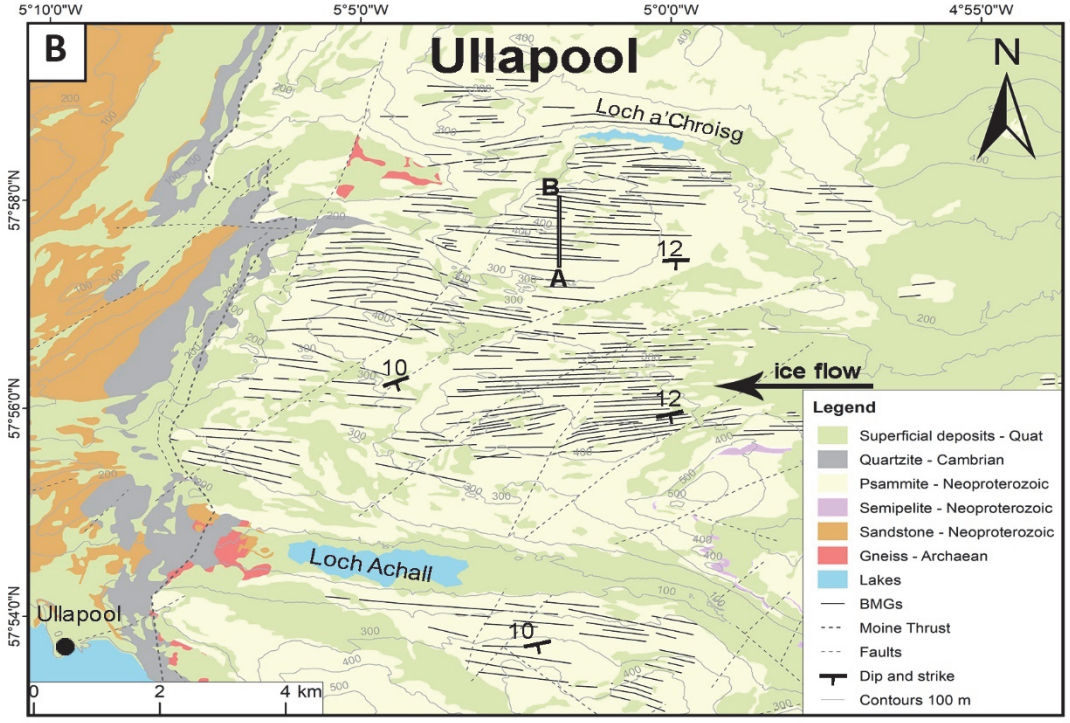
B
Ullapool
Loch a'Chroisg
N
B
A
12
10
12
ice flow
Loch Achall
Ullapool
10
0 2 4 km
Legend
Superficial deposits - Quat
Quartzite - Cambrian
Psammite - Neoproterozoic
Semipelite - Neoproterozoic
Sandstone - Neoproterozoic
Gneiss - Archaean
Lakes
BMGs
Moine Thrust
Faults
Dip and strike
Contours 100 m
5°10'0"W
5°5'0"W
5°0'0"W
4°55'0"W
57°58'0"N
57°56'0"N
57°54'0"N

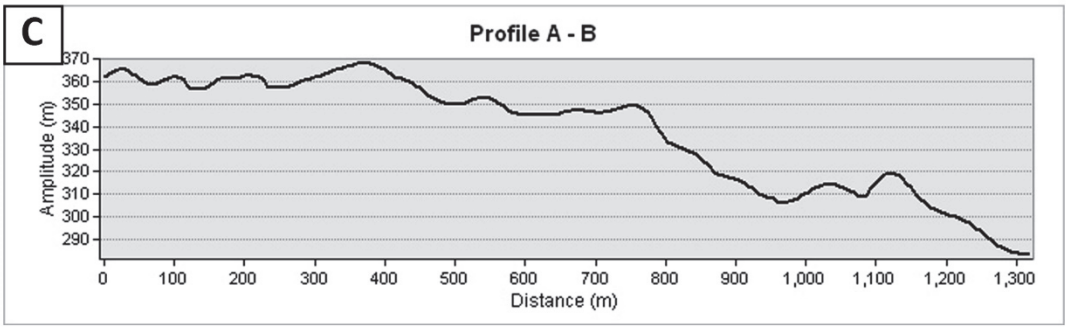
C
Profile A - B
Amplitude (m)
370
360
350
340
330
320
310
300
290
0 100 200 300 400 500 600 700 800 900 1,000 1,100 1,200 1,300
Distance (m)

Figure 3.5. A: Hill-shaded relief NEXTMap digital terrain model showing the grooved terrain north-east of Ullapool in Assynt, Scotland, UK. Illumination angle at 45° from the north-west. Inset shows location of the Ullapool site in NW Scotland, UK; outline of inset map © vemaps.com. Base image © NERC BGS UK. **B:** Simplified map of bedrock geology. Note the grooves being confined to psammitic rocks. A–B marks the transect of profile in Figure 3.5C. The dip and strike of the bedding planes was manually digitised from the geological map Sheet 101 Ullapool bedrock (British Geological Survey, 2008). Map modified from digital version of geology map (DigMapGB_50, 2016 https://digimap.edina.ac.uk/webhelp/digimapsupport/about_1.htm). **C:** Profile across the grooved area. The profile transect A–B is marked in Figure 3.5B. The southern, shallow flank of the grooves corresponds to the bedrock dip plane.

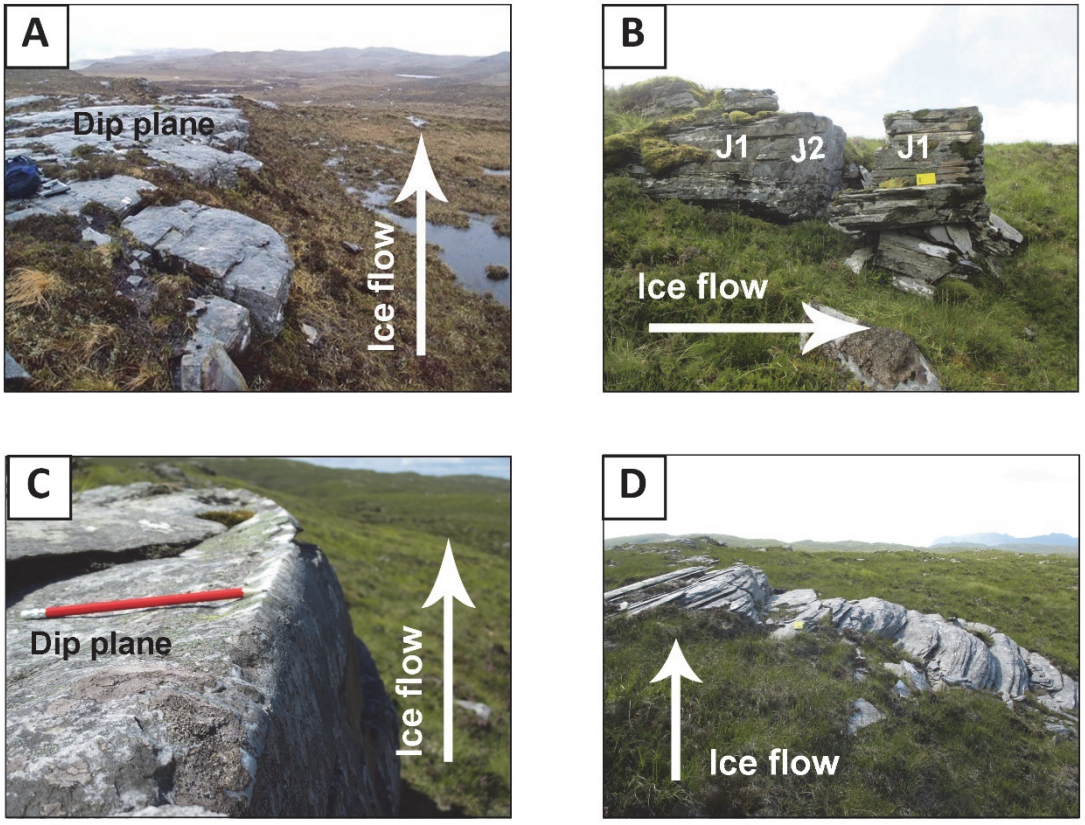

Figure 3.6. A: Plucking along the edge of a groove. Note the zig-zag profile of the groove edge. Photo M Krabbendam © NERC, UK. **B:** psammite block dislocated through plucking southeast of Loch a'Chroisg. The plucked rock has been dislocated along the sub-vertical joint planes J1 and J2, perpendicular to each other, and the bedding plane on which the yellow field book is resting. **C:** abraded quartz-rich edge of bedrock strata. Pencil resting on the bedrock dip slope. **D:** strata edges rounded by abrasion in thinly layered psammitic rocks, close to the floor of a mega-groove. Ice flow was from east to west.

Typically, the plucked rock faces have a fresh aspect, with smooth surfaces and sharp edges, and sometimes the dislocated blocks are present close to the place of dislocation (Figure 3.6B). Abrasion occurs in the form of rounded strata edges (Figures 3.6C and D) rather than glacial striations, as they have likely been removed through post-glacial erosion aided by

the susceptibility of metasandstone to exfoliation. Striations with a general east–west alignment are abundant on other lithologies along the same flow corridor (Lawson, 1996; Krabbendam and Glasser, 2011), which verifies that the BMGs are aligned parallel to former ice flow direction. The Ullapool BMGs have a stair-case profile that is characteristic of grooves in layered rocks (Figure 3.5C) (Krabbendam and Bradwell, 2011; Krabbendam et al., 2016), where the shallow groove flank typically corresponds to the bedrock dip plane (Figure 3.6A and C), and the steep flank was developed along sub-vertical joints (see also Figure 2.10 in Chapter 2).

3.2.2.4 Franklin

These mega-grooves are located on the western flank of the Franklin Mountains Range, on a slope positioned on the lee side relative to the palaeo-ice flow direction, to the WNW (Figure 3.7A). Franklin is the most easterly site described by Smith (1948) in his benchmark paper, where BMGs up to 60 m deep occur in the Bear Rock formation, and represent the deepest BMGs reported on-shore (see Table 2.1 in Chapter 2). The Bear Rock formation is the lower member in the normal Devonian stratigraphy (Figure 3.7B). It consists of brecciated limestone with a rubbly and massive structure (Fallas, 2013) and is prone to water dissolution as suggested by the widespread occurrence of well-developed karstic landforms (Hamilton and Ford, 2002). The BMGs attain considerable depth in the Devonian limestone, while in the Cretaceous sedimentary rocks they reach 1–2 km in length (Figure 3.7B) and are relatively shallow, being only 1–5 m deep (Smith, 1948). The Cretaceous sequence consists of soft sedimentary rocks, comprising mudstone, shale and sandstone; the latter is described as friable and porous in most Cretaceous formations (Fallas, 2013). Some mega-grooves show continuity when crossing the lithological boundaries between the Devonian and the Cretaceous, but they are mostly discontinuous across the lithological boundaries between the Devonian limestone and the Bear Rock formation (Figure 3.7B). The BMGs are aligned on the dip slope of an anticline,

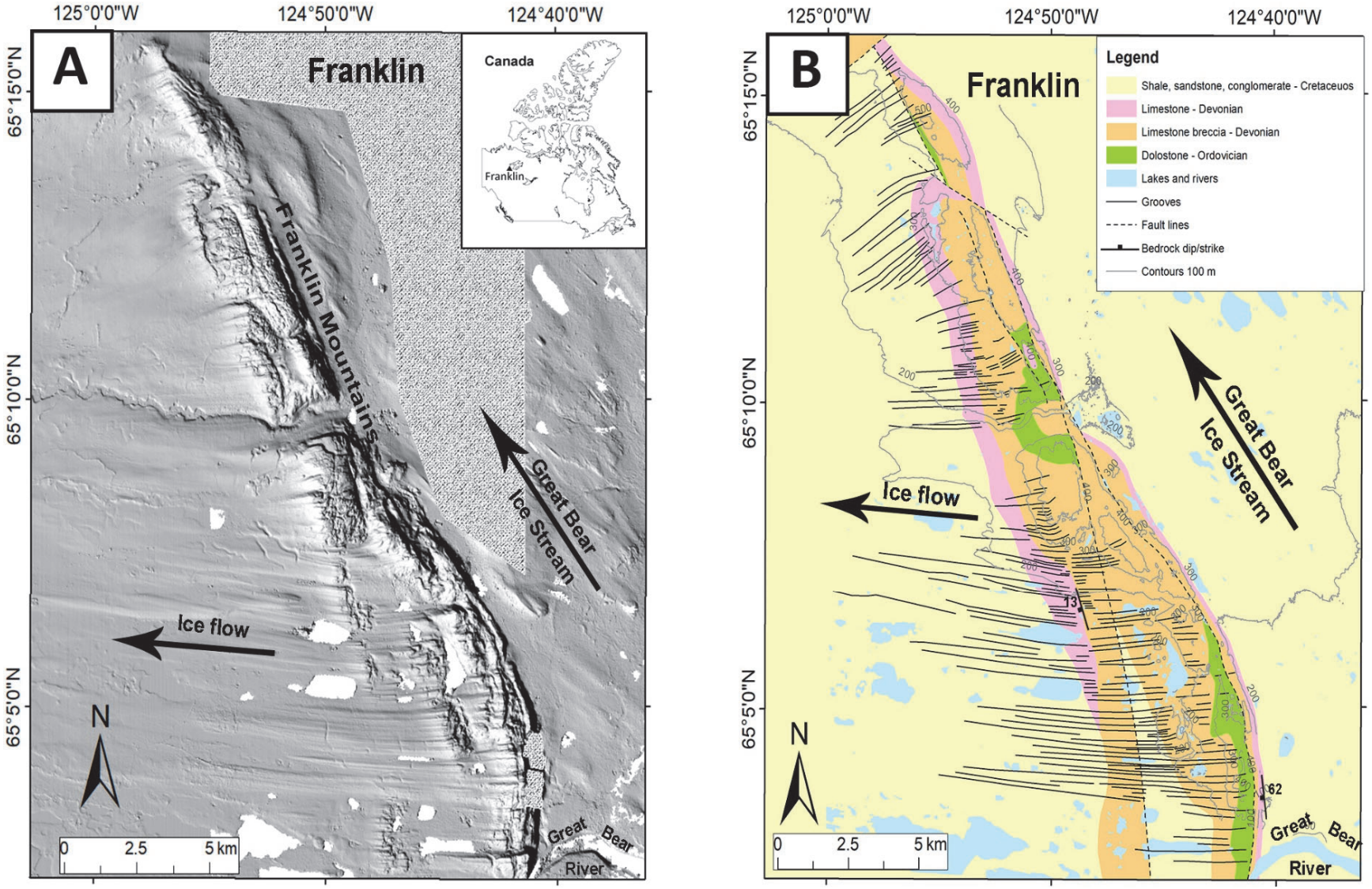
A
Franklin
Canada
Franklin
Franklin Mountains
Great Bear
Ice Stream
Ice flow
N
0
2.5
5 km
Great Bear
River
125°0'0"W
124°50'0"W
124°40'0"W
65°15'0"N
65°10'0"N
65°5'0"N
B
Franklin
Legend
Shale, sandstone, conglomerate - Cretaceuos
Limestone - Devonian
Limestone breccia - Devonian
Dolostone - Ordovician
Lakes and rivers
Grooves
Fault lines
Bedrock dip/strike
Contours 100 m
Great Bear
Ice Stream
Ice flow
13
62
N
0
2.5
5 km
Great Bear
River

Figure 3.7. A: Digital elevation model of the grooved terrain at Franklin Mountains, Northwest Territories, Canada. The site lies halfway between the southwest termination of the Great Bear Lake and the Mackenzie River, and the Franklin Mountains ridge is traversed by the Great Bear River. Textured fill represents data voids on the Arctic DEM due to data collection methods (see Section 3.3.1) and the white areas are lakes or rivers. Illumination angle at 45° from the south. Inset shows location of the Franklin site in the Northwest Territories, Arctic Canada. Outline of inset map © vemaps.com. Arctic DEM provided by the Polar Geospatial Centre under NSF-OPP awards 1043681, 1559691, and 1542736. **B:** Schematic geology and geomorphology map showing the mega-grooves and the main rock units. The Devonian limestone breccia is commonly referred to as the Bear Rock Formation. The geology map was simplified from Fallas (2013).

perpendicular to bedrock strike and at an angle to other major structural lines, such as faults (Figure 3.7B). Although not recorded on the geological maps consulted for this study, medium-scale structural features, such as fractures and joints, are typically present in Cretaceous rocks and Devonian sedimentary rocks, as documented to the west of the Franklin Ridge (Tassonyi i, 1969; see also Section 3.2.2.4), which likely enabled glacial plucking.

Regarding the palaeo-glaciology, there is some uncertainty as to whether the flow was through streaming or slower, non-streaming ice sheet flow conditions. The paleo-glacier east of the Franklin Mountains has been interpreted as a branch of the Great Bear Ice Stream (Margold et al., 2015), identified as an area of fast-flowing ice based on its characteristic streamlined bedform imprint, mostly in unconsolidated sediment (Brown et al., 2011; Brown, 2012; Margold et. al., 2015). West of the Franklin Mountains the streamlined terrain is composed of BMGs rather than MSGLs, which occur over large but discontinuous areas. In addition, the BMGs trend in a general NNW direction, being broadly parallel to the Mackenzie River valley (Smith, 1948), and at an angle of approximately 45° to the inferred flow direction of the Great Bear Ice Stream (Figure 3.7A) (Margold et. al., 2015). Although ice streaming cannot be ruled out, a degree of uncertainty remains over the ice flow regime at Franklin.

3.2.2.5 Hanna

The site is referred to in the geological literature as “East Mountain” (Hume, 1954; Tassonyi, 1969) and “Site J” in Smith’s (1948) nomenclature, but here it is assigned the name “Hanna” after the adjacent Hanna River (Figure 3.8A). Hanna is the western-most site described by Smith (1948), who noted that the grooves occur in fossiliferous Devonian limestone (Figure 3.8B) and also that they change their alignment from ESE–WNW to SE–NW (Figure 3.8C), which he attributed to a change in ice flow direction. The ice flow direction was up-slope, and the grooves occur on the southern flank of an anticline with an east-west axis and are aligned sub-parallel to the anticline a-axis (Figure 3.8B).

The BMGs are confined to the Ramparts formation, of middle Devonian age (Figure 3.8B), consisting of two members of marine limestone: the lower Platform Member comprises well-bedded strata, and the upper Reef member is coralline and more massive (Tassonyi, 1969). The Ramparts formation in and around the study site comprises both the well-bedded and jointed limestone interbedded with shale, as well as the more massive and porous coraline beds (Hume, 1954 and references therein to the unpublished Canol Reports). Albeit speculative, it could be regarded that the change in mega-groove orientation noted by Smith (1948) (Figure 3.8C) reflects a stratigraphic boundary between the two members, rather than a change in the ice-flow direction.

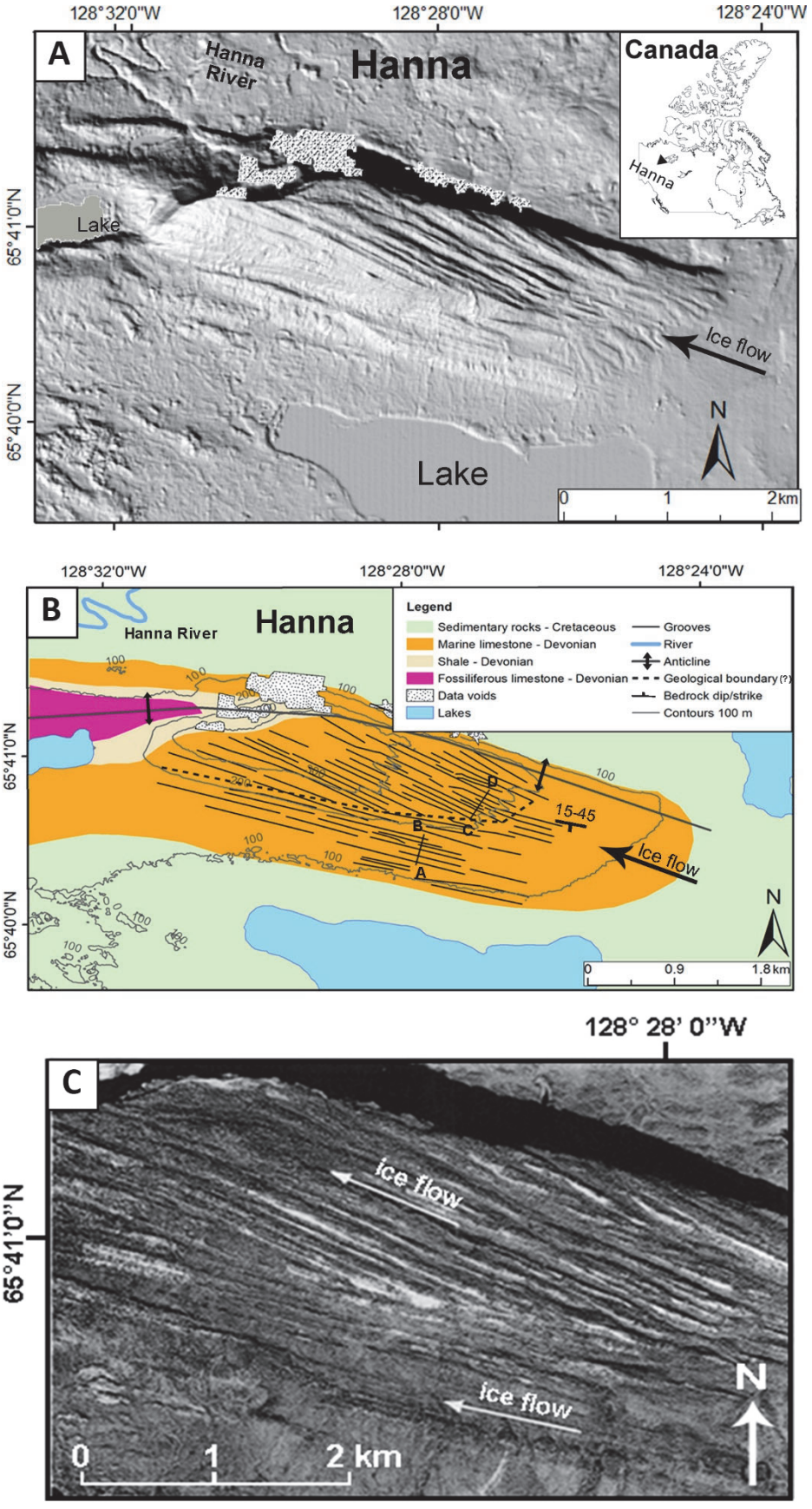
A
Hanna River
Hanna
Canada
Hanna
Lake
Ice flow
N
Lake
0 1 2km
128°32'0"W
128°28'0"W
128°24'0"W
65°41'0"N
65°40'0"N
B
Hanna River
Hanna
Legend
Sedimentary rocks - Cretaceous
Marine limestone - Devonian
Shale - Devonian
Fossiliferous limestone - Devonian
Data voids
Lakes
Grooves
River
Anticline
Geological boundary (?)
Bedrock dip/strike
Contours 100 m
15-45
Ice flow
N
0 0.9 1.8 km
C
128° 28' 0"W
65°41'0"N
ice flow
ice flow
N
0 1 2 km

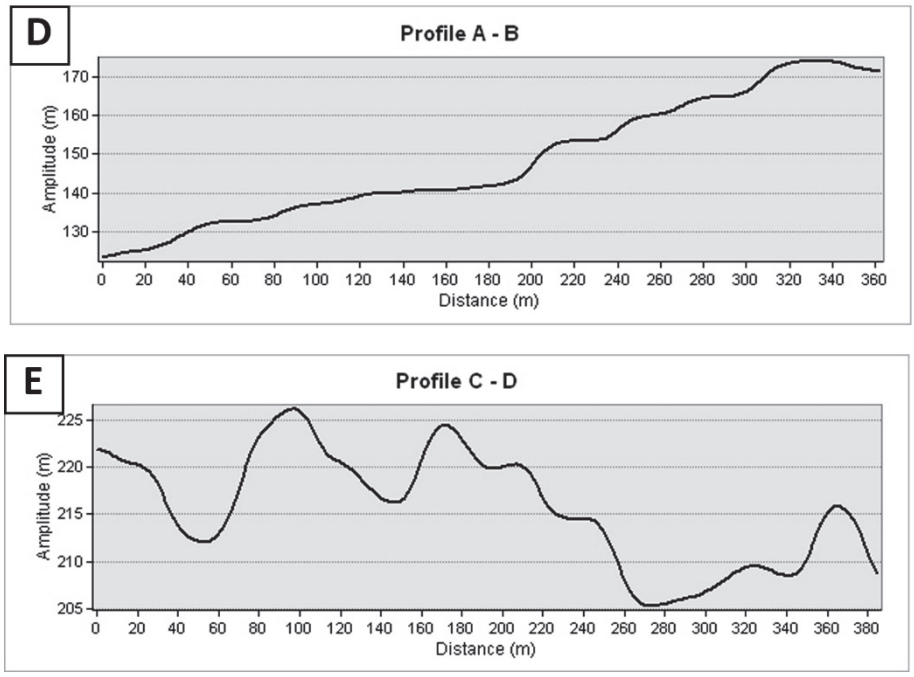

Figure 3.8. A: Digital elevation model of the grooved terrain at Hanna, Northwest Territories, Canada. Illumination angle at 45° from the north-east. Arctic DEM provided by the Polar Geospatial Centre under NSF-OPP awards 1043681, 1559691, and 1542736. Textured areas represent data voids due to data collection methods (see Section 3.3.1). Inset shows location of the Hanna site in the Northwest Territories, Canada. Outline map © vemaps.com. **B:** Schematic geological map showing BMG occurrence in the marine Devonian limestone. The geology map was manually digitised and simplified from Aitken and Cook (1979). **C:** Aerial photograph of the Hanna site modified from Smith (1948) and reproduced with permission from the American Bulletin of Science. The white arrows show the two different orientations of the mega-grooves, attributed by Smith (1984) to different ice-flow directions. Base image © *RCAF.* **D, E:** profiles across the grooved area along transects A–B and C–D, marked in Figure 3.8B.

The author is not aware of any detailed empirical evidence pertaining to either the bedrock structure or to glacial erosion of the BMGs at Hanna, but a few inferences regarding these aspects could be attempted. First, considering the bed thickness for the Ramparts formation of 1.2–3.6 m as inferred from McLaren (1962), a conservative expectation is that the joint spacing is equal to the bed thickness, which has been found to be valid in bedded and jointed rocks regardless of scale (see Figure 8.13 in Fossen, 2016). This could be used as a minimum boundary value for rock debris dislocated through plucking, if plucking did occur. Second, the BMGs south of this limit are parallel to the bedrock strike (Figure 3.8D) and have a stepped profile (Figure 3.8D), typical of grooves formed in layered rocks due to lateral plucking (Krabbendam and Bradwell, 2011; Figure 3.5C). The BMGs north of this boundary form a corrugated surface of alternating grooves and ridges (Figure 3.8E), characteristic of mega-grooves eroded into a flat surface, similar to that at Elphin (Figure 3.3C).

Collectively the data suggest that there is scope for structural control of the BMGs at Hanna, with plucking likely to have occurred particularly where the BMGs are aligned parallel to the bedrock strike. The palaeoglaciological conditions are regarded as slower ice sheet flow, rather than ice streaming, due to the absence of a coherent palaeo-ice landsystem in the area, and a considerable distance of approximately 200 km to the Great Bear Ice Stream, which is the nearest reconstructed palaeo-ice stream (Margold et al., 2015).

3.2.2.6 Beavertail

The Beavertail Range is located ca. 12 km north of the Hanna site. The grooves occur on the north-western flank of the Beavertail Range, on the lee side relative to the palaeo-ice flow direction (Figure 3.9A). The grooves were mapped by Duk-Rodkin and Hughes (1993) as prominent landforms with a thin veneer of till of 0–2 m, which likely conforms to the bedrock topography, but no further description was provided. Their alignment to the north-west is consistent with the regional ice-flow direction as well as with the alignment of other BMGs documented in the wider area (Smith, 1948) and based on this, they are regarded as BMGs formed subglacially. The BMGs occur in the Reef member of the Ramparts Formation, comprising both coralline, more massive rocks, as well as harder and bedded limestone (Hume, 1954). The grooves are located on the dip slope of the Beavertail anticline flank, perpendicular to the bedrock strike (Figure 3.9B) and are independent of major geological structures. Regarding potential mechanisms for BMG formation, there is scope for glacial abrasion considering the massive and porous bedrock, as well as for plucking, given the presence of potentially well-jointed sedimentary rocks. Chemical erosion through dissolution may also have played a part in erosion considering the calcareous nature of the rocks. However, in the absence of detailed empirical evidence, it remains difficult to assess the prevalence of a specific erosion mechanism.

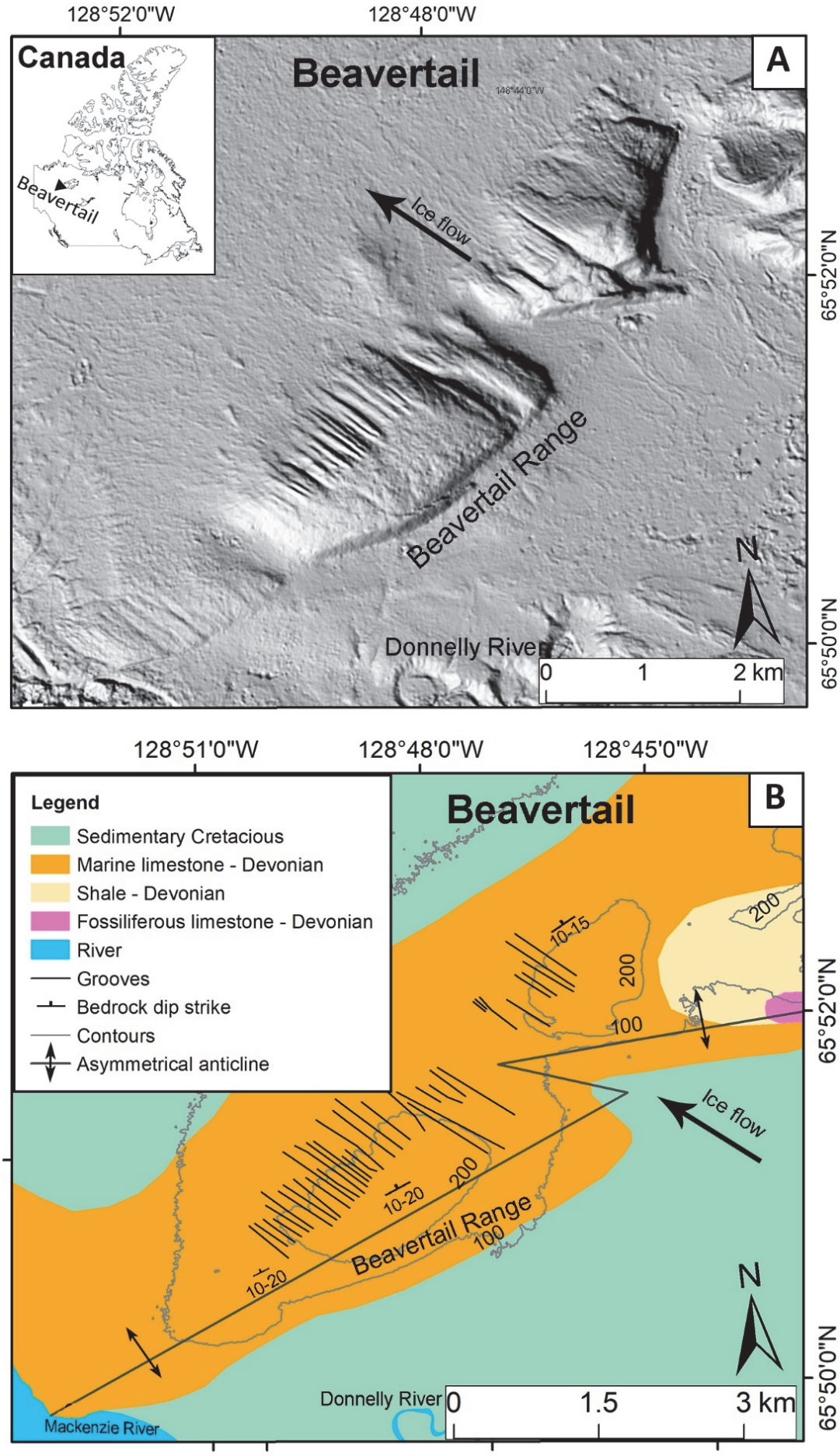
128°52'0"W
128°48'0"W
Canada
Beavertail
A
Ice flow
Beavertail Range
Donnelly River
N
0
1
2 km
65°52'0"N
65°50'0"N
128°51'0"W
128°48'0"W
128°45'0"W
Legend
Sedimentary Cretacious
Marine limestone - Devonian
Shale - Devonian
Fossiliferous limestone - Devonian
River
Grooves
Bedrock dip strike
Contours
Asymmetrical anticline
Beavertail
B
10-15
200
100
10-20
Mackenzie River
0
1.5
3 km

Figure 3.9. A: Digital elevation model of the grooved terrain at Beavertail, Northwest Territories, Canada. Illumination angle at 45° from the north-east. Inset shows location of the Beavertail site in the Northwest territories, Canada. Outline of inset map © vemaps.com. Arctic DEM provided by the Polar Geospatial Centre under NSF-OPP awards 1043681, 1559691, and 1542736. **B:** Schematic geological map showing the mega-groove occurrence in the context of the bedrock geology. The geology map was manually digitised and simplified from Aitken and Cook (1979).

The area was glaciated multiple times during the Quaternary considering its location in Arctic Canada (Batchelor et al., 2019), but no ice streaming has yet been inferred at Beavertail, and the grooved terrain is a rather isolated occurrence (Figure 3.9A). It is therefore assumed that the palaeoglaciological conditions were of slower, ice sheet flow.

3.2.2.7 Iivaara

The mega-grooves at Iivaara are located in eastern Finland, on a lee-side slope relative to the palaeo-ice flow direction (Figure 3.10A). The landforms were included in the Kuusamo ice lobe complex (Punkari, 1980), and later interpreted as part of a Kuusamo palaeo-ice stream based on the high elongation ratio of streamlined bedforms (up to 48:1) and the abrupt termination of the wider streamlined complex to the south (Sutinen et al., 2010). The grooves are interpreted to have formed through glacial erosion and they lack any structural control (Sutinen et al., 2010).

The Iivaara site is underlain by an igneous alkaline complex comprising syenite, present within the gneissic parent rock (Geological Survey of Finland, 2016) (Figure 3.10B). Outside the alkaline complex, on the gneissic parent rock, the landforms are mostly flutings of large dimensions and widely spaced out, in contrast with the narrow and closely spaced BMGs at Iivaara (see Fig. 2 in Sutinen et al., 2010). This conspicuous morphological contrast suggests a lithological control over the landform development. The alkaline complex at Iivaara is petrographically heterogeneous on a micro-scale (millimetre to centimetre), comprising rocks of different mineralogy separated by a dense and chaotic network of cross-cutting mineral veins (Lehijärvi, 1960; Sindern and Kramm, 2000) (Figure 3.10C). The structure and the relationship between different types of rocks and minerals remain poorly understood (Lehtinen et al., 2005), but any heterogeneity in the composition of a rock is potentially subject to differential weathering and can lead to mechanical weaknesses, which are subsequently exploited by erosion. It is difficult to speculate with regards to a mechanism of BMG formation in the absence of detailed field evidence. However, considering the lack of bedding, the chaotic spatial arrangement of the mineral veins and the small scale at which petrographic heterogeneities occur, it is unlikely that plucking was systematic (*sensu* Krabbendam and Bradwell, 2011) or that it dislocated large enough rock fragments to have contributed substantially to BMG modification, so there is reduced scope for structural control over BMG genesis in this location.

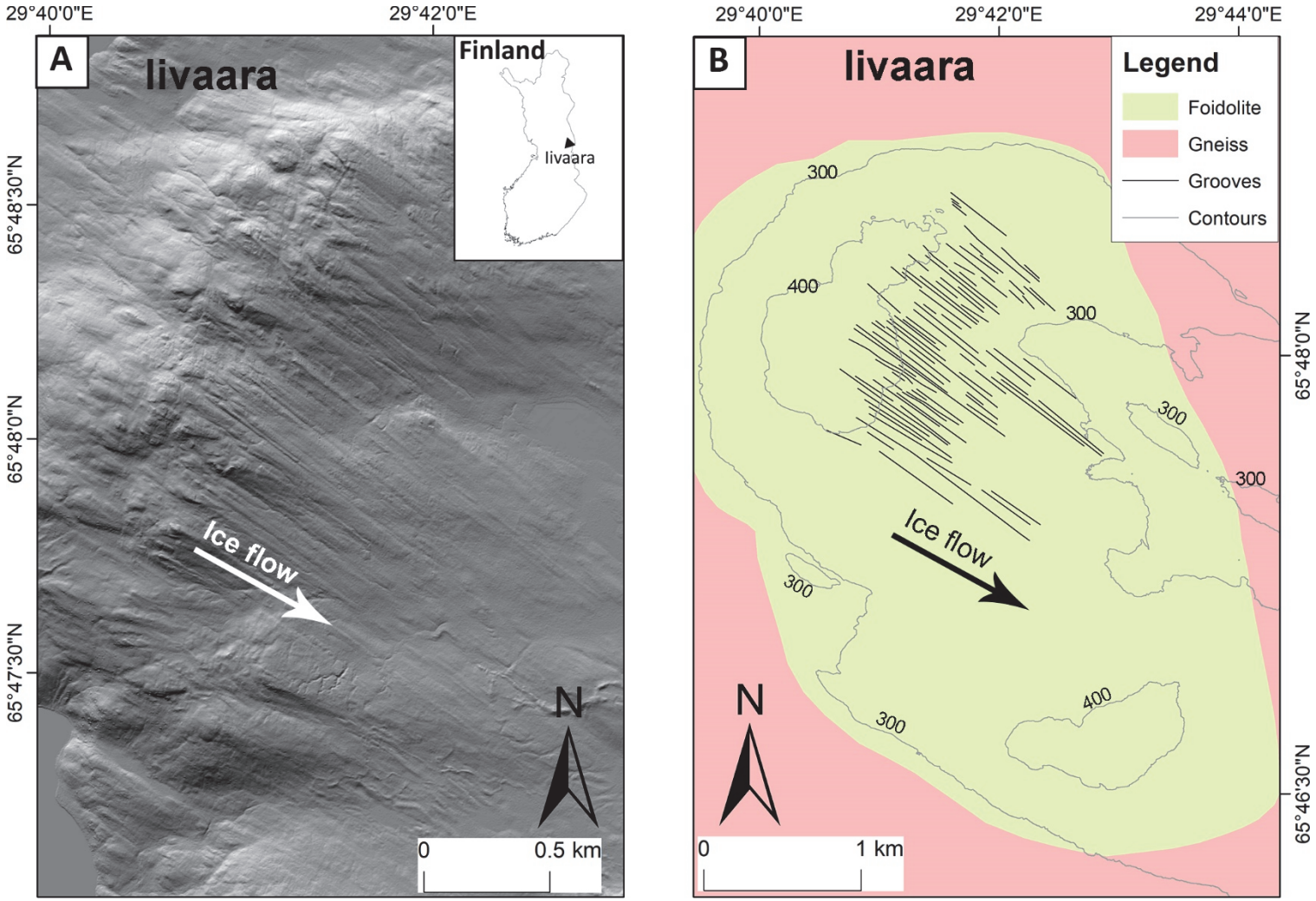
A
Iivaara
Finland
Iivaara
Ice flow
N
0
0.5 km
29°40'0"E
29°42'0"E
65°48'30"N
65°48'0"N
65°47'30"N
B
Iivaara
Legend
Foidolite
Gneiss
Grooves
Contours
300
400
Ice flow
N
0
1 km
29°40'0"E
29°42'0"E
29°44'0"E
65°48'0"N
65°46'30"N

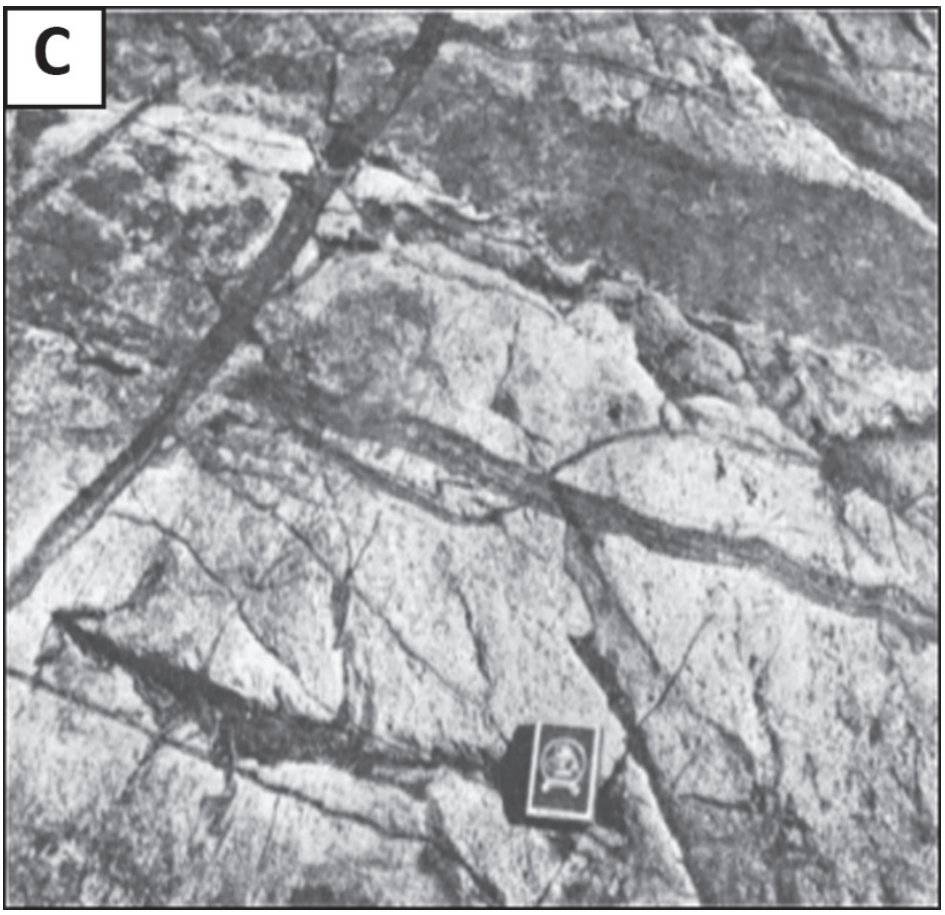

Figure 3.10. A: Digital elevation model of the Iivaara site, located in the Kuusamo area, eastern Finland. Inset shows location of the Iivaara site in eastern Finland; outline of inset map © vemaps.com. Base image © National Land Survey of Finland. **B:** Geological map of Iivaara modified from the GIS database of the Geological Survey of Finland (2016). **C:** Pyroxene-rich veins criss-crossing the paler rock. Image reproduced from Lehijärvi (1960).

3.2.2.8 Vikna

The BMGs at Vikna are situated offshore, on the Norwegian continental shelf (inset in Figure 3.11A). Typically, the inner Norwegian continental shelf is composed of Precambrian metamorphic rocks, whereas the mid-shelf consists of younger sedimentary rocks of Palaeozoic and Mesozoic age, with the strike broadly parallel to the coastline (Bugge et al., 1984). At Vikna, the likely lithological units have been inferred based on the differences in the general aspect of the topography (Figure 3.11A and B). The grooving becomes more attenuated towards the west, possibly due to the presence of thicker unconsolidated sediment (Figure 3.11B).

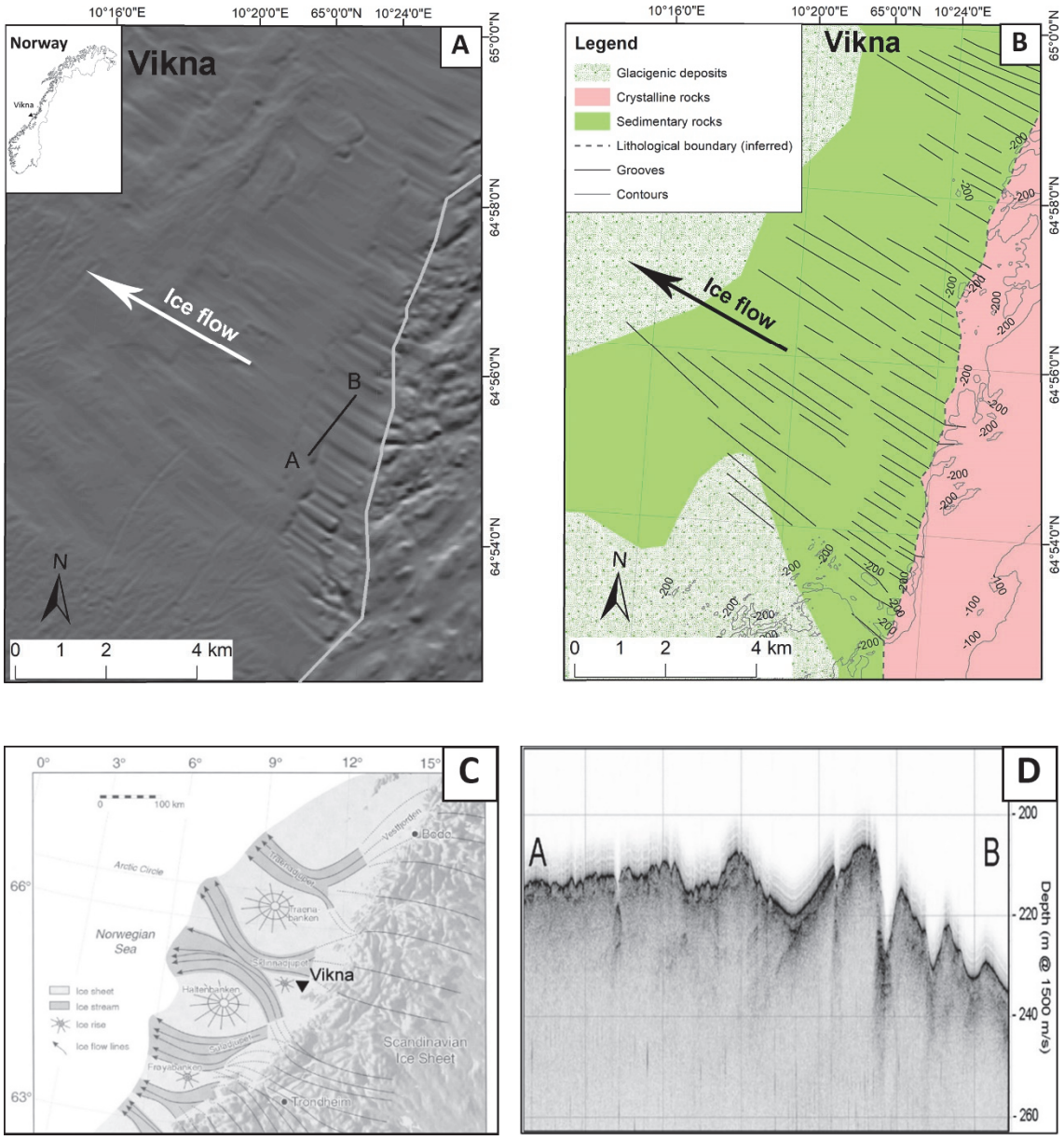

Figure 3.11. A: Digital elevation model of the Vikna site. The grey line represents the inferred lithological boundary between crystalline and sedimentary bedrock. A–B represents the transect of the seismic profile in Figure 3.9D. Inset shows location of the Vikna site in western Norway; outline map © vemaps.com. Base image © Norwegian Hydrographic Service. **B:** Inferred geological map of the Vikna site. **C:** Location of the Vikna site in relation to palaeo-ice streams. Image modified from Ottesen et al., 2002. Base image © Geological Society of London **D:** Seismic profile at Vikna with substrate aspect showing that the grooves occur in bedrock. Profile transect shown in Figure 3.11A. Image courtesy Dag Ottesen.

The BMGs occur in the fast-flow onset zone of the Sklinnadjupet palaeo-ice stream (Figure 3.11C), one of the numerous ice streams which drained the Fennoscandian Ice Sheet to the west during the last deglaciation (Ottesen et al., 2005). Palaeo-ice stream reconstructions on the Norwegian continental shelf were based on the characteristic streamlined bedrock forms closer to the fast-flow onset zone, followed to the west by long trains of MSGLs in

unconsolidated sediments stretching across the outer continental shelf (Ottesen et al., 2002). The Sklinnadjupet ice stream flowed to the north-west and formed a large streamlined bedform assemblage down-flow from the grooves at Vikna (Ottesen et al., 2005), but it is at Vikna where the BMGs have the clearest geomorphic expression and dominate the topography. Seismic profiles show that the grooves at Vikna were eroded in bedrock (Figure 3.11D). The geological and palaeoglaciological scenario at Vikna is similar to that in Ontario, Canada, where the Huron palaeo-ice stream initiated its fast flow over the gneissic bedrock of the Canadian Shield and flowed westwards over the Palaeozoic sedimentary bedrock where it produced streamlined bedforms, including BMGs (Eyles, 2012; Krabbendam at al., 2016).

3.2.2.9 Hazelton

The BMGs occur on the south-western flank of the Hazelton Ridge, on the lee side relative to the regional palaeo-ice flow direction (Figure 3.12A) and have been eroded in sedimentary rocks of the Lower Cretaceous formations, along the dip planes, sub-perpendicular to the bedrock strike (Figure 3.12B). The rocks consist of sandstone, siltstone and mudstone (Aldrick et al., 2006; Evenchick et. al., 2008). The BMGs, previously assigned a glacial origin by Krabbendam et al. (2016), have recently been interpreted as part of a wider streamlined bedform assemblage formed by the Skeena Ice Stream (Eyles et al., 2018). The Skeena Ice Stream was a land-terminating ice stream which flowed southwards in the British Columbia Cordillera and left a rich archive of streamlined bedrock forms along the main valleys and across high-altitude plateaus, as well as MSGLs in the lowlands outside the mountainous area (Eyles et al., 2018). In the absence of empirical evidence pertaining to the BMGs, or a more detailed relationship to geological structure, it is difficult to assess the main mechanism of erosion responsible for their formation. In general, sedimentary Cretaceous strata comprise bedded rocks, with beds of varying thickness and hardness (Aldrick et al., 2006; Evenchick et.al., 2008), which may have enabled plucking to occur.

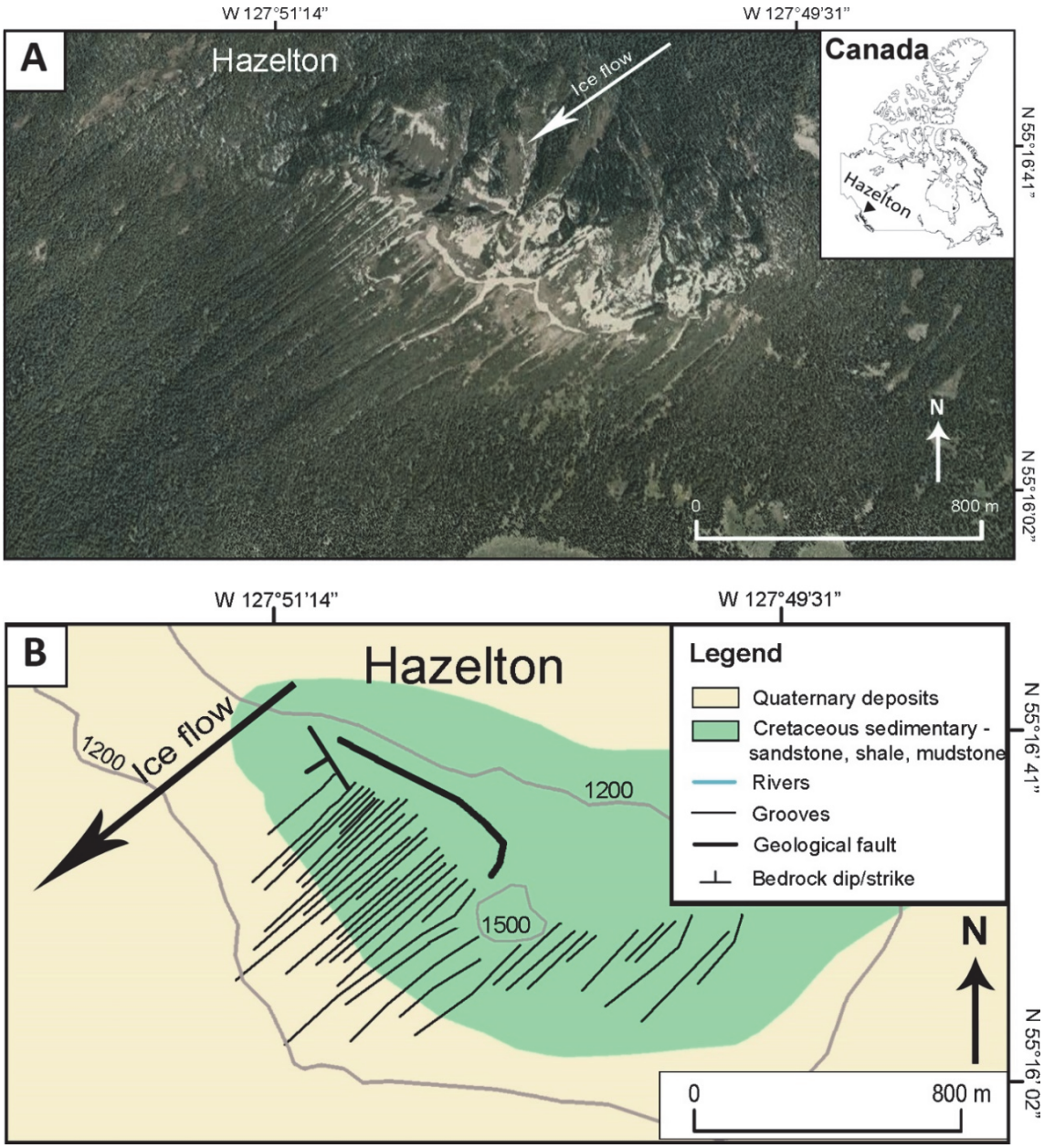

Figure 3.12. A: Aerial photograph of the grooved terrain at Hazelton. The site is located west of Skeena River, ca 10 km north-west from New Hazelton town, British Columbia, Canada. Image © GoogleEarth Pro. **B:** Simplified geological map, digitised from Evenchick et al. (2008).

3.2.2.10 Pine Island

The Pine Island study area is situated on the inner West Antarctic continental shelf, relatively close to the current ice margin (Figure 3.12A) and comprises grooves and streamlined ridges interpreted as being formed through a combination of glacial erosion and subglacial meltwater under ice-streaming conditions (Lowe and Anderson, 2002 and 2003). Meltwater, in particular, is regarded as an important erosive agent on the ice stream bed at Pine Island, with the recognition of a huge anastomosing system of large-scale

bedrock channels upstream from the grooved terrain, thought to have formed through rapid meltwater erosion following subglacial lake outbursts (Kirkham et al., 2019). The Pine Island glacier has repeatedly advanced and retreated during the late Quaternary (Graham et al., 2010) and its bed has been identified as an area subject to intense erosion upstream from the grooved area (Smith et al., 2012). The palaeo-ice stream at Pine Island has left a clear geomorphic signature in the substrate, with BMGs being a common occurrence in the upper part of a palaeo-ice stream landsystem, alongside other bedrock forms elongated in the ice flow direction, including canyons, rock drumlins and crag-and-tails (Lowe and Anderson, 2003). The results of geophysical investigations show that the substrate consists of crystalline bedrock with unconsolidated deposits forming a thin and patchy cover, which suggests groove occurrence in bedrock. Collectively, the evidence strongly suggests a glacial origin for the BMGs, which formed through erosion into the crystalline bedrock under fast-ice flow conditions.

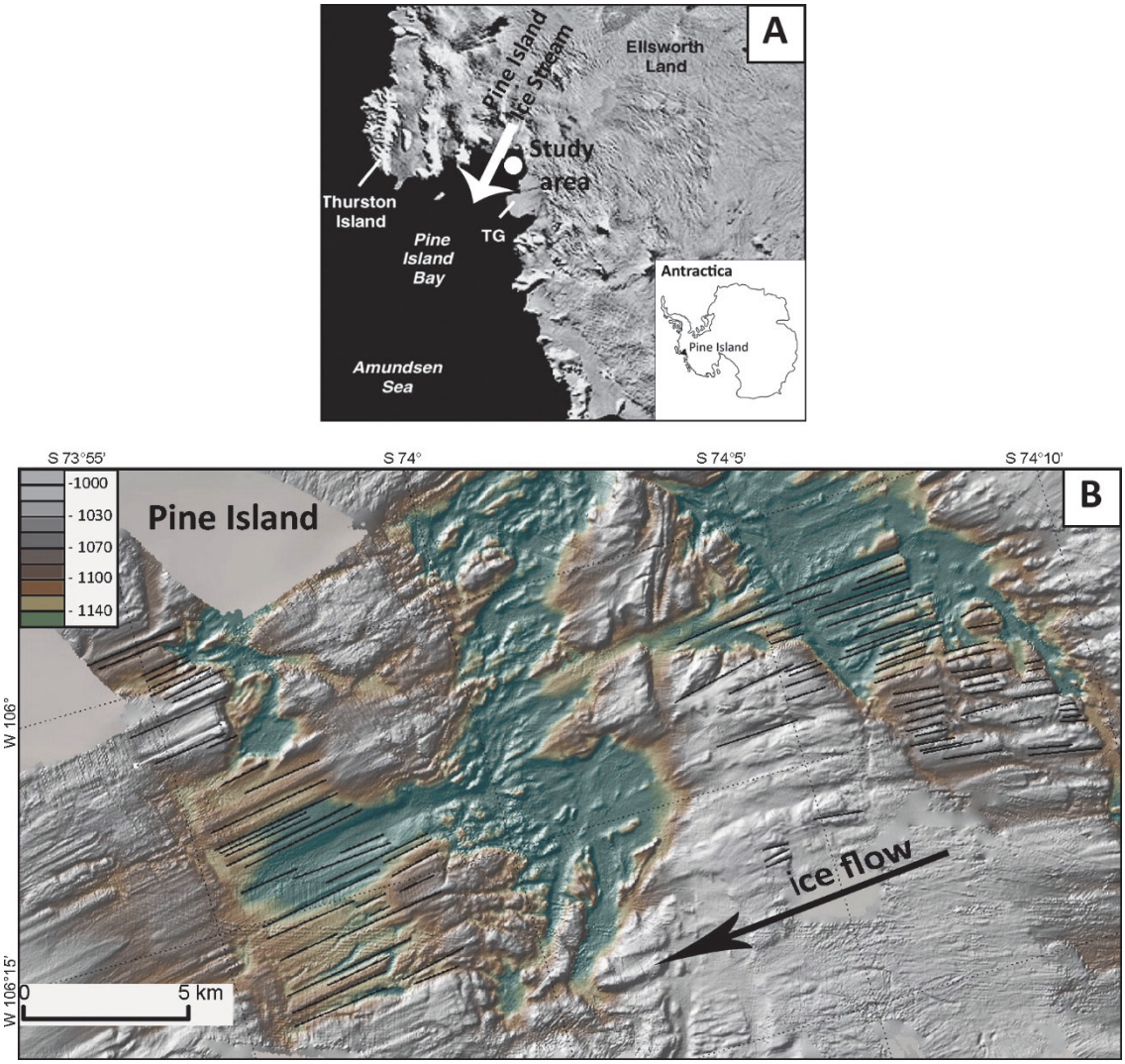

Figure 3.13. A: Satellite image of the Pine Island Glacier flowing into the sea at Pine Island Bay, Antarctica. Inset shows location of study area within Antarctica. Image modified from Lowe and Andreson, 2002. Image © Elsevier. **B:** DEM of the grooved site at Pine Island situated on the West Antarctic continental shelf in Pine Island Bay. The units in the colour key represent meters. Base image © GeoMapApp.

3.3 Methods

3.3.1 Digital datasets

DEMs at various resolutions were used for landform mapping and measurement at all sites except Hazelton, for which 2D Google Earth imagery was used (Table 3.2). A brief description is presented below of the protocols for image acquisition, data collection and processing, and the specifications of the resulting terrain models, including their associated errors and uncertainties.

NEXTMap digital terrain model (DTM) files were used for the two Scottish sites, at Elphin and Ullapool, and they are available through https://www.intermap.com/nextmap. The NEXTMap DTM is a bare-earth model containing elevations of natural terrain features in the UK. Elevations of vegetation and anthropogenic artefacts have been digitally removed. The resolution is 5 m posting and it has a vertical accuracy of 1 m root-mean-square error in unobstructed areas having slopes <10°. The data rendition on DTMs is void-free and seamless because the data-collecting technology is not hindered by any weather effect or cloud coverage.

The ArcticDEM files used for Haarefjord, Franklin, Hanna and Beavertail are stereo-derived elevation models covering the terrain above 60°N and are available to download from https://www.pgc.umn.edu/data/arcticdem/. The in-track and/or cross-track stereo imagery was collected by satellites and processed into 2-meters posting using photogrammetric techniques. The files used in this study are mosaic files obtained by joining multiple strips, which have been co-registered, blended and feathered to reduce the edge-matching effects. One weakness is that the terrain image is not a bare-earth product because the vegetation and any human interference and infrastructure add to the overall ground elevation, whereas water surfaces (e.g. lakes) obscure any submerged topography. As the product is optically derived, there are sometimes data voids resulting from atmospheric obstruction present at the time the data were acquired (e.g. clouds, fog, shadows). Overall, the accuracy is approximately 2 m in horizontal and vertical planes.

The elevation model for the site at Vikna, located on the Norwegian continental shelf, was obtained through the Norwegian Hydrographic Service https://kartkatalog.geonorge.no/. The hydrographic survey data were compiled in the form of a 50-m resolution DEM from depth measurements using multibeam echo sounders, laser and single beam echo sounders.

The DEM for the Iivaara site, provided by the National Land Survey of Finland through https://www.maanmittauslaitos.fi/en/maps-and-spatial-data, has a grid size of 2 × 2 m and is based on laser scanning data with a point density of at least 0.5 points per m^2. The accuracy of the elevation data is 0.3–1 m.

The topographic data for the continental shelf at Pine Island Bay, Antarctica were collected through multibeam swath bathymetry at a scale of tens of meters and processed into a hill-shaded terrain model, with features smaller than 10 m recorded locally using a deep-tow apparatus (Lowe and Anderson, 2002). The data were collected between 1999 and 2010, and later compiled into a comprehensive 35-m grid by Nitsche et al. (2013) available to view and manipulate in 3D in GeoMapApp http://www.geomapapp.org/.

The raw DEMs were imported and rendered in ArcMap, following best practice outlined in Smith and Clark (2005) for optimum visualisation of linear landforms. Thus, the DEMs used as a mapping base were rendered as greyscale hill-shaded terrain, the light-source azimuth was applied perpendicular to the mega-grooves at an illumination height of 45°. The DEMs were also viewed with the light source parallel to the mega-grooves/ridges, which made the landforms less obvious, but still observable, due to their large dimensions. This was done to rule out illumination biases known to produce false appearance of landforms. The imagery from Pine Island Bay, Antarctica was visualised in GeoMapApp where the 3D-effect is obtained through altitude colour-coding.

3.3.2 BMG mapping and sampling

BMGs were identified as multiple straight and parallel features aligned in the ice flow direction, visually enhanced on the DEM by the differences in shading where the angle of slope exposure to the light source changes. As the same visual effect occurs along ridges, cross profiles were traced where in doubt, to ensure that the focus was on grooves rather than ridges. Cross-profiles were also traced to verify the BMG presence in the topography in the case of shallow grooves, where the shading variation is hardly visible (e.g. Figure 1D and 1G in Appendix; see groove 14 in Figure 3.14 - Inset 1). In cases where the bounding

ridges are of different length, establishing the start/end point of a BMG was guided by the shortest of the two bounding ridges, despite the fact that the change in shading may continue to be visible along the longer ridge (see groove 27 Inset 1 in Figure 3.14). BMGs were mapped as continuous lines over cross-cutting bedrock incisions only where this continuation was visually unequivocal on the aerial imagery (Inset 2 in Figure 3.14). At Ullapool and Haarefjord this may have influenced the result for groove length (see Section 3.3.4) as well as the overall number of landforms (see Section 3.4.1 and Section 4.3.1). Following these assessments, the BMGs were mapped as solid lines along the deepest part of the groove. In total 1,242 mega-grooves were mapped across all sites (Table 3.3).

At each site, BMGs were sampled for length, width, depth and lateral spacing. At Hazelton, where only 2D measurements could be carried out, there is no data for groove depth. There were large variations in the number of grooves across sites (e.g. 37 at Elphin, Beavertail and Hazelton compared to 397 at Franklin). Consequently, at sites comprising fewer than 40 grooves the entire groove population was sampled, leaving out only the grooves with a poorly defined cross-profile, while at sites with a large number of landforms, approximately 15% of grooves were sampled to balance the time incurred with the aim of obtaining a representative database (c.f. Spagnolo et al., 2014). The exact number of features sampled for each metric as well as the number of data points at each individual site, are recorded in Table 3.3.

In order to select the areas best suited for sampling, with well-defined grooves and minimum interference from other landforms or geological features, landform mapping was pursued in more detail, whereby linear features other than BMGs were also recorded on maps. These comprise breaks of slope along geological fractures and faults aligned across the grooved area (e.g. Figure 3.2B and 3.5B), or along lithological contacts (Figure 3.7B), or changes in the general aspect of topography (Figure 3.11A). Areas of fluvial erosion or deposition interspersed with or superimposed on to the grooved terrain were also mapped, as well as areas of glacifluvial deposits or in-filled basins (Figure 3.2B). Where possible, maps were checked against pre-existing geomorphic and geological maps. In order to obtain realistic values for groove metrics and to minimise uncertainties, BMG sampling was not carried out in areas where other landforms and deposits were present, as these could potentially have altered groove profiles (see Section 3.3.4).

3.3.3 BMG measurements

The length, depth, width and lateral spacing of the BMGs were measured using semi-automated methods facilitated by tools and features available in ArcMap, GeoMapApp and Google Earth. Length was automatically retrieved in ArcMap from the attribute table of the shape file where each polyline corresponds to an individual groove. At Hazelton and Pine Island, BMGs were manually measured in Google Earth and GeoMapApp, respectively. Width, depth and lateral spacing were measured in the palaeo-ice flow direction, at 100-m intervals (Figure 3.14; see also Figure 1 in the Appendix). To correctly gauge the distance between data points, a fishnet overlay was applied on the DEM in ArcMap, or a digitised graded-ruler guide was moved along each groove and metrics were extracted manually (e.g Figure 1G in the Appendix). The minimum number of data points for each sampled groove was three. The sampling protocols were followed as closely as possible, but sometimes small compromises had to be made to keep the measurements systematic. Thus, occasionally the cross-profile location had to be shifted up to a few 10s of metres along the groove in order to avoid interference with cross-cutting geological features (e.g. fault lines, fractures) or erosional/depositional features (e.g. meltwater channels/eskers).

Measurement of depth and width first required the identification of the groove as a geomorphic entity. This equates to establishing the groove's upper and lower limit, or separating groove from ridge, in order to ensure the measurements were focused on the groove rather than the ridge. As grooves and ridges exist in conjunction with each other, it can be difficult to clearly distinguish between them when the top of the groove does not coincide with the crest of the intervening ridge. The protocol followed here is summarised in Figure 3.15, whereby the top of the groove represents the point of maximum inflexion on the flank profile (c.f. Spagnolo et al., 2014). It was found that most cross profiles fell into one of four categories. In the case of sinusoidal profiles, the peak of the ridge is also the uppermost part of the groove (Figure 3.15A).

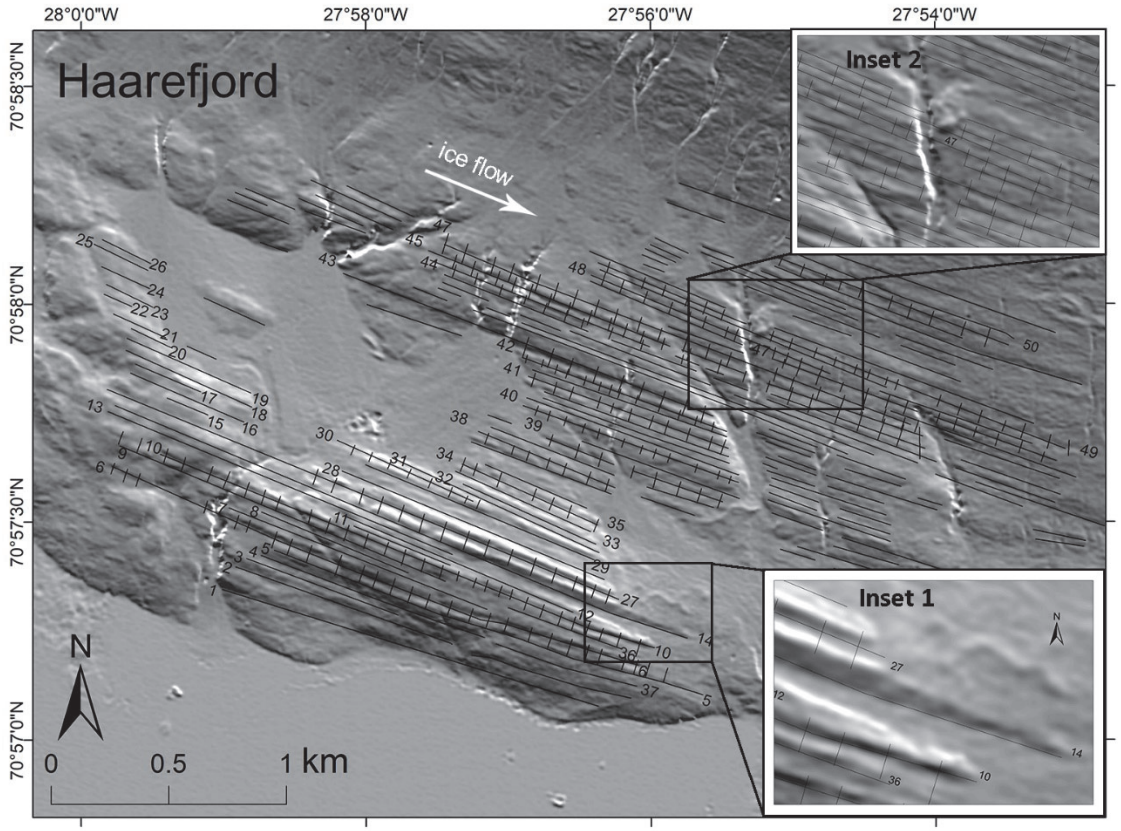

Figure 3.14. Example of a sampled site (Haarefjord), showing the location of the cross-profiles on which depth and width were measured. The numbered BMGs with cross-profile transects represent those BMGs for which depth and width were measured. The numbered BMGs with no cross profile transects (e.g. 15–26) were used for measuring lateral spacing. For the remaining nine sites the sampled grooves and the data point locations are represented in Figure 1 in the Appendix. Inset 1 illustrates BMG mapping in relation to the bounding ridges, whereby the groove end-point corresponds to the shortest of the two ridges (e.g. groove 27). Inset 2 illustrates BMG mapping in areas of cross-cutting channels, where BMGs are mapped as continuous lines only where groove continuity can be visually matched on both sides of the cross-cutting landform.

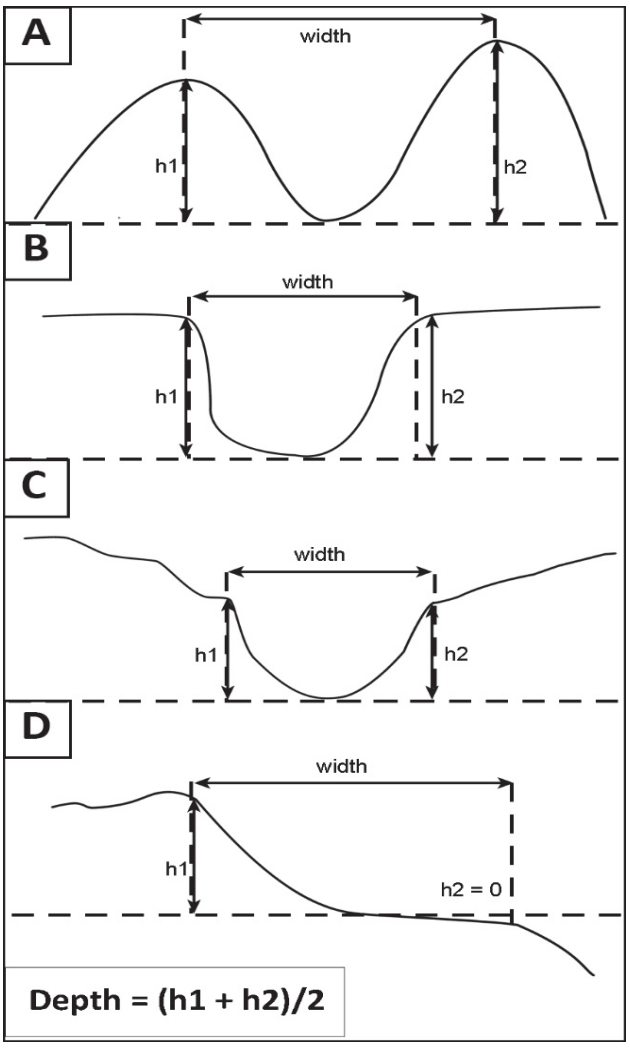

Figure 3.15. A–D: Measurements of groove width and depth on different types of BMG cross-profile.

Where the grooves were eroded into a relatively flat, plateau-like surface, the top of the groove coincides with the plateau edge (Figure 3.15B). Where the cross-profile had an irregular shape, the break of slope closest to the groove floor was considered the top of the groove flank. In cross-profile, this occurs either as a ledge eroded into the slope of the ridge or a change in the slope convexity (Figure 3.15C). Often there is an inflexion in the slope profile on the opposite ridge, at a matching altitude, except for grooves with a stepped profile, where only one side is defined (Figure 3.15D). Once the groove geometry was established, depth was calculated as the average height of the two flanks, and width was measured as the distance between the tops of the two groove flanks opposite each other in the cross profile (Figure 3.15). Spacing was measured at 100-m intervals, along the ice-flow direction (Figure 3.16A), as the distance between the centre-line (i.e. groove floor) of two adjacent grooves (Figure 3.16B).

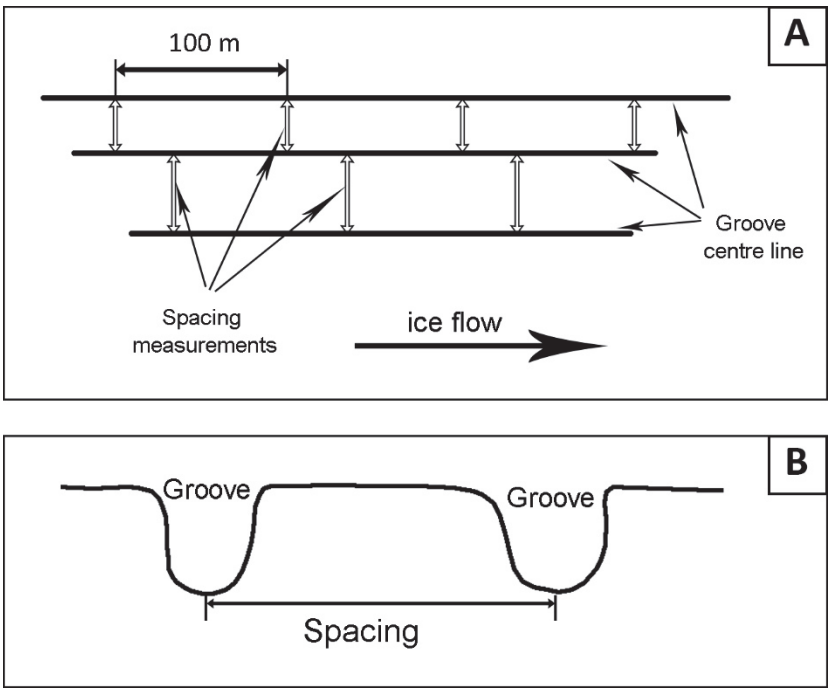

Figure 3.16. A: Schematic representation of spacing measurements along adjacent grooves at 100-m inervals in the ice-flow direction; **B:** spacing measurement between the centre line of adjacent grooves. Ice flow direction perpendicular to the page.

For azimuth calculations, the grooves mapped as polylines were first split at vertices, which resulted in a series of segments, so that the azimuth could be calculated for each segment using ArcGIS tools. The summary statistics were subsequently calculated based on the azimuth values for individual segments between vertices rather than the individual grooves. The elongation ratios (length:width) were calculated only for the grooves with measured widths, by dividing the mean length value by groove width.

3.3.4 Errors and uncertainties

Most sites were mapped and sampled on high-resolution imagery (see Section 3.3.1), with horizontal gridding 2–5 m, and vertical accuracy of at least 1 m (Table 3.2). This means that the BMGs were fully visible; any groove narrower than 2-5 m or shallower than 1 m which may not have been picked out would be better described as a macro- or meso-groove (see Section 2.5.2 in Chapter 2). At Pine Island and Vikna, where the horizontal resolutions of the DEMs were 35 m and 50 m, respectively, some BMGs may have not been visible and therefore not mapped (Table 3.2 and Section 3.3.1). This may have resulted in higher values for lateral spacing and width. Conversely, at Iivaara, the high vertical accuracy of <0.5 m (Table 3.2 and Section 3.3.1) means that very shallow grooves became visible, and which may have skewed the value range towards the lower end at this site, relative to the other sites mapped at a coarser resolution. At Hazelton, the width measurements are estimations

rather than exact measurements, extracted from high-quality Google Earth imagery, aided by the presence of snow inside the grooves when the photographs were taken (Figure 3.12A). However, these represent estimated minimum values in the absence of 3D profiles, which may have resulted in underestimations of width. These factors will be considered in the interpretation of results.

The internal consistency of the results is ensured by the fact that the mapping and measurements at all sites were undertaken by the same person over a relatively short period of time, spanning no more than 10 months, and following consistent protocols. At Haarefjord, Ullapool and Elphin, the metrics were checked against those reported by Funder (1978), Bradwell et al. (2008) and Bradwell (2005), respectively (see Table 3.1), and found to be consistent overall (see Section 3.4.1). BMG mapping in areas with cross-cutting channels (see Section 3.3.2) may have resulted in underestimation of BMG mean length by a few hundred meters. These situations are not common and only applicable to two sites out of ten, namely Ullapool (Figure 3.5 B) and Haarefjord (Figure 3.2 B). While they may be of local importance (see Section 4.3.3), these instances did not significantly alter the BMG length values in the global dataset.

In conclusion, the aerial imagery used here allowed for consistent measurements across sites, with only three gaps in the dataset, namely one for depth and two for azimuth values. At most sites, the BMG visibility on the aerial imagery is excellent due to the high-resolution horizontal gridding combined with high vertical accuracy for most sites, and the data at Elphin and Ullapool were checked during a fieldwork campaign in 2018. At Vikna and Pine Island, however, the relatively coarse resolution may have resulted in some landforms being missed, which in turn may have resulted in overestimation of groove width and spacing. Nevertheless, the consistency in data collection from digital datasets with similar resolution ranges for most sites is considered to have produced an overall robust basis for quantitative analysis.

3.4 Results

3.4.1 BMG metrics

The results of the summary statistics for length, width, depth, spacing, elongation and azimuth are presented in Table 3.3 and the frequency distributions for the overall populations are illustrated in Figure 3.17. The site-specific spatial distribution for each metric is presented in Figures 2–6 in the Appendix. Upper and lower values at the 10th and

90th percentile are reported rather than the minimum and maximum, to avoid data skewing by extreme values that may have been unrepresentative (cf. Spagnolo et al., 2014). The value ranges for individual sites are represented in the box plots in Figures 3.17A–E.

Dimensions for most BMGs were as follows:

- length 220–2270 m (mode 400–500 m, median 662 m) (Table 3.3; Figure 3.17A),
- width 21–210 m (mode 200 m, median 76 m) (Table 3.3; Figure 3.17B),
- lateral spacing 35–315 m (mode 84 m, median 95 m) (Table 3.3; Figure 3.17C),
- depth 2–15 m (mode 3 m, median 5 m) (Table 3.3; Figure 3.17D).
- elongation ratios 5:1–41:1 (a mode of 8:1–10:1, median of 15:1) (Table 3.3; Figure 3.17E).

Table 3.3. Summary statistics for BMG metrics. The mode was established based on a visual examination of the graphs, whereby those graphs with a clear peak were regarded as unimodal.

Metric	Summary statistics	Haarefjord	Elphin	Ullapool	Franklin	Hanna	Beavertail	Iivaara	Vikna	Hazelton	Pine Island	All sites
Length	No. of BMGs (n)	162	37	248	397	64	37	87	74	37	99	**1242**
	Min	65	94	135	113	167	155	57	302	136	450	**57**
	10 pct	142	177	356	243	356	361	113	533	223	908	**224**
	Median	447	382	843	661	656	605	316	1117	445	1580	**662**
	Mean	594	449	1039	1228	776	610	352	1350	439	1888	**1018**
	90 pct	1203	688	2032	2760	1303	877	628	2487	671	3330	**2269**
	Max	2628	1465	4258	9713	1867	1259	1354	3200	854	4210	**9713**
	Std dev	508	272	734	1357	417	241	242	752	176	956	**1005**
	Mode	200–300	200–300	400–500	300–500	600–600	polymodal	100–200	800–900	400–500	1500–1600	**400–500**
Width	No. of BMGs	18	12	33	40	38	30	30	20	34	21	**276**
	No. of data points	259	61	416	640	359	211	202	213	170	255	**2966**
	Min	11	24	30	28	22	30	7	105	8	20	**7**
	10 pct	19	36	60	55	34	40	13	145	13	100	**21**
	Median	30	71	88	130	55	60	22	218	18	180	**76**
	Mean	30	74	91	137	58	64	23	220	18	180	**98**
	90 pct	43	110	130	223	85	95	35	280	23	260	**210**
	Max	55	160	194	370	114	150	56	450	43	500	**370**
	Std dev	9	29	28	65	19	22	9	61	5	61	**75**
	Mode	20–30	60–70	70–90	Polymodal	50–60	50–70	10–30	Polymodal	10–20	200–210	**20–30**
	(continued)											

Metric	Summary statistics	Haarefjord	Elphin	Ullapool	Franklin	Hanna	Beavertail	Iivaara	Vikna	Hazelton	Pine Island	All sites
Lateral spacing	No. of BMG pairs	25	26	36	57	49	33	47	26	32	24	**355**
	No. of data points	207	124	447	757	332	197	210	233	143	363	**2986**
	Min	19	35	38	37	19	6	10	121	10	127	**6**
	10 pct	27	43	58	74	39	54	19	207	17	159	**35**
	Median	42	80	88	142	68	87	30	300	30	270	**95**
	Mean	45	86	82	158	72	100	35	313	37	271	**134**
	90 pct	62	126	112	289	116	158	59	404	77	362	**315**
	Max	109	246	145	405	172	262	110	734	126	421	**405**
	Std dev	16	42	20	79	29	48	19	104	22	72	**104**
	Mode	40	72	84	142	73	112	30	295	27	149	**84**
Depth	No. of BMGs	18	14	33	40	38	30	30	20	-	21	**244**
	No. of data points	259	72	416	640	359	211	202	213	-	255	**2627**
	Min	1	1	1	1	1	1	1	1	-	1	**1**
	10 pct	2	2	2	1	2	2	1	3	-	5	**2**
	Median	4	7	6	3	5	5	2	7	-	14	**5**
	Mean	4	7	7	5	6	6	2	8	-	18	**7**
	90 pct	7	14	13	13	13	10	3	15	-	40	**15**
	Max	13	20	25	63	20	27	6	40	-	60	**63**
	Std dev	2	5	4	6	4	4	1	6	-	13	**7**
	Mode	4	5	5	5	3	3	1	6	-	10	**3**
	(continued)											

Metric	Summary statistics	Haarefjord	Elphin	Ullapool	Franklin	Hanna	Beavertail	Iivaara	Vikna	Hazelton	Pine Island	All sites
Elongation	No. of BMGs	18	12	33	40	38	30	30	20	34	21	**276**
	No. of data points	N/A	N/A	N/A	N/A	N/A	N/A	N/A	N/A	N/A	N/A	**N/A**
	Min	20	4	9	3	6	4	9	2	11	4	**2**
	10 pct	23	5	10	6	9	5	11	3	12	5	**5**
	Median	41	8	21	22	15	9	22	5	25	7	**15**
	Mean	42	10	22	25	16	10	27	5	25	7	**20**
	90 pct	63	15	32	45	24	15	46	8	38	11	**41**
	Max	72	19	49	99	42	18	59	10	50	14	**99**
	St dev	16	4	10	19	7	4	15	2	11	3	**15**
	Mode	Polymodal	Poly modal	Polymodal	Poly modal	Poly modal	Polymodal	Poly modal	4–6	Poly modal	4–6	**8–10**
Azimuth	No. of BMGs	199	36	371	757	109	41	87	83	-	-	**-**
	Min	71	258	246	157	272	298	111	271	-	-	**-**
	10 pct	116	272	264	240	280	306	119	297	-	-	**-**
	Median	119	284	274	265	290	311	124	302	-	-	**-**
	Mean	119	281	274	262	286	311	124	302	-	-	**-**
	90 pct	123	288	285	276	299	314	128	308	-	-	**-**
	Max	143	292	299	280	304	329	136	323	-	-	**-**
	Std dev	5	8	8	14	22	5	4	7	-	-	**-**
	Mode	119	285	270	266	297	313	124	303	-	-	**-**
BMG density	No. BMGs/area (grooves/km^2)	31.2	14.8	5.7	3.1	15.2	13.5	43.5	1.7	12.3	0.7	

The deepest grooves occur at Pine Island, with a median of 14 m, which is double the median range of 2–7 m for all the other sites (Table 3.3; Figure 3.17D). The highest values for length, width and spacing occur at Vikna and Pine Island, whereas the lowest values apply to BMGs at Iivaara, Hazelton and Haarefjord (Figures 3.17A-C). This hierarchy is reversed for elongation ratios, with the highest values at Haarefjord (mean 42:1), and lowest values at Vikna (mean 5:1) and Pine Island (mean 7:1), (Figure 3.17E). At most sites, the azimuth of the BMGs has a low standard deviation of 4–8 degrees (Table 3.3), indicative of a strong parallel conformity between grooves within individual sites. The mean azimuth value coincides with that of the regional ice-flow direction inferred from independent evidence (see Section 3.2.2), which confirms the empirical observations that BMGs are aligned parallel to former ice flow. Relatively high values for azimuth standard deviation are 14 degrees at Franklin and 22 degrees at Hanna (Table 3.3), indicative of a change in BMG alignment within these sites. At Franklin, BMG alignment changes from westwards to north-westwards (Figure 3.7). At Hanna there are two slightly divergent orientations for the BMGs (Figure 3.8C), likely due to changes in the geological structure (see Section 3.2.2.5).

BMG density, calculated as number of landforms per unit area, was highest at Iivaara and Haarefjord (>30/km^2), and lowest at Vikna and Pine Island (<2/km^2) (Table 3.3).

In summary, the metrics confirm that BMGs are large-scale elongate landforms, with a high degree of parallelism to former regional ice-flow directions. Thus, 80% of the sampled population have lengths of 224–2269 m, widths of 21–210 m, depths of 2–15 m, elongation values of 5:1–41:1, and a spacing between adjacent individuals of 35–315 m (Table 3.3). The frequency distribution of all metrics for the aggregated groove population is unimodal with a positive skew and relatively high kurtosis indicative of a wide spread on values to the right of mode (Figure 3.17).

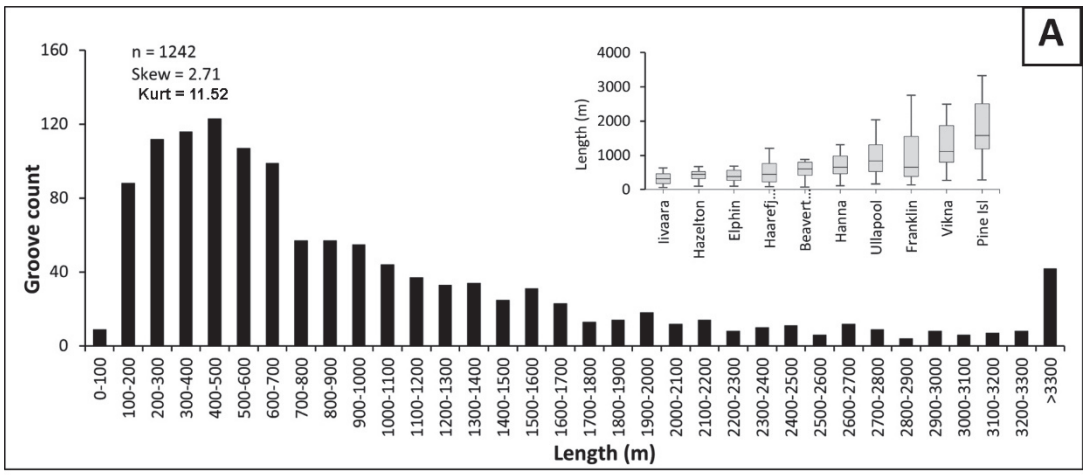
A
n = 1242
Skew = 2.71
Kurt = 11.52
Groove count
Length (m)
Length (m)
Iivaara
Hazelton
Elphin
Haarefj...
Beavert...
Hanna
Ullapool
Franklin
Vikna
Pine Isl

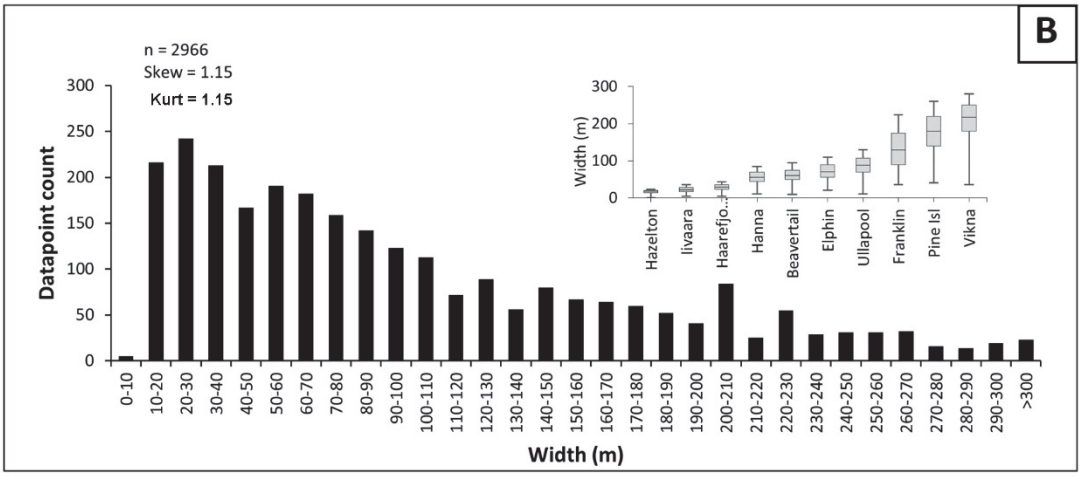
B
n = 2966
Skew = 1.15
Kurt = 1.15
Datapoint count
Width (m)
Width (m)
Hazelton
Iivaara
Haarefjo...
Hanna
Beavertail
Elphin
Ullapool
Franklin
Pine Isl
Vikna

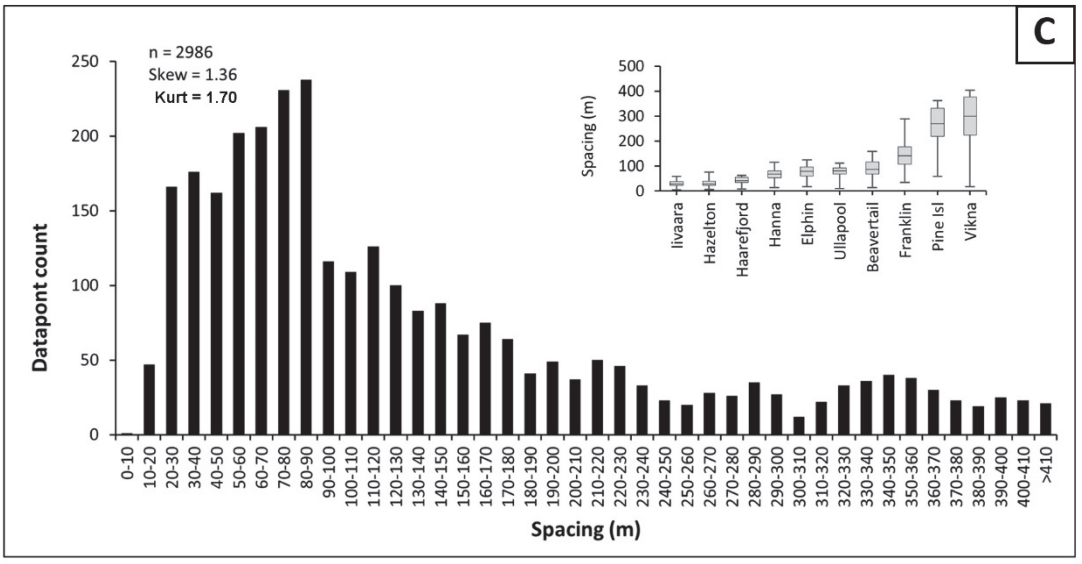
C
n = 2986
Skew = 1.36
Kurt = 1.70
Datapont count
Spacing (m)
Spacing (m)
Iivaara
Hazelton
Haarefjord
Hanna
Elphin
Ullapool
Beavertail
Franklin
Pine Isl
Vikna

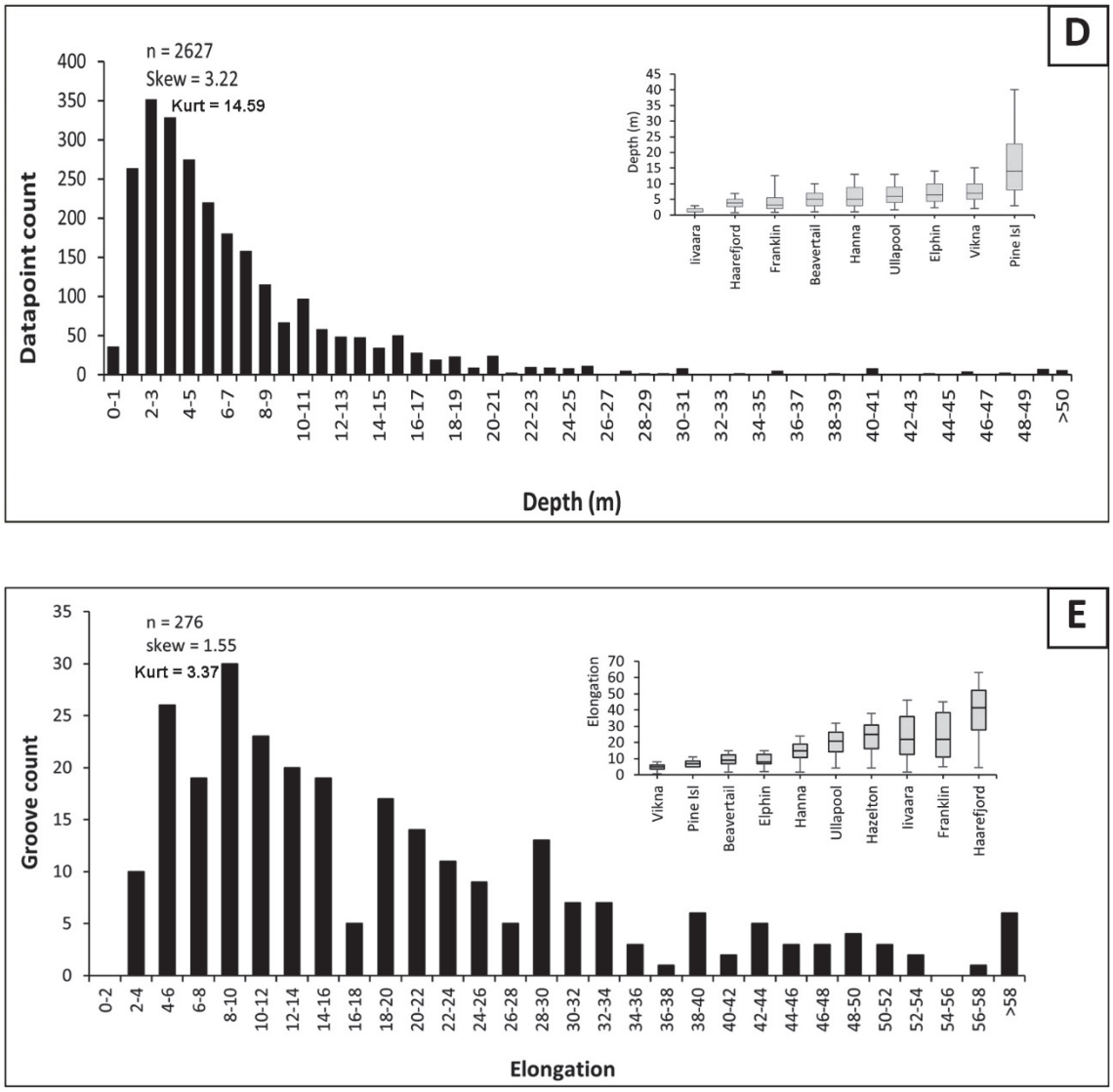

Figure 3.17. Frequency distribution for the length (**A**), width (**B**), spacing (**C**), depth (**D**) and elongation (**E**) for the entire mapped population of BMGs. The statistical box plots for individual parameters show the 10th, 25th, 50th, 75th and 90th percentiles of the value range. Kurt = kurtosis.

Comparisons between metrics reported here to those reported in previous studies show various degrees of consistency. At Haarefjord there is good consistency between length, width and depth between the value ranges of 10th – 90th per centile reported here and the average values reported by Funder (1978). For example, lengths of 50- 2000 m (Funder, 1078) and 142 – 1203 m (Table 3.3.); width 45 m on average (Funder, 1978) and 19 – 43 m (Table 3.3.); spacing 45 m (Funder, 1978) and 27 – 62 (Table 3.3.); depth 1 -5 m (Funder, 1978) and 2-7 (Table 3.3). This consistency may reflect the fact that mapping was done on high-resolution imagery in both studies and covered the same area. The discrepancy in the number of landforms reported, namely 50 by Funder (1978) versus 162 reported here (Table 3.3), may reflect the acknowledgement herein of the more fragmented result of mapping from areas where BMGs are cross-cut by other bedrock channels (see Section

3.3.4). At Ullapool and Elphin the values for length, depth and spacing reported here are lower than those of Bradwell et al. (2008) and Bradwell (2005), respectively. The greatest discrepancy applies to BMG depth at Ullapool, whereby there is only a small overlap between the range of 2-13 meters reported here (Table 3.3) and that of 10-20 m reported by Bradwell et al. (2008). Metrics differences are likely due to the fact that the area studied by Bradwell et al. (2008) is larger, covering the entire length of the Ullapool tributary glacier, which spans different lithologies with likely variable susceptibility to erosion (c.f. Krabbendam and Glasser, 2011; see Section 4.5.3.). The area sampled in the present study is confined to the Moine Schist lithology (Figure 3.5 B), therefore the metrics (Table 3.3) are representative of this particular lithology. The same argument applies to Elphin, where the grooves reported by Bradwell (2005) are both deeper and longer than those reported here. In addition, there are differences between the protocol for groove selection between the two studies. For example, some BMGs reported by Bradwell (2005) occur along geological faults, which may explain their relatively high depth, such as groove 'o' in Figure 2 in Bradwell (2005). Such grooves were left out in the present study, to avoid the results being skewed by structural factors (see Section 3.3.2).

In conclusion, the results reported here for BMG metrics are comparable to those from previous studies covering similar areas. Inconsistencies occur due to differences in the mapping protocols and areal extent of the sampled terrain.

3.4.2 Relationships between BMG dimensions

The relationships between various BMG dimensions have been derived by plotting mean values for metrics against each other, derived from all sampled individuals (Figure 3.18). The underlying aim is to explore at different levels possible relationships between metrics, for example, width *versus* depth or length *versus* width, which may lead to new insights regarding their formative mechanism(s).

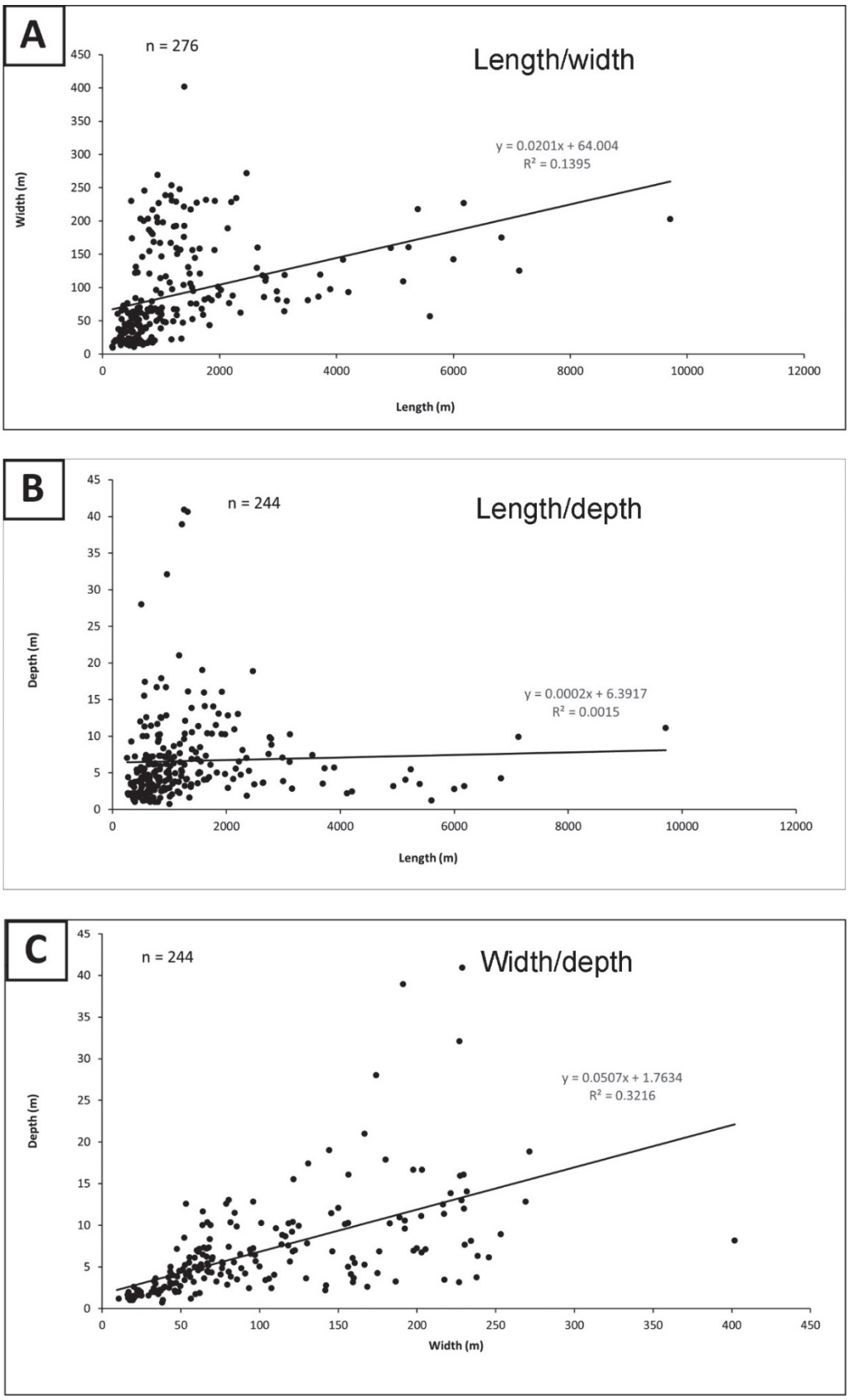

Figure 3.18. A–C: Length, width and depth plotted against each other for the entire sampled population. Each datapoint represents the mean value of that respective metric corresponding to a sampled groove. The plots are fitted with a linear trendline.

Table 3.4. P-values indicative of the degree of statistical significance for the plotted metrics in Figure 3.18. Note the frequent occurrence of $p < 0.05$ in the width/depth regression (shaded cells), indicative of statistical significance for the relationship between these two metrics. L = length; D = depth; W = width. The p-values correspond to Figures 7–9 in the Appendix.

Site	Haare-fjord	Elphin	Ullapool	Franklin	Hanna	Beavertail	Iivaara	Vikna	Hazel-ton	Pine Island	All
L/W	0.005	0.064	0.345	0.3	0.005	0.545	0.166	0.369	0.936	0.041	3.6×10^{-10}
L/D	0.030	0.087	0.08	0.467	0.003	0.377	0.481	0.687	-	0.685	0.548
W/D	0.001	0.0003	0.0003	0.0001	5.4×10^{-7}	1.22E-06	4.7×10^{-7}	0.447	-	0.001	1.3×10^{-22}

All correlations between metrics based on values derived from individual sampled BMGs (Figure 3.18) show a positive linear trend, albeit generally weak, as indicated by the low R^2 values, between 0.001–0.321 (Figure 3.18; see also Figure 7–9 in the Appendix). The strongest correlation is that between width and depth (Figure 3.18C), indicating that BMGs consistently grow wider as they get deeper. This relationship is apparent at all individual sites (Figure 9 in the Appendix) and the correlation is always statistically significant ($p < 0.05$) (Table 3.4) indicating a non-random causality for the progressive increase in groove depth with width (see Section 3.5.4). The much weaker length/width and length/depth correlations apparent across the global population as well as within individual sites (Figures 7 and 8 in the Appendix) mean that the widest and deepest BMGs can be either short or long. The general lack of statistical significance characterising these relationships (Table 3.4) suggests an apparent randomness in what may control these relationships, and points to a high variability in the local factors (see Section 3.5.2).

To examine whether various metrics might be related to or associated with processes governing BMG evolution across sites and also to enable comparisons of BMG metrics between sites, the relationships between length, width, depth and spacing were explored in combinations of two metrics (Figure 3.19). The plotted values represent site-specific values for these metrics, calculated as overall mean values of the sampled BMG population within each individual site. Each plot is fitted with a linear trendline. All relationships show strong positive trends with $R^2 = 0.4–0.9$ (Figure 3.19) and all are statistically significant as reflected in the p-values <0.05 (Figure 3.19).

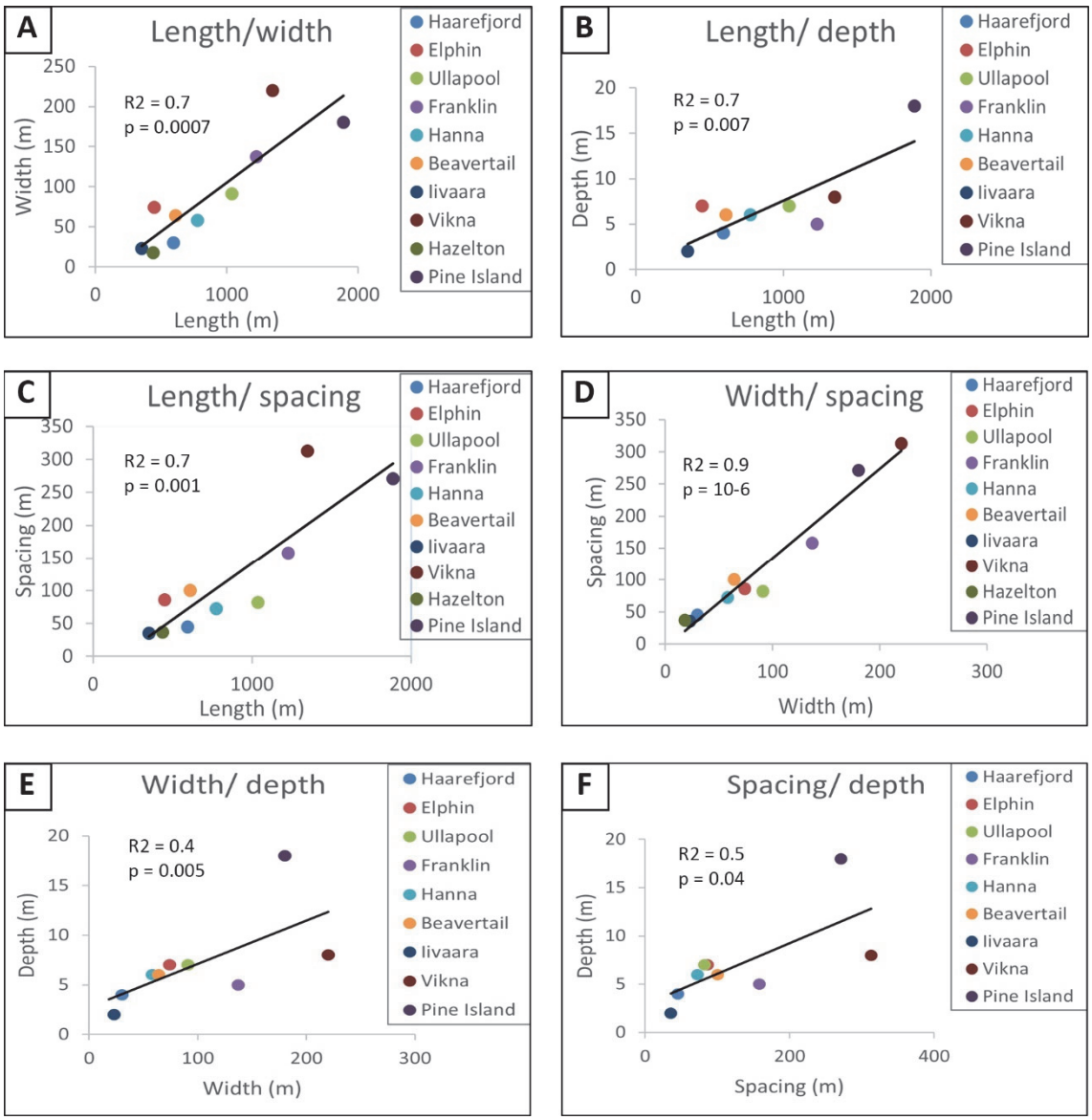

Figure 3.19. A–F: Overall site-specific mean values for length, width, depth and spacing plotted against each other. Each value represents the overall mean of that metric for a study area (Table 3.3). The trendlines correspond to the linear equations. R^2 (written "R2" in the diagrams) indicates the correlation strength between plotted metrics, and the p-value represents the statistical significance. Note the low p-values on all graphs (<0.05; in Part D "10-6" means "10^{-6}"), suggesting that the correlations are statistically significant.

The correlations between length and all the other metrics are positive and strong, as reflected in the high R^2 values of 0.7 (Figures 3.19A–C). The almost perfectly linear relationship between width and spacing (R^2 = 0.9; Figure 3.19D) needs to be treated with care because the two metrics co-vary with each other and are therefore semi-independent. This is because two adjacent grooves need to merge for spacing between grooves to grow, which would result in the formation of a wider groove. If this is replicated across the population at any site, the resulting mean values for both width and spacing would increase. The width/depth and spacing/depth relationships with R^2 values for the linear trends

sitting at 0.4 and 0.5, respectively, also support a convincing positive correlation between those metrics, albeit somewhat weaker than the correlations involving length (Figure 3.19E and F).

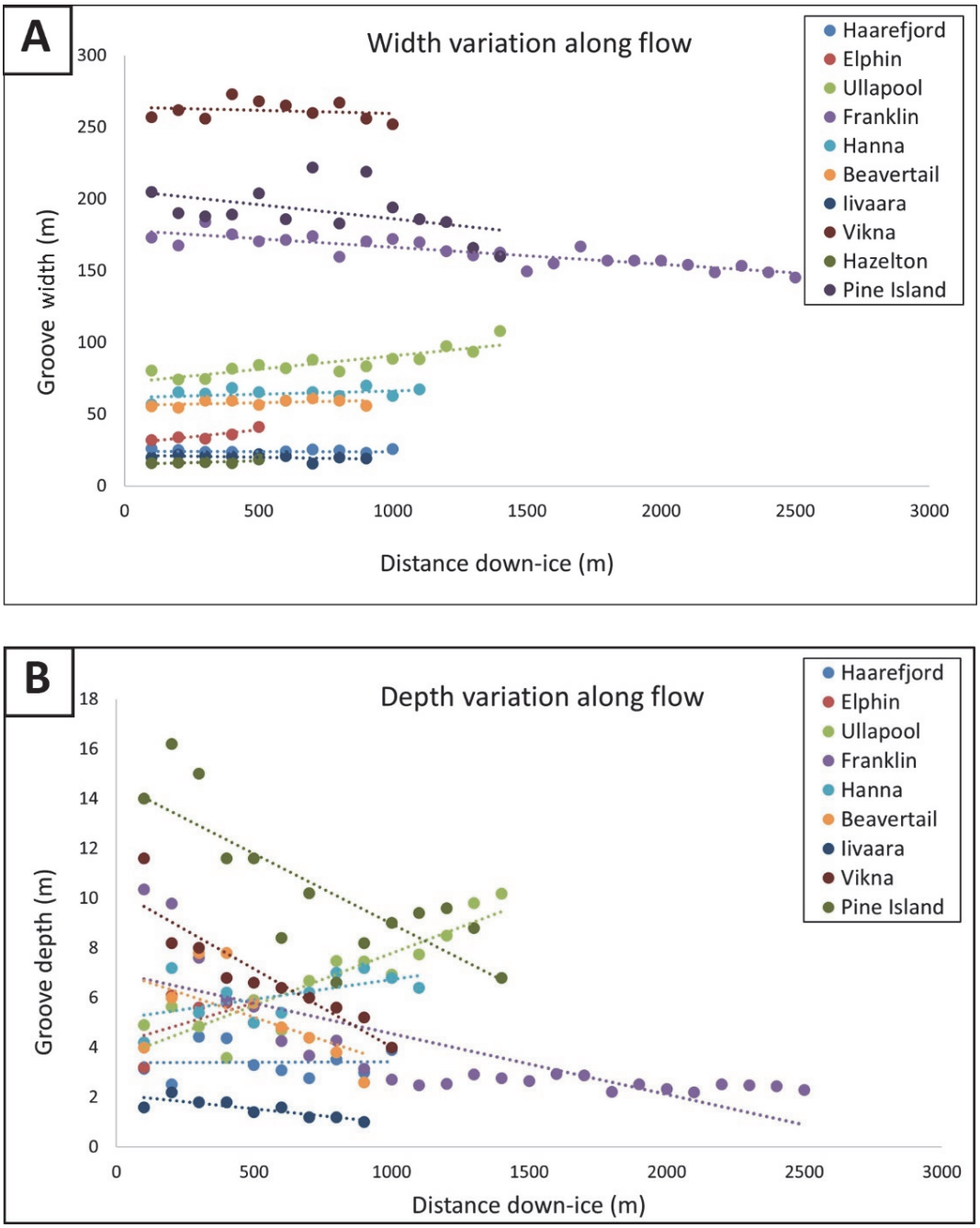

Figure 3.20. Variation of width (**A**) and depth (**B**) along the grooves in the down-ice direction. Each datapoint represents the width and depth value, respectively calculated as an average between five datapoints from five different grooves, whereby each datapoint is found at the same distance from the starting point of the groove. The starting point is at 100 m, so that the graphs are slightly offset from the x-axis, and the datapoints are spaced-out by 100 m, consistent with the protocol for sampling frequency (see Section 3.3.2). The ice-flow direction is from left to right.

In order to investigate the efficiency of erosion processes, the variations in width and depth along the grooves were plotted in the down-ice direction and the graphs fitted with a linear trendline (Figure 3.20A and B). The results show different trends between sites, which can be either positive or negative, but there is usually consistency within the same site for variation in depth and width with flow distance down-ice. Thus, at Elphin, Ullapool and Hanna the trends are positive showing the tendency of BMGs to widen and deepen along the ice-flow direction, whereas Franklin, Iivaara, Vikna and Pine Island have downward trends, meaning that BMGs become narrower and shallower with distance downstream.

In summary, the correlations between metrics derived from BMGs within individual sites are positive, but weak (Figure 7–9 in the Appendix), indicative of a high degree of variability in BMG development within sampled sites. Relationships between overall site-specific mean values show much stronger positive correlations of basic metrics between sites, indicative of possible overarching relationships. The variations in depth and width along the grooves is positive at some sites and negative at others, but the two trends are usually consistent within individual sites.

3.5 Discussion

3.5.1 Spatial and statistical distribution of BMG dimensions

The frequency distribution patterns of the aggregated dataset is unimodal for all metrics, with no obvious breaks or stepped patterns to suggest separate sub-populations or different scenarios of formation (Figure 3.17). In addition, the value ranges for all metrics always overlap, regardless of discrepancies between end members (see Figure 3.17). Collectively, these observations imply that, at least morphometrically, BMGs appear to form a single landform population, which justifies their treatment as a distinctive landform type and the use of specific terminology. In other words, no morphometric evidence was found to indicate that BMGs at any of the sampled sites might be split into separate categories of landform based on their dimensions. The same conclusion has been reached based on similar analyses for other subglacial bedforms, such as drumlins (Clark et al., 2009), ribbed moraine (Dunlop and Clark, 2006), MSGLs (Spagnolo et al., 2014) and eskers (Storrar et al., 2014).

Notably, however, there is marked variation between individual sites in the spatial distribution of BMG metrics. In particular, the degree of value spread is different between sites for the same metric (e.g. Figure 3A and 3J in the Appendix). The high standard deviation for length reflects the fact that BMGs of very different lengths can occur within most sites. Depth has the lowest standard deviation across the sampled sites, reflecting a strong internal consistency in the development of this metric, likely due to the bedrock-specific susceptibility to erosion. Most frequency distributions at individual sites are unimodal (e.g. Figures 3C, 3E, 4C, 4D, 5E, 5H in the Appendix), whereas some have a less obvious modal value (e.g. Figures 2F, 2E, 3D, 3H, 4A, 4B, 4F in the Appendix) which could reflect a more evenly balanced presence of BMGs of various dimensions. Albeit less frequently, the skew can be symmetrical with tails left and right of equal length, so the distribution patterns at individual sites do not consistently mirror those for the aggregated population. In the case of MSGLs, the frequency distribution patterns of individual sites mirror those of the aggregated landform population, likely due to the uniformity of the substrate (Spagnolo et al., 2014). Overall, the inter-site variability in frequency distributions of BMG metrics is interpreted to reflect a strong influence of local conditions over individual BMG development (see Section 3.5.2). This variability is also apparent from the weak correlations between metrics, especially those between length/width and length/depth derived from both the aggregated sampled population (Figure 3.18A and 3.18B) as well as from the sampled BMGs within individual sites (Figures 7 and 8 in the Appendix). Nevertheless, despite pronounced local variability in BMG formation, the fact that metrics across the aggregated global population produce unimodal frequency distributions (Figure 3.17) with overlapping value ranges between sites (box plots in Figure 3.17) strengthens the conclusion that BMGs represent a single landform population.

In contrast to the weak metrics relationships between sampled individuals, the site-specific, overall mean values for BMG metrics show strongly consistent and positive linear correlations (Figure 3.19; see Section 3.4.2). This is surprising considering the geological differences between sites, the potential differences in glaciological conditions and in landform age, and differences in topography. These strong correlations mean that, regardless of any geomorphic constraints or any differences in BMG initiation (Chapter 5), the overall evolution of BMG dimensions within any site is quite predictable. Thus, if a site-specific mean value for groove length was known, the equivalent mean value for width, depth and spacing could be estimated within relatively narrow margins of error, based on the equations derived from the trendlines in Figure 3.19. These results could be further refined by reducing potential overestimations of BMG width and depth at Vikna and Pine

Island if mapping could be done at higher resolution (see Section 3.3.2). In principle, modelling experiments could use these results to further explore BMG evolution through time (see also Section 3.5.4) and further unravel overarching rules that seem to be governing BMG development.

In conclusion, BMGs represent a discreet landform type, which, once initiated, appear to develop under an overarching scenario, considering the strong correlations between mean metric values *between* sites. This is despite pronounced local variability in metric correlations manifested *within* individual sites and variations in physical and glaciological characteristics between sites.

3.5.2 What controls BMG morphometry: geology *versus* glaciology

In this section the results of morphometric analyses are used to explore the primary factors controlling BMG formation, considering that BMG formation results as an interplay between bedrock resistance to erosion and the efficiency of various subglacial erosion processes at overcoming that resistance.

At Vikna and Pine Island, a series of common characteristics of the BMGs point to a primary glaciological control over their development, through enhanced erosion beneath fast-flowing glacier ice. Firstly, both sites experienced a similar glaciological history, with the BMGs being situated on continental shelves in polar regions affected by marine-terminating ice streams during the last glacial, and in zones of fast-flow onset (Ottesen et al., 2002 and 2005; Lowe and Anderson, 2002 and 2003; Kirkham et al., 2019). Secondly, the value ranges for the BMG metrics are strikingly similar between the two sites, and they stand out in the global dataset at the higher end of the spectrum (Figures 3.17A–D). Thirdly, the two sites are underlain by different bedrock geology, namely sedimentary at Vikna (Figure 3.9B) and crystalline at Pine Island (Figure 3.11B), with each rock type known to produce its characteristic topography through glacial erosion under slow ice flow conditions. Thus, sedimentary rocks typically enable the formation of streamlined bedrock forms (Eyles, 2012; Eyles and Putkinen, 2014), whereas crystalline bedrock leads to the development of classic cnoc-and-lochan topography, with reduced streamlining, common in glaciated shield terrain (Linton, 1963; Sugden, 1974; Krabbendam and Bradwell, 2014). However, at Pine Island, the dominant mode is that of grooved and streamlined bedrock, similar to the crystalline streamlined bedforms in West Greenland, formed by enhanced abrasion under ice-streaming conditions (Roberts and Long, 2005; Roberts et al., 2010; Roberts et al.,

2013). At Vikna, the streamlined topography is not uncommon for the bedrock type, but the BMG dimensions exceed by far those of BMGs in similar types of bedrock (e.g. Ullapool, Hanna, Beavertail; Figure 3.17).

The elongation ratios for the BMGs at Vikna and Pine Island have the lowest values in the dataset (Figure 3.17E). Considering that the grooves at these two locations are among the longest in the dataset (Figure 3.17A), the low elongation ratios are explained by the relatively high values for width, compared to the rest of the sites. This result may be skewed towards somewhat lower values for the elongation ratios due to possible overestimations of width (see Section 3.3.4). However, it is interesting that the elongation ratios have a strikingly similar unimodal frequency distribution spanning a short range of low values, with similar mode values between the two sites of 4:1–6:1 (Figure 5 in the Appendix), which differs from those at all other sites (Figure 5 in the Appendix). In addition, the modal value for elongation is similar to that for the streamlined gneissic bedrock forms at Jakobshavns, West Greenland (approximately 5:1) from an area also affected by ice streaming (Roberts and Long, 2005). The frequency distribution of elongation ratios at Vikna and Pine Island could represent a tendency for scaling (c.f. Clark et al., 2009) following either prolonged subglacial erosion or a relatively short period of efficient lateral erosion beneath fast-flowing ice. In other words, as the BMGs evolve, they may get wider, which would be consistent with the relatively low values for groove density at these locations. Collectively the characteristics of the BMGs from Vikna and Pine Island strongly indicate BMG development under the primary influence of fast-flowing ice, under streaming conditions (see Section 1.1) which enabled high rates of subglacial erosion and superseded geological controls.

Apart from Vikna and Pine Island, the other sampled areas comprise BMGs which have much smaller dimensions, especially regarding length and width (Figure 3.17A-D), and up to one order of magnitude higher elongation ratios and density compared to BMGs interpreted as primarily controlled by ice streaming (Table 3.3). The prevailing erosion mechanism, i.e. plucking or abrasion, in BMG formation at most other sites was either established with direct empirical evidence (e.g. Smith, 1948; Funder, 1978; Krabbendam and Bradwell, 2011), or inferred from published geological information (Hume, 1954; McLaren, 1962; Tassonyi, 1969). The two glacial erosion mechanisms are plucking (also referred to as ‘quarrying`) and abrasion, and the prevalence of one over the other was found to be directly related the geological structure or lithology (see Section 3.2). As pointed out by Iverson (1995), “at a fundamental level, both abrasion and quarrying involve the fracture

and dislodgement of rock from the bed". For abrasion to occur, rock fragments in subglacial traction have to be in frictional contact with the bedrock, and the stress differences in the bedrock lead to crushing of the latter beneath the abrading fragments, which produces fine debris and leaves behind in the topography a groove (see Section 2.4.1.1). Other factors governing the efficiency of abrasion are the relative hardness between erodent and substratum, the contact forces at the erodent/bedrock interface, the clast velocity, the areal concentration of erodent clasts in contact with the bed and the contact area between the erodent and the bedrock (Drewry, 1986; Iverson, 1995). Abrasion has been found to prevail over plucking in poorly jointed rocks, of a more massive nature (e.g. Chamberlain, 1888; Eyles, 2012; Krabbendam et al., 2016). Plucking requires the existence of joints in the bedrock, and these can be either preglacial, possibly structurally controlled, or formed subglacially, through crushing induced by the action of applied shear stress to the underlying substrate. Subglacial crushing is most efficient beneath large rock fragments in contact with the bedrock, or on the lip of bedrock steps (Boulton, 1979; Benn and Evans, 2010). Subsequently, joints need to be loosened in preparation for glacial entrainment, and this can happen through the injection into cracks of glacier ice (Rea and Whalley, 1994) or soft sediment (Evans et al., 1998). The lose fragments can then be effectively "plucked out" of the parent bedrock by the glacier in motion due to contact pressure differences which lead to freeze-on processes beneath fast-flowing thin ice. The latter can occur through the heat pump effect (Robin, 1976; Rösliberger and Iken, 1981) or cavity opening (Hallet, 1996). The results of quantitative analyses are now being deployed to identify morphometric commonalities between BMGs at sites other than Vikna and Pine Island, and to further explore the likelihood of BMG development through plucking or abrasion as the prevailing mechanism, in conjunction with the geological characteristics at each site.

At Elphin and Ullapool it has been established through fieldwork that plucking was the main mechanism that modified the BMGs during the last glaciation, enabled by a dense, three-dimensional network of joints in the bedrock (Bradwell, 2005; Krabbendam and Glasser, 2011; Krabbendam and Bradwell, 2011; see also Section 4.4.2.2 in Chapter 4). Abrasion and meltwater erosion were operational, but their effects were assessed as minimal based on the shallowness of striations and meltwater-sculpted cavities (Bradwell, 2005; Krabbendam and Glasser, 2011; see Sections 3.2.2.2 and 3.2.2.3; see also Section 4.5.1 in Chapter 4). The inferred presence of joints and their alignment relative to the BMGs (Hume, 1954; McLaren, 1962; Tassonyi, 1969) deems plucking as highly plausible at Hanna and Beavertail (see Sections 3.2.2.5 and 3.2.2.6), and possibly just as effective as it was at Elphin and Ullapool. At Hanna in particular, the BMG alignment parallel to bedrock strike and the

two different directions in BMG orientation could indicate structural control over BMG formation (see Section 3.2.2.5). Furthermore, the positive correlation between groove depth and width with distance down-stream at all four sites (Figure 3.20) is consistent with plucked rocks becoming entrained into glacial transport and acting as erosive tools further down-ice, thus leading to groove widening and deepening. Also, BMG density at Hanna, Beavertail and Elphin is similar and within a narrow range of 13.5–15.5 landforms/km^2 (Table 3.3), possibly indicative of groove development under similar constraints, most likely pertaining to structural geology at all four sites, considering the differences in lithology, at least with respect to susceptibility to abrasion (see Sections 3.2.2.2., 3.2.2.3, 3.2.2.5 and 3.2.2.6).

At Haarefjord and Iivaara abrasion, rather than plucking, is likely to have been the main mechanism of erosion considering the massive and poorly jointed bedrock, which deems pervasive plucking less likely. Importantly, the results of quantitative analyses show close similarities between the grooves at Haarefjord and Iivaara, consistent with the expected geomorphic outcomes of abrasion (see Sections 3.2.2.1 and 3.2.2.7; Iverson, 1991; Krabbendam and Glasser, 2011). Thus, the relatively small dimensions of the BMGs at these two sites (Figure 3.17) are consistent with low efficiency of glacial abrasion in comparison to plucking, documented in both glacial and fluvial environments (Whipple et al., 2000; Dühnforth et al., 2010). The relatively high groove densities of 31.2 grooves/km^2 at Haarefjord and 43.5 at Iivaara (more than double the density at any other site; Table 3.3), could reflect the reduced effect of lateral plucking, which inhibited groove widening, and which also explains the low values for width and spacing (Figures 3.17B and 3.17C). Furthermore, at Iivaara the grooves become narrower and shallower with distance down-ice, consistent with the wearing out of abrasive tools with distance downstream, as in the case of striations (Iverson, 1991), suggesting that BMGs may essentially be giant striations (see Section 5.3.1.1. in Chapter 5). At Haarefjord abrasion was suggested as the primary mechanism of BMG formation based on field evidence, by Funder (1978).

The role of water erosion in BMG formation can be difficult to quantify because of the various regimes of its manifestation, which can be subglacial under glaciostatic pressure (Bradwell, 2005) or free flowing either subglacially or subaerially (Eyles, 2006). It is significant perhaps that the deepest BMGs reported both on-shore at Franklin (Smith, 1948; Hamilton and Ford, 2002; Table 3.3; Figure 3.17D) and off-shore at Pine Island (Lowe and Anderson, 2003; Kirkham et al., 2019) (see Section 3.2.2.1; Table 3.3; Figure 3.17D) are associated with the effects of water erosion. Thus, at Franklin, the porous limestone of the

Great Bear Formation containing some of the deepest BMGs ever reported of up to 60 m (Smith, 1948), has been affected by dissolution (Hamilton and Ford, 2002; see Section 3.2.2.4), which likely contributed to BMG overdeepening alongside the formation of karstic landforms (Hamilton and Ford, 2002). The exceptional depth of the BMGs at Pine Island (Figure 3.17D) could reasonably be associated with sudden discharges of large meltwater volumes following subglacial lake outbursts (Kirkham et al., 2019), which would have resulted in high-energy turbulent flow, known to be an efficient erosion mechanism in bedrock (Whipple et al, 2000). Overall, despite the limited and often equivocal data available regarding meltwater erosion, its contribution can lead to BMGs attaining great depths.

Attempts to differentiate between the prevalence of plucking or abrasion would need to be validated by field evidence pertaining to BMGs at Hanna, Beavertail and Iivaara, so at this stage the results here should be regarded as provisional. Nevertheless, if glacial abrasion was the main mechanism of erosion in the massive, poorly jointed rocks, then it would not be unexpected to find that the resulting BMGs would have the smallest dimensions, highest density of landforms/km^2 and the highest elongation ratios in the dataset. Plucking was likely prevalent in the well-jointed rocks and it probably explains why the resulting BMGs occupy the mid-range position in the size spectrum and in all morphometric analyses.

The BMGs interpreted as being formed under primary geological control analysed in this study have experienced different glaciological conditions, comprising either slow- or fast-flowing ice (Bradwell et al., 2008; Sutinen et al., 2010; Krabbendam et al., 2016), which adds to the complexity of differentiating between the prevalence of control factors. In as much as erosion rates beneath fast-flowing ice are high, which is expected to produce large BMGs in a relatively short time, BMGs of similar dimensions should in theory result from slow-ice flow providing the necessary time is allowed for erosion to act. It could be that the BMGs at Vikna and Pine Island are among the most evolved grooves, having been subject to long-term intense erosion by fast-ice flow throughout repeat cycles of ice streaming, and that the BMGs at other sites are following the same evolutionary path but have not reached that stage yet due to slower erosion rates or to an insufficiently long period of time of high erosion rates (see Section 4.5.3).

In summary, morphometric correlations in conjunction with geological characteristics enable an initial assessment of the primary control factors over BMG development. Results so far seem to indicate that when fast-flowing ice is the primary control factor, the BMGs

have the largest dimensions, lowest density and lowest elongation ratios. Importantly, the values of these metrics are remarkably similar between BMGs from sites located far from each other and underlain by different geology. Where bedrock geology has been interpreted as the primary control factor, the BMGs dimensions also have comparable values across lithologies, but they sit at the low end of the values spectrum and have formed under a range of glaciological conditions.

3.5.3 Comparisons between BMGs and MSGLs

This section provides the first quantitative comparison between the dimensions of BMGs and those of MSGLs, as a first step towards understanding whether they represent different landform populations, considering their similar morphology as assemblages of multiple grooves and ridges parallel to each other and to (palaeo)ice-flow directions (Krabbendam et al., 2016; Eyles et al., 2018; Newton et al., 2018). MSGLs are largely regarded as a diagnostic landform for identifying palaeo-ice streaming (Clark, 1993; Stokes and Clark, 1999; Stokes and Clark, 2001; Ottesen et al., 2005) and their ongoing formation has been detected beneath fast-flowing ice in Antarctica (King et al., 2009). As for BMGs, it has been asserted that their formation is a direct result of enhanced glacial erosion in onset zones of fast-flow onset based on their common occurrence upstream from MSGLs (Bradwell et al., 2008; Eyles 2012; Krabbendam et al., 2016; Eyles et al., 2018). Thus far, morphometric analyses have shown that fast-flowing ice under streaming conditions (see Section 1.1) can be a primary control factor in BMG formation (see Section 3.5.2), but the association of BMGs with other component landforms within the ice-stream landsystem needs further exploration. Landform dimensions are compared here based on the aggregated global populations of BMGs and MSGLs to test whether they are two different landform types.

The two landform datasets used for general comparisons are of a similar magnitude, comprising nine sites for the MSGLs (Spagnolo et al., 2014) and ten sites for the BMGs from across the world, which makes them comparable in size and global representation. Despite differences between the two studies in the mapping and measurement protocols, the results are regarded as comparable. Thus, MSGLs were mapped as lines along the crest line of ridges rather than grooves, but the result is expected to have been the same if the grooves had been mapped instead, because the corrugated land surfaces have a sinusoidal profile (Spagnolo et al., 2014), and ridges mirror grooves (Figure 3.15 A). MSGLs onshore were mapped as elongated polygons where 3D shading effects made this possible, and only at those sites where values for amplitude and width could be derived. The protocols for

measuring length and amplitude (referred to as `depth` for BMGs) are identical in both studies (see Section 3.3.3). For MSGLs, width measurements were based on mapped polygons, approximated to highly elongate ellipses, and calculated as a function of the ellipse's short axis (Spagnolo et al., 2014). For BMGs, width measurements were done between points of inflexion in the slope angle, identified in cross-profiles. However, if these inflexion points were to be joined together, the result would be an elongate polygon delineating the BMG in planform, similar to the way that onshore MSGLs were originally mapped. In other words, width measurements targeted the same feature in both landform types but did so by using a different graphic basis. The measurements for spacing are somewhat different between the two datasets, in that for MSGLs spacing was considered as the mean between adjacent landforms on *either* side, whereas for BMGs spacing values were extracted between the next adjacent individual moving in one direction across ice flow. What matters here, however, is that in both cases spacing represents the distance between the centre line of landforms, and that both approaches carry out systematic measurements along and across ice flow, which likely return realistic mean values for each site. The main differences between the two datasets relate to the number of sampled landforms. Thus, the MSGL population selected for width, spacing and amplitude measurements consists of 1929, 3543 and 1607 features, respectively (Table III in Spagnolo et al., 2014), whereas for the BMGs these metrics were extracted from 276, 355 and 244 features, respectively (see Table 3.3). However, this discrepancy in numbers is balanced by the grid size on which measurements were done, namely every 1,000 m for MSGLs and every 100 m for mega-grooves, so the number of datapoints is within comparable ranges between the two landform types. For both BMGs and MSGLs the range for each metric is representative for 80% of the landform population, comprising data between the 10^{th} and the 90^{th} percentile. Although it is not an exact comparison, the overall results are likely realistic considering it has been done at a very general level, based on the aggregated landform populations.

The results (Table 3.5) show that BMGs are on average approximately 4× shorter, 3.5× narrower, 3.5× more closely spaced and about 2× deeper than MSGLs (Figure 3.21A). Modal values for length, width and spacing are an order of magnitude higher for MSGLs. Significantly, there is no overlap between the modal value for any given metric, whereas the difference in depth is less pronounced. The results show that BMGs are consistently shorter, narrower, deeper and denser than MSGLs (Figure 3.21B), so at least morphometrically, BMGs and MSGLs appear to represent different landform populations.

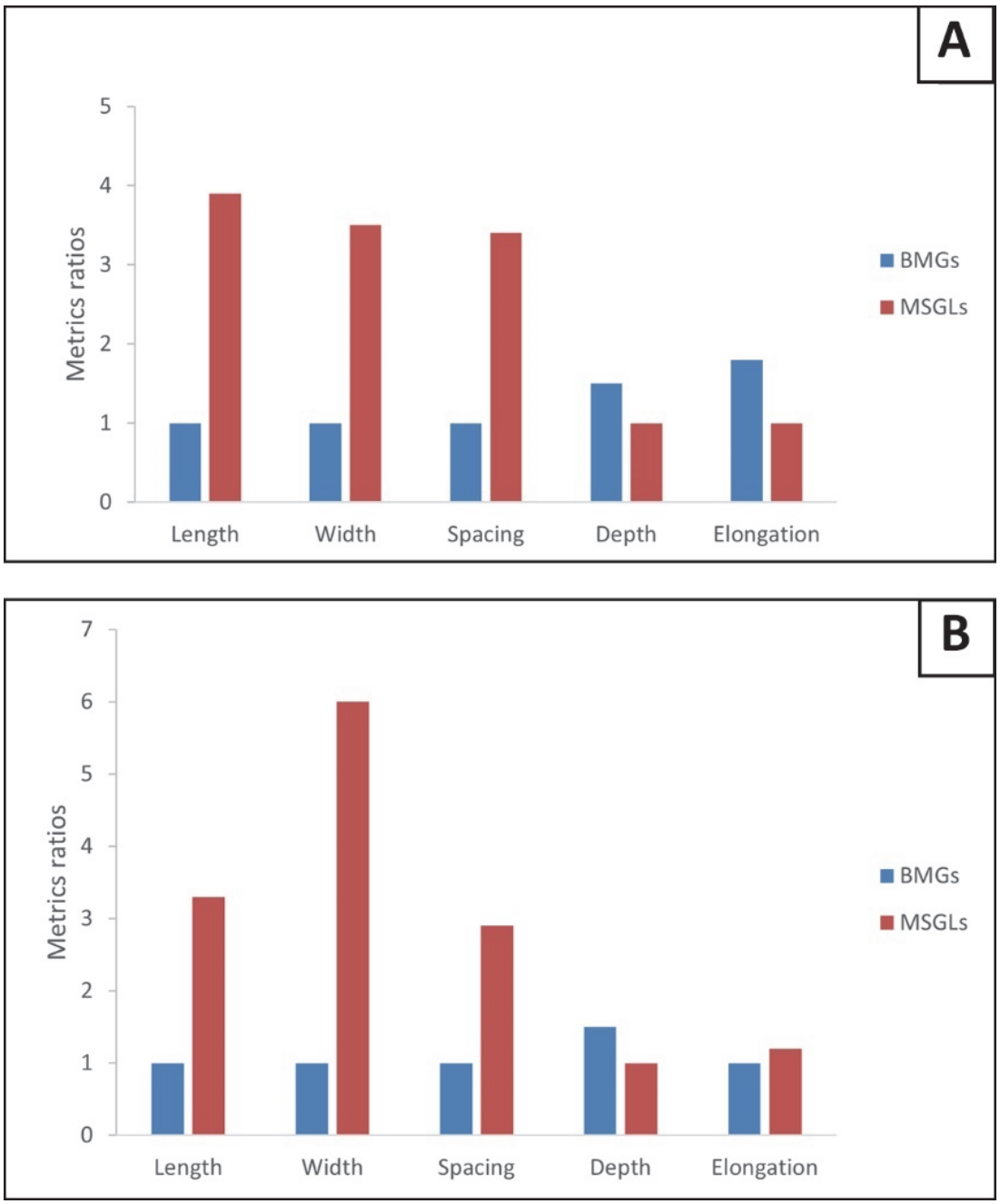

Figure 3.21. Comparative representation of metrics for BMGs and MSGLs, based on mean values (**A**) and modal values (**B**) corresponding to the aggregated landform population for each landform type (see Table 3.5 for details).

In order to further refine comparisons between BMGs and MSGLs, the landforms are further analysed within the palaeo-ice stream landsystem in which they occur, because the glaciological conditions can be assumed uniform, thus reducing the number of variables.

The sites selected for this analysis are Pine Island and Vikna because the BMGs there are of similar magnitude (see Section 3.5.2) and they are situated in the zone of fast-flow onset within ice-stream landsystems comprising MSGLs for which morphometric data is available. The ratios of mean metrics between BMGs and their associated MSGLs were calculated, and the results presented in Table 3.6 and illustrated in Figure 3.22. The results show that BMGs are 1–1.6× narrower, 0.8–1.5× more closely spaced, and ~2.5× shorter than their corresponding MSGLs (Figures 3.22A and 3.22B). Although this is a crude comparison, it shows that when analysed within a (palaeo)ice-stream landsystem, the discrepancy between dimensions of BMGs and their associated MSGLs is greatly reduced in comparison to results of the same analyses based on aggregated global populations. This creates scope for further investigations into links between the BMGs and MSGLs (see Section 6.2.2).

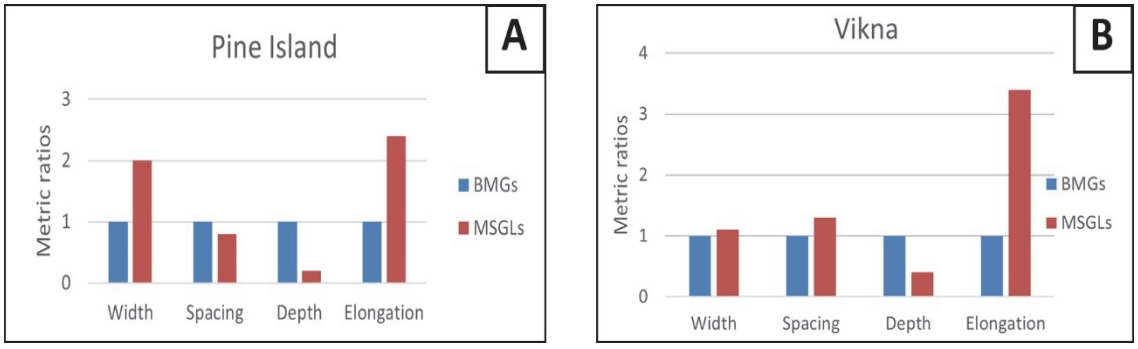

Figure 3.22. Ratios of BMG and MSGL metrics from Pine Island (**A**) and Vikna (**B**), based on mean values listed in Table 3.6. The landform pairs belong to the same palaeo-ice stream landsystem for Pine Island, and to associated landsystems for Vikna (see heading for Table 3.6 for details).

Table 3.5. Summary of metrics for BMGs and MSGLs. The figures for MSGL metrics were extracted from Spagnolo et al. (2014).

Landform	Length (m)			Width (m)			Spacing (m)			Depth (m)			Elongation ratios		
	Range	Mode	Mean	Range	Mode	Mean	Range	Mode	Mean	Range	Mode	Mean	Range	Mode	Mean
BMGs	224–2,269	400–500	1018	21–210	20–30	98	35–315	80–90	134	2–15	3	7	5–41	8–10	20
MSGLs	940–9,050	1,000–2,000	3,967	90–720	100–200	348	140–960	200–300	458	1–9	1–2	4	6–33	6–8	17

Table 3.6. Mean values for metrics of BMGs at Pine Island and Vikna, and for their associated MSGLs. The MSGL values at Pine Island are extracted from Spagnolo et al. (2014), apart from width which is from Evans et al. (2006). At Vikna, in the absence of MSGL metrics from the associated Sklinnadjupet palaeo-ice stream landsystem, the MSGLs from three other landsystems along the Norwegian coast were used for comparison, where a similar transition from crystalline to sedimentary bedrock has been documented within each fast-flow onset zone, namely Skagerrak, Trænadjupet and Andfjorden (Ottesen et al., 2002 and 2005). Where an interval was provided, the average between the end members was calculated and reported here. The BMG metrics are mean values (Table 3.3). N/D= not determined.

Ice stream ID	Ice stream location	Landform and site ID	Mean Length (m)	Length ratio MSGLs/BMGs	Mean Width (m)	Width ratio MSGLs/BMGs	Mean Spacing (m)	Spacing ratio MSGLs/BMGs	Mean Depth (m)	Depth ratio BMGs/MSGLs
Pine Island	W Antarctica	BMGs (Pine Island)	1580	2.5	180	1.6	270	0.8	14	4.6
		MSGLs (Pine Island)	4,019		290		228		3	
Sklinnadjupet	W Norway	BMGs (Vikna)	1,117	N/D	218	1–1.2	300	1.2–1.5	7	1.4–2
Norwegian Channel	SW Norway	MSGLs (Skagerrak)	N/D		275		400		3.5	
Trænadjupet	W Norway	MSGLs (Trænadjupet)	N/D		250		450		<5	
Tromsøflaket	N Norway	MSGLs (Andfjorden)	N/D		210		370		<3	

A high elongation ratio for subglacial bedforms (mean 17:1 for MSGLs, Spagnolo et al., 2014) is considered diagnostic of their formation through ice streaming (Stokes and Clark, 2002). The opposite seems true for BMGs formed under the primary control of fast-ice flow conditions, which yield the lowest mean values in the global BMG population with ratios of 5:1 and 7:1 (Table 3.3) and classify BMGs as approximately 3× less elongated than MSGLs. Potential underestimation of width due to the coarse resolution of the DEMs may have skewed the results towards higher values to some extent (see Section 2.3.3.4), which may have reduced elongation ratios, but it cannot account for the consistency in elongation ratio, which remains striking considering all the other differences between the two sites (see Section 3.5.2). Despite both BMGs and MSGLs being elongate landforms formed subglacially, the discrepancy between their elongation ratios could reflect the essentially different geomorphic mechanisms which drive their evolution and make them different landforms. Thus, MSGLs evolve through an interplay between erosion and deposition, whereby the soft sediment in the deformation layer is transported and deposited downstream (King et al., 2009). This can lead to MSGLs lengthening without widening, and thus their elongation ratios increasing as they grow longer over time. The low elongation ratios for the BMGs formed through enhanced erosion due to high ice-flow velocities are explained by groove widening over time, and possibly adjacent groove merging as erosion progresses laterally. The different feedback mechanisms driving landform development show that BMGs and MSGLs are essentially different landform types, despite their similar shape and formation under similar glaciological conditions. However, this does not rule out the likelihood of possible connections between BMGs and MSGLs as component parts of ice-stream landsystems. One possible link is that the supply of new debris eroded from BMGs upstream may add to the deforming layer in MSGLs. BMGs may also have the potential to act as "moulds" for the formation of ice keels that could plough through unlithified sediment downstream, contributing to MSGL formation (Clark et al., 2003; Piasecka et al., 2018). Also, the fact that BMGs can channel meltwater leading to the formation of channels in the base of the ice down-flow, beyond the grooved terrain (Jeofry et al., 2018; Drews et al., 2020), may direct and focus processes of erosion down-ice flow, which could potentially affect MSGLs.

In summary, quantitative comparisons between BMGs and MSGLs based on aggregated global datasets show that they represent two landform types. Morphometrically they are discrete landform populations with BMGs approximately 4× shorter, 3.5× narrower, 3.5× more closely spaced and about 2× deeper than MSGLs. However, these differences are reduced by half when BMGs and MSGLs are analysed within their associated ice-stream

landsystems. The most marked difference between BMGs and their associated MSGLs resides in their elongation ratios, which could be explained by the different feedback mechanisms driving their development and are a strong indication that they represent different landform types. However, the morphometric differences between BMGs and MSGLs does not prevent them forming close together, particularly where an ice stream bed is composed of both hard bedrock and soft substrate.

3.5.4 How do BMGs evolve through time?

Two questions lie at the core of BMG research: how are BMGs initiated and how do they evolve? The first question remains to be investigated elsewhere (see Chapter 5), but the second question can be explored here using the results of quantitative analyses. Unlike drumlins (Ely et al., 2018), BMGs cannot shrink through erosion unless the intervening ridges are lowered at a higher rate than the grooves deepen (which would lead to landform obliteration). However, considering that, once initiated, a bedrock groove is likely to act as a "trap" for any agents of erosion such as ice, debris, water (Boulton, 1974), it could be argued that continued erosion leads to BMG growth through simultaneous lengthening, widening and deepening. Landform growth is indicated by the existence of the longer tail to the right of the mode in the frequency distribution graphs for length, width and depth, reflected in the positive skew (Figure 3.17), and in the high values for kurtosis especially for length and depth, indicating that BMGs are capable of attaining large dimensions (c.f. Clark et al., 2009). BMG growth is also reflected in the positive correlations between length, width and depth at individual localities (Figures 7–9 in the Appendix), despite such correlations being weak for the length/width and length/depth relationships (see Section 3.4.2; Figure 3.18A and 3.18B). This means that, overall, the longer BMGs tend to be the deeper and wider specimens. The stronger and consistently positive width/depth correlations show that deep grooves are also wide (Section 3.4.2; Figure 3.18C). This confirms that BMGs have a strong tendency to grow deeper as they become wider, a trend that is reflected in the statistical significance of the width/depth correlations (Table 3.4) and which explains the high preservation potential of these landforms, as suggested by early studies (Smith, 1948; Funder, 1978). However, the steeper length/width trend than the length/depth trend, as shown by the comparison between equations corresponding to each linear trendline within individual sites (Figures 7 and 8 in the Appendix), may indicate that lateral erosion is more efficient than in-depth erosion. In theory, this would first result in adjacent grooves merging, leading to an increase in width and spacing (Figure 3.19D), and given time, it would lead to landform obliteration unless the erosion cycle is somehow reset. This is

another aspect that could be tested through numerical modelling experiments by future research (see Section 6.2.3).

Theoretically there are several scenarios of long-term BMG evolution, considering the way frequency distribution of landform metrics could change over time, namely remain unchanged, shift to the right/left of the current modal value, or become more evenly spread (Ely et al., 2018). Currently, the distribution patterns of the BMG metrics are unimodal, with a positive skew (Figure 3.17A–D). For the distribution patterns to remain unchanged through time, the current equilibrium between the production rate of new, smaller grooves coming into the system and the growth rate of the existing grooves needs to be maintained, so that the mode remains unchanged (Figure 3.23A). The mode would shift to the left if the production rate of small grooves exceeded that of landform growth (Figure 3.23B), and it would be expected to shift to the right if too few new grooves came into the system as the existing ones continued growing (Figure 3.23C). Notably, at sites comprising the largest BMGs, the values of landform dimensions tend to be more widely and uniformly spread out. This applies to Vikna and Pine Island, where BMG formation was controlled primarily by ice streaming (see Section 3.5.2; Figures 2–5 in the Appendix). The same trend has been noted for drumlins, where one common reason for non-uniformity in landform evolution has been proposed as landform initiation at different times during pattern evolution (Ely et al., 2018). For drumlins, this trend has been supported by results of statistical and numerical models (Fowler et al., 2013; Barchyn et al., 2016), techniques as yet not applied to BMGs. Assuming the BMGs at Vikna and Pine Island are the oldest and therefore most evolved landforms, the current distribution pattern may suggest BMG evolution towards a flat distribution, with a reduced preference for scaling relative to a mode as the landforms mature (Figure 3.2.3D). It is still not known whether this pattern emerges only under ice-streaming conditions, applicable so far to these two sites, or whether it would be the end result of prolonged glacial erosion under slow flowing conditions given the necessary time for the landforms to grow (see Section 3.5.3). Modelling experiments will hopefully be able to test these scenarios in the future.

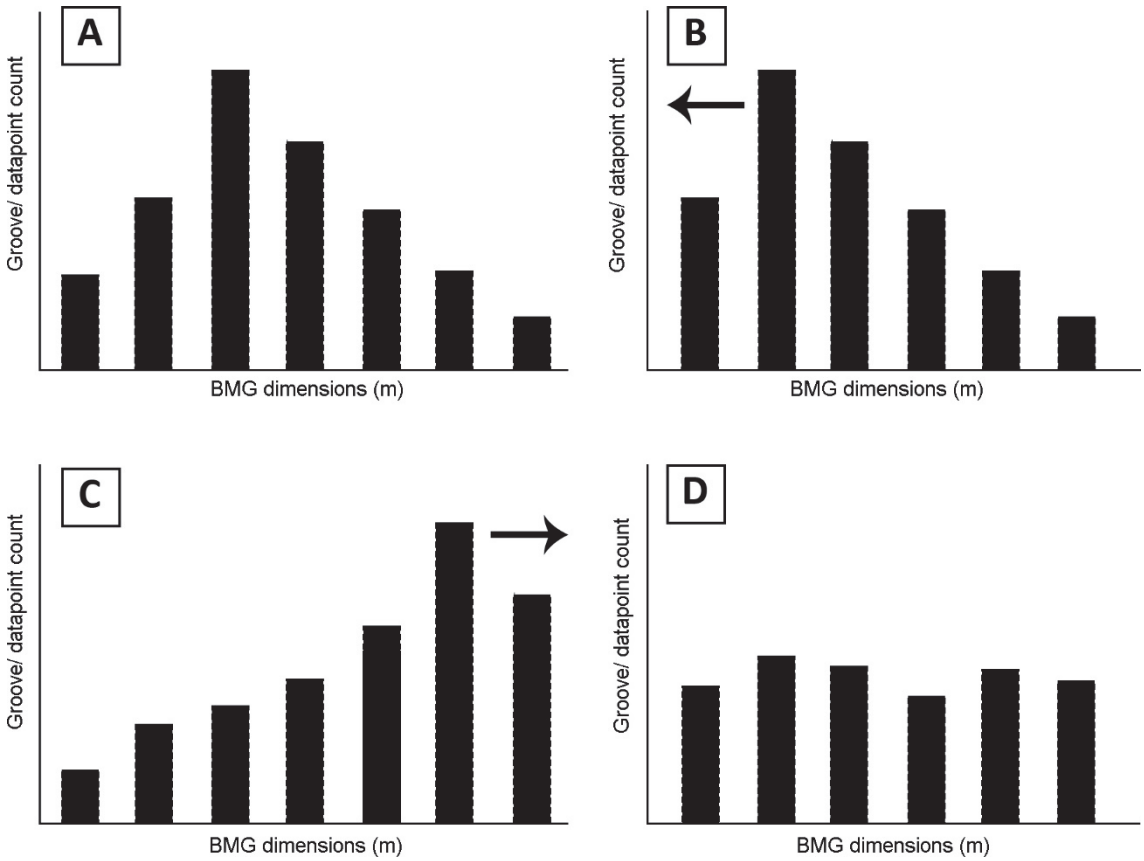

Figure 3.23. Schematic diagram illustrating how BMG evolution over time would affect dimensional frequency distribution. **A:** the current distribution patterns for BMG length, width and depth are unimodal with a positive skew. **B:** mode shifting to the left, over time, would imply that the rate of new grooves being formed is higher than the rate at which grooves grow in size. **C:** mode shifting to the right, over time, would imply fewer new grooves being formed relative to the rate of development of existing grooves. **D:** a shift over time to a flat distribution with no obvious mode would imply an equilibrium between groove formation and development at all stages in their evolution.

The lengths, widths and depths of the aggregated BMG population show a tendency towards smaller values, reflected in median values lower than means (Table 3.3), positioned at the low end of the value spectrum (Figures 3.17A, 3.17B and 3.17D). Considering that the resolution at which mapping and measurements were done prevented the recording of small grooves, the mode may actually be situated further to the left. However, the distribution patterns are similar to those for length and width of drumlins, a possible explanation being that not enough time has yet passed for the landforms to attain larger dimensions (c.f. Clark et al., 2009). This explanation remains speculative for the BMGs and is difficult to test without knowing their age or how they were initiated, in addition to the fact that aggregated global populations may comprise landforms of different age. Knowing for how long a particular set of BMGs had spent under the ice would enable comparison of samples that lay under ice sheets for a long time with those found in ice marginal areas and were not under the ice for long, and to infer rates of BMG evolution from any differences.

However, most BMG sites in the northern hemisphere are located within the limits of the area that has been most frequently glaciated (Batchelor et al., 2019) and unless more peripheral BMG sites are discovered, this spatial distribution could indicate that BMGs were initiated earlier in the Quaternary, by glaciations which pre-date the most recent.

In summary, BMGs evolve by lengthening, widening and deepening, as suggested by the positive correlations between these metrics at all levels of analysis. The particularly strong positive correlation between width and depth may explain the high preservation potential of BMGs as they continue to deepen while becoming wider. As the BMGs attain larger dimensions, individual metrics show a reduced preference for scaling, reflected by the more evenly spread frequency distribution patterns. However, it is uncertain whether this is the effect of fast-flowing ice or simply equifinality under any glaciological conditions.

3.6 Conclusions

The results of landform measurements confirm that BMGs are elongate landforms of considerable length, depth and width in the suite of landforms formed subglacially, and with a high degree of parallelism to former regional ice-flow directions. Based on the aggregated global population, BMGs have lengths of 224–2269 m, widths of 21–210 m, depths of 2–15 m, elongation ratios of 5:1–41:1 and spacing of 35–315 m. Morphometrically the BMGs plot as a single landform population with a unimodal spatial distribution and overlapping value ranges for all metrics, which implies that they represent one landform type. There is a pronounced inter-site variability both in the spatial and the statistical distribution of the BMG metrics, as well as in the non-linear landform development of BMG length in relation to width and depth, likely due to highly variable local control factors.

The BMGs formed under streaming ice are the largest in the dataset and have the lowest elongation ratios. This is interpreted as the result of enhanced erosion induced by fast-flowing ice in contact with the bedrock, possibly over long periods of time. When bedrock geology is hypothesised to be the primary control, the BMGs have smaller dimensions, with plucking-dominated grooves occupying mid-range position in the metrics spectrum, and with abrasion-dominated grooves positioned at the lower end. There is independent evidence to suggest that the deepest BMGs may have been enhanced by meltwater erosion. Strongly positive and consistent linear correlations between site-specific mean values for BMG metrics, analysed across the site populations, show a uniformity in the development

of BMG metrics. This points to an overarching scenario of BMG development likely to be inherent to the physics of the process of bedrock erosion by glacier ice.

Morphometrically BMGs and MSGLs plot as different populations. BMGs are on average approximately 4× shorter, 3.5× narrower, 3.5× more closely spaced and about 2× deeper. The lower elongation ratios of BMGs than MSGLs are the result of the different mechanisms of landform evolution, with the former widening through lateral erosion and the latter lengthening as soft sediment is mobilised and deposited downstream. Despite similarities in their morphology and occurrence within the same ice-stream landsystems, BMGs and MSGLs are different landform types due to their different morphometry and formation mechanisms.

Future research could advance understanding of BMG development through numerical modelling experiments. These could test rates of erosion in different bedrock substrates under varying glaciological conditions, which might also provide constraints on uncertain landform age from their dimensions. Empirical evidence remains key in validating geological controls over BMG formation and in assessing the efficiency of erosion mechanisms, ideally done through direct field observation. At the same time, analyses of morphometric data retrieved through remote sensing for BMGs and MSGLs within the same ice-stream landsystem could help elucidate links between the two types of landform and fast-ice flow.

Acknowledgements: Thanks to Dag Ottesen from the Geological Survey of Norway for access to the 3D imagery for Vikna and the seismic profiles for this site reproduced in Figure 3.11D; to Nikos Putkinen from the Geological Survey of Finland, for signposting the Iivaara site to us; to Brian Anderson, from Rice University of Texas, for making MN aware of GeoMapApp; to Terry Allen (https://www.allenfotowild.com/) for providing the photograph of the Røde Ø conglomerate, Greenland, reproduced in Figure 3.2C.

3.7 References

Aitken, J D; Cook, D G., 1979. Geology, Sans Sault Rapids, District of Mackenzie; Geological Survey of Canada, "A" Series Map 1453A, 1 sheet, https://doi.org/10.4095/123316 (Open Access)

Alldrick, D.J., MacIntyre, D.G. and Villeneuve, M.E., 2006. Geology, Mineral Deposits and Exploration Potential of the Skeena Group (NTS 093E, L, M; 103I), Central British Columbia. *Geological Fieldwork*, pp.2007-1.

Barchyn, T.E., Dowling, T.P., Stokes, C.R. and Hugenholtz, C.H., 2016. Subglacial bed form morphology controlled by ice speed and sediment thickness. *Geophysical Research Letters*, *43*(14), pp.7572-7580.

Batchelor, C.L., Margold, M., Krapp, M., Murton, D.K., Dalton, A.S., Gibbard, P.L., Stokes, C.R., Murton, J.B. and Manica, A., 2019. The configuration of Northern Hemisphere ice sheets through the Quaternary. *Nature Communications*, *10*(1), pp.1-10.

Benn, D.I. and Evans D.J.A., 2010. *Glaciers and Glaciation*. Second edition. Routledge, London.

Boulton G.S. 1974. Processes and Patterns of Glacial Erosion. In: Coates, D.R. (ed), *Glacial Geomorphology.* University of New York, Binghampton, pp. 41–87.

Bradwell, T., 2005. Bedrock megagrooves in Assynt, NW Scotland. *Geomorphology*, *65*(3-4), pp.195-204.

Bradwell, T., Stoker, M. and Krabbendam, M., 2008. Megagrooves and streamlined bedrock in NW Scotland: the role of ice streams in landscape evolution. *Geomorphology*, *97*(1-2), pp.135-156.

Bradwell, T., Stoker, M. and Larter, R., 2007. Geomorphological signature and flow dynamics of The Minch palaeo-ice stream, northwest Scotland. *Journal of Quaternary Science 22*(6), pp.609-617.

British Geological Survey (BGS), 2008. Ullapool. Scotland Sheet 101E. Bedrock. 1:50,000 Geology Series.

British Geological Survey (BGS), 2011. Bedrock Geology of the United Kingdom. DIGMAP50k. Digital GeologicalMap and Database.British Geological Survey, Keyworth, Nottingham, UK.

Brown, V.H. 2012. Ice stream dynamics and pro-glacial lake evolution along the north-western margin of the Laurentide Ice Sheet. Unpublished PhD thesis, Durham University.

Brown, V.H., Stokes, C.R. and Ó Cofaigh, C., 2011. The glacial geomorphology of the north-west sector of the Laurentide Ice Sheet. *Journal of Maps*, *7*(1), pp.409-428.

Boulton, G.S., 1979. Processes of glacier erosion on different substrata. *Journal of glaciology*, *23*(89), pp.15-38.

Bugge, T., Knarud, R. and Mørk, A., 1984. Bedrock geology on the mid-Norwegian continental shelf. In *Petroleum geology of the North European margin* (pp. 271-283). Springer, Dordrecht.

Chamberlin, T.C., 1888. *The rock-scorings of the great ice invasions*. US Geological Survey, 7th Annual Report, pp.155-254.

Chandler, B.M., Lovell, H., Boston, C.M., Lukas, S., Barr, I.D., Benediktsson, Í.Ö., Benn, D.I., Clark, C.D., Darvill, C.M., Evans, D.J.A. and Ewertowski, M.W., 2018. Glacial geomorphological mapping: A review of approaches and frameworks for best practice. *Earth-Science Reviews*, *185*, pp.806-846.

Clark, C.D., 1993. Mega-scale glacial lineations and cross-cutting ice-flow landforms. *Earth Surface Processes and Landforms*, *18*(1), pp.1-29.

Clark, C.D., Tulaczyk, S.M., Stokes, C.R. and Canals, M., 2003. A groove-ploughing theory for the production of mega-scale glacial lineations, and implications for ice-stream mechanics. *Journal of Glaciology*, *49*(165), pp.240-256.

Clark, C.D., Hughes, A.L., Greenwood, S.L., Spagnolo, M. and Ng, F.S., 2009. Size and shape characteristics of drumlins, derived from a large sample, and associated scaling laws. *Quaternary Science Reviews*, *28*(7-8), pp.677-692.

Collinson, J.D., 1972. *The Røde Ø Conglomerate of Inner Scoresby Sund and the Carboniferous and Permian Rocks West of the Schuchert Flod*. Reitzel.

DigMapGB_50, 2016. Tile sc101e. Geological Map Data, British Geological Survey © UKRI 2016

Drewry, D.J., 1986. *Glacial geologic processes*. E. Arnold.

Drews, R., Schannwell, C., Ehlers, T.A., Gladstone, R., Pattyn, F. and Matsuoka, K., 2020. Atmospheric and Oceanographic Signatures in the Ice Shelf Channel Morphology of Roi Baudouin Ice Shelf, East Antarctica, Inferred From Radar Data. *Journal of Geophysical Research: Earth Surface*, *125*(7), p.e2020JF005587.

Duk-Rodkin, A; Hughes, O. L., 1993. Surficial Geology, Sans Sault Rapids, District of Mackenzie, Northwest Territories; Geological Survey of Canada, "A" Series Map 1784A, 1 sheet, https://doi.org/10.4095/184008 (Open Access).

Dühnforth, M., Anderson, R.S., Ward, D. and Stock, G.M., 2010. Bedrock fracture control of glacial erosion processes and rates. *Geology*, *38*(5), 423-426.

Dunlop, P. and Clark, C.D., 2006. The morphological characteristics of ribbed moraine. *Quaternary Science Reviews*, *25*(13-14), 1668-1691.

Dunlop, P., Clark, C.D. and Hindmarsh, R.C., 2008. Bed ribbing instability explanation: testing a numerical model of ribbed moraine formation arising from coupled flow of ice and subglacial sediment. *Journal of Geophysical Research: Earth Surface*, *113*(F3).

Ely, J.C., Clark, C.D., Spagnolo, M., Stokes, C.R., Greenwood, S.L., Hughes, A.L., Dunlop, P. and Hess, D., 2016. Do subglacial bedforms comprise a size and shape continuum? *Geomorphology*, *257*, 108-119.

Ely, J.C., Clark, C.D., Spagnolo, M., Hughes, A.L. and Stokes, C.R., 2018. Using the size and position of drumlins to understand how they grow, interact and evolve. *Earth Surface Processes and Landforms*, *43*(5), pp.1073-1087.

Evans, D.J.A., Rea, B.R. and Benn, D.I., 1998. Subglacial deformation and bedrock plucking in areas of hard bedrock. *Glacial Geology and Geomorphology* rp04/1998 (http://ggg.qub.ac.uk/papers/frame.htm)

Evans, J., Dowdeswell, J.A., Ó Cofaigh, C., Benham, T.J. and Anderson, J.B., 2006. Extent and dynamics of the West Antarctic Ice Sheet on the outer continental shelf of Pine Island Bay during the last glaciation. *Marine Geology*, *230*(1-2), pp.53-72.

Evenchick, C.A., McMechan, M.E., Mustard, Ferri, F and Waldron, J.W.F., 2008. Geology, Hazelton, British Columbia. Geological Survey of Canada, Open File 5704. BC Ministry of Energy, Mines and Petroleum Resources, Petroleum Geology Open Files 2008-6, scale 1: 125 000.

Eyles, N., 2006. The role of meltwater in glacial processes. *Sedimentary Geology*, *190*(1-4), 257-268.

Eyles, N., 2012. Rock drumlins and megaflutes of the Niagara Escarpment, Ontario, Canada: a hard bed landform assemblage cut by the Saginaw–Huron Ice Stream. *Quaternary Science Reviews*, *55*, 34-49.

Eyles, N., Moreno, L.A. and Sookhan, S., 2018. Ice streams of the Late Wisconsin Cordilleran Ice Sheet in western North America. *Quaternary Science Reviews*, *179*, pp.87-122.

Eyles, N. and Putkinen, N., 2014. Glacially-megalineated limestone terrain of Anticosti Island, Gulf of St. Lawrence, Canada; onset zone of the Laurentian Channel ice stream. *Quaternary Science Reviews*, *88*, 125-134.

Fallas, K.M., 2013. Geology, Mahony Lake (southeast), Northwest Territories; Geological Survey of Canada, Canadian Geoscience Map 90, scale 1:100 000. doi:10.4095/292282 https://doi.org/10.4095/292282 (Open Access).

Fettes, D.J., Long, C.B., Bevins, R.E., Max, M.D., Oliver, G.J.H., Primmer, T.J., Thomas, L.J. and Yardley, B.W.D., 1985. Grade and time of metamorphism in the Caledonide Orogen of Britain and Ireland. *Geological Society, London, Memoirs*, *9*(1), pp.41-53.

Fowler, A.C., Spagnolo, M., Clark, C.D., Stokes, C.R., Hughes, A.L.C. and Dunlop, P., 2013. On the size and shape of drumlins. *GEM-International Journal on Geomathematics*, *4*(2), pp.155-165.

Fossen, H., 2016. *Structural geology*. Cambridge University Press, Cambridge.

Funder, S., 1978. Glacial flutings in bedrock, an observation in East Greenland. *Bulletin of the Geological Society of Denmark*, *27*, pp.9-13.

Geological Map of Greenland 1:500,000. 2014. Format ESRI ArcGIS package. Geological Survey of Denmark and Greenland

Geological Survey of Finland, 2016. Bedrock of Finland 1:200,000 https://hakku.gtk.fi/en/

Graham, A.G., Larter, R.D., Gohl, K., Dowdeswell, J.A., Hillenbrand, C.D., Smith, J.A., Evans, J., Kuhn, G. and Deen, T., 2010. Flow and retreat of the Late Quaternary Pine Island-Thwaites palaeo-ice stream, West Antarctica. *Journal of Geophysical Research: Earth Surface*, *115*(F3).

Gravenor, C.P. and Meneley, W.A., 1958. Glacial flutings in central and northern Alberta. *American Journal of Science*, *256*(10), pp.715-728.

Hallet, B., 1996. Glacial quarrying: A simple theoretical model. *Annals of Glaciology*, *22*, pp.1-8.

Hamilton, J. and Ford, D., 2002. Karst geomorphology and hydrogeology of the Bear Rock Formation—a remarkable dolostone and gypsum megabreccia in the continuous permafrost zone of Northwest Territories, Canada. *Carbonates and Evaporites*, *17*(2), pp.114-115.

Heikkinen, O. and Tikkanen, M., 1989. Drumlins and flutings in Finland: their relationships to ice movement and to each other. *Sedimentary geology*, *62*(2-4), pp.349-355.

Henriksen, N. (1983). Geological map of RØdefjord 70 Ø3 Nord 1: 100,000. Map compiled by Henriksen in 1977. Geological Survey of Greenland.

Hillier, J.K., Smith, M.J., Clark, C.D., Stokes, C.R. and Spagnolo, M., 2013. Subglacial bedforms reveal an exponential size–frequency distribution. *Geomorphology*, *190*, pp.82-91.

Hillier, J.K., Kougioumtzoglou, I.A., Stokes, C.R., Smith, M.J., Clark, C.D. and Spagnolo, M.S., 2016. Exploring explanations of subglacial bedform sizes using statistical models. *PloS one*, *11*(7), p.e0159489.

Hume, G.S., 1954. The lower Mackenzie River area, Northwest Territories and Yukon: Geol. *Survey Canada Mem*, *273*. https://doi.org/10.4095/101498 (Open Access)

Iverson, N.R., 1991. Morphology of glacial striae: implications for abrasion of glacier beds and fault surfaces. *Geological Society of America Bulletin*, *103*(10), pp.1308-1316.

Iverson, N.R., 1995. Processes of erosion. In: Menzies, J. (ed.), *Modern Glacial Environments: Processes, Dynamics and Sediments.* Butterworth-Heinemann, Oxford, pp.241-260.

Jeofry, H., Ross, N., Le Brocq, A., Graham, A.G., Li, J., Gogineni, P., Morlighem, M., Jordan, T. and Siegert, M.J., 2018. Hard rock landforms generate 130 km ice shelf channels through water focusing in basal corrugations. *Nature communications*, *9*(1), pp.1-9.

Jezek, K., Wu, X., Gogineni, P., Rodríguez, E., Freeman, A., Rodriguez-Morales, F. and Clark, C.D., 2011. Radar images of the bed of the Greenland Ice Sheet. *Geophysical Research Letters*, *38*(1) L01501.

King, E.C., Hindmarsh, R.C. and Stokes, C.R., 2009. Formation of mega-scale glacial lineations observed beneath a West Antarctic ice stream. *Nature Geoscience*, *2*(8), pp.585-588.

Kirkham, J.D., Hogan, K.A., Larter, R.D., Arnold, N.S., Nitsche, F.O., Golledge, N.R. and Dowdeswell, J.A., 2019. Past water flow beneath Pine Island and Thwaites glaciers, West Antarctica. *The Cryosphere*, *13*(7), pp.1959-1981.

Krabbendam, M., Prave, T. and Cheer, D., 2008. A fluvial origin for the Neoproterozoic Morar Group, NW Scotland; implications for Torridon–Morar group correlation and the Grenville Orogen Foreland Basin. *Journal of the Geological Society*, *165*(1), pp.379-394.

Krabbendam, M. and Bradwell, T., 2011. Lateral plucking as a mechanism for elongate erosional glacial bedforms: explaining megagrooves in Britain and Canada. *Earth Surface Processes and Landforms*, *36*(10), pp.1335-1349.

Krabbendam, M. and Bradwell, T., 2014. Quaternary evolution of glaciated gneiss terrains: pre-glacial weathering vs. glacial erosion. *Quaternary Science Reviews*, *95*, pp.20-42.

Krabbendam, M., Eyles, N., Putkinen, N., Bradwell, T. and Arbelaez-Moreno, L., 2016. Streamlined hard beds formed by palaeo-ice streams: A review. *Sedimentary Geology*, *338*, pp.24-50.

Krabbendam, M. and Glasser, N.F., 2011. Glacial erosion and bedrock properties in NW Scotland: abrasion and plucking, hardness and joint spacing. *Geomorphology*, *130*(3-4), pp.374-383.

Lawson, T.J., 1996. Glacial striae and former ice movement: the evidence from Assynt, Sutherland. *Scottish Journal of Geology*, *32*(1), pp.59-65.

Lehijärvi, M., 1960. *The alkaline district of Iivaara, Kuusamo, Finland* (Vol. 185). Valtioneuvoston kirjapaino. Open access through https://books.google.co.uk/

Lehtinen, M., Nurmi, P.A. and Ramo, O.T., 2005. *Precambrian Geology of Finland*. Elsevier, Amsterdam.

Linton, D.L., 1963. The forms of glacial erosion. *Transactions and Papers (Institute of British Geographers)*, (33), pp.1-28.

Livingstone, S.J., Ó Cofaigh, C. and Evans, D.J.A., 2008. Glacial geomorphology of the central sector of the last British-Irish Ice Sheet. *Journal of Maps*, *4*(1), pp.358-377.

Livingstone, S.J., Storrar, R.D., Hillier, J.K., Stokes, C.R., Clark, C.D. and Tarasov, L., 2015. An ice-sheet scale comparison of eskers with modelled subglacial drainage routes. *Geomorphology*, *246*, pp.104-112.

Lowe, A.L. and Anderson, J.B., 2002. Reconstruction of the West Antarctic ice sheet in Pine Island Bay during the Last Glacial Maximum and its subsequent retreat history. *Quaternary Science Reviews*, *21*(16-17), pp.1879-1897.

Lowe, A.L. and Anderson, J.B., 2003. Evidence for abundant subglacial meltwater beneath the paleo-ice sheet in Pine Island Bay, Antarctica. *Journal of Glaciology*, *49*(164), pp.125-138.

Margold, M., Stokes, C.R. and Clark, C.D., 2015. Ice streams in the Laurentide Ice Sheet: Identification, characteristics and comparison to modern ice sheets. *Earth-Science Reviews*, *143*, pp.117-146.

McLaren, D.J., 1962. *Middle and Early Devonian Rhynchonelloid Brachiopods from Western Canada*. Geological Survey of Canada, Bulletin 86, Department of Mines and Technical Surveys. https://doi.org/10.4095/100604 (Open Access)

Newton, M., Evans, D.J.A., Roberts, D.H. and Stokes, C.R., 2018. Bedrock mega-grooves in glaciated terrain: A review. *Earth-Science Reviews*, *185*, pp.57-79.

Nitsche, F.O., Gohl, K., Larter, R.D., Hillenbrand, C.D., Kuhn, G., Smith, J.A., Jacobs, S.S., Anderson, J.B. and Jakobsson, M., 2013. Paleo ice flow and subglacial meltwater dynamics in Pine Island Bay, West Antarctica. *The Cryosphere 7*, pp.249-262.

Ottesen, D., Dowdeswell, J.A., Rise, L., Rokoengen, K. and Henriksen, S., 2002. Large-scale morphological evidence for past ice-stream flow on the mid-Norwegian continental margin. *Geological Society, London, Special Publications 203*(1), pp.245-258.

Ottesen, D., Dowdeswell, J.A. and Rise, L., 2005. Submarine landforms and the reconstruction of fast-flowing ice streams within a large Quaternary ice sheet: The 2500-km-long Norwegian-Svalbard margin (57–80 N). *GSA Bulletin*, *117*(7-8), pp.1033-1050.

Peach, B.N., Horne, J., Gunn, W., Clough, C.T., Teall, J.J.H. and Hinxman, L.W., 1907. *The geological structure of the North-West Highlands of Scotland*. HM Stationery Office.

Piasecka, E.D., Stokes, C.R., Winsborrow, M.C. and Andreassen, K., 2018. Relationship between mega-scale glacial lineations and iceberg ploughmarks on the Bjørnøyrenna Palaeo-Ice Stream bed, Barents Sea. *Marine Geology*, *402*, pp.153-164.

Punkari, M., 1980. The ice lobes of the Scandinavian ice sheet during the deglaciation in Finland. *Boreas*, *9*(4), pp.307-310.

Rea, B.R. and Brian Whalley, W., 1994. Subglacial observations from Øksfjordjøkelen, north Norway. *Earth Surface Processes and Landforms*, *19*(7), pp.659-673.

Roberts, D.H. and Long, A.J., 2005. Streamlined bedrock terrain and fast ice flow, Jakobshavns Isbrae, West Greenland: implications for ice stream and ice sheet dynamics. *Boreas 34*(1), pp.25-42.

Roberts, D.H., Long, A.J., Davies, B.J., Simpson, M.J. and Schnabel, C., 2010. Ice stream influence on west Greenland ice sheet dynamics during the last glacial maximum. *Journal of Quaternary Science*, *25*(6), pp.850-864.

Roberts, D.H., Rea, B.R., Lane, T.P., Schnabel, C. and Rodés, A., 2013. New constraints on Greenland ice sheet dynamics during the last glacial cycle: evidence from the Uummannaq ice stream system. *Journal of Geophysical Research: Earth Surface*, *118*(2), pp.519-541.

Robin, G.D.Q., 1976. Is the basal ice of a temperate glacier at the pressure melting point?. *Journal of Glaciology*, *16*(74), pp.183-196.

Röthlisberger, H. and Iken, A., 1981. Plucking as an effect of water-pressure variations at the glacier bed. *Annals of Glaciology*, *2*, pp.57-62.

Sharpe, D.R. and Shaw, J., 1989. Erosion of bedrock by subglacial meltwater, Cantley, Quebec. *Geological Society of America Bulletin*, *101*(8), pp.1011-1020.

Shaw, J., 2002. The meltwater hypothesis for subglacial bedforms. *Quaternary International*, *90*(1), pp.5-22.

Sindern, S. and Kramm, U., 2000. Volume characteristics and element transfer of fenite aureoles: a case study from the Iivaara alkaline complex, Finland. *Lithos*, *51*(1-2), pp.75-93.

Smith, A.M., Bentley, C.R., Bingham, R.G. and Jordan, T.A., 2012. Rapid subglacial erosion beneath Pine Island glacier, west Antarctica. *Geophysical Research Letters*, *39*(12) L12501

Smith, H.T.U., 1948. Giant glacial grooves in northwest Canada. *American Journal of Science*, *246*(8), pp.503-514.

Smith, M.J. and Clark, C.D., 2005. Methods for the visualization of digital elevation models for landform mapping. *Earth Surface Processes and Landforms*, *30*(7), pp.885-900.

Sørensen K., 1970. Geological map of the northern Røde Fjord area 1:50, 000. Field observations. Open access through the Greenland Portal of the Geological Survey of Denmark and Greenland https://eng.geus.dk/

Spagnolo, M., Clark, C.D., Ely, J.C., Stokes, C.R., Anderson, J.B., Andreassen, K., Graham, A.G. and King, E.C., 2014. Size, shape and spatial arrangement of mega-scale glacial lineations from a large and diverse dataset. *Earth Surface Processes and Landforms*, *39*(11), pp.1432-1448.

Stemmerik, L. and Piasecki, S., 2004. Isotopic evidence for the age of the Røde Ø Conglomerate, inner Scoresby Sund, East Greenland. *Bulletin of the Geological Society of Denmark*, *51*, pp.137-140.

Stoker, M. and Bradwell, T., 2005. The Minch palaeo-ice stream, NW sector of the British–Irish Ice Sheet. *Journal of the Geological Society*, *162*(3), pp.425-428.

Stokes, C.R. and Clark, C.D., 1999. Geomorphological criteria for identifying Pleistocene ice streams. *Annals of Glaciology*, *28*, pp.67-74.

Stokes, C.R. and Clark, C.D., 2001. Palaeo-ice streams. Quaternary Science Reviews 20(13), pp.1437-1457.

Stokes, C.R. and Clark, C.D., 2002. Are long subglacial bedforms indicative of fast ice flow?. *Boreas*, *31*(3), pp.239-249.

Stokes, C.R., Spagnolo, M., Clark, C.D., Ó Cofaigh, C., Lian, O.B. and Dunstone, R.B., 2013. Formation of mega-scale glacial lineations on the Dubawnt Lake Ice Stream bed: 1. size, shape and spacing from a large remote sensing dataset. *Quaternary Science Reviews*, *77*, pp.190-209.

Storrar, R.D., Stokes, C.R. and Evans, D.J.A., 2014. Morphometry and pattern of a large sample (> 20,000) of Canadian eskers and implications for subglacial drainage beneath ice sheets. *Quaternary Science Reviews*, *105*, pp.1-25.

Sugden, D.E., 1974. Landscapes of glacial erosion in Greenland and their relationship to ice, topographic and bedrock conditions. *Institute of British Geographers Special Publication*, *7*, pp.177-195.

Sutinen, R., Hyvönen, E., Närhi, P., Haavikko, P., Piekkari, M. and Middleton, M., 2010. Sedimentary anisotropy diverges from flute trends in south-east Finnish Lapland. *Sedimentary Geology*, *232*(3-4), pp.190-197.

Tassonyi i, E.J., 1969. Subsurface geology, lower Mackenzie River and Anderson River area, District of Mackenzie (Vol. 25). Department of Energy, Mines and Resources, https://doi.org/10.4095/103335 (Open Access)

Wardlaw, N.C., Stauffer, M.R. and Hoque, M., 1969. Striations, giant grooves, and superposed drag folds, Interlake area, Manitoba. *Canadian Journal of Earth Sciences*, *6*(4), pp.577-593.

Whipple, K.X., Hancock, G.S. and Anderson, R.S., 2000. River incision into bedrock: Mechanics and relative efficacy of plucking, abrasion, and cavitation. *Geological Society of America Bulletin*, *112*(3), pp.490-503.

Witkind, I.J., 1978. Giant glacial grooves at the north end of the Mission Range, northwest Montana. *J. Res. US Geol. Surv*, *6*(4), pp.425-433.

Zumberge, J.H., 1955. Glacial erosion in tilted rock layers. *The Journal of Geology*, *63*(2), pp.149-158.

Chapter 4. Glacial erosion in metasandstone: implications for fast-ice flow and bedrock mega-groove (BMG) formation at Ullapool, Scotland, UK

Abstract

Recent studies have proposed that bedrock mega-grooves (BMGs) represent a signature landform of the onset zone of ice streams flowing over a bedrock substrate. This interpretation has been applied to the BMGs at Ullapool, Scotland, UK, where they were hypothesised to have formed in the onset zone of the Minch palaeo-ice stream, which drained the NW sector of the British–Irish Ice Sheet. The genesis of the BMGs within this hard-bed landform assemblage is appraised here, in conjunction with other linear features of the structural geology. The results show that all bedrock landforms follow medium-to-large structural lineaments, and their present-day topographic expression is the result of glacial erosion through abrasion and plucking, with the latter directly controlled by the availability and orientation of bedrock joints and fractures. The BMGs are the most conspicuous landforms in the study area due to the orientation of bedrock strike sub-parallel to the former ice-flow direction, which enabled lateral plucking. Although the BMGs remain traceable throughout the study area, their dominance in the landscape varies in relation to imprints of other bedrock landforms in the local landsystem, such as roches moutonnées, whalebacks, lineaments of plucked cliffs and assemblages of bedrock channels. Overall, the landscape is one of areal scouring, best described as groove-and-lochan topography, characterised by a grid of cross-cutting linear landforms underpinned by ancient structural features, with lakes commonly present at the intersection of structural lines. Despite their presence in an area of fast-flow onset, it is argued that the BMGs do not constitute unequivocal evidence for fast-ice flow nor was fast-flowing ice a necessary condition for BMG initiation. This conclusion is supported by independent empirical evidence from an area comprising landforms akin to the BMGs at Ullapool, formed in similar Moine Schist lithology beneath slower ice-sheet flow.

4.1 Introduction

In recent decades, the understanding of ice streams and their geomorphic signature has evolved from an initial focus on the development of streamlined bedforms in soft-bed settings to a greater focus on hard-bed settings (Clark, 1993; Stokes and Clark, 1999; Ottesen et al., 2005; Livingstone et al., 2012; Spagnolo et al., 2014; Margold et al., 2015;

Bradwell et al., 2007; Eyles, 2012; Krabbendam et al., 2016). In soft-bed settings it been demonstrated that elongate, subglacial bedforms, termed mega-scale glacial lineations (MSGLs) (Clark, 1993), evolve in response to sediment transport and deposition at the ice–bed interface through basal sliding and sediment deformation (Smith et al., 2007; King et al, 2009; Spagnolo et al., 2016; Stokes, 2018). Soft-bed landforms can evolve in response to short-lived, single-flow phase events. Their morphometry can develop in response to changing ice-flow velocity, which has been linked to a subglacial bedform continuum (Ely et al., 2016; Ely et al., 2018). Changing ice-flow dynamics (e.g. flow direction) are reflected in the orientation of superimposed flow sets of soft-bed landforms (Stokes et al., 2009), hence their invaluable role in the reconstruction of ice sheet dynamics (Dowdeswell et al., 2006; Ó Cofaigh et al., 2010; Van Landeghem and Chiverrell, 2020).

In hard-bed settings the evolution of streamlined bedforms is more complex and controlled principally by erosional processes heavily influenced by the bedrock geology (Roberts et al., 2010; Krabbendam and Bradwell, 2011; Bradwell, 2013; Lane et al., 2015). The erosional processes comprise glacial abrasion and plucking, and also meltwater erosion operating beneath warm-based ice, with resulting landscapes of areal scour and selective linear erosion (Sudgen 1968 and 1974; Roberts et al., 2010). Hard-bed landforms do not evolve through a single glacial phase, but are the product of long term, multi-cycle glacial erosion, and they can retain their orientation despite changes in ice-flow direction (Roberts and Long, 2005; Finlayson et al, 2014).

In ice-stream settings, hard- and soft-bed environments are often transitional in nature and directly linked to the dynamic evolution of the ice stream through flow convergence, resulting in the formation of onset and trunk zones (Stokes and Clark, 1999; De Angelis and Kleman, 2008; Ottesen et al., 2016). Beneath an ice-stream onset zone, increased ice thickness and flow acceleration trigger enhanced erosion and bedrock excavation (Ottesen et al., 2016). This can lead to the development of streamlined bedrock terrain characterised by rock drumlins, whalebacks, mega-grooves and mega-ridges (Dyke and Morris, 1988; Lowe and Anderson, 2003; Roberts and Long, 2005; Bradwell et al., 2008b; Roberts et al., 2010; Eyles, 2012; Eyles et al., 2016; Krabbendam et al., 2016). Based on their spatial association to ice-stream landsystems, BMG and mega-ridge development across previously glaciated terrain has been assigned a glaciological causality, being specifically linked to ice streaming (Bradwell et al., 2008b; Eyles and Putkinen, 2014; Krabbendam et al., 2016; Eyles et al., 2018), but the relationship between fast-ice flow and geological structure has been only partially researched (Roberts and Long, 2005; Roberts et al., 2010; Lane et al, 2015).

At Ullapool, in Assynt, Northwest Scotland, UK (Figure 4.1), empirical evidence has demonstrated that BMG modification through lateral plucking was strongly controlled by the presence of small-scale structural joints (Krabbendam and Bradwell, 2011). Furthermore, an overall primary geological control over the BMG formation at Ullapool has been inferred from morphometric analyses, whereby groove dimension, density and elongation ratios are typical of BMGs formed under a slow-ice or interstream-flow regime (see Chapter 3). Collectively, these results deem glaciological control secondary, despite the area being situated in a fast-flow onset zone (Figure 4.2) and show that the role of fast-ice flow in bedrock erosion and groove formation at Ullapool needs to be reappraised. This is done here by adding new morphometric data and empirical observations pertaining to BMGs, and by extending landform analysis to other bedrock landforms. The latter occur in conjunction with the BMGs and pertain to the same hard-bed terrain in this former zone of ice stream onset. Firstly, we map and describe the major geological structures. Secondly, we describe the glacial landforms, with emphasis on the efficiency of plucking and abrasion enabled by local geological features. Finally, we consider the influence of ice dynamics, structural geology and pre-glacial conditioning with respect to the long-term evolution of this hard-bed zone of the last British–Irish Ice Sheet.

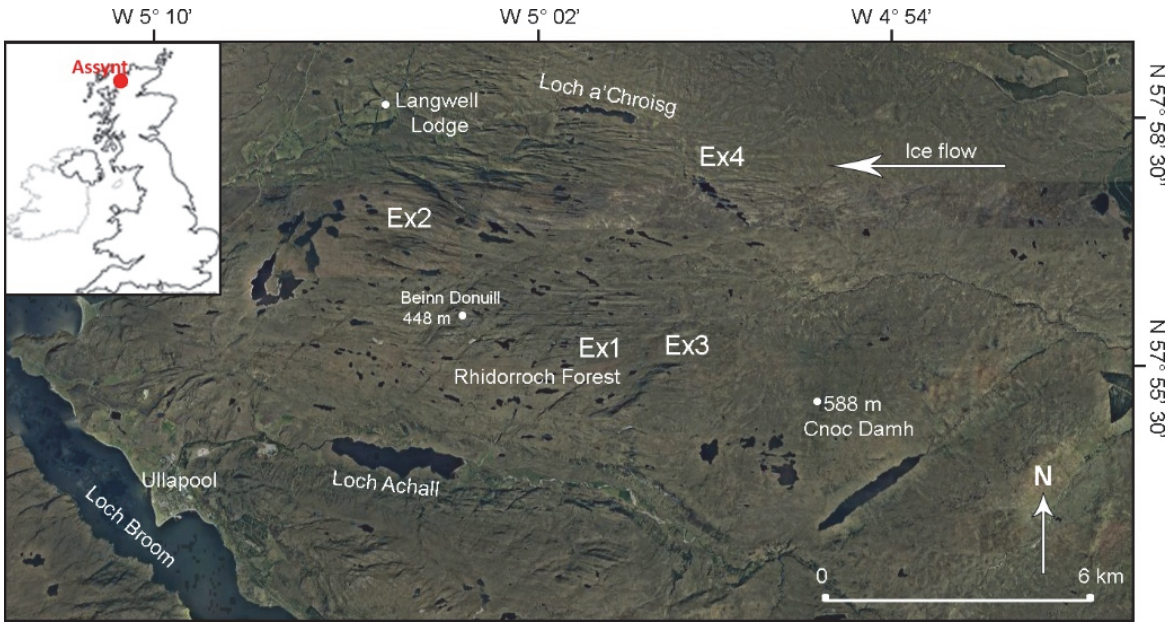

Figure 4.1. Satellite image of the study area near Ullapool centred around Rhidorroch Forest. Inset shows location of the study area in Assynt, Northwest Highlands, Scotland. Ex1–4 indicate areas where fieldwork excursions were conducted (see Section 4.3.2). Base image © Google Earth. Outline of inset map © EnnchantedLearning.com.

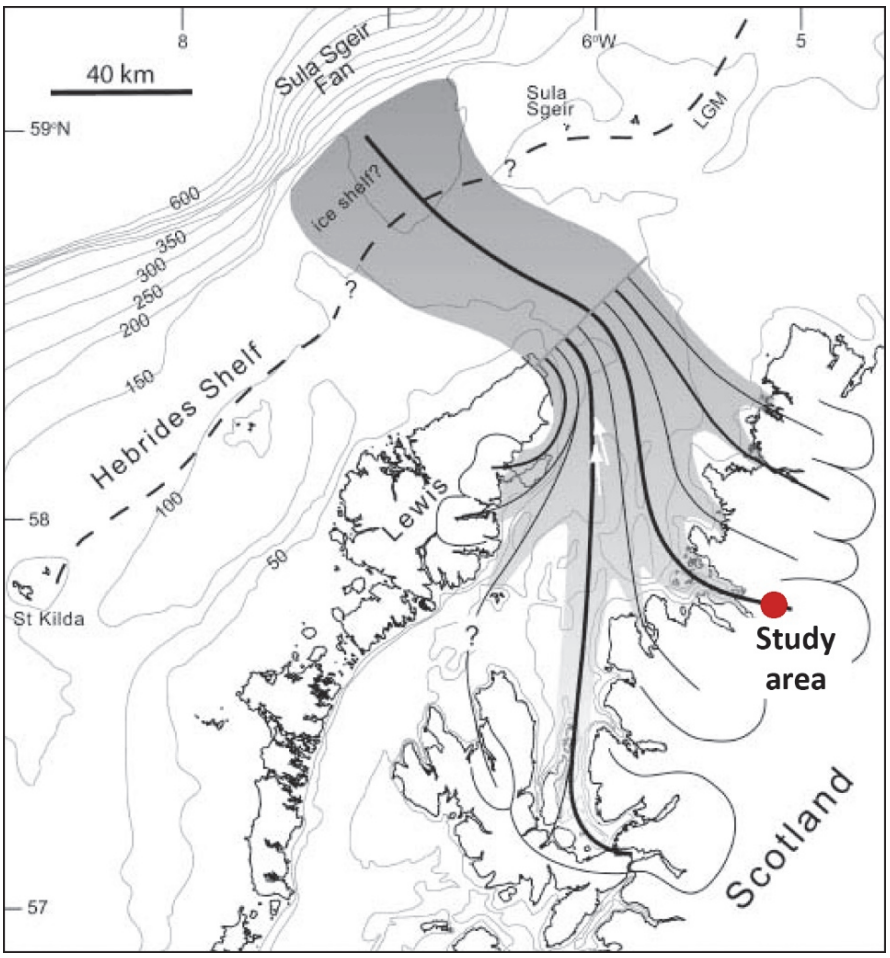

Figure 4.2. Reconstruction of the Minch Ice Stream during the Last Glacial Maximum (Bradwell et al., 2007). The position of the Ullapool tributary glacier draining the study area (red dot) was inferred based primarily on the presence of the streamlined bedrock grooves and ridges. Figure modified from Bradwell et. al. (2007). Base image © John Wiley & Sons.

4.2 Study area

The study area is situated north-east of Ullapool, in Assynt, the Northwest Highlands of Scotland, UK (Figure 4.1) and comprises the highland terrain around Loch Achall with an average altitude of 300 m a.s.l. and area of approximately 60 km^2 (Figure 4.3). The general aspect is that of a plateau sloping gently to the north. The topography is highly dissected in the west and dotted by a myriad of elongated lakes (Figure 4.4), whereas in the east it is smooth and gently undulating (Figure 4.3), with several high peaks rising above the overall surface (e.g. Beinn Donuill 448 m). The area is devoid of forest, despite the toponym Rhidorroch Forest north of Loch Achall (Figure 4.1), and is covered by shrub vegetation of heather, alongside grasses and mosses, with frequent bedrock outcrops across the central-western parts.

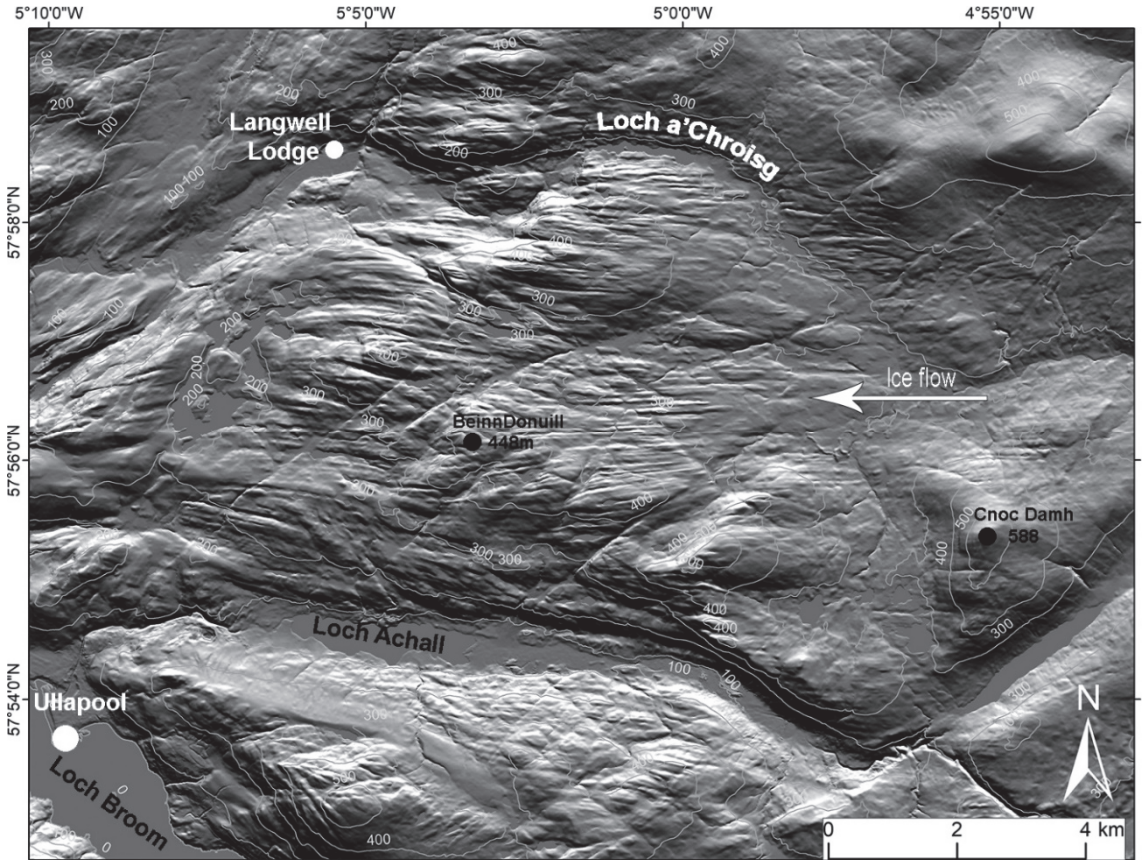

Figure 4.3. Digital terrain model of the study area, showing BMGs aligned parallel to the palaeo-ice flow direction and the relief (at 300–400 m a.s.l.) across the grooved area. Note the grooved and dissected terrain in the western-central part in comparison to the more subdued relief in the east, with less well pronounced grooving north of Cnoc Damh. Illumination source from the north. Image © NEXTMap Technologies, BGS NERC, UK.

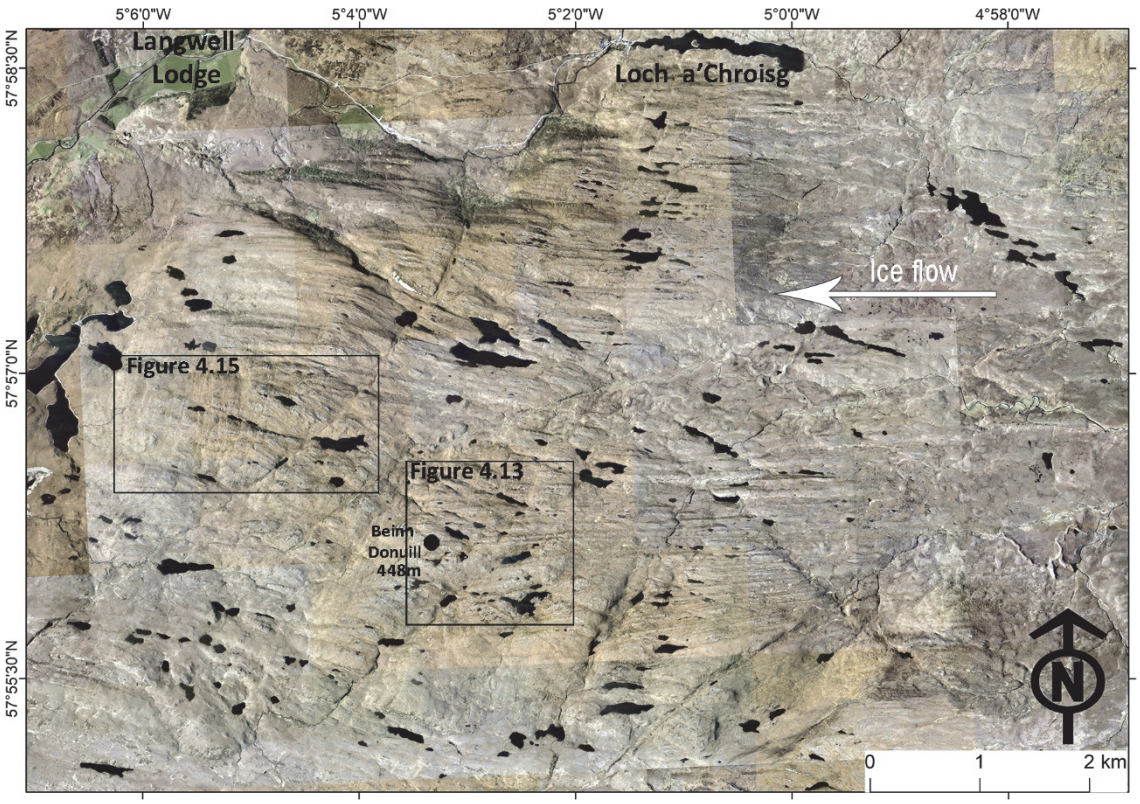

Figure 4.4. Aerial photograph mosaic of the study area. Note the presence of closely spaced BMGs aligned east–west, cross-cut by series of less conspicuous, linear features with different but consistent orientations, parallel to each other. Base image © Edina Digimap.

4.2.1 Geology

The bedrock outcrops close to or at the surface, and the area is largely devoid of unconsolidated glacigenic sediment (British Geological Survey, 2016). The bedrock lithology is uniform across the area (Peach et al., 1907) and consists of metasandstones of the Morar Formation, which belong to the Moine Schists Supergroup (Figure 4.5A). The Moine Schists were originally deposited as sandstone in a shallow marine environment (Strachan, 1986). Medium-grade metamorphism resulted in bed thinning and the formation of cleavage planes parallel to bedding, so that in the field the rocks appear thinly stratified and they split easily along cleavage planes. Although the original depositional structure is well preserved, the bedding planes are not easily recognisable due to intense foliation (Johnstone et al., 1969). Several major tectonic events have affected the sequence of the Moine meta-sediments, of which the most recent took place approximately 400 Ma ago at the end of the Caledonian Orogeny. This event involved the mobilisation and transportation of a thick sequence of Moine Schists many kilometres north-westwards to form large nappe folds (Figure 4.5B), after which they were thrust over younger rocks (Gillen, 2003). The

thrusting of the Moine Schists occurred along the Moine Thrust, but other thrust planes (i.e. Ben More, Glencoul, Sole) are present further to the west (Figure 4.5C) and were active during the same tectonic event.

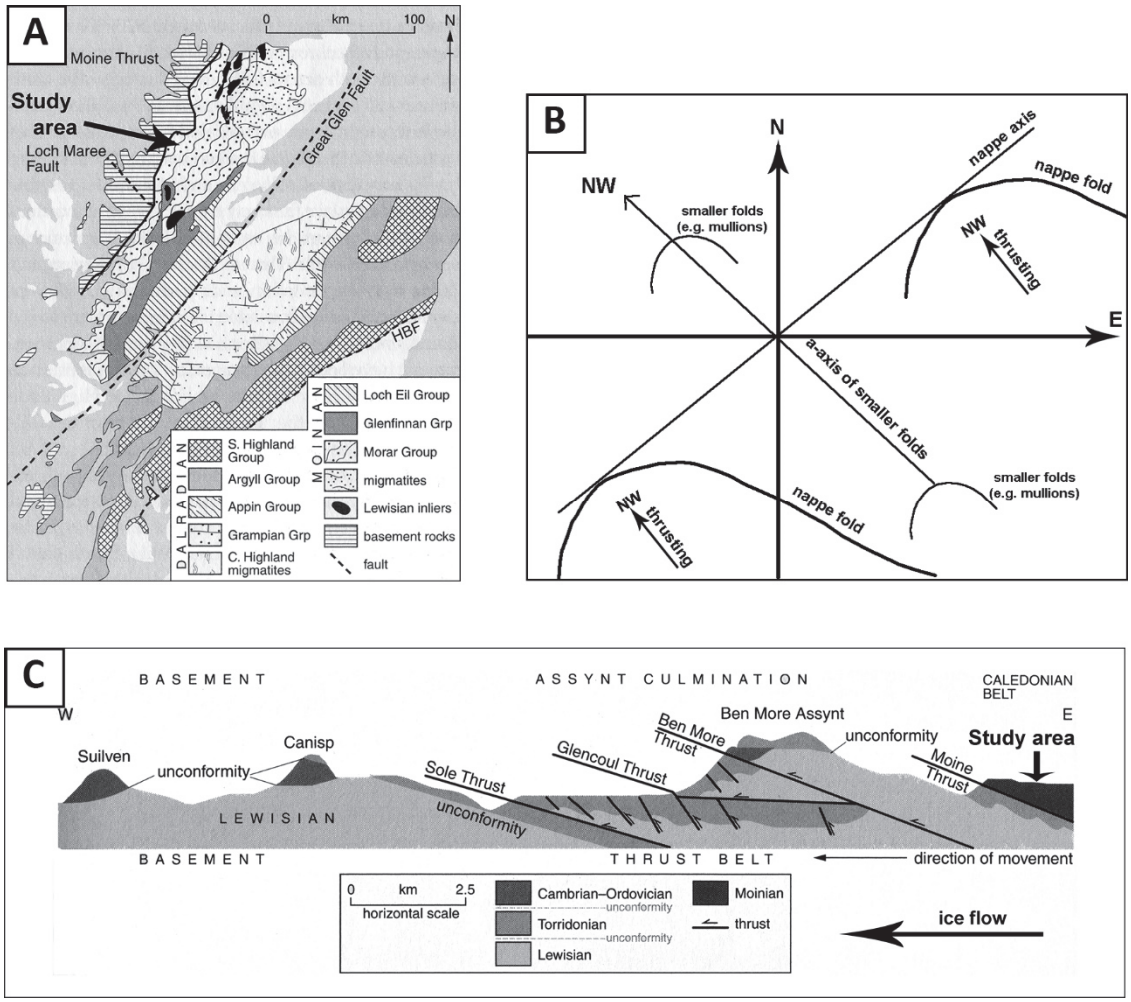

Figure 4.5. A: Location of the study area within the Morar Group Formation, in the wider lithological context of northern Scotland. Image modified from Gillen (2003). Image © Terra Publishing. **B:** Double-folding system in the Moine rocks, with large-scale primary nappe folding and secondary folding superimposed on the nappes, in the form of mullions; schematic representation following the description in Peach et al. (1907, p 601). **C:** The location of the study area in the wider context of structural geology, typical for the contact between the Caledonian Belt in the Northwest Highlands, and the foreland, underlain by Lewisian gneiss, which was unaffected by the Caledonian thrusting. Image modified from Gillen (2003). Base image © Terra Publishing.

The Caledonian movements led to the development of complex, imbricate and folded structures in the rocks between the thrust planes west of the Moine Thrust, due to movement and deformation along smaller, high-angle reverse faults situated between the major, low-angle faults (Peach et al., 1907; Strachan et al., 2010; Gillen, 2003; Figure 4.5C). The Moine Schists, which underlie the BMGs (Figure 4.5A), are situated above the Moine

Thrust and have a double system of folding (Figure 4.5B). One folding system strikes NNE–SSW, with the axial plane dipping to the ESE, aligned with the regional movement of the thrusting to the WNW and with the Moine thrust plane which formed the nappes; and a second fold system, with a-axis aligned WNW–ESE or NW–SE, perpendicular to those of the nappes (Figure 4.5B), comprising series of smaller folds along the foliation planes, termed mullions or rods, which have also been identified in Moine Schists at Loch Eriboll (Peach et al., 1907) and Glen Okyel (Wilson, 1953).

4.2.2 Glacial history

The study area has been subject to multiple Quaternary glaciations, but most recently was glaciated during Marine Isotope Stage 2 and was occupied by the Minch Ice Stream. The Minch Ice Stream was a topographically-constrained, marine-terminating ice stream which drained the north-western sector of last British–Irish Ice Sheet, originating in the Assynt region of western Scotland and reaching the edge of the continental shelf (Bradwell et al., 2007; 2019; Figure 4.2).

Nine tributary glaciers of the Minch Ice Stream were reconstructed as having flowed off the north-west Scottish mainland, northern Skye and north-east Lewis, and coalesced into the main trunk of the Minch trough (Bradwell et al., 2007; Figure 4.2). The Ullapool tributary glacier is highly constrained by topography, occupying the widest glacial breach in the Northwest Highlands of Scotland, bounded to the north and south by much higher ground (Bradwell et al., 2008b). Throughout successive glaciations, topographically-constrained flow would have been channelled through this hard-bed corridor (Bradwell et al., 2008b), which likely became a zone of preferential ice flow during successive glaciations. The offshore record indicates that the Minch Ice Stream activity was episodic (Graham et al., 1990; Stoker, 1995; Stoker and Bradwell, 2005; Bradwell et al., 2019) making it likely that subglacial conditions beneath the fast-flow onset zone mirrored this, with bedform and BMG modification occurring through repeated phases of ice stream onset during successive glacial cycles.

The Minch Ice Stream imparted a distinctive signature in the geomorphic and stratigraphic record offshore (Bradwell et al., 2019), with the main trunk zone comprising a field of mega-scale glacial lineations (MSGLs) in the Minch trough and being bordered by shear-margin moraines on the Hebridean shelf which converge towards to the Sula Sgeir trough-mouth fan (Stoker and Holmes, 1991; Stoker, 1995; Stoker and Bradwell, 2005). The configuration

of the Minch Ice Stream onshore was reconstructed by Bradwell et al. (2007) *after* the offshore record had been identified (Stoker and Bradwell, 2005), based on the presence of streamlined bedrock upstream from the Minch trough. Of critical importance to the reconstruction of the on-shore record of this palaeo-ice stream is the assertion that the BMGs situated at the upstream end of the Ullapool tributary are evidence of bedrock streamlining as a direct product of fast ice-flow in the onset zone of the ice stream (Stoker and Bradwell, 2005; Bradwell et al., 2007; Bradwell et al., 2008b).

In the context of ice-stream landsystems BMGs are commonly regarded as landforms produced by the onset of fast-flow in hard-bed terrains (Krabbendam et al, 2016; Eyles et al., 2018), alongside mega-flutes and streamlined bedrock ridges (Bradwell, 2005; Roberts and Long, 2005; Roberts et al., 2010; Eyles, 2012), rock drumlins (Dyke and Morris, 1988), crag-and-tails and whalebacks (Evans, 1996; Roberts and Long, 2005; Roberts et al., 2010; Bradwell, 2013). At some locations, one landform type can dominate the landscape (e.g. the BMGs at Ullapool; Bradwell et al., 2008b), whereas at other locations there is a mixed set of bedrock forms, such as meltwater canyons, rock drumlins, whalebacks, mega-grooves and mega-ridges (Dyke and Morris, 1988; Lowe and Anderson, 2003; Roberts and Long, 2005; Bradwell et al., 2008b; Roberts et al., 2010; Eyles, 2012; Krabbendam et al., 2016; Eyles, 2018). Despite morphologic differences, all forms are typically elongate and streamlined in the ice-flow direction. They are assumed to have been initiated due to enhanced abrasion beneath warm-based, fast-flowing ice and collectively they have been referred to as "hard-bed landform assemblages" (Eyles, 2012) or "mega-lineated terrain" (Krabbendam et al., 2016), and are typically followed downstream by MSGLs (Stokes and Clark, 1999; Bradwell et al., 2007; Eyles, 2012; Krabbendam et al., 2016; Eyles et al, 2018). At many locations the geological structure underpins BMG formation, while at other sites BMGs could not be linked to any structural controls and are often developed obliquely to major geological structure (Smith, 1948; Funder, 1978; Krabbendam and Bradwell, 2011; Krabbendam et al., 2016; Newton et al., 2018). The BMGs at Ullapool belong to the category of grooves controlled by geological structure which enabled lateral plucking to occur systematically (Krabbendam and Bradwell, 2011; Krabbendam et al., 2016), but the current interpretation is that they have been initiated through enhanced abrasion beneath fast-flowing ice by subglacial debris bands (Bradwell et al., 2008b).

In summary, the study area is situated at the upstream end of the Ullapool tributary to the Minch Ice Stream which may have undergone multiple episodes of ice streaming. The BMGs have been regarded as key landforms in response to enhanced erosion by fast-flowing ice

and have been used as principal geomorphic evidence for the reconstruction of the Ullapool tributary and ice stream onset onshore.

4.3 Methods

4.3.1 Mapping

A composite geomorphological and geological map of the study area was compiled (Figure 4.6) using geological data downloaded from the British Geological Survey (British Geological Survey, 2016) superimposed on a NEXTMap digital terrain model (DTM). The NEXTMap DTM is a bare-earth model containing elevations of natural terrain features. Elevations of vegetation and anthropogenic artefacts have been digitally removed. The resolution is 5 m posting and it has a vertical accuracy of 1 m in unobstructed areas having slopes <10°. The data rendition on DTMs is void-free and seamless because the data-collecting technology is not hindered by any weather effect or cloud coverage. The NEXTMap DTM files are available through https://www.intermap.com/nextmap. High-resolution vertical aerial photographs were used in conjunction with the DTM to visualise the landforms in more detail, especially over small areas (e.g. Figure 4.4). The data are in the form of 25 cm-resolution vertical ortho-photography, available to download from https://digimap.edina.ac.uk/aerial. All digital imagery was imported, labelled and georeferenced in ArcMap 10.5.1, and subsequently annotated in Adobe Photoshop CC2017. The 3D viewing of the aerial photographs was done in ArcScene 10.5.1, with a vertical exaggeration of up to 3× (e.g. Figure 4.4).

Landform mapping focussed on linear features with a negative surface expression, i.e. grooves rather than ridges. These were mapped as lines, being visually guided by changes in the shading along the groove floors on the DTM (Figure 4.3), where the angle of exposure to the illumination source changes. The mapped BMGs were imported from the ArcGIS files in Chapter 3, therefore the mapping protocol detailed in Section 3.3.2 applies and the same errors potentially occur. These refer especially to a possible underestimation of length in some places where BMGs are cross-cut by faults and their continuity across the latter is equivocal (see Section 3.3.2), but such instances are not common and they are unlikely to have skewed the mean result considering the size of the dataset, comprising 248 ladfroms (Table 3.3 in Section 3.4.1). The bedrock units, fault lines and superficial deposits were imported in digital form, as shapefiles (.shp), from the British Geological Survey (2016). The superficial deposits (e.g. peat, glacigenic, alluvial, mass movement) were collated into one unit to simplify the map for the purpose of this research. The bedrock dip and strike were

manually digitised from the paper version of the Scotland Sheet 101E Ullapool map (British Geological Survey, 2008). Topographic profiles were traced using the Spatial Analyst tool in ArcGis 10.5.1 to help assess changes in the terrain topography at key locations.

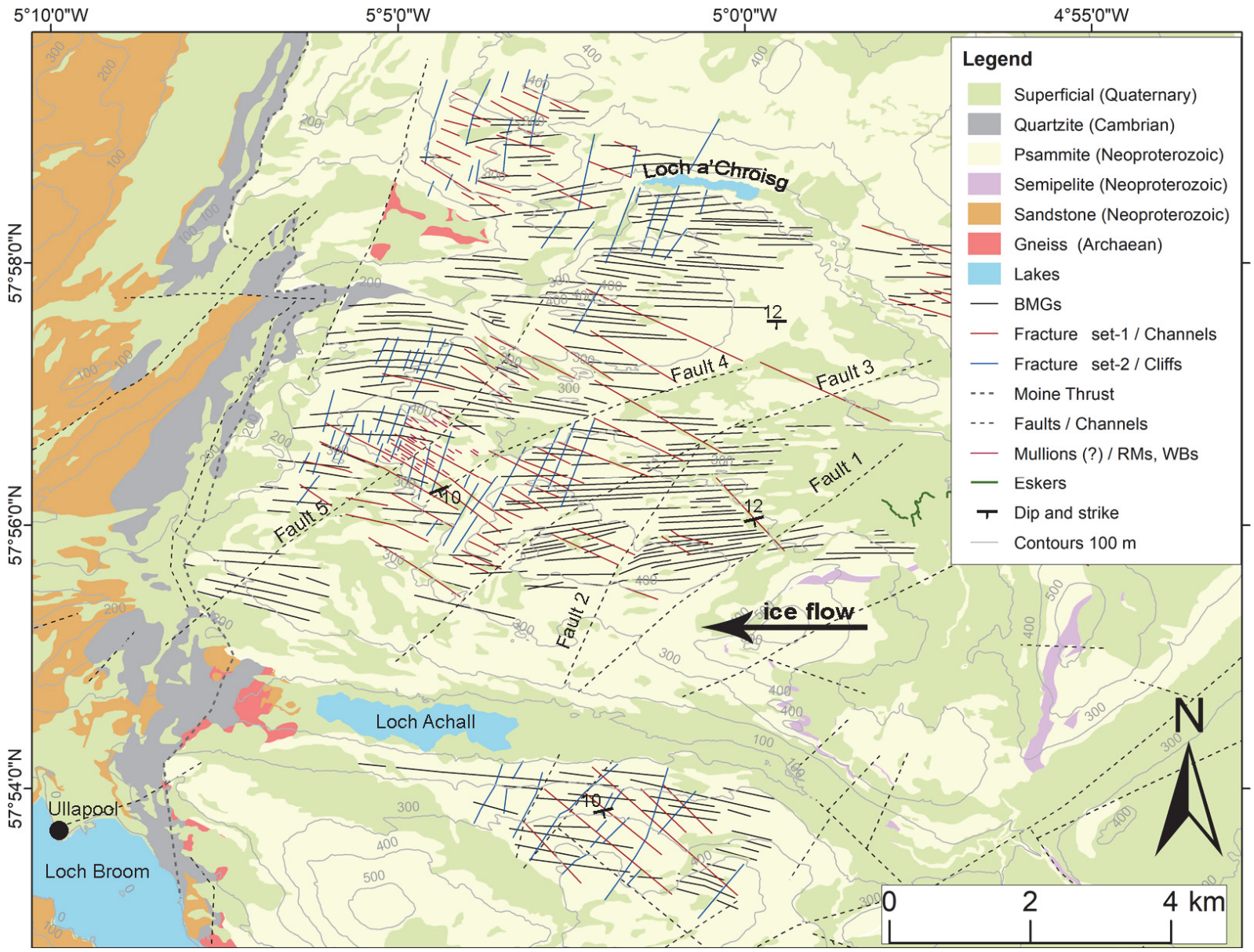
5°10'0"W
5°5'0"W
5°0'0"W
4°55'0"W
57°58'0"N
57°56'0"N
57°54'0"N
Legend
Superficial (Quaternary)
Quartzite (Cambrian)
Psammite (Neoproterozoic)
Semipelite (Neoproterozoic)
Sandstone (Neoproterozoic)
Gneiss (Archaean)
Lakes
BMGs
Fracture set-1 / Channels
Fracture set-2 / Cliffs
Moine Thrust
Faults / Channels
Mullions (?) / RMs, WBs
Eskers
Dip and strike
Contours 100 m
Loch a'Chroisg
Fault 1
Fault 2
Fault 3
Fault 4
Fault 5
ice flow
Loch Achall
Ullapool
Loch Broom
N
0
2
4 km

Figure 4.6. Composite geological and geomorphological map of the study area. The solid bedrock geology, fault lines and superficial deposits were downloaded from the British Geological Survey (2016) digital database, and the bedrock dip and strike were manually transferred from the British Geological Survey Sheet 101E Bedrock Ullapool map (British Geological Survey, 2008). The BMGs and lineations were mapped on the NEXTMap shaded DTM. See Section 4.2.1 for more detail. Abbreviations in the map legend: RMs = roches moutonnées; WBs = whalebacks.

4.3.2 Fieldwork

Fieldwork was conducted in the summer of 2018 following preliminary mapping and examination of aerial imagery, which highlighted the need to clarify three key aspects related to landform and landscape characteristics. Firstly, the mechanisms of BMG erosion and the influence of geological structure on BMG development were assessed in the south-eastern part of Rhidorroch Forest (Ex1 in Figure 4.1). This area was chosen due to the continuity of the BMGs across the landscape, which is largely devoid of cross-cutting landforms. Bedrock outcrops pertaining to the BMGs were examined for signs of plucking, abrasion and meltwater erosion. The orientation of dip and strike of the bedrock joints was recorded systematically along six grooves in Rhidorroch Forest and plotted using RockWorks software available at https://www.rockware.com/product/rockworks/. The new data were intended to supplement previous findings reported from further west, around Beinn Donuill (Bradwell et al., 2008b; Krabbendam and Bradwell., 2011). Secondly, in the west of the study area, the presence of numerous short and closely spaced bedrock lineations prompted a second excursion (Ex2 in Figure 4.1) to examine the geology underpinning these features and their relationship with the BMGs. Thirdly, the relationships between superficial deposits and BMGs in the eastern part of the study area were examined (Ex3 and Ex4 on Figure 4.1), prompted by the generally subdued relief there with fewer BMGs and seemingly few bedrock outcrops.

4.3.3 Statistical analyses of length and spacing

The bedrock lineations were first mapped on the NEXTMap DTM and then grouped into discrete assemblages, according to their prevailing orientation. For each assemblage of lineations the length and spacing were measured, following the protocols detailed in Chapter 3 (see Section 3.3). For the BMGs, the metrics are as described in Chapter 3 (see Section 3.3.3), including the associated errors (see Section 3.3.4). The size frequency distributions for all data series are represented on the same graphs (Figure 4.7), to help compare populations and assess their nature.

4.4 Results

4.4.1 Structural geology

This section describes the nature and origin of the linear structural features mapped in the study area (Figure 4.6) that occur in conjunction with BMGs.

4.4.1.1 Fractures

Two sets of linear features occur in this area in addition to the BMGs, aligned NW–SE and NNE–SSW, respectively. Based on their pervasive occurrence in bedrock, consistent orientation and parallel conformity (Table 4.2), they are structural features, referred henceforth as fracture set-1 (NW–SE) and set-2 (NNE–SSW) (Figure 4.6). Within each group there is a high degree of parallel conformity between individual features (Figure 4.6), reflected in the small values for the standard deviation for the azimuth (Table 4.1). For both fracture sets spacing has a more evenly spread distribution, with no obvious preference for a mode, and with spacing values ranging between 75 and 375 m. This contrasts with the BMGs, which exhibit unimodal spacing at 75–99 m and span a narrow range of relatively low values, 75–150 m (Figure 4.7A). The frequency distribution pattern for length is rather consistent across the three lineation groups in that they are all unimodal, with a positive skew (Figure 4.7B), but both sets of fractures have lower mean values (below 1,000 m) than the BMGs, which have a mean length of >1,000 m (Table 4.1). Collectively, these morphometric results suggest a commonality between the fracture sets and a marked difference to the BMGs. The internal parallel conformity within the fracture sets, and their alignment at an angle to the BMGs and therefore to bedrock strike, justify the choice of the term “fractures” adopted here; this term is also preferred because it does not imply any terrain dislocation. Regarding age, the fractures likely relate to the post-orogenic Caledonian tectonic movement. The alignment of fracture set-2 broadly parallel to the thrust faults aligned NE–SW (Figure 4.5B) and their occurrence confined between fault lines (Figure 4.6) point to a tectonic-related origin for their formation; fracture set-1 are a common occurrence throughout the Moine Series in Scotland and have been associated with thrust movements (Law and Johnson, 2010 and Figure 5a therein). Collectively this implies that the fractures pre-date the Quaternary and are likely related to major tectonic movements of the Moine rocks in the geological past.

Table 4.1. Mean values for spacing, length and azimuth for the three assemblages of cross-cutting lineations, namely fracture set-1 and set-2 and BMGs.

Lineation type	Mean Spacing (m)	Mean Length (m)	Mean Azimuth (°) (Standard deviation)
BMGs	82	1039	274 (8)
Fracture set-1 (NW–SE)	243	929	119 (10)
Fracture set-2 (NNE–SSW)	180	653	208 (14)

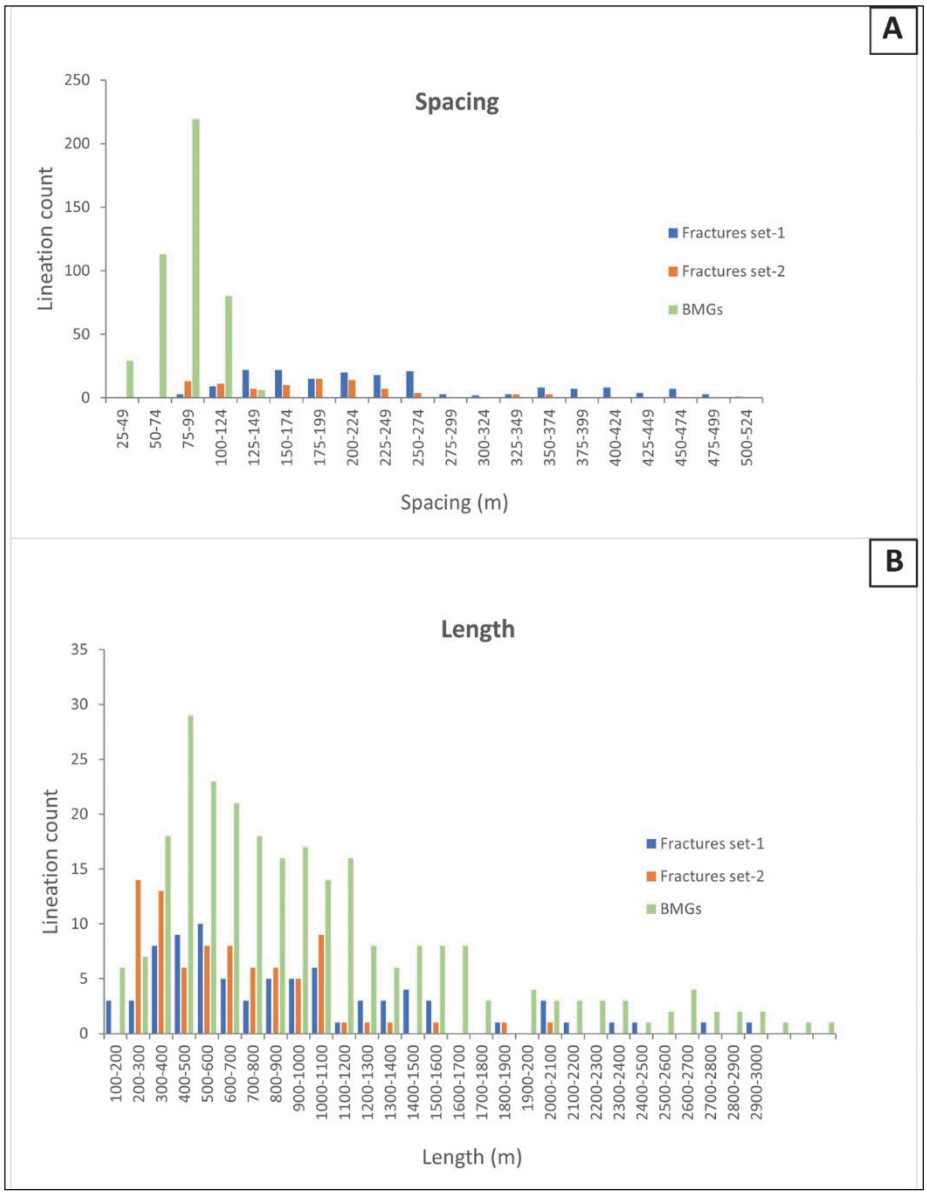

Figure 4.7. Frequency distribution histograms for spacing (**A**) and length (**B**) of the BMGs and fracture set-1 and set-2. The data for BMGs was imported from Chapter 3 (Supplementary Material).

4.4.1.2 Mullion-type folds

In the western part of the study area, the topography is controlled by small-scale folds, with long axis oriented NW–SE and plunging 20–30° to the SE. In places, the folding forms parallel and densely-packed rods, with their north-western end truncated by joints and affected by rock falls due to weathering (Figure 4.8A). These structures are similar to the mullions described at Okyel Bridge (Wilson, 1953), as they occur in the same lithology, have similar orientation and a-axis dips (Figure 4.8A and B), and similar microfabric. The microfabric similarities comprise cleavage structures (Figure 9C and D), typical of cleavage mullions, and highly irregular yet compact cross-section structures (Figure 9E and F) characteristic of irregular mullions (Wilson, 1953). Mullions occur due to metamorphism at the interface between a competent and an incompetent rock (Fossen, 2016). In the Northwest Highlands, the stress field that led to folding was oriented NE–SW, perpendicular to the mullions' long axis and to the direction of thrusting (Peach et al., 1907; Wilson, 1953; Figure 4.5B). Considering that these are only preliminary geological considerations, the structures in the study area will hitherto be referred to as 'mullion-type folds', to avoid a too prescriptive geological label. The topographic expression of mullion-like folds is that of semi-cylindrical, elongate ridges rising several meters above the general surface.

In summary, several assemblages of linear features have been identified in the study area, comprising faults, fractures and mullion-type folds. All of these features are structural, likely pre-date the Quaternary, and have a clear topographic expression, producing landforms in addition to BMGs.

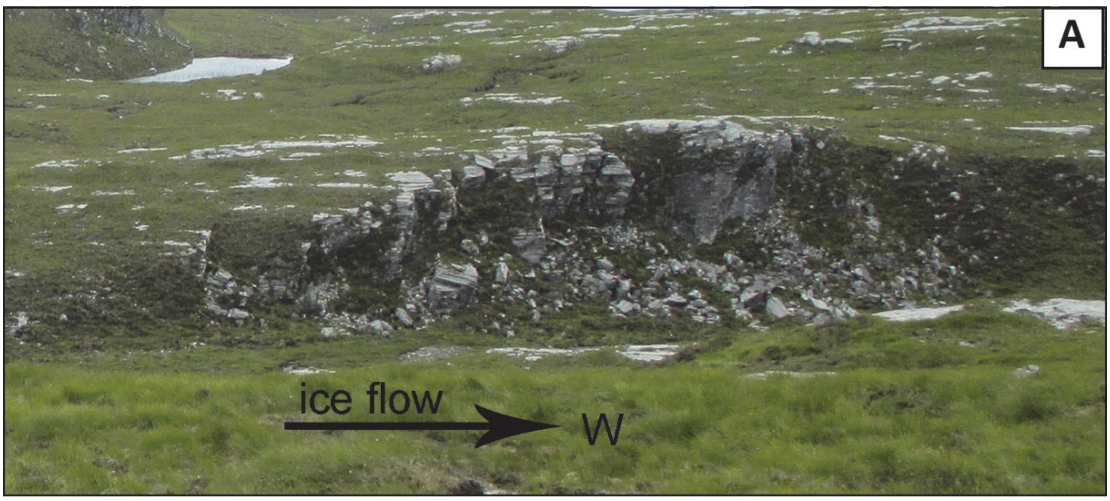
A
ice flow
W


B

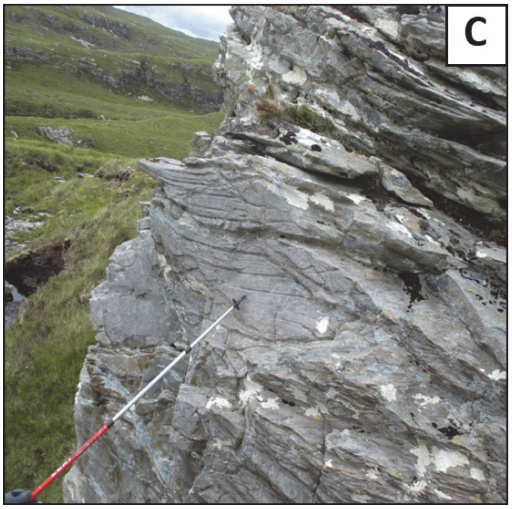
C

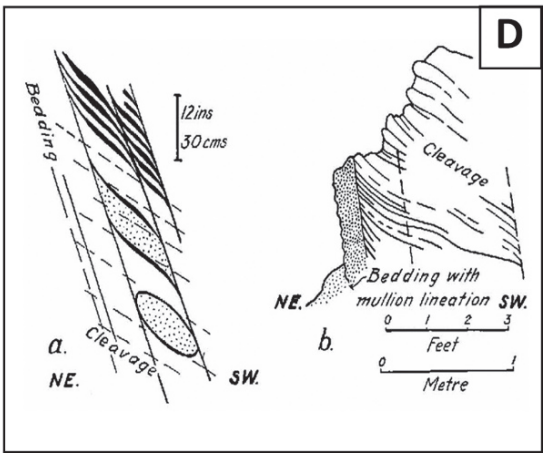
D
Bedding
12ins
30cms
Cleavage
a.
NE.
SW.
Cleavage
Bedding with
mullion lineation
NE.
SW.
0 1 2 3
Feet
b.
0 1
Metre

Figure 4.8. A: Bedrock structure similar to mullions, with cylindrical tight folding, west of fault 5; location in the landscape marked on Figure 4.19. **B:** mullion structure at Okyel Bridge, 7 km to the ENE of the study area **C:** Microfabrics in the rock structure showing cleavage in bedrock **D:** cleavage mullion structure at Okyel Bridge identified by Wilson (1953). **E:** Profile characteristic to irregular mullions at Ullapool. **F:** Profile characteristic to irregular mullions at Okyel Bridge identified by Wilson (1953). Images B, D and F have been reproduced from Wilson (1953) © Elsevier.

4.4.1.3 Faults

Several geological faults cross the landscape, being aligned broadly NE–SW. The faults are expressed in the topography as elongate channels, cross-cutting the BMGs at angles in the range 35–55° (Figure 4.6). The faults in the study area occur east of the Moine Thrust and their nature is unknown (Faults 1–5 in Figure 4.6) because the terrain displacement along them has not been established (British Geological Survey, 2008 and 2016; c.f. Goodenough et al., 2009). The grooves and ridges either side of the faults are continuous, showing no obvious horizontal displacement (Figure 4.3), while any vertical displacement is difficult to assess due to the lithological uniformity. Regarding the time of faulting, it is noted that the alignment of the faults is broadly perpendicular to the direction of thrusting (see section 2.1 and Figure 4.5B), which points to a pre-Quaternary age for the faulting, possibly related to the thrusting of Moinian rocks at the end of the Caledonian Orogeny. Post-glacial Quaternary faults described elsewhere in Moine rocks are typically oriented NW–SE, consistent with the late Cenozoic stress fields thought to be responsible for their formation (Ringrose et al., 1991). They are located in zones of maximum isostatic uplift, which contributed to their activation; and their recognition in the topography has been achieved primarily through their associated low-amplitude terrain dislocation, with a subtle topographic expression (Ringrose et al., 1991). The faults in the study area differ, having a well-defined relief (see section 4.2.4) and NE–SW orientation, indicating a greater, pre-Quaternary age.

4.4.2 Glacial landforms

All landforms identified here follow structural alignments and have been modified by glacial erosion through plucking and abrasion. Landforms occur in assemblages of multiple parallel and linear individuals which often cross-cut each other angles in the range 35–75°. Each landform assemblage is described in this section and their appearance in the landscape explained.

4.4.2.1 BMGs

The most distinctive set of glacial landforms in this area are BMGs. These are over-deepened, linear grooves eroded in bedrock, which traverse the landscape from east to west and are aligned subparallel to bedrock strike and to former regional ice-flow direction (Figure 4.9A). The BMGs are asymmetric in cross-profile, with a shallow northern side at 10–14° coinciding with the dip plane of the Moine schist bedding, and a steeper southern side at 35–45° (Figure 4.9B). Lithologically the bedrock is formed of stacks of thin layers of Moine metasandstone with intercalated quartz and white mica, prone to exfoliation (Figure 4.9C); and the bedrock is present close to the surface, as shown by the numerous rock outcrops (Figure 4.9A).

The evidence for glacial plucking is widespread along the north-facing side of the BMGs in the form of dislocated cuboid blocks (30–50 cm on average), sometimes slightly rotated, and found in the vicinity of the parent rock (Figure 4.9D). Rock dislocation occurred along three structural planes (Figure 4.9C and D), defined by two systems of vertical joints striking 110/290 and 040/220, respectively (Figure 4.10), and a third system formed by bedding planes, or foliation planes parallel to bedding, that strike approximately east–west, and with a sub-horizontal dip to the south. The orientation of these joints and the size of the plucked debris is similar to that identified by Krabbendam and Bradwell (2011) further west around Beinn Donuill (Figure 4.3). This consistency indicates that lateral plucking was a pervasive mechanism of BMG modification that occurred across the study area. Abrasion was also operational and is commonly reflected in the general ‘roundness’ of bedrock eminences (Figure 4.9E). Bedrock polish and striations are less common, as surface weathering, especially exfoliation, has removed the evidence.

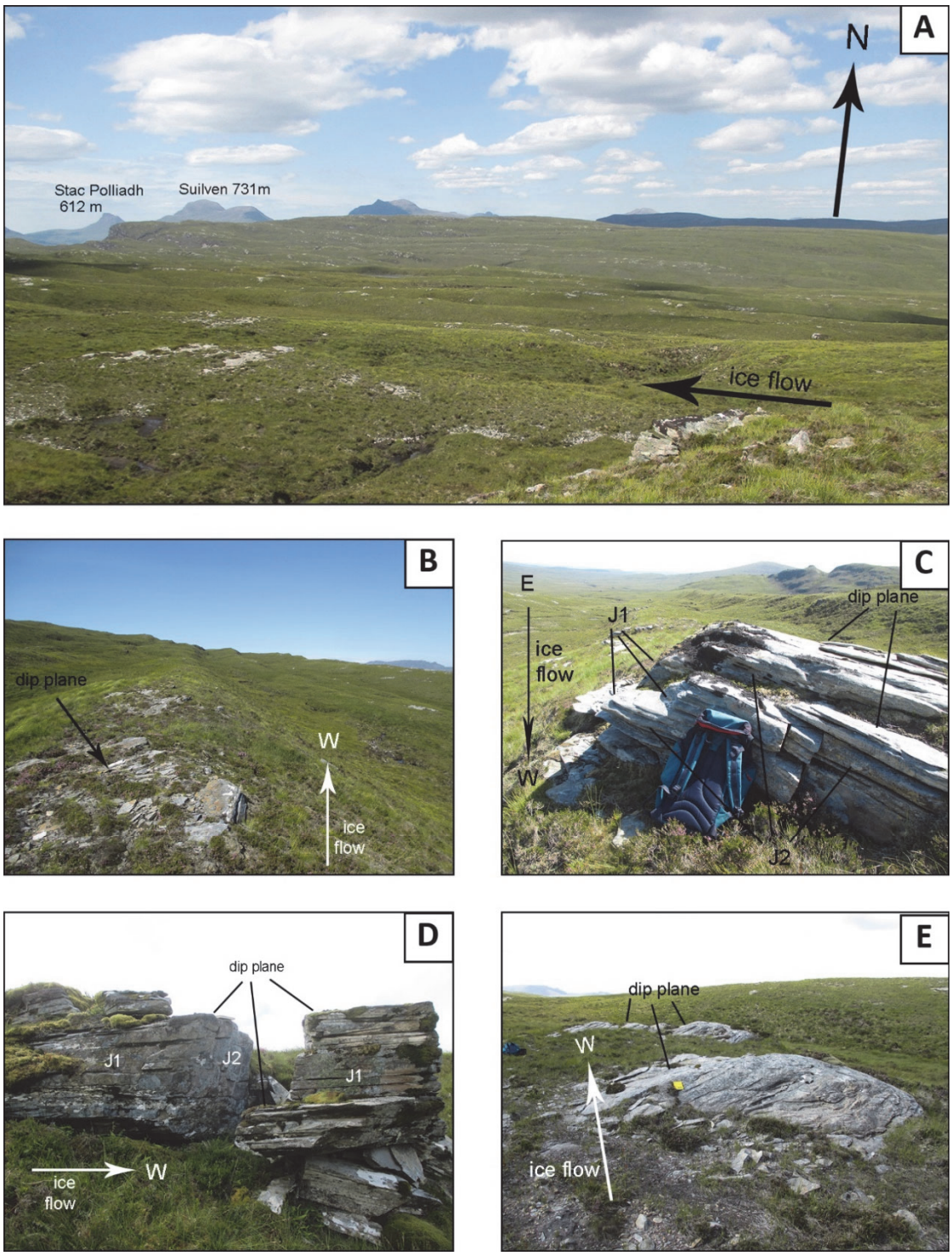

Figure 4.9. A: Landscape dominated by rows of parallel BMGs and ridges aligned east–west, along the palaeo-ice flow direction, in Rhidorroch Forest, north-east of Loch Achall. Note the widespread occurrence of bedrock outcrops indicating the presence of the bedrock close to the surface. **B:** Asymmetric grooves and ridges looking west (in the direction of ice-flow) in Rhidorroch Forest, north-east of Loch Achall. The shallow side of the ridges follow the dip plane of the bedrock strata. Note the stepped cross-profile of the grooved landscape, projected against the horizon. **C:** Bedrock outcrop of plucked psammite in the northern flank of a BMG at Rhidorroch Forest, north-east of Loch Achall. Note joints trending 110/290 (J1) and 040/220 (J2), as well as the bedding/foliation planes dipping to the right (south) and striking approximately east–west. **D:** Plucked block dislocated along vertical joints trending 110/290 (J1) and 040/220 (J2), on a BMG south-east of Loch a'Chroisg. **E:** Bedrock outcrop rounded by glacial abrasion, in a shallow BMG from Rhidorroch Forest.

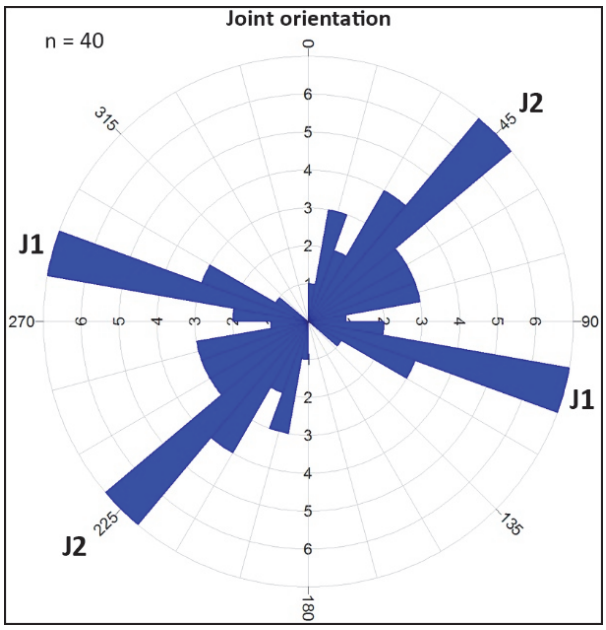

Figure 4.10. Rose diagram of bedrock joint orientation in Rhidorroch Forest. Joints J1 and J2 are pervasive across the whole study area, and they have been identified by Krabbendam and Bradwell (2011) around Beinn Donuill, approximately 2 km to the west (Figure 5d in Krabbendam and Bradwell, 2011).

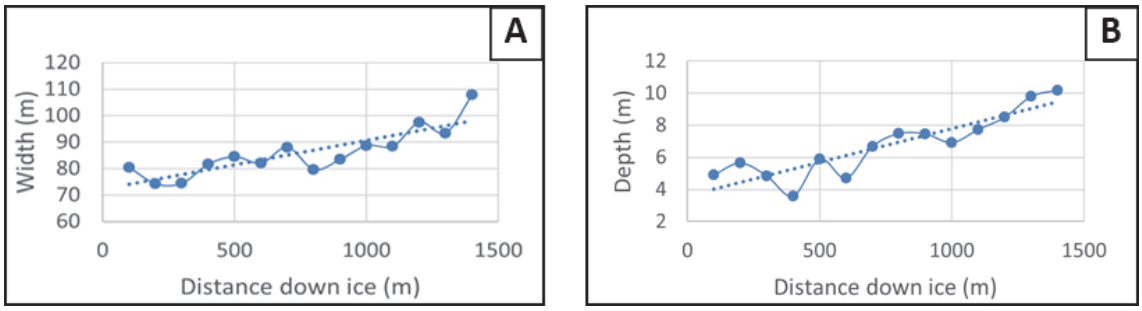

Figure 4.11. Variation in width (**A**) and depth (**B**) along the BMGs in the study area in the down-ice direction. Each datapoint represents the width value calculated as an average of five datapoints from five different grooves, whereby each datapoint is found at the same distance from the starting point of the groove. The starting point is established at 100 m, so that the data are slightly offset from the y-axis, and the datapoints are spaced at 100 m intervals, consistent with the protocol for sampling frequency established in Chapter 3 (see Section 3.3.2 in Chapter 3). The ice flow direction is from left to right. The statistical significance is p = 0.01 for width variation (A) and p = 0.001 for depth variation (B).

The BMGs at Ullapool have a mean width of 91 m, mean depth of 7 m, length:width ratios of 22:1 (see Table 3.3. in Chapter 3) and become wider and deeper with distance down-ice (Figure 4.11A and B). These morphometric characteristics are common for BMGs formed primarily under geological control, regardless of the glaciological regime (see Section 3.5.2). The BMGs can be traced across the whole study area, and they are the dominant landform

in Rhidorroch Forest, NNE of Loch Achall and south of Loch a'Chroisg (Figure 4.3), where their length reaches 2–3 km due to minimal cross-cutting by other linear features, such as faults and fractures.

4.4.2.2 Glacially modified fractures

Fracture set-1 cross-cut the BMGs at an angle of 35–55° (Figures 4.12 and 4.13). Where the fractures cross-cut the ridges separating the BMGs, a depression is noticeable in the ridge profile ca. 2–10 m deep (Figure 4.14), whereas the intersection with the BMGs is often marked by the presence of a lake, indicative of an over-deepening into a bedrock basin (Figures 4.12 and 4.13). Fracture set-1 have been exploited by both abrasion and plucking, likely aided by mechanical weaknesses in the bedrock due to fracturing.

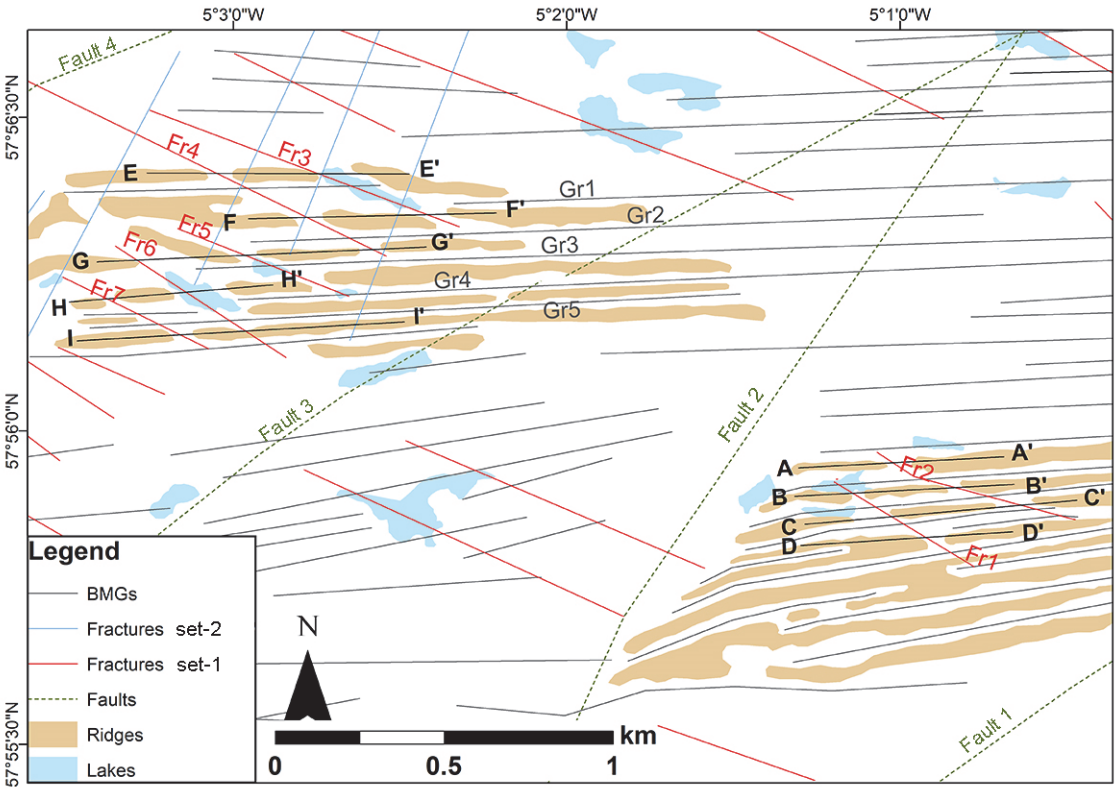

Figure 4.12. Diagram of the cross-cutting linear bedrock features in the central-western study area. Fr1–Fr7 occur within fracture set-1. Gr1–Gr5 represent the BMGs. Note how the BMGs are cross-cut at an angle by fracture set-1. The black lines A–A' to I-I' represent the trajectory of profiles along the bedrock ridges cross-cut by fractures. See Figure 4.13 for a real-life 3D perspective. Note the higher density of cross-cutting lines between Faults 3 and 4 compared to the rest of the area. For the location of this area please refer to Figure 4.13.

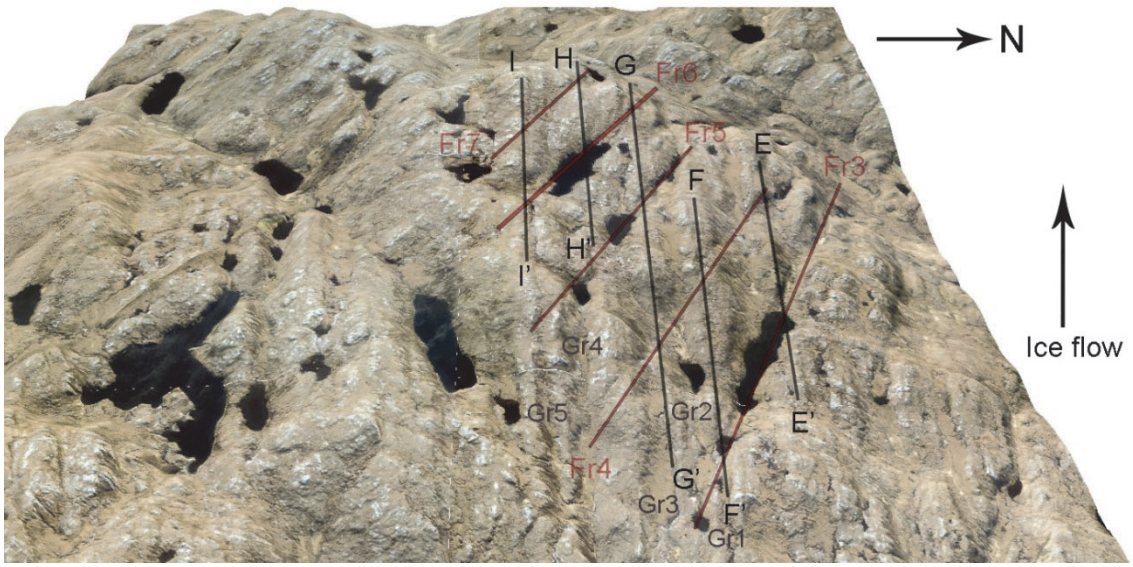

Figure 4.13. 3D aerial image of the area between Faults 3 and 4 marked in Figure 4.12. The BMGs are marked Gr1–Gr5 in grey. Fr3–Fr7 occur within fracture set-1 and are aligned NE–SW. The black lines E–E' to I–I' are the long profiles traced along the ridges and illustrated in Figure 4.14. Note how the BMGs and ridges are less dominant in the landscape, their continuity often being interrupted by intersection with other structural features. Image processed in ArcScene with vertical exaggeration of 2.5×. The location of this area is marked in Figure 4.4. Base image © Edina Digimap.

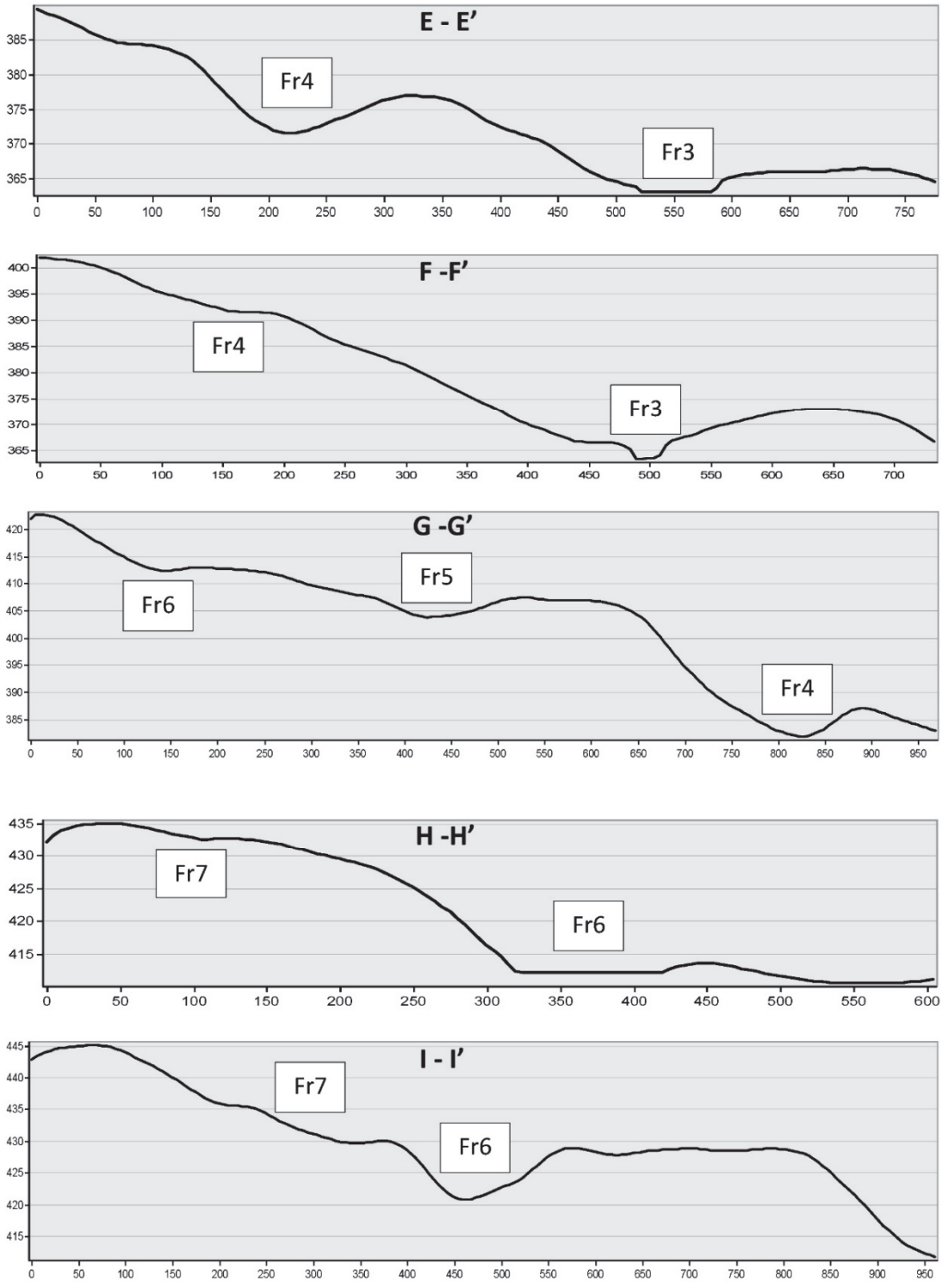

Figure 4.14. Long profiles of ridges situated between Faults 3 and 4 marked on Figure 4.12. Labels Fr3–FR7 mark a lowering in the ridge topography at the intersection between ridges and fractures. Profile transects are represented in Figures 4.12 and 4.13. The x-axes represent distance (m) and the y-axes represent amplitude (m).

Fracture set-2 forms distinctive lineaments of steep cliffs trending NNW–SSE as they cross-cut the BMGs and their intervening ridges (Figure 4.15). The fracture alignment sub-perpendicular to former ice-flow direction enabled quarrying and plucking, which produced west-facing cliffs (Figure 4.16) or slopes with a staircase profile (Figure 4.17). The landscape in the central-western part of the study area has a densely dissected aspect due to frequent cross-cutting between fracture set-1 and set-2 with the BMGs (Figure 4.6), which diminishes the dominance of the BMGs in the landscape (Figure 4.13).

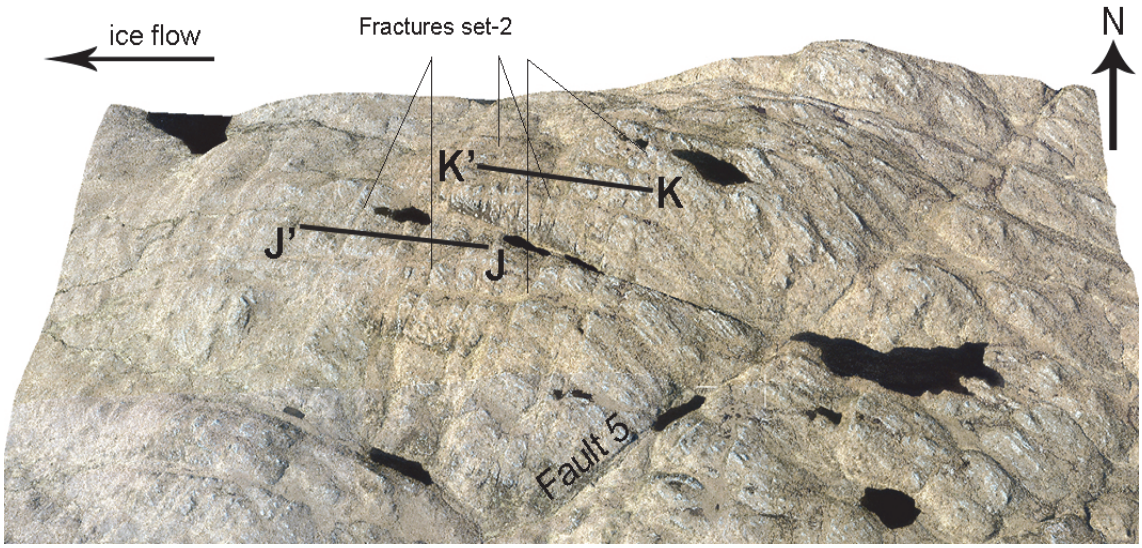

Figure 4.15. 3D aerial image of the area situated west of Fault 5, with the dense network of fracture set-2 aligned NNE–SSW, almost perpendicular to the palaeo-ice-flow direction. Black lines marked J–J' and K–K' represent the trajectories of the topographic profiles illustrated in Figure 4.17. Image processed in ArcScene with vertical exaggeration of 2.5×. Note the white grain of the closely-spaced mullion-type ridges aligned NW–SE, modified into roches moutonnées and whalebacks by glacial erosion (see Section 4.4.2.3). The location of the area is marked in Figure 4.4. Base image © Edina Digimap.

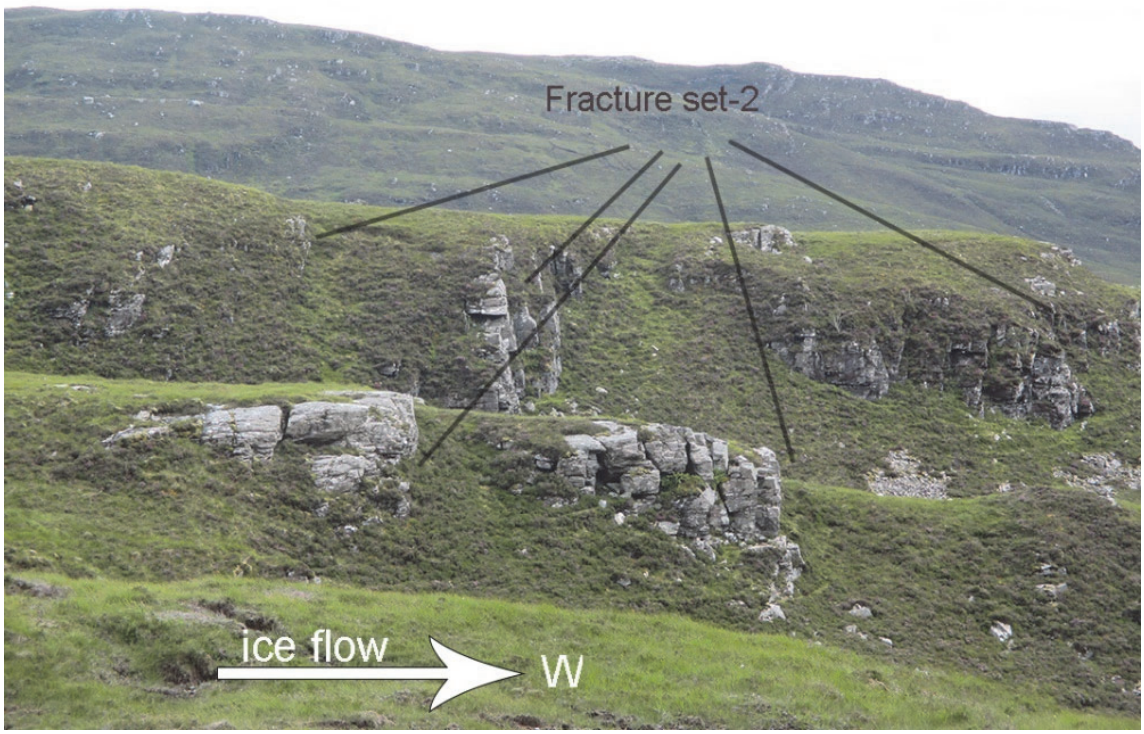

Figure 4.16. Cliffs facing west enhanced by quarrying and plucking at the intersection between the bedrock ridges aligned east–west and fracture set-2, trending NNE–SSW. The photograph was taken south-west of Loch a'Chroisg.

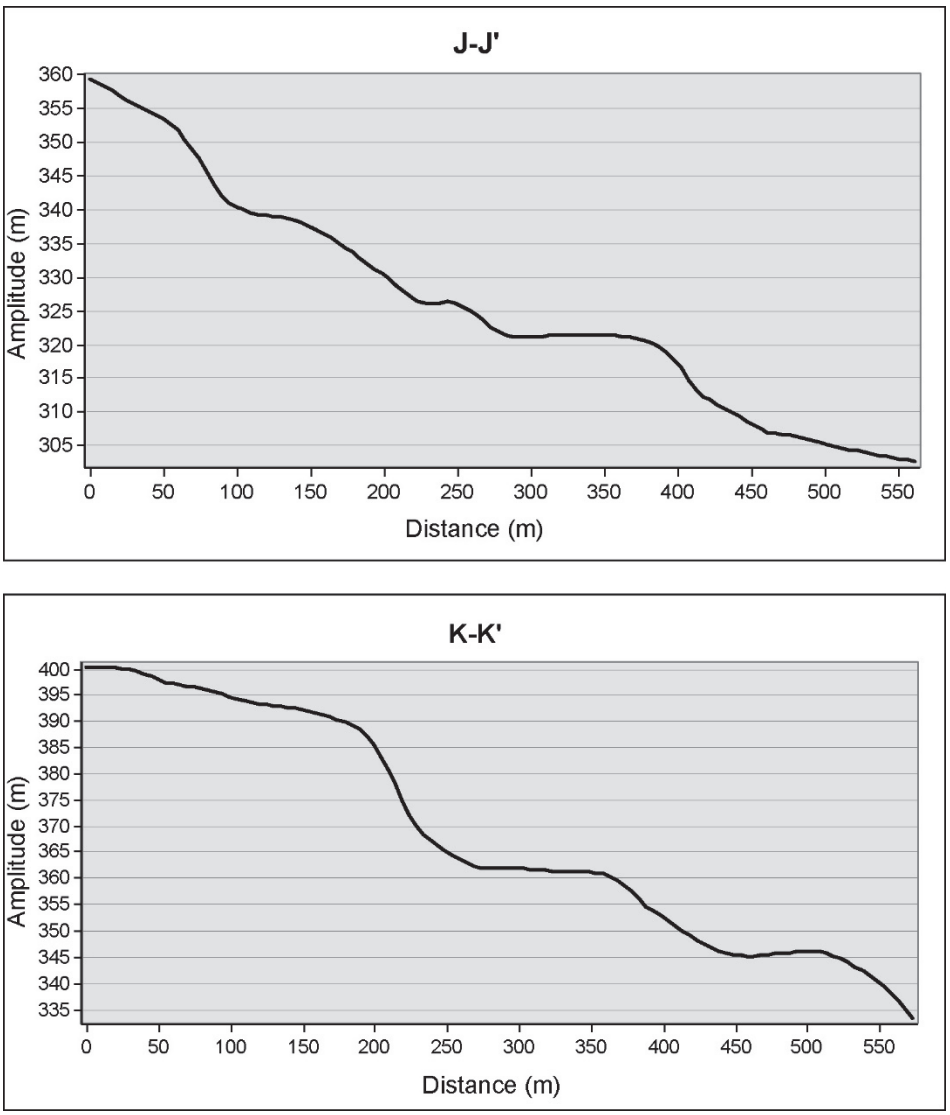

Figure 4.17. Stepped slope profile enhanced by plucking, resembling giant roches moutonnées, similar to those described in the eastern Cairngorms by Sugden et al. (1992). The steep slopes represent the topographic expression of fracture set-2. The profile transects are marked on Figure 4.15. Ice flow was from left to right.

4.4.2.3 Mullions, whalebacks and roches moutonnées

In the western part of the study area, either side of Fault 5 (Figure 4.6), the landscape is dominated by lineaments of low-amplitude ridges aligned parallel to each other and rising 1–3 m above the general ground surface (Figure 4.18). The ridges are mullion-type anticlines that have been modified into whalebacks or roches moutonnées by abrasion and plucking (Figure 4.19A). The rock surface sometimes has shallow and smooth grooves, parallel to the fold long axis (Figure 4.19B), which could be either structural due to folding (Wilson, 1953) or glacial due to abrasion, being aligned sub-parallel to ice flow. Plucking

exploited the vertical joints, perpendicular to the fold axis (Figure 4.19A) and facing north-west, which resulted in the formation of small cavities (Figure 4.19A and B) or roches moutonnées (Figure 4.19C). The plucked faces observed in the field are aligned perpendicular to the fold long axis at an angle of ~75° to the inferred regional ice-flow and are generally not considered reliable indicators of the ice-flow direction (Gordon, 1981; Glasser and Bennett, 2004; Roberts and Long, 2005). In the absence of unequivocal evidence of abrasion indicative of ice-flow direction, this is assumed to have been from east to west, consistent with the regional ice-flow.

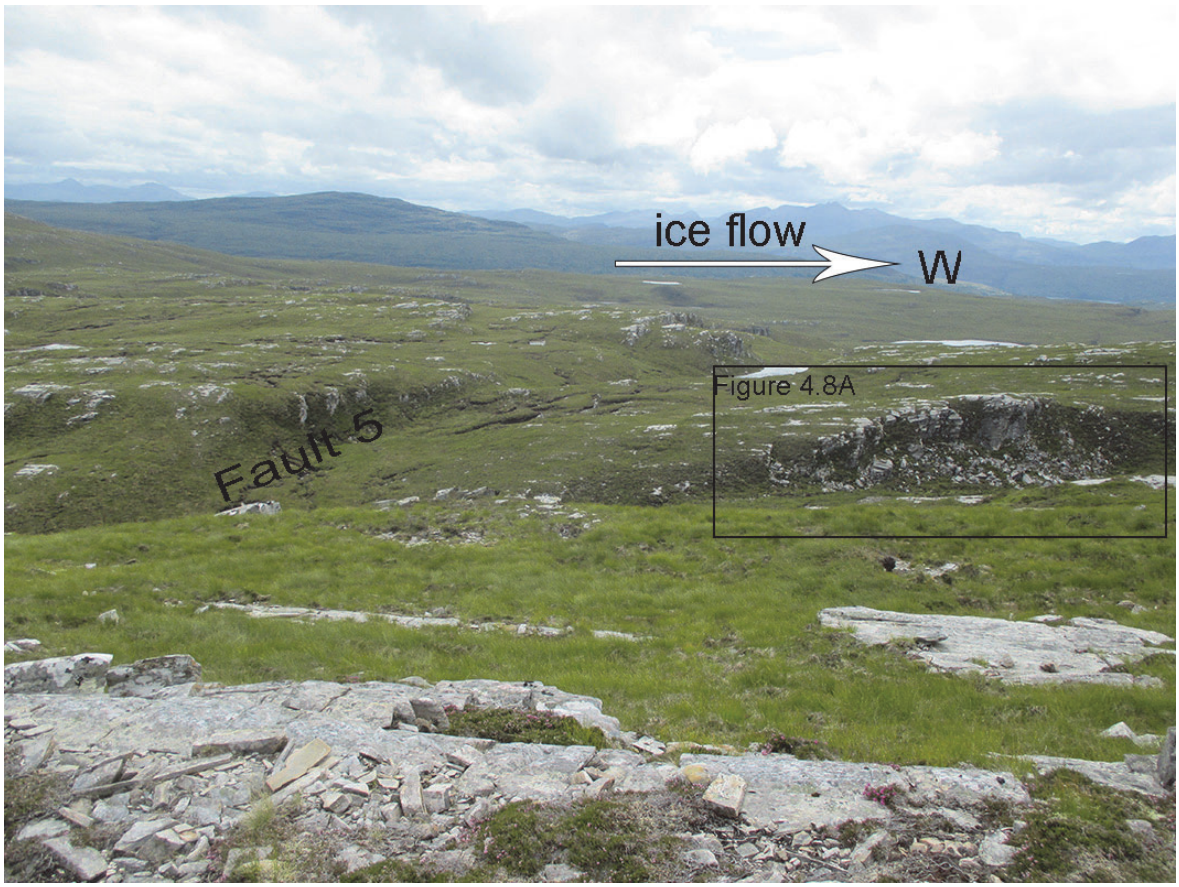

Figure 4.18. Roches moutonnées and whalebacks formed through plucking and abrasion along mullion-type folds forming an overall landscape of low-rising bedrock corrugations aligned NW–SE, obliquely to the BMGs.

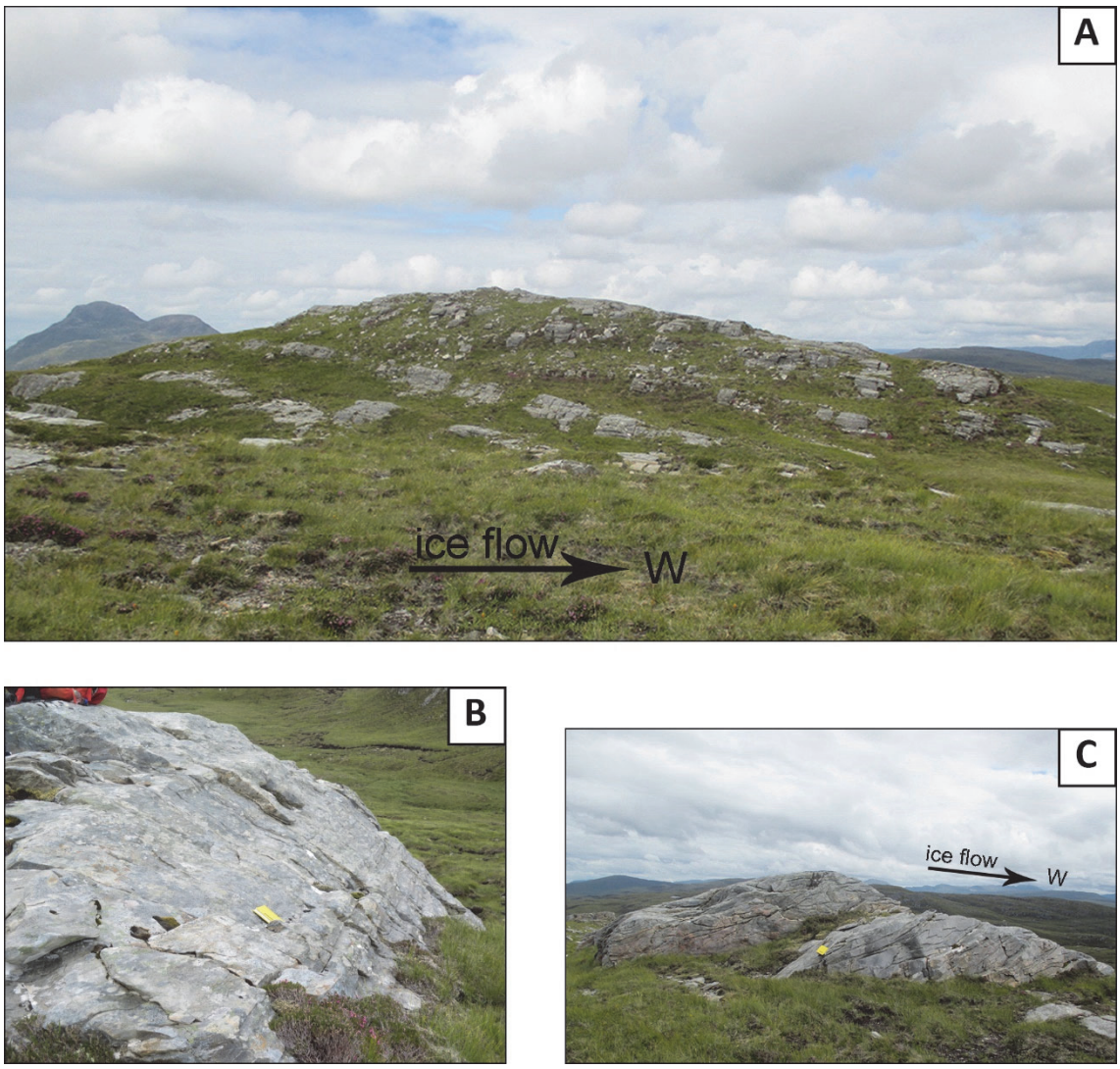

Figure 4.19. A: whaleback form aligned sub-parallel to palaeo-ice flow direction underpinned by mullion-type bedrock fold. Note the abundant vertical joints, which enabled plucking to occur. **B:** Grooved surface of a roche moutonnée. It is uncertain whether the grooving was glacial or geological (see Section 4.4.2.3). Note the small cavities formed through plucking as ice flow was towards the reader. **C:** Plucked rock face of a roche moutonnée perched on a mullion-type fold.

4.4.2.4 Glacially-modified faults

Throughout the study area geological faults are major structural features with a general NE–SW alignment, sub-perpendicular to the palaeo-ice flow (Figure 4.6). The faults have been excavated by erosion and form channels approximately 50 m wide and 4–7 km long, with an up-and-down profile and well-defined sides. The effects of glacial erosion are observable in the plucked cliffs bordering the fault-channel side facing NW, aligned at an angle to the palaeo-flow direction and in the lee-side relative to it (Figure 4.20). The opposite side faces east and has a smooth profile with bedrock ridges rounded by abrasion as a result of glacier

ice crossing the fault channel from east to west (Figure 4.20). The faults appear devoid of glacial debris, although sometimes the contact with the bedrock is obscured by thick peat deposits. They are drained by small burns and, in several places, elongate lakes are present.

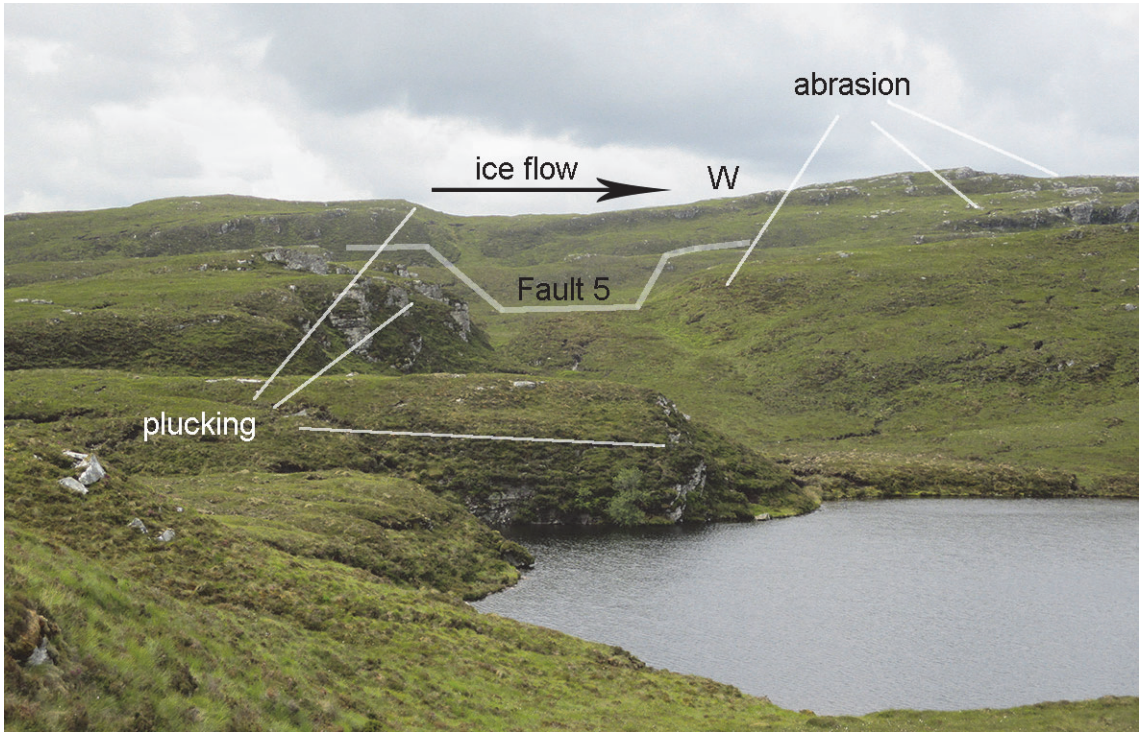

Figure 4.20. View to the south, along Fault 5 marked on Figure 4.6. Note the well-defined profile of the channel developed along the geological fault, approximately 50 m wide and 5 m deep. The fault cuts through the BMGs and ridges at an angle of 45°. Note the plucked rocks along the eastern side of the fault, positioned on the lee side relative to palaeo-ice flow, compared to the smooth, abraded profile of the western side (see Section 4.4.2.4). The photograph was taken at the northern end of Fault 5.

4.4.2.5 Drift covered terrain

East of the grooved terrain, the landscape is dominated by rounded or elongate low-amplitude mounds and ridges (Figure 4.21) consisting of poorly-sorted, unconsolidated glacigenic sediments (inset in Figure 4.21) and with a preferential east–west alignment. The sediment cover is several meters thick in places and the bedrock is rarely visible at the surface. The surface expression of the geological structure is gradually less discernible towards the east (e.g. north of Cnoc Damh) as it tails off beneath the sediment cover, and the BMGs are less numerous and poorly defined (Figure 4.3). North of Cnoc Damh there is a cluster of eskers 3–10 m high and 60 m wide, with no preferential alignment, indicative of

glacifluvial activity (Figure 4.6). Topographically, the drift-covered terrain sits ca. 200 m lower than the grooved area to the west.

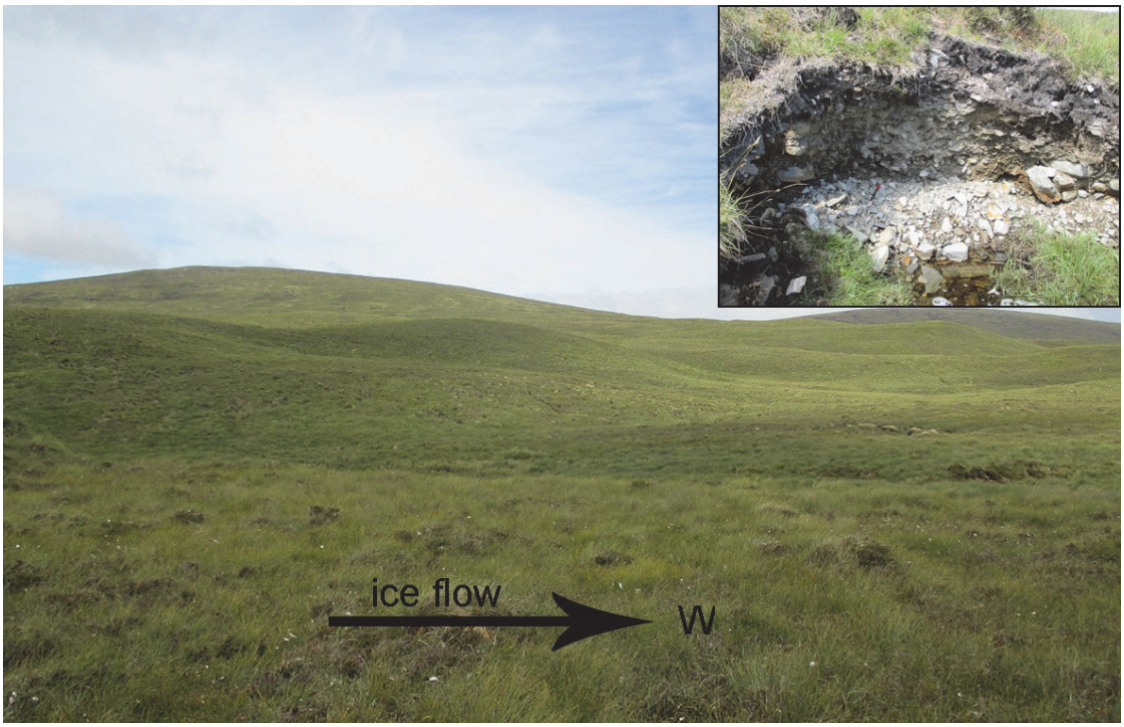

Figure 4.21. Landscape dominated by subdued and broad landforms, with rounded to slightly elongate mounds, south-east of Loch a'Chroisg, characteristic to the east of the grooved terrain (see Section 4.4.2.5). The inset shows glacigenic deposits exposed in a burn bank south-east of Loch a'Chroisg; such exposures are a common occurrence in burn banks throughout the area east of the grooved terrain.

In summary, the results show the presence of several assemblages of bedrock landforms which occur in conjunction with the BMGs. The BMGs, the fracture set-1 and the geological faults have a negative topographic expression as either grooves or channels, whereas the whalebacks or roches moutonnées in the west, developed along the mullion-type anticlines, have a positive expression. Fracture set-1 form lineaments of plucked cliffs. The landforms occur in series of parallel individuals aligned either sub-parallel or obliquely relative to regional ice-flow direction and have been modified by glacial plucking and abrasion. The spatial distribution of landforms and their cross-cutting relationships are reflected at landscape scale (see Section 4.5.2).

4.5 Discussion

4.5.1 Structural geomorphology

This section discusses the overarching relationships between mechanisms of glacial erosion, landforms and geological structure and are summarised in Table 4.2. The results suggest that the landforms present in the study area reflect a close connection between the geological structure pre-dating the Quaternary and the mechanisms of glacial erosion.

Plucking was controlled by the presence of joints in the bedrock and the spatial arrangement of linear structural features relative to palaeo-ice flow direction. The joints are associated with bedding, foliation, folding, faulting and fracturing (see Section 4.4.2.1), all factors associated with mechanical weaknesses in the bedrock and which enabled block dislocation through plucking. The geomorphic effects of plucking range in size from mini-cavities in the lee of small-scale fractures along the spine of mullion-type anticlines (Figure 4.19B), to cliffs several meters high (Figure 4.17) developed along fracture set-2, (Figure 4.15) or along slopes of fault channels positioned on the lee-side relative to palaeo-ice flow direction (Figure 4.20). The same type of terrain with steep cliffs facing into the former ice direction has been described in glaciated terrain in numerous other locations where palaeo-ice flow direction was (sub)perpendicular to structural lineaments, leading to the formation of large-scale stoss-and-lee forms (Gordon, 1981; Sugden et al., 1992; Rea, 1994; Glasser, 2002; Dühnforth et al., 2010; Glasser et al., 2020). Lateral plucking, which modified the BMGs, occurred parallel to ice flow and to bedrock strike and involved block rotation rather than translation forwards (Krabbendam and Bradwell, 2011). Considering the pervasive occurrence of lateral plucking and its strong influence on BMG modification (see Section 4.4.2.1), the BMGs represent yet another example of large-scale landforms produced by the cumulative spatial effect of a small-scale process, as noted elsewhere (Glasser and Warren, 1990).

Table 4.2. A summary of geological and geomorphological evidence pertaining to all landscape types and their relationships with the BMGs.

Landform	Geological feature	Erosion mechanism	Relationship to BMGs
BMGs	Bedrock strike	Lateral plucking; also abrasion and meltwater erosion	-
Sub-grooves	Fracture set-1	Plucking and abrasion	Cross-cutting
Whalebacks and Roches moutonnées	Mullion-like folds	Abrasion and plucking	Cross-cutting
Plucked cliffs	Fracture set-2	Plucking	Cross-cutting
Channels	Faults NW–SE	Abrasion and plucking; possibly meltwater erosion	Cross-cutting

The evidence for abrasion is observable in landforms ranging from medium- to large-scale and is best preserved on slopes oriented proximal to ice-flow. Examples comprise the roches moutonnées and whalebacks underpinned by mullion-type folds (Figure 4.19A); the west-facing sides of the channels along major faults, with a smooth abraded profile (Figure 4.20); and the abraded bedrock outcrops along the BMG floors (Figure 4.9E). Similar structural underpinning of whalebacks and roches moutonnées has been described in southern Sweden in gneissic bedrock, where medium-scale folds other than mullions were modified into whalebacks or roches moutonnées (Larsson, 1954). No unequivocal small-scale evidence for abrasion was identified in the field, despite such evidence being ubiquitous on all lithologies down-ice along the same flow corridor (Gordon, 1981; Lawson, 1996; Bradwell, 2005; Krabbendam and Glasser, 2011). Striations were most likely removed through post-glacial weathering considering the susceptibility of metasandstone to exfoliation (Figure 4.9C).

The visibility of BMGs in the landscape (Figure 4.3) is due to the combined effect of their well-defined relief, length, density and long-distance traceability in comparison to other landforms. Besides lateral plucking, recognised as the principal mechanism in recent BMG modification (Krabbendam and Bradwell., 2011; see Section 4.4.2.1), abrasion also contributed to increasing BMG dimensions, as the plucked rocks became entrained in glacial transportation and acted as abrading tools down-flow. This scenario is reflected in the widening and deepening of the BMGs with distance down-ice (Figure 4.11). It is difficult to know to what extent glacial erosion contributed to BMG lengthening, as their initiation is still poorly understood (see Chapter 5). However, the main cause for their remarkable

length (>1,000 m) is likely to reside in groove development along the bedrock strike, aided by the topographic slope perpendicular to dip (Krabbendam and Bradwell, 2011). The high density of the BMGs, reflected in their closer spacing in comparison to the bedrock forms developed along the fracture sets (Table 4.1), also contributes to the visibility of the BMGs in the landscape. BMG density could be an inherited reflection of their initiation conditions, whether this was related to debris banding beneath fast-ice flow (proposed by Bradwell et al., 2008b) or caused by some structural feature in existence prior to initial bedrock grooving (see section 5.4.1 in Chapter 5). Unlike other bedrock forms observed in the field area, which tend to form more localised clusters, the BMGs remain traceable across the terrain (Table 4.2), even in areas where their visibility is diminished by interference from other landforms.

In summary, the topographic expression of bedrock landforms, in conjunction with their underpinning geological features, indicates a strong geological control over the process of glacial erosion across the study area. Abrasion, plucking and meltwater were directed by the alignment of landforms developed along ancient, pre-Quaternary structural features present in the bedrock. Their action is recognisable at a range of scales and it has enhanced rather than obliterated structural features. Thus, overall, the present-day topography reflects the structural architecture of the bedrock rather than the palaeo-ice flow direction. BMGs remain conspicuous across the landscape, and their relatively high visibility is the result of glacial erosion enhanced by the parallel alignment of the bedrock strike and palaeo-ice flow direction over multiple glaciations.

4.5.2 A landscape of areal scour

Understanding the style of glaciation provides a framework for the reconstruction of palaeoglaciological conditions that shaped a particular landscape, and for the exploration of long-term landscape evolution. Areal scouring appears most applicable glacial erosion style to the landscape across the grooved terrain at Ullapool, based on similarities to landscapes reconstructed from palaeo-glacial environments (Linton, 1963; Sugden 1974 and 1978), as well as modern settings (Jamieson et al., 2014). The criteria for areal scouring have been derived from the characteristics of the cnoc-and-lochan topography, commonly encountered over gneissic bedrock in glaciated shield terrain (Linton, 1963; Sugden, 1974 and 1978; Rea and Evans, 1996), but rarely mentioned in other lithologies (e.g. Sugden, 1978; Gordon, 1981). These criteria refer to the scale and spatial distribution of glacial

erosion in bedrock across a large area, and once established, they could be applied to any type of bedrock. Here they are tested on the Moine Schists.

At Ullapool the evidence for plucking and abrasion is present at a range of scales across the grooved terrain, as detailed in Section 4.5.1. The presence of numerous lakes at the intersection of structural lines (see Section 4.4.2.2 and Figures 4.12 and 4.13) is consistent with enhanced erosion in bedrock zones of mechanical weakness, as noted on gneiss (Linton, 1963; Sugden, 1978). The evidence for glacial erosion is present across the area regardless of altitude, as proven by the grooving over the highest ground around Beinn Donuill (Figure 4.3), as well as in the lower reaches where abraded and plucked bedrock has been observed around Loch a'Chroisg (Figure 4.16). Thus, the spatial distribution of glacial erosion has both a lateral dimension, through its areal extent, as well as a vertical one, on altitude. Collectively, there is compelling evidence for widespread glacial erosion at all scales across the landscape, which is fully consistent with a landscape of areal scouring described elsewhere (Sugden, 1978).

The overall topography at Ullapool is defined by a network of linear, criss-crossing erosional lines with remarkable geometric regularity (Figure 4.6), with lakes present at the intersection between BMGs and fractures, which could be named 'groove-and-lochan' (Figure 4.22.). This differs from the cnoc-and-lochan landscape, typically associated with areal scouring, developed on relatively flat lowland areas of gneissic bedrock, and characterised by a non-regular combination of bedrock protuberances rounded by abrasion with depressions excavated and modified by glacial erosion along ancient structural lines (Linton, 1963; Sugden 1974 and 1978; Rea and Evans, 1996; Krabbendam and Bradwell, 2014). Unlike the cnoc-and-lochan landscape, recognisable on glaciated gneiss across the world (Sugden 1974 and 1978; Rea and Evans, 1996) the groove-and-lochan style may not be applicable to any glaciated landscape in layered rocks, because its development is directly conditioned by the right spatial combination of structural lines relative to each other and to ice-flow direction. Hence this spatial combination is not typically recognisable across the extent of the Moine Schists, despite these occupying a large area in Scotland (Figure 4.5A) (Gillen, 2003). Nevertheless, the groove-and-lochan topography could be encountered elsewhere in glaciated bedrock terrain provided the underpinning structural geology offers a suitable framework.

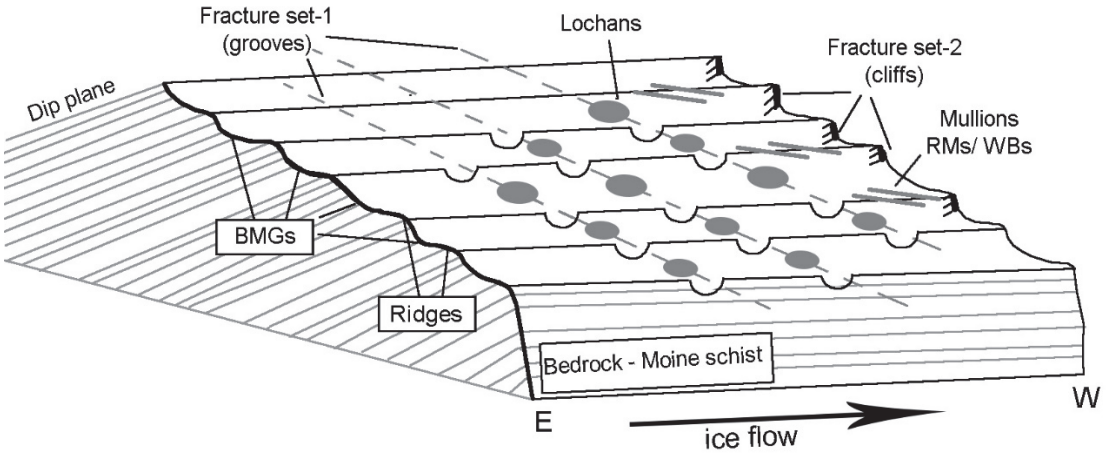

Figure 4.22. Schematic representation of the cross-cutting relationships between landforms developed along structural lineaments. The resulting landscape is one of groove-and-lochan, a type of areal scouring on Moine schists (see Section 4.5.2). Abbreviations: RMs = roches moutonnées; WBs = whalebacks.

Notably, two aspects of selective linear erosion (*sensu* Sugden, 1974) add to the understanding of the style of glacial erosion in the study area. One relates to the inferred channelling of the Ullapool tributary of the Minch Ice Stream along the same route throughout multiple glaciations and phases of ice streaming (see Section 4.2.2). In the wider context of the British–Irish Ice Sheet, the emergence of a fast-flowing artery becomes a preferential flow corridor, which changes the ice bed conditions and enhances bed erosion; so, the area occupied by the Ullapool tributary could be regarded as a corridor of linear erosion (c.f. Sugden, 1978). The other aspect relates to the potential for BMGs to act as predefined concavities which trapped ice, debris, and meltwater (Boulton, 1974), and channelled the flow as well as the erosion process, with the intervening ridges experiencing less erosion (Roberts and Long, 2005; Roberts et al., 2010; Krabbendam et al., 2016). The erosion process inside the grooves is further aided by the effect of cumulative geothermal energy, as the heat-flow lines converging towards the groove floor (Figure 2.15 in Chapter 2) are expected to have enhanced melting and abrasion (Nobles and Weertman, 1971; see also Newton et al., 2018 for a discussion; see Section 5.3 in Chapter 5). It could be argued that, at a small scale, the BMGs are essentially landforms of selective linear erosion, with the same ice–bedrock interaction feedbacks as those operating in glacial troughs in landscapes of selective linear erosion (Sugden, 1974 and 1978). It is perhaps along the same 'lines' that Glasser and Bennett (2004, p. 59) classified bedrock grooves as landforms of selective linear erosion as part of a "landscape of linear ice sheet erosion " rather than areal scouring (Figure

1 in Glasser and Bennett, 2004), but overall, the landscape in the study area is one of areal scouring.

Another defining aspect of landscapes of areal scouring is long-term ice flow through basal sliding (Sugden, 1974 and 1978; Rea and Evans, 1996). At Ullapool, ice flow was through fast-flowing ice, as inferred from onshore and offshore evidence (Stoker and Bradwell, 2005; Bradwell et al., 2007; see Section 4.2.2). These conditions would have allowed for partial ice–bedrock (de)coupling and enabled both plucking and abrasion to occur at the same time. However, the evidence for plucking and abrasion may not be coeval, considering the dynamic setting and temporal evolution of bedforms in an ice-stream onset zone throughout repeat glaciations and episodes of ice streaming. At the start and end of each glacial and streaming cycle the ice bed conditions would have changed in response to variations in ice thickness and velocity, potentially alternating conditions for plucking and abrasion (Roberts and Long, 2005). The likelihood is that the landscape of areal scour at Ullapool developed episodically throughout the Quaternary, as phases of partial ice–bedrock coupling favourable to both plucking and abrasion alternated with phases of thick ice flow through widespread basal sliding favourable to abrasion, and with reduced scope for plucking. It is reasonable to assume that the fresh evidence for plucking, ubiquitous across the study area (Figure 4.9D), is the result of thin ice flow, during deglaciation under maritime conditions, with production of abundant meltwater (Bradwell et al, 2008a). This is also consistent with the dearth of subglacial debris which was probably efficiently removed by meltwater during deglaciation.

Despite variations in ice-bed conditions, basal sliding would have prevailed throughout the Quaternary glaciations in the wider area of north-west Scotland. This is suggested by the limited evidence for potential landform preservation beneath non-erosive ice (Stone et al., 1998) and a dearth of pre-Quaternary regolith, which is generally regarded as the result of removal through glacial erosion (Krabbendam and Bradwell, 2014; Sissons, 1967). In contrast, in eastern Scotland the less erosive action of glacier ice is reflected in the preservation of granite tors (Phillips et al., 2006) and pre-glacial regolith (Hall, 1985), as well as in the generally reduced density of relief fragmentation (Gordon and Sutherland, 1993; Sissons, 1967), underpinning a landscape of selective linear erosion (Sugden, 1968). In the study area at Ullapool, the apparent lack of regolith and the alignment between glacial landforms and ancient structural lineaments point to the possibility of an etched landscape, whereby areal scouring may have revealed an old erosion surface by removing the weathering mantle. This type of scenario has been recognised in shield rocks in West

Greenland (Bonow et al, 2006) and Sweden (Lidmar-Bergström, 1989; 1996 and 1997; Olvmo et al., 1999; Hall et al., 2013). The cnoc-and-lochan topography in Scotland has been shown to resemble the geological structure of non-glaciated gneissic terrain subjected to long-term weathering (Krabbendam and Bradwell, 2014). These examples apply to shield rocks, where glacial erosion is thought to have removed a relatively thin cover of rock in comparison to other geological periods and agents of denudation (e.g. Lidmar-Bergström, 1996). This cannot be extrapolated to apply to metasandstone at Ullapool without specific knowledge of its erosion rates under glacial conditions, therefore the possibility of the study area being an inherited landscape remains speculative.

In summary the groove-and-lochan topography at Ullapool represents a type of landscape of areal scouring on metasandstone, defined by a network of cross-cutting grooves with a geometric regularity, formed through glacial erosion along pre-Quaternary structural lines. The landscape evolution was likely episodic, with variations in the ice-bed conditions, but basal sliding by warm-based ice is inferred to have been the prevailing ice-flow mode. The lack of regolith in conjunction with the alignment between glacial landforms and ancient structural lines point to the existence of an inherited landscape, revealed and enhanced by glacial erosion.

4.5.3 Ice streaming and BMG formation

The existing interpretation of BMG formation at Ullapool is that they are the product of fast-ice flow, formed in a zone of streaming onset, although no quantitative constraints on the ice-flow velocity under streaming conditions are known from that area (see Section 1.1). This interpretation has been advocated by Bradwell et al. (2008b), following several studies pertaining to the Minch Ice Stream (e.g. Stoker and Bradwell, 2005; Bradwell et al., 2007) (see Section 4.2.2), and based on the presence of BMGs, with little or no mention of other bedrock landforms. While the BMGs are arguably the most conspicuous landforms, traceable throughout the area, several other groups of linear landforms exist, having either positive (e.g. roches moutonnées and whalebacks) or negative (channels and narrow depressions) topographic expressions, and cross-cutting the BMGs at various angles (see Section 4.5.1 and Table 4.2). Collectively, these observations mean that the fast-flow onset zone of the Ullapool tributary to the Minch Ice Stream comprises a structurally-controlled hard-bed landform assemblage (*sensu* Eyles, 2012). This raises the question to what extent BMGs owe their formation to fast-flowing ice? Could the glaciological signal be separated from the geological one in the BMG formation process, and ultimately would BMGs be

present if ice flow velocities had been slow, under slow ice-sheet flow conditions? Here these questions are explored through a reappraisal of the evidence for fast-flowing ice and a comparative analysis of BMGs to similar landforms in a regional geological and glaciological context.

Geographically, the location of the grooved terrain at Ullapool is consistent with a zone of fast-flow onset that links to the wider geomorphic context pertaining to a fast ice flow corridor offshore (see Section 4.2.2 and Figure 4.2). The study area lies at the transition between soft- and hard-bed, a transitional context reported elsewhere in palaeo-ice stream landsystems and interpreted as typical of onset zones due to the enhanced erosion rates at the glacier bed, induced by ice-flow acceleration (Livingstone et al., 2012; Eyles, 2012; Ottesen et al., 2016). There is uncertainty regarding the age of the glacigenic sediment in the east of the study area (Figure 4.6), in that it could have been deposited during deglaciation by active ice, as suggested by the presence of eskers and streamlined glacigenic mounds (see Section 4.4.2.5; Figure 4.21). In this case, the fast-flow onset zone may have extended further to the east. Nevertheless, the substrate transition from soft- to hard-bed remains consistent with the grooved area representing a zone of enhanced erosion and fast-flow onset.

A more equivocal piece of evidence resides in the proposed links between BMGs and fast-flowing ice, derived from the spatial distribution of elongation ratios of bedrock forms (Bradwell et al., 2008b). It has been inferred that ice flow attained maximum velocities along the central corridor of the Ullapool tributary glacier, which coincides with the area occupied by BMGs (Bradwell et al., 2008b). This is based on the relatively high density and higher elongation ratios of the grooves in comparison to adjacent, peripheral zones to the north and south, where streamlined bedforms are less numerous and less elongate (Bradwell et al., 2008b). Down-ice from the BMGs, the presence of longer bedrock grooves with increasingly higher elongation ratios has been interpreted as the result of ice-flow acceleration along the Ullapool ice-stream tributary (Bradwell et al., 2008b; and Figure 3C therein). This interpretation is potentially problematic for two reasons. Firstly, the variation in elongation ratios could be due to geological rather than glaciological causes. For example, across the flow corridor, this variation could reflect changes in the geological structure, known to produce different landforms in the Moine Schists, as the alignment of bedrock structure relative to the ice flow-direction changes (Gordon, 1981). Along the flow corridor, it could be that changes in lithology rather than ice-flow velocity may account for the variation in BMG elongation, considering the sequence of different lithologies down-flow

and their variable susceptibility to erosion (Gordon, 1981; Krabbendam and Glasser, 2014). Although the influence of fast-ice flow cannot be ruled out based on these theoretical considerations, comparisons of bedrock landforms between areas underlain by different geology need to first assess underpinning geological causes before defaulting to glaciological causes to explain morphometric differences.

Secondly, high elongation ratios may not necessarily be indicative of ice flow acceleration in the case of bedrock grooves, as they are in the case of MSGLs (Stokes and Clark, 2002), due to different feedbacks operating at the ice–bed interface on soft- *versus* hard-bed substrate. This is because, over time, BMGs tend to widen through lateral erosion, which leads to a reduction in elongation (Roberts et al., 2010), whereas MSGLs become longer through sediment transfer and deposition down-ice, which leads to increased elongation ratios (King et al., 2009). This is consistent with results of recent morphometric analyses derived from a global BMG dataset (see Chapter 3), which show that the BMGs in areas of enhanced erosion rates due to fast-ice flow have lower elongation ratios of 5:1–7:1 than those developed primarily under geological control with elongation ratios of 10:1–27:1 (see Section 3.5). The mean elongation ratio of the BMGs at Ullapool is 22:1, which strengthens the argument for their belonging to the category of BMGs developed primarily under geological control.

In the absence of quantitative data on erosion rates and landform dating controls, it remains difficult to separate the effect of slow- *versus* fast-flowing ice on bedrock erosion (see also Section 1.1). However, considering the potentially long-term ice streaming in the Minch (Stoker and Bradwell, 2005), one question is why the Ullapool BMGs are not more similar morphometrically to those from the Antarctic and Norwegian continental shelves (see Section 3.5.2)? This could be due to the relatively slow flow over the study area in comparison to the rest of the Minch, considering its location at the upstream end on the tributary glacier and the potentially gradual increase of ice velocity down-flow (c.f. Bindschadler et al., 2000). It is also possible that over repeat phases of ice-streaming in the Minch, the onset zones migrated further inland, and that the study area was a fast-flow onset zone perhaps only during the last ice-streaming episode. It may therefore be that neither the time span was sufficiently long, nor the ice velocity sufficiently high for glaciological control to overrun the geological resistance in BMG formation. This interpretation is speculative, but it has the benefit of reconciling the BMG formation primarily under geological rather than glaciological constraints, with the site location in an area of fast-ice flow.

Not least, independent empirical evidence implies that BMGs can form in similar geological conditions, under slower ice-sheet flow. Thus, at Invermoriston, north of Loch Ness, where ice flow was parallel to bedrock strike in Moine Schists, the topography is dominated by "a series of benches delimited by rock ribs and steps [which] run parallel to the former ice movement direction" (Gordon, 1981, p. 60) — a description which matches the Ullapool BMGs. To the author's knowledge, no palaeo-ice streaming has been documented in that area, therefore it is assumed that the area underwent slow, ice-sheet flow. The wider implication is that fast-ice flow is not a pre-condition to BMG formation, and therefore BMGs should not be regarded as a diagnostic landform for fast-ice flow. This is consistent with the suggestion that BMGs can be a velocity–duration product, formed either relatively fast beneath streaming ice, or over longer periods of time under slow-flow conditions (see Section 3.5.4).

In conclusion, the location within the Minch ice-stream landsystem and the fact that the bedrock substrate is devoid of glacigenic sediment strongly support the scenario of ice stream onset for BMG formation, although the contribution of fast-ice flow to BMG formation is still poorly understood, due to the equivocal interpretation of their elongation ratios. Results of morphometric analyses alongside the occurrence of BMGs in conjunction with other bedrock forms within a hard-bed landforms assemblage strongly suggest a primary geological rather than glaciological control over BMG formation. Independent empirical evidence of bedrock grooves developed in similar geology under slower, ice-sheet flow conditions indicate that fast-ice flow is not a precondition for BMG formation in Moine Schists. The new insights into BMG formation at Ullapool do not rule out the potentially significant influence fast-ice flow could have had on BMG modification, but the presence of the BMGs does not represent unequivocal evidence for fast-ice flow in the area. The wider implication is that BMGs in general is not a robust indicator of fast-ice flow.

4.6 Conclusions

All bedrock landforms in the study area follow medium-to-large structural lineaments, namely the bedrock strike, fractures, faults, and anticline folds. The present-day landforms are the result of glacial erosion through abrasion and plucking, with the latter directly controlled by the availability and orientation of bedrock joints and fractures. The BMGs are the most conspicuous landforms in the study area due to the orientation of bedrock strike sub-parallel to the former ice-flow direction, which enabled efficient lateral plucking. The

glacial origin of the BMGs is supported by empirical evidence as well as groove widening and deepening with distance down-flow. Although the BMGs remain traceable across the studied terrain, their dominance in the landscape varies in relation to the variable occurrence of other landforms in the topography. Overall, the landscape is one of areal scouring, best described as groove-and-lochan topography, characterised by a grid of cross-cutting linear landforms that reflect the underlying structural geology, with lakes commonly present at the intersection of structural lines. The study area is situated at the upstream end of a tributary glacier feeding into the Minch Ice Stream during the last glaciation. Contrary to earlier hypotheses that BMGs are a direct manifestation of the onset of fast flow conditions, it is more likely that they are a velocity–duration product generated either by slow ice flow over long timescales or faster ice flow over shorter timescales, and consequently they may not be a diagnostic indicator of ice streaming over bedrock terrain.

Acknowledgements

The fieldwork at Ullapool was funded through a New Researcher Working Award offered by the Quaternary Research Association. Iain MacFadyen of Langwell Estate and Kim Scobie of Rhidorroch Estate kindly facilitated access into the more remote parts of the area.

4.7 References

Bindschadler, R., Chen, X. and Vornberger, P., 2000. The onset area of Ice Stream D, West Antarctica. *Journal of Glaciology*, *46*(152), pp.95-101.

Bonow, J.M., Lidmar-Bergström, K. and Japsen, P., 2006. Palaeosurfaces in central West Greenland as reference for identification of tectonic movements and estimation of erosion. *Global and Planetary Change*, *50*(3-4), pp.161-183.

Boulton G.S. 1974. Processes and Patterns of Glacial Erosion. In: Coates, D.R. (ed), *Glacial Geomorphology.* University of New York, Binghampton, pp. 41–87.

Bradwell, T., 2005. Bedrock megagrooves in Assynt, NW Scotland. *Geomorphology*, *65*(3-4), pp.195-204.

Bradwell, T., 2013. Identifying palaeo-ice-stream tributaries on hard beds: Mapping glacial bedforms and erosion zones in NW Scotland. *Geomorphology*, *201*, pp. 397-414.

Bradwell, T., Small, D., Fabel, D., Smedley, R.K., Clark, C.D., Saher, M.H., Callard, S.L., Chiverrell, R.C., Dove, D., Moreton, S.G. and Roberts, D.H., 2019. Ice-stream demise dynamically conditioned by trough shape and bed strength. *Science advances*, *5*(4), pp.eaau1380.

Bradwell, T., Stoker, M.S., Golledge, N.R., Wilson, C.K., Merritt, J.W., Long, D., Everest, J.D., Hestvik, O.B., Stevenson, A.G., Hubbard, A.L. and Finlayson, A.G., 2008a. The northern sector of the last British Ice Sheet: maximum extent and demise. *Earth-Science Reviews*, *88*(3-4), pp.207-226.

Bradwell, T., Stoker, M. and Krabbendam, M., 2008b. Megagrooves and streamlined bedrock in NW Scotland: the role of ice streams in landscape evolution. *Geomorphology*, *97*(1-2), pp.135-156.

Bradwell, T., Stoker, M. and Larter, R., 2007. Geomorphological signature and flow dynamics of The Minch palaeo-ice stream, northwest Scotland. *Journal of Quaternary Science 22*(6), pp.609-617.

British Geological Survey (BGS), 2008. Ullapool. Scotland Sheet 101E. Bedrock 1:50,000 Geology Series. British Geological Survey, Keyworth, Nottingham, UK

British Geological Survey (BGS), 2016. DiGMapGB-50 [bedrock, linear and superficial], Scale 1:50000, Tiles: sc101e, sc102w, downloaded from EDINA Geology Digimap Service https://digimap.edina.ac.uk

Clark, C.D., 1993. Mega-scale glacial lineations and cross-cutting ice-flow landforms. *Earth Surface Processes and Landforms*, *18*(1), pp.1-29.

De Angelis, H.D. and Kleman, J., 2008. Palaeo-ice-stream onsets: examples from the north-eastern Laurentide Ice Sheet. *Earth Surface Processes and Landforms 33*(4), pp.560-572.

Dowdeswell, J.A., Ottesen, D. and Rise, L., 2006. Flow switching and large-scale deposition by ice streams draining former ice sheets. *Geology*, *34*(4), pp.313-316.

Dühnforth, M., Anderson, R.S., Ward, D. and Stock, G.M., 2010. Bedrock fracture control of glacial erosion processes and rates. *Geology*, *38*(5), pp.423-426.

Dyke, A.S. and Morris, T.F., 1988. Drumlin fields, dispersal trains, and ice streams in Arctic Canada. *Canadian Geographer 32*(1), pp.86-90.

Ely, J.C., Clark, C.D., Spagnolo, M., Stokes, C.R., Greenwood, S.L., Hughes, A.L., Dunlop, P. and Hess, D., 2016. Do subglacial bedforms comprise a size and shape continuum? *Geomorphology*, *257*, pp.108-119.

Ely, J.C., Clark, C.D., Spagnolo, M., Hughes, A.L. and Stokes, C.R., 2018. Using the size and position of drumlins to understand how they grow, interact and evolve. *Earth Surface Processes and Landforms*, *43*(5), pp.1073-1087.

Evans, I.S., 1996. Abraded rock landforms (whalebacks) developed under ice streams in mountain areas. *Annals of Glaciology*, *22*, pp.9-16.

Eyles, N., 2012. Rock drumlins and megaflutes of the Niagara Escarpment, Ontario, Canada: a hard bed landform assemblage cut by the Saginaw–Huron Ice Stream. *Quaternary Science Reviews*, *55*, pp.34-49.

Eyles, N. and Putkinen, N., 2014. Glacially-megalineated limestone terrain of Anticosti Island, Gulf of St. Lawrence, Canada; onset zone of the Laurentian Channel ice stream. *Quaternary Science Reviews*, *88*, pp.125-134.

Eyles, N., Putkinen, N., Sookhan, S. and Arbelaez-Moreno, L., 2016. Erosional origin of drumlins and megaridges. *Sedimentary Geology*, *338*, pp.2-23.

Eyles, N., Moreno, L.A. and Sookhan, S., 2018. Ice streams of the Late Wisconsin Cordilleran Ice Sheet in western North America. *Quaternary Science Reviews*, *179*, pp.87-122.

Finlayson, A., Fabel, D., Bradwell, T. and Sugden, D., 2014. Growth and decay of a marine terminating sector of the last British–Irish Ice Sheet: a geomorphological reconstruction. *Quaternary Science Reviews*, *83*, pp.28-45.

Fossen, H., 2016. *Structural geology*. Cambridge University Press, Cambridge.

Funder, S., 1978. Glacial flutings in bedrock, an observation in East Greenland. *Bulletin of the Geological Society of Denmark*, *27*, pp.9-13.

Gillen, C., 2003. *Geology and Landscapes of Scotland*. Terra Publishing, Harpenden.

Glasser, N.F., 2002. The large roches moutonnées of Upper Deeside. *Scottish Geographical Journal*, *118*(2), pp.129-138.

Glasser, N.F. and Bennett, M.R., 2004. Glacial erosional landforms: origins and significance for palaeoglaciology. *Progress in Physical Geography*, *28*(1), pp.43-75.

Glasser, N.F., Roman, M., Holt, T.O., Žebre, M., Patton, H. and Hubbard, A.L., 2020. Modification of bedrock surfaces by glacial abrasion and quarrying: Evidence from North Wales. *Geomorphology*, pp.107-283.

Glasser, N.F. and Warren, C.R., 1990. Medium scale landforms of glacial erosion in south Greenland; process and form. *Geografiska Annaler: Series A, Physical Geography*, *72*(3-4), pp.211-215.

Goodenough, K.M., Krabbendam, M., Bradwell, T., Finlayson, A. and Leslie, A.G., 2009. Digital surface models and the landscape: interaction between bedrock and glacial geology in the Ullapool area. *Scottish Journal of Geology*, *45*(2), pp.99-105.

Gordon, J.E., 1981. Ice-scoured topography and its relationships to bedrock structure and ice movement in parts of northern Scotland and West Greenland. *Geografiska Annaler: Series A, Physical Geography*, *63*(1-2), pp.55-65.

Gordon, J.E., Sutherland, D.G., 1993. Quaternary of Scotland. Chapman and Hall, London.

Graham, D.K., Harland, R., Gregory, D.M., Long, D. and Morton, A.C., 1990. The biostratigraphy and chronostratigraphy of BGS Borehole 78/4, North Minch. *Scottish Journal of Geology*, *26*(2), pp.65-75.

Hall, A.M., 1985. Cenozoic weathering covers in Buchan, Scotland and their significance. *Nature*, *315*(6018), pp.392-395.

Hall, A.M., Ebert, K. and Hättestrand, C., 2013. Pre-glacial landform inheritance in a glaciated shield landscape. *Geografiska Annaler: Series A, Physical Geography*, *95*(1), pp.33-49.

Jamieson, S.S., Stokes, C.R., Ross, N., Rippin, D.M., Bingham, R.G., Wilson, D.S., Margold, M. and Bentley, M.J., 2014. The glacial geomorphology of the Antarctic ice sheet bed. *Antarctic Science*, *26*(6), pp.724-741.

Johnstone, G. S., Smith, D. I. and Harris, A. L., 1969. The Moinian Assemblage of Scotland. In: Kay, M. (ed.) North Atlantic Geology and Continental Drift. American Association of Petroleum Geologists, Memoirs, 12, 159–180.

King, E.C., Hindmarsh, R.C. and Stokes, C.R., 2009. Formation of mega-scale glacial lineations observed beneath a West Antarctic ice stream. *Nature Geoscience*, *2*(8), pp.585-588.

Krabbendam, M. and Bradwell, T., 2011. Lateral plucking as a mechanism for elongate erosional glacial bedforms: explaining megagrooves in Britain and Canada. *Earth Surface Processes and Landforms*, *36*(10), pp.1335-1349.

Krabbendam, M. and Bradwell, T., 2014. Quaternary evolution of glaciated gneiss terrains: pre-glacial weathering vs. glacial erosion. *Quaternary Science Reviews*, *95*, pp.20-42.

Krabbendam, M., Eyles, N., Putkinen, N., Bradwell, T. and Arbelaez-Moreno, L., 2016. Streamlined hard beds formed by palaeo-ice streams: A review. *Sedimentary Geology*, *338*, pp.24-50.

Krabbendam, M. and Glasser, N.F., 2011. Glacial erosion and bedrock properties in NW Scotland: abrasion and plucking, hardness and joint spacing. *Geomorphology*, *130*(3-4), pp.374-383.

Lane, T.P., Roberts, D.H., Rea, B.R., Ó Cofaigh, C. and Vieli, A., 2015. Controls on bedrock bedform development beneath the Uummannaq Ice Stream onset zone, West Greenland. *Geomorphology*, *231*, pp.301-313.

Larsson, I., 1954. *Structure and landscape in western Blekinge, southeast Sweden*. Royal University of Lund, Department of Geography, Paper 7.

Law, R.D. and Johnson, M.R.W., 2010. Microstructures and crystal fabrics of the Moine Thrust zone and Moine Nappe: history of research and changing tectonic interpretations. *Geological Society, London, Special Publications*, *335*(1), pp.443-503.

Lawson, T.J., 1996. Glacial striae and former ice movement: the evidence from Assynt, Sutherland. *Scottish Journal of Geology*, *32*(1), pp.59-65.

Lidmar-Bergström, K., 1989. Exhumed Cretaceous landforms in south Sweden. *Zeitschrift für Geomorphologie. Supplementband*, *72*, pp.21-40.

Lidmar-Bergström, K., 1996. Long term morphotectonic evolution in Sweden. *Geomorphology*, *16*(1), pp.33-59.

Lidmar-Bergström, K., 1997. A long-term perspective on glacial erosion. *Earth Surface Processes and Landforms 22*(3), pp.297-306.

Linton, D.L., 1963. The forms of glacial erosion. *Transactions and Papers (Institute of British Geographers)*, (33), pp.1-28.

Livingstone, S.J., Ó Cofaigh, C., Stokes, C.R., Hillenbrand, C.D., Vieli, A. and Jamieson, S.S., 2012. Antarctic palaeo-ice streams. *Earth-Science Reviews*, *111*(1-2), pp.90-128.

Lowe, A.L. and Anderson, J.B., 2003. Evidence for abundant subglacial meltwater beneath the paleo-ice sheet in Pine Island Bay, Antarctica. *Journal of Glaciology*, *49*(164), pp.125-138.

Margold, M., Stokes, C.R. and Clark, C.D., 2015. Ice streams in the Laurentide Ice Sheet: Identification, characteristics and comparison to modern ice sheets. *Earth-Science Reviews*, *143*, pp.117-146.

Newton, M., Evans, D.J.A., Roberts, D.H. and Stokes, C.R., 2018. Bedrock mega-grooves in glaciated terrain: A review. *Earth-Science Reviews*, *185*, pp.57-79.

Nobles, L.H., Weertman, J., 1971. Influence of irregularities of the bed of an ice sheet on deposition rate of till. In: Goldthwait, R.P. (Ed.), Till, a Symposium. Ohio State Univ. Press, Columbus, Ohio, pp. 117–126.

Ó Cofaigh, C., Evans, D.J.A. and Smith, I.R., 2010. Large-scale reorganization and sedimentation of terrestrial ice streams during late Wisconsinan Laurentide Ice Sheet deglaciation. *Bulletin of the Geological Society of America 122*(5-6), pp.743-756.

Olvmo, M., Lidmar-Bergström, K. and Lindberg, G., 1999. The glacial impact on an exhumed sub-Mesozoic etch surface in southwestern Sweden. *Annals of Glaciology*, *28*, pp.153-160.

Ottesen, D., Dowdeswell, J.A. and Rise, L., 2005. Submarine landforms and the reconstruction of fast-flowing ice streams within a large Quaternary ice sheet: The 2500-km-long Norwegian-Svalbard margin (57–80 N). *Geological Society of America Bulletin*, *117*(7-8), pp.1033-1050.

Ottesen, D., Stokes, C.R., Bøe, R., Rise, L., Longva, O., Thorsnes, T., Olesen, O., Bugge, T., Lepland, A. and Hestvik, O.B., 2016. Landform assemblages and sedimentary processes along the Norwegian Channel Ice Stream. *Sedimentary Geology*, *338*, pp.115-137.

Peach, B.N., Horne, J., Gunn, W., Clough, C.T., Hinxman, L.W., Teall, J.J.H., 1907. The Geological Structure of the North-West Highlands of Scotland. Memoir of the Geological Survey of Great Britain, HMSO, Glasgow, 668 pp.

Phillips, W.M., Hall, A.M., Mottram, R., Fifield, L.K. and Sugden, D.E., 2006. Cosmogenic 10Be and 26Al exposure ages of tors and erratics, Cairngorm Mountains, Scotland: timescales for the development of a classic landscape of selective linear glacial erosion. *Geomorphology*, *73*(3-4), pp.222-245.

Rea, B.R., 1994. Joint control in the formation of rock steps in the subglacial environment. In Robinson, D. A. and Williams, R. B. G. (eds.): *Rock Weathering and Landform Evolution,* pp. 473-486.

Rea, B.R. and Evans, D.J., 1996. Landscapes of areal scouring in NW Scotland. *Scottish Geographical Magazine*, *112*(1), pp.47-50.

Ringrose, P.S., Hancock, P., Fenton, C. and Davenport, C.A., 1991. Quaternary tectonic activity in Scotland. *Geological Society, London, Engineering Geology Special Publications*, *7*(1), pp.679-686.

Roberts, D.H. and Long, A.J., 2005. Streamlined bedrock terrain and fast ice flow, Jakobshavns Isbrae, West Greenland: implications for ice stream and ice sheet dynamics. *Boreas*, *34*(1), pp.25-42.

Roberts, D.H., Long, A.J., Davies, B.J., Simpson, M.J. and Schnabel, C., 2010. Ice stream influence on west Greenland ice sheet dynamics during the last glacial maximum. *Journal of Quaternary Science*, *25*(6), pp.850-864.

Sissons, J.B., 1967. *The Evolution of Scotland's Scenery*. Oliver and Boyd, Edinburgh.

Smith, A.M., Murray, T., Nicholls, K.W., Makinson, K., Aðalgeirsdóttir, G., Behar, A.E. and Vaughan, D.G., 2007. Rapid erosion, drumlin formation, and changing hydrology beneath an Antarctic ice stream. *Geology*, *35*(2), pp.127-130.

Smith, H.T.U., 1948. Giant glacial grooves in northwest Canada. *American Journal of Science*, *246*(8), pp.503-514.

Spagnolo, M., Clark, C.D., Ely, J.C., Stokes, C.R., Anderson, J.B., Andreassen, K., Graham, A.G. and King, E.C., 2014. Size, shape and spatial arrangement of mega-scale glacial lineations from a large and diverse dataset. *Earth Surface Processes and Landforms*, *39*(11), pp.1432-1448.

Spagnolo, M., Phillips, E., Piotrowski, J.A., Rea, B.R., Clark, C.D., Stokes, C.R., Carr, S.J., Ely, J.C., Ribolini, A., Wysota, W. and Szuman, I., 2016. Ice stream motion facilitated by a shallow-deforming and accreting bed. *Nature communications*, *7*(1), pp.1-11.

Stoker, M.S., 1995. The influence of glacigenic sedimentation on slope-apron development on the continental margin off Northwest Britain. *Geological Society, London, Special Publications*, *90*(1), pp.159-177.

Stoker, M.S. and Holmes, R., 1991. Submarine end-moraines as indicators of Pleistocene ice-limits off northwest Britain. *Journal of the Geological Society*, *148*(3), pp.431-434.

Stoker, M. and Bradwell, T., 2005. The Minch palaeo-ice stream, NW sector of the British–Irish Ice Sheet. *Journal of the Geological Society*, *162*(3), pp.425-428.

Stokes, C.R., 2018. Geomorphology under ice streams: moving from form to process. *Earth Surface Processes and Landforms*, *43*(1), pp.85-123.

Stokes, C.R. and Clark, C.D., 1999. Geomorphological criteria for identifying Pleistocene ice streams. *Annals of Glaciology*, *28*, pp.67-74.

Stokes, C.R. and Clark, C.D., 2001. Palaeo-ice streams. Quaternary Science Reviews 20(13), pp.1437-1457.

Stokes, C.R. and Clark, C.D., 2002. Are long subglacial bedforms indicative of fast ice flow?. *Boreas*, *31*(3), pp.239-249.

Stokes, C.R., Clark, C.D. and Storrar, R., 2009. Major changes in ice stream dynamics during deglaciation of the north-western margin of the Laurentide Ice Sheet. *Quaternary Science Reviews*, *28*(7-8), pp.721-738.

Stone, J.O., Ballantyne, C.K. and Keith Fifield, L., 1998. Exposure dating and validation of periglacial weathering limits, northwest Scotland. *Geology*, *26*(7), pp.587-590.

Strachan, R.A., 1986. Shallow marine sedimentation in the Proterozoic Moine succession, northern Scotland. *Precambrian Research*, *32*(1), pp.17-33.

Strachan, R.A., Holdsworth, R.E., Krabbendam, M. and Alsop, G.I., 2010. The Moine Supergroup of NW Scotland: insights into the analysis of polyorogenic supracrustal sequences. *Geological Society, London, Special Publications*, *335*(1), pp.233-254.

Sugden, D.E., 1968. The selectivity of glacial erosion in the Cairngorm Mountains, Scotland. *Transactions of the Institute of British Geographers*, 45, pp.79-92.

Sugden, D.E., 1974. Landscapes of glacial erosion in Greenland and their relationship to ice, topographic and bedrock conditions. *Institute of British Geographers Special Publication*, *7*, pp.177-195.

Sugden, D.E., 1978. Glacial erosion by the Laurentide ice sheet. *Journal of Glaciology*, *20*(83), pp.367-391.

Sugden, D.E., Glasser, N.F. and Clapperton, C.M., 1992. Evolution of large roches moutonnées. *Geografiska Annaler: Series A, Physical Geography*, *74*(2-3), pp.253-264.

Van Landeghem, K.J. and Chiverrell, R.C., 2020. Bed erosion during fast ice streaming regulated the retreat dynamics of the Irish Sea Ice Stream. *Quaternary Science Reviews*, *245*, 106526.

Wilson, G., 1953. Mullion and rodding structures in the Moine Series of Scotland. *Proceedings of the Geologists' Association*, *64*(2), pp.118-IN3.

Chapter 5. On the origin of bedrock mega-grooves (BMGs)

Abstract
Understanding bedrock mega-groove (BMG) formation equates to being able to explain their initiation as well as their subsequent evolution. The latter can be inferred by assessing the efficiency of erosion mechanisms in relation to the susceptibility of bedrock to that erosion, provided both the environment of erosion and the geological characteristics of the bedrock are known in considerable detail. In contrast, BMG initiation remains poorly understood. Any model of BMG formation must be able to explain their main physical characteristics, specifically in relation to their large dimensions, straightness and relationships to bedrock geology. Several scenarios of BMG initiation are proposed here, based on the assumptions that BMGs pre-date the last glaciation and were initiated subglacially, through erosion by glacier ice. In cases where geological controls have been inferred from the BMG morphology or location, groove initiation was likely either structural through the exploitation of linear features, or lithological, whereby the origin of harder erodents necessary for abrading softer rocks can be explained by the succession of adjacent lithologies across former ice flow directions. Where no geological control over BMG initiation could be inferred, it is hypothesised that their initiation was due to antecedent geological conditions, through gradual bedrock removal due to erosion, or was related to pre-Quaternary regolith, which was potentially a source of erodents no longer visible in the landscape.

5.1 Introduction

Previous chapters have shown that BMG metrics or characteristics fall within well-defined ranges, and the grooves attain large dimensions through widening, deepening and possibly lengthening as erosion progresses (see Chapter 3). Any genetic model of BMG evolution must explain these characteristics. Clearly, the close association of BMGs with bedrock structure in many locations (Zumberge, 1955; Krabbendam and Bradwell, 2011; Krabbendam et al., 2016; see also Section 2.5.1.2) supports the notion that they have been evolving as a result of the exploitation of the geological structure by glacial erosion, and presumably through relatively uniform ice-flow directions. Hence, BMG development could be inferred by assessing the bedrock susceptibility to erosion in conjunction with various agents of erosion expected to have acted upon the land surface throughout the Quaternary (Newton et al., 2018). In contrast, BMG initiation continues to be poorly understood and

difficult to explore other than theoretically. This is thought to be due to BMGs being potentially older than the last glaciation, especially those that are independent of bedrock structure, because long-term erosion responsible for their persistence has also likely obliterated the physical characteristics of the land surface (i.e. the antecedent conditions) which may have triggered groove initiation (see Section 2.5.2; Newton et al., 2018).

Crucial questions that require addressing include: i) given the highly dynamic evolution of ice-sheet flow dynamics (Boulton and Clark, 1990), how is persistent, uni-directional glacier flow maintained for long enough to create straight grooves in bedrock, especially in situations where bedrock structure has not been exploited? ii) Is the sparsity of BMGs in the glacial landscape record a reflection of their blanketing by glacigenic deposits? iii) Do BMGs relate to the earliest Quaternary glaciation footprints and hence result from a land surface whose characteristics are significantly different from those of today and relatively recent glaciations?

Invariably, in the absence of evidence for key factors that led to initial bedrock grooving, the construction of theoretical and often speculative models of BMG initiation remain the best option, which can be tested by future research (e.g. through numerical modelling). This chapter proceeds with proposing several plausible scenarios for BMG initiation and development, in which the characteristics of grooved terrain are explained by considering the interactions of known glacial erosion processes with topography and long-term weathering. First, the BMG characteristics that require explaining need to be summarised and then, arising from that, the underlying assumptions are formulated.

5.2 BMG characteristics

Several general characteristics of BMGs have been derived based on mapping and morphometric analyses at ten sites, spanning different lithologies, across the world (see Chapter 3). Firstly, it has been consistently noted that BMGs tend to be confined to one lithology despite the ice having traversed sequences of different adjacent bedrock types (see Section 3.2.2 in Chapter 3 and the geology maps therein). This strongly indicates that BMG formation is underpinned by geological controls. Secondly, the large dimensions of BMGs have been confirmed through systematic measurements, as has their straightness and parallelism, reflected in the low standard deviation values for azimuth (see section 3.4.1 in Chapter 3). Groove depth, in particular, yields high values of between 2–15 m, approximately twice those for MSGLs (Spagnolo et al., 2014), which are soft-bedded

landforms of similar shape and magnitude. The width/depth linear correlations have a consistently positive trend across the analysis spectrum (Figures 3.18C and 3.19E in Chapter 3), whereas the length/width and length/depth correlations, albeit positive, are weak within individual sites (Figures 7 and 8 in the Appendix; also Figure 3.18A and 3.18B in Chapter 3). This means that, regardless of length, any individual site comprises BMGs which can be either narrow or wide, and deep or shallow. The variation of width and depth along flow is inconsistent between sites, with some showing a positive trend and others a negative one (Figure 3.20 in Chapter 3). It is noticeable, however, that width varies relatively little with distance down-ice flow as indicated by the nearly-horizontal trendlines (Figure 3.20A in Section 3.5.1), whereas the variation in depth is greater whether the values increase or decrease with distance down-flow (Figure 3.20B in Section 3.5.1).

A potentially viable, overarching explanation for the evolution of BMGs must obviously explain the range of general characteristics outlined above. Importantly, it must also satisfy some fundamental genetic factors that are clearly necessary for grooving bedrock. Firstly, as with striations, BMG production needs the provision of suitably sized and resistant striator clasts (mega-blocks) or erodents. As BMGs are located, and therefore formed, on ice sheet beds, such blocks must be sourced from the bed relatively adjacent to the grooved site, whether through plucking (quarrying) and/or through the formation or re-mobilization of a deformable substrate containing erodents (*sensu* Eyles et al., 2016). Secondly, in the absence of bedrock structural control, relative uniformity of parallel-aligned and straight grooves requires either fast glacier flow (Krabbendam et al., 2016) or a consistent ice flow direction over long periods of time (see Section 3.5.4 in Chapter 3 and Section 4.5.3 in Chapter 4). The latter is particularly important for bedrock grooving and would conceivably imply repeat occupation of similar ice flow trajectories by erosive agents throughout multiple glaciations to ensure the length of time required for groove growth, under slower ice-flow conditions. Thirdly, grooves must have been initiated in bedrock that was relatively weaker than the erodents. As this weak rock is not represented in the grooved landscape today, it must have been removed by erosion, pointing to antecedent conditions for BMG initiation, at least in some cases (e.g. at Elphin, Scotland, UK; Bradwell, 2005). Fourthly, BMG fields display groove initiation either at approximately the same position, along a linear source zone (e.g. Figures 3.7B, 3.10B and 3.11B in Chapter 3), or at various points down-flow (e.g. Figures 3.2B, 3.5B, 3.8B in Chapter 3). Consequently, there are two different modes of BMG initiation driven by either linear source-outcrops or randomly distributed, *in situ* erodents contained in antecedent materials. Finally, remarkably few examples of BMG fields exist, relative to other subglacial landforms, so either the requisite

conditions for their formation were rarely met (Funder, 1978) or many are buried beneath glacigenic deposits and hence date to glaciations that pre-date the last glacial maximum (LGM), or many have been removed by subsequent erosion. These factors are now considered in the review of underlying assumptions and construction of genetic models for BMGs.

5.3 Assumptions

The groove initiation scenarios developed here are based on two underlying assumptions. Firstly, it is assumed that groove initiation took place subglacially, through erosion by glacier ice. However, once initiated, a groove will inevitably be the focus of subglacial meltwater drainage, and hence glacifluvial erosion is likely to play a not insignificant role during phases of substantial subglacial meltwater production. Secondly, BMGs that are independent of bedrock structure are assumed to pre-date at least the last glaciation, in order to accommodate the long-term erosion needed to remove any antecedent conditions for groove initiation.

5.3.1 Glacial erosion of BMGs

5.3.1.1 Abrasion

It has long been suggested that BMGs are the product of abrasion by glacier ice, as this is the only mechanism that can account for groove straightness and parallelism over long distances (Smith, 1948; Funder, 1978; Heikkinen and Tikkanen, 1989; Bradwell et al., 2008; Newton et al., 2018; see also Section 5.2). Striations were among the first features to be recognised as vestiges of glacial erosion and their occurrence is ubiquitous across glaciated terrain (Chamberlin, 1888; Geikie, 1894; Laverdiere et al., 1979 and 1985; Veillette et al., 1999; Rea et al., 2000). Their formation has been observed in the field (e.g. Boulton, 1979) and simulated in the laboratory (e.g. Lister et al., 1968; Iverson, 1990; Rea, 1996). Although striations and BMGs have morphological similarities and are both initiated through glacial abrasion, bedrock grooves are orders of magnitude larger than striations (see Table 2.2 in Chapter 2) and hence presumably develop into mega-scale features (Bukhari et al., 2021), as a result of a combination of erosional mechanisms beyond that of a single striator clast impact (Krabbendam et al., 2016; Newton et al., 2018). Importantly, the dominant role of mega-blocks in mega-groove initiation in soft bedrock and Quaternary sediment has been identified recently by Evans et al. (2021) in Alberta, Canada, and is particularly evident where groove floors contain possible mega-scale chattermarks (Figure 5.1). This remains a

qualitative consideration in the absence of numerical constraints, but it is reasonable to assume that, like abraded and striated surfaces, the rate of groove deepening must be higher than the rate of ridge lowering for a BMG to develop. The availability and abundance of mega-blocks and/or bedrock rafts on former ice sheet beds, often referred to as "rubble terrain", and their widespread association with grooves (Evans et al., 2020 and 2021; Bukhari et al., 2021) demonstrates their crucial role as erodents or mega-striators.

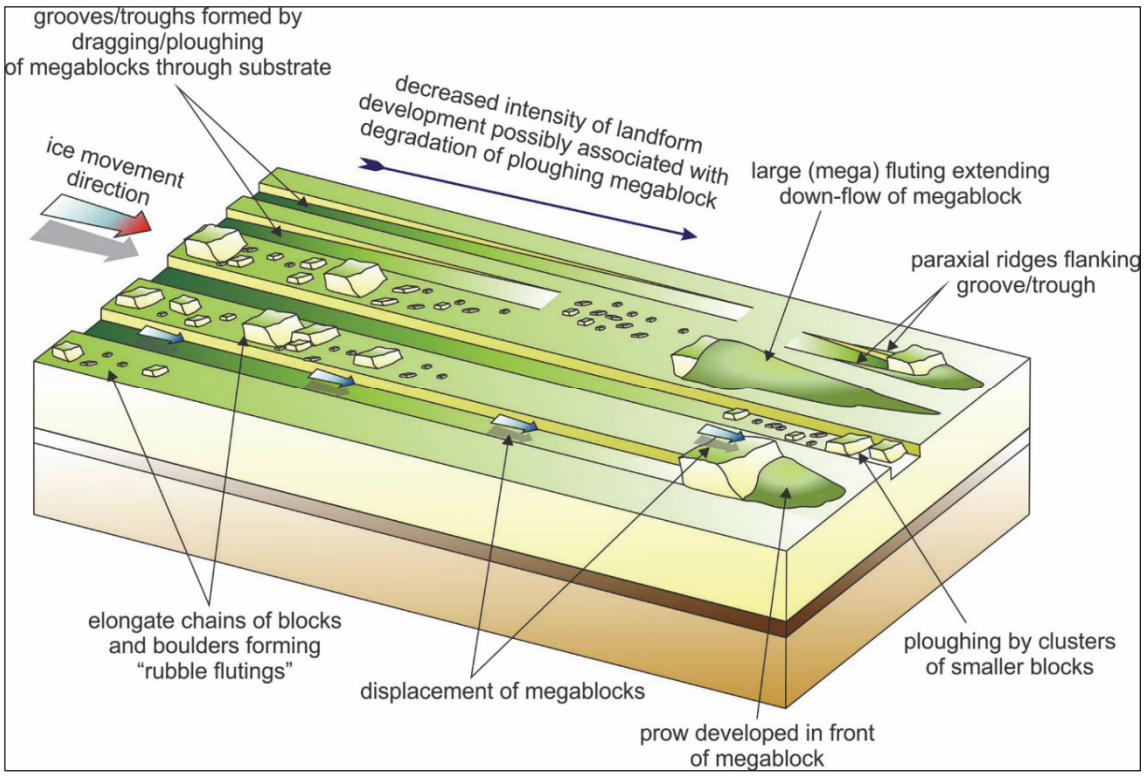

Figure 5.1. Conceptual model of bedrock and/or sediment grooving through mega-block ploughing after the production of rubble terrain by bedrock plucking/rafting (from Evans et al., 2021). Image © Elsevier.

Although BMGs have been widely associated with palaeo-ice stream beds (e.g. Ó Cofaigh et al., 2002; Bradwell et al., 2008; Eyles, 2012; Krabbendam et al., 2016; Eyles et al., 2018; Bukhari et al., 2021), fast-ice flow is not in itself necessarily capable of groove initiation, and it has been acknowledged that multiple glaciations with similar ice flow trajectories are likely required to form grooved terrain (Livingstone et al., 2012). Critical in this respect is the availability of mega-striators capable of groove initiation and indeed their continued, or at least punctuated, availability through time. Intermittent ice stream freeze-on/shutdown (Iverson, 2000; Bougamont et al., 2003a, b; Christoffersen and Tulaczyk, 2003a, b; Christoffersen et al., 2006) has been proposed as a potential source of mega-striators, viable in situations where the exposure of well-jointed bedrock leads to enhanced plucking (e.g.

Hall et al., 2020; Bukhari et al., 2021; Evans et al., 2021). The gradual thinning and exhaustion of subglacial deforming layers also has the potential to expose jointed bedrock and thereby refresh the supply of erodents through plucking (Evans et al., 1998; Alley, 2000; Iverson, 2010).

It follows that some form of sustained and focussed bedrock grooving is needed to form a proto-BMG, which in the case of structurally controlled examples is ensured by a constant supply of erodents derived through plucking, subsequently entrained into relatively fast-flowing basal ice (i.e. warm-based thermal regimes) and moving in predominantly the same direction (cf. Bradwell et al., 2008; Krabbendam and Bradwell, 2011; Eyles, 2012). Early assessments of the macro-scale Kelleys Island grooves at Lake Erie by Carney (1910) inferred the importance of the localized impact of abrading tools and their constant supply to basal ice in the area. With larger scale BMGs developed independent of bedrock structure, it is more difficult to envisage groove initiation, especially as the groove needs to attain sufficient size rapidly in order to further concentrate the erosion processes required for enlargement and entrenchment at a stable position on the ice sheet bed. The focussing of tools, and hence erosional processes after bed perturbations have been created, has been explained theoretically by Nobles and Weertman (1971) through geothermal heat flow concentration in depressions (Figure 5.2A), and by Boulton (1975 and 1979) through flow diversion of debris-rich ice towards depressions (Figure 5.2B).

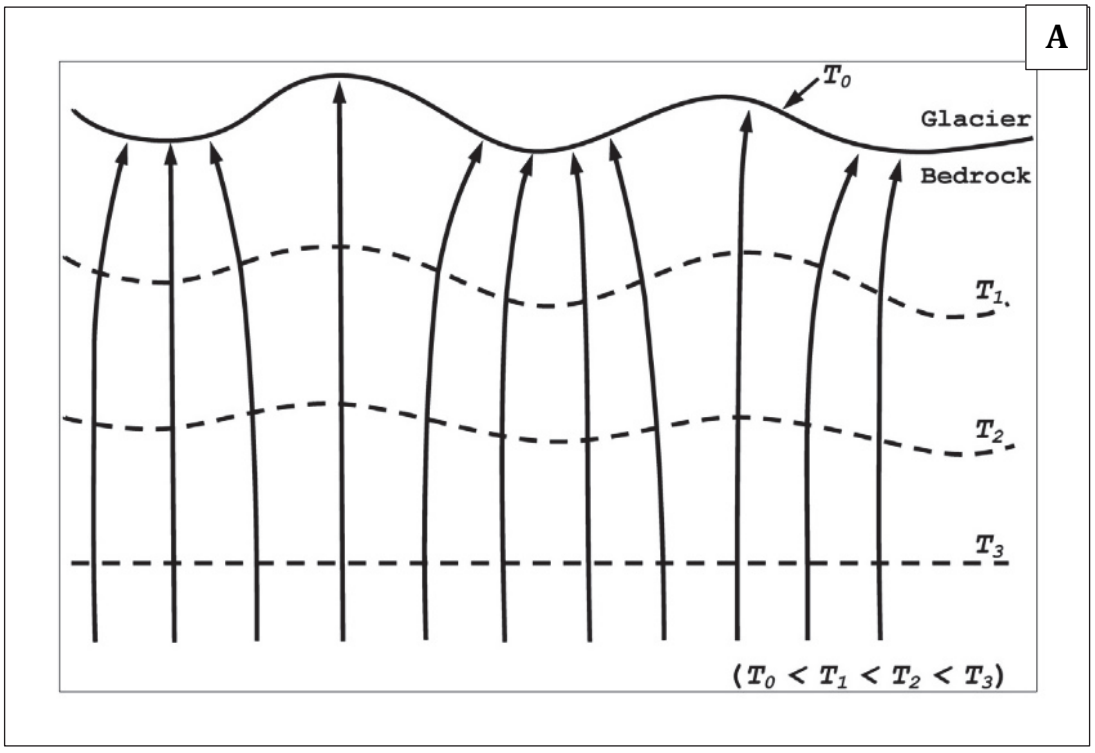

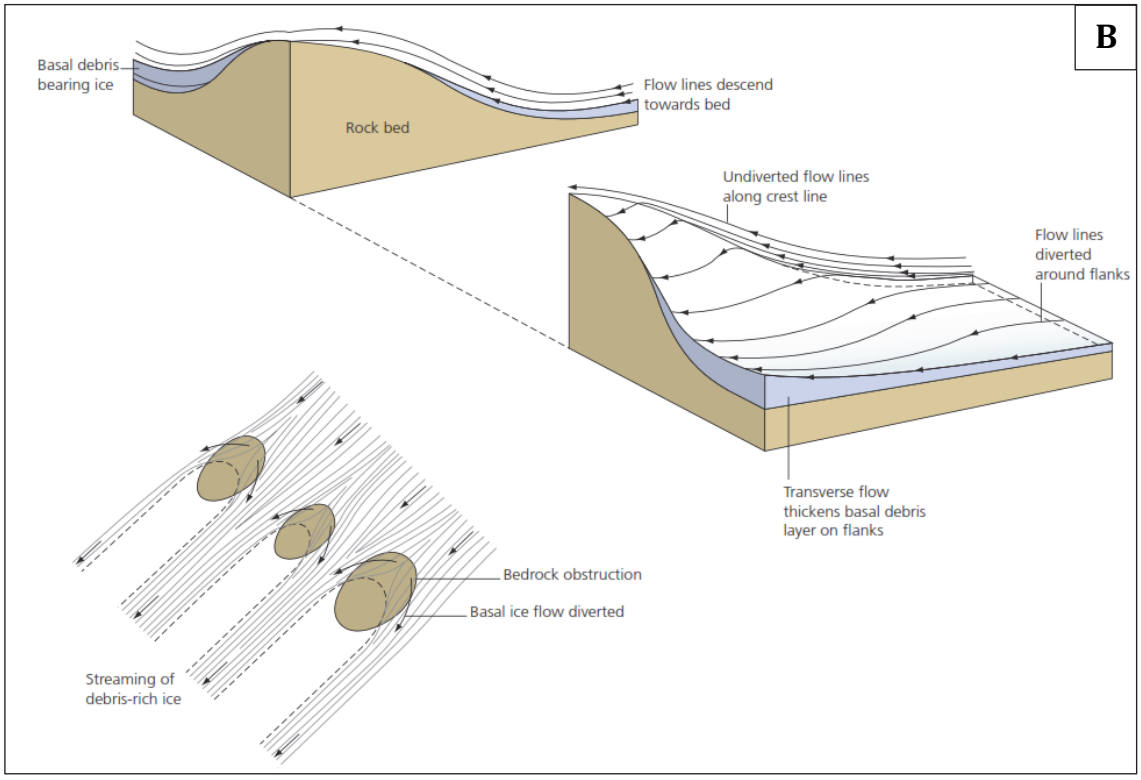

Figure 5.2. Theoretical models that explain preferential till sedimentation and debris-rich ice in low areas of glacier beds. **A:** Geothermal heat flow intercepting isotherms (T_0 – T_3) at right angles, thus leading to more heat being delivered into the bedrock depressions than the topographic highs., leading in turn to elevated basal ice melt rates in depressions (Figure 15 in Newton et al., 2018, after Nobles and Weertman, 1971); image © Elsevier. **B:** basal debris-rich ice thickening due to bed obstructions (after Boulton, 1975 and 1979). Figure 5.2.B was digitised by Chris Orton.

5.3.1.2 Plucking

Plucking cannot incise the bedrock in the same way as abrasion does, but it could, in theory, initiate a groove by the gradual migration up-ice of a plucked rock face. This is possible if a cavity forms between the bedrock substrate and the overriding ice due to pre-existing topographic high points (Hallet, 1996) and if the up-ice migration of the plucking front occurs along straight lineaments in order to lead to the formation of straight BMGs. So far it has been demonstrated that plucking is more efficient than abrasion in the glacial erosion process (Dühnforth et al., 2010) and there is evidence that plucking has been effective in BMG enlargement during the last glaciation in areas of layered, well-jointed rocks (Bradwell, 2005; Krabbendam and Bradwell, 2011; Krabbendam et al., 2016) (see Section 3.2.2 and Section 3.5.2 in Chapter 3). This implies that, overall, a higher bedrock volume may have been removed through plucking compared to abrasion in the long-term process of BMG development, but it is perhaps less certain whether plucking started to operate *after* BMG initiation through abrasion, or it was directly involved in BMG initiation alongside abrasion. Either way, it could be argued that plucking begins to play a part in BMG

development at an early stage, considering that striations are essentially microscale grooves the floors of which are characterised by quarrying (i.e. plucking) features such as chattermarks (Iverson, 1990 and 1995; Rea, 1996).

5.3.1.3 Glacifluvial erosion

Cases have been made for the glacifluvial erosion of subglacially streamlined bedrock, especially in the development of P-forms (e.g. Dahl, 1965; Shaw and Sharpe, 1987; Sharpe and Shaw, 1989; Shaw and Gilbert, 1990; Kor et al., 1991; Shaw, 2002). Even multiple, parallel-aligned and straight grooves have been explained exclusively as the product of meltwater erosion, specifically by multiple vortices developed down-flow from protuberances (Bradwell 2005; Munro-Stasiuk et al., 2005; Shaw et al., 2008), thereby potentially explaining larger-scale grooves and ridges in fields of crag-and-tails. The limitations of an exclusive meltwater origin for such landforms has been widely demonstrated (e.g. Clarke et al., 2005; Benn and Evans, 2006; Ó Cofaigh et al., 2010b), but the pathways for subglacial meltwater are undoubtedly influenced by pre-existing topographic lows in the substrate and hence, once initiated, grooves are very likely to have been enhanced by glacifluvial erosion due to their ability to channel substantial meltwater flows (Eyles, 2006; Le Broque et al., 2013; Jeofry et al., 2018; Drews et al., 2020). This is entirely consistent with heat fluxes, as modelled by Nobles and Weertman (1971), and the concentration of debris-rich ice in grooves, as proposed by Boulton (1975 and 1979; Figure 5.2). To elaborate further, fluctuations in subglacial effective pressures and associated meltwater production will result in switches from strong to weak ice-bed coupling. The latter enables subglacial meltwater flows in Nye channels. In contrast, strong ice-bed coupling leads to ice creep towards such channels and freeze-on of residual meltwater and debris concentrated in channel floors. Hence, once grooves are initiated, they become the increasing focus of meltwater erosion and abrasion by flow-parallel, debris-rich basal ice stripes or bands (Boulton, 1975 and 1979; Bradwell et al., 2008; Catania et al., 2005; Roberts et al. 2010), providing till advection to the site does not seal them off from the glacier sole. This concept of temporal switching between ice-bed interface conditions is compatible with previous theories of a hybrid genesis for P-forms, which invoke debris-rich basal ice, saturated till at the ice-bed interface, pressurised subglacial meltwater and ice–water mixtures (Gjessing, 1965; Gray, 1981). In particular, it promotes the concept of ice–debris mixtures for P-form development as advocated by Gjessing (1965). Previous models of bedrock grooving have invoked these ice–debris mixtures (Figure 5.3) in terms of longitudinal, ice flow-parallel “debris streams” (Goldthwait, 1979). The relatively strong, positive correlations between depth and width across the analysis spectrum in the

morphometry study (see Section 3.4.2 and Section 5.2) strengthen the idea that erosion progresses both laterally and in depth, in synchrony, as the groove develops, and they also support the case for the high preservation potential of BMGs (see Section 3.5.4 in Chapter 3).

Figure 5.3. Example of debris-rich basal ice in a sub-polar glacier, Ellesmere Island, Arctic Canada, illustrating the erosional potential of ice-debris mixtures, created when ice–bedrock coupling is achieved through freeze-on. Note particularly the large boulders that may act as mega-striators (Photo: D. J. A. Evans).

In summary, BMGs are most likely to have been initiated through glacial abrasion, through the agency of large, relatively resistant bedrock blocks (erodents) dragged by the ice over relatively weaker lithologies. The contribution of plucking is likely to have increased as the grooves developed, although plucking cannot be ruled out as a mechanism of groove initiation. Although the role of glacifluvial erosion can be accommodated through potentially any combination of ice, water and debris slurry, such processes are difficult to envisage as *initiators* of parallel-aligned, kilometres-long BMGs. Consequently, the BMG models compiled below integrate these processes only in the more advanced stages of groove development, alongside concentrated abrasion.

5.3.2 BMGs pre-dating the last glaciation

The links between BMGs and Quaternary glaciations, in terms of ice flow direction and spatial extent, strongly suggest a Quaternary age for the grooves (Newton et al., 2018 and references therein), but in the absence of absolute dates it is difficult to establish how far back into the Quaternary the BMGs were initiated. Furthermore, initiation dates are likely to have varied both between and within sites (see Chapter 3). However, several observations indicate that, once established, BMGs have a high preservation potential, and that this is consistent with significant age.

First, there is a lack of cross-cutting between BMGs, although smaller grooves, especially striations, can occur at an angle to the BMGs and ridges (Funder, 1978; Witkind, 1978; Bradwell, 2005). In addition, BMGs can be aligned at a low angle to that of the latest inferred ice-flow direction (Finlayson et al., 2014; Krabbendam et al., 2016). Collectively, these observations indicate that BMGs can survive changes in ice-flow direction and even continue to grow in size while maintaining their initial alignment. In contrast, MSGLs, glacial corrugations of similar morphology and magnitude to BMGs, can develop cross-cutting flow sets driven by changes in ice-flow direction (e.g. Clark, 1993, 1994 and1999; Ó Cofaigh et al., 2010a). This is due to the fact that MSGLs are composed of unlithified sediment and hence prone to subglacial reworking within the deformable substrate. This contrast in permanence of orientation between bedrock-cored BMGs and sediment-cored MSGLs highlights not only the relatively high preservation potential of BMGs but also their persistence through time.

Second, the dendritic drainage pattern typical of long-term subaerial fluvial denudation is missing across grooved terrain (e.g. Witkind, 1978). Instead, the drainage pattern often follows the BMG alignment, as displayed by their floors commonly being drained by shallow streams or hosting elongate lakes (Figure 3.7 in Chapter 3; see also Figure Chapter 4), indicating that surface drainage follows subglacial ice-flow indicators. At sites where the BMGs underpin a landscape of areal scouring, the long-term development of drainage patterns is directly linked to bedrock grooving (e.g. Ullapool, in Scotland, UK – see Section 4.5.2 in Chapter 4). A similar argument for long-term landscape development throughout the Quaternary has been invoked for cnoc-and-lochan topography on gneissic substrate, where the dendritic drainage pattern is missing, and surface water bodies typically follow the glacially-modified topography (Sugden, 1978).

Third, the typical BMG depth of 2-15 m (see Table 3.3) is within the same order of magnitude as the average surface lowering through glacial erosion during the Quaternary. Overall, the latter it is estimated to have been well under 100 m, for example 35-48 m in Eastern Scotland (Glasser and Hall, 1997), or as little as between 9 m (+/-8m) and 27 m (+/-11 m) in northern Sweden (Hall et al., 2013). The efficiency of glacial erosion is known to vary locally and regionally, according to the style of glacial erosion. Thus, deep glacial troughs underwent deepening of 100s of meters through glacial erosion (Sugden, 1968 and 1974), whereas other areas have hardly been affected by glacial erosion (e.g. Sugden, 1968; Lidmar-Bergström et al., 1997; Phillips et al., 2006). If grooved terrain are regarded as the result of areal scouring (see Section 4.5.2), then the amount of surface lowering through glacial erosion is expected to sit between extreme values. Significantly, if the amount of ridge lowering is added to the BMG depth, the figure thus obtained would reflect more realistically the overall surface lowering through Quaternary glacial erosion, and it would bring the amount of erosion closer to the estimated ranges of several 10s of meters constrained across glaciated terrain elsewhere (Glasser and Hall, 1997; Hall et al., 2013).

Although this is a crude and generalised comparison, it strongly supports an age at least older than the last glacial cycle for the BMGs and the plausibility of their initiation in the earlier stages of the Quaternary. More specifically, this conclusion is supported by the mean BMG depth of 7m at Elphin, developed exclusively in quartzite, which need more than 150,000 years to develop if a continuous glacial erosion rate of 0.04 mm/yr was assumed, based on the estimations of Colgan et al. (2013). This exceeds the duration of the last glacial cycle and strongly suggests BMG initiation earlier in the Quaternary.

Finally, the fact that so few BMGs appear to exist in glaciated terrain compared to other subglacial landforms may well relate to the fact that they are buried by glacigenic sediments deposited after BMG production. This is being increasingly verified by offshore seismic stratigraphy evidence, wherein multiple ice sheet flow trajectories are recorded in mega-scale lineations in the lower/older glacigenic deposits (e.g. Rafaelsen et al., 2002; Dowdeswell et al., 2006; Graham et al. 2007; Riedel et al., 2021). It follows that many BMGs may have been formed during earlier Quaternary glaciations but are now obscured by the tills left by subsequent ice sheets. Additionally, it may be that the conditions necessary for BMG initiation and indeed growth have been reduced or possibly even removed over time (see Section 5.4.2) and hence, there has been a reduction in the number of locations providing optimum conditions for their development. This implies that the precursor shapes and necessary erosional ingredients of some glacial landforms are inherited from

older, non-glacial land surfaces such as etchplains (cf. Lindström, 1988; Lidmar-Bergström, 1989, 1995 and 1997; Lidmar-Bergström et al., 1997; Olvmo et al., 1999 and 2005; Olvmo and Johansson, 2002; Hall et al., 2013; Krabbendam and Bradwell, 2014), which strengthens the presumption of an old age for the BMGs.

5.4 Hypotheses for BMG initiation

In this section various hypotheses of BMG formation are presented based upon the common physical characteristics of specific sites, and explanations are suggested for those occurrences. The underlying assumptions are that BMGs were created by subglacial abrasion and that they are pre-LGM landforms (see Section 5.3). In doing so, three crucial aspects are specifically addressed: the persistence of unidirectional glacier flow; the sparsity of BMGs; and BMG initiation on a land surface significantly different from that of today (antecedent conditions).

5.4.1 BMGs controlled by bedrock structure and lithology

The confinement of most BMGs to one lithology strongly indicates the susceptibility of that particular lithology to grooving, whether the original striators belonged to that specific rock type or were transported from adjacent lithologies up-ice. In this respect, it appears that primary bedrock control over BMG formation can be classified under two scenarios (Figure 5.4). Firstly, structure and lithology can exert a primary control on BMG location through the occurrence of features such as steps in tilted strata, surface-parallel synclinal folds, folded strata of different resistance and multiple surface exposures of intrusive dykes (Newton et al., 2018). Secondly, the juxtaposition of lithologies of contrasting resistance, for example at fault or lithological boundaries, can result in the passage of relatively hard striator blocks plucked from fault scarps or faulted zones which are then dragged across the softer bedrock located down-ice flow (Figure 3.7 in Chapter 3; see also Section 3.5.2).

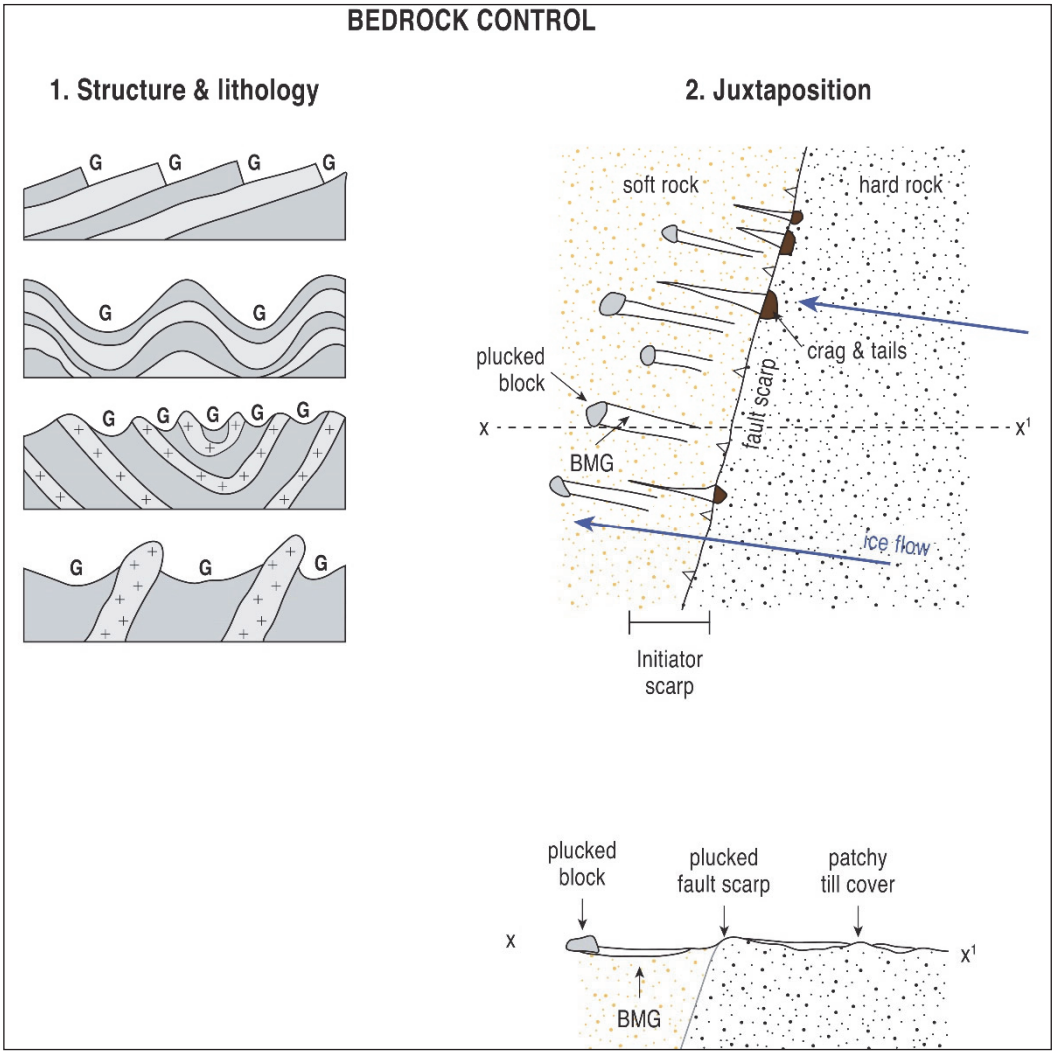

Figure 5.4. Two typical scenarios for bedrock control over BMG formation. Diagram 1: BMG development under structural control; image modified from Figure 10 in Newton et al., 2018. Diagram 2: BMG development under lithological control with boulders derived from hard lithology at a geological boundary (initiator scarp) subsequently dragged by the ice over softer bedrock, susceptible to abrasion. Diagram 2 was digitised by Chris Orton.

In the BMGs at Ullapool (Bradwell et al., 2008), Isle Royale (Zumberge, 1955), and Kaladar and Cape Smith Belt, Ungava, Canada (Krabbendam and Bradwell, 2011), the host bedrock comprises layered and tilted rock strata (see Table 2.1 in Chapter 2). The BMGs are parallel to strike and typically have a stepped, asymmetric profile. Lateral plucking during the last glaciation has been proposed as the most effective mechanism of erosion of these landforms (Zumberge, 1955; Krabbendam and Bradwell, 2011), although the age of BMG initiation is unknown. Considering the strong coincidence of linear major bedrock structure and BMG alignment, it has been suggested that the grooves were initiated through differential weathering and denudation, controlled by the variable rock characteristics under subaerial conditions, presumably both pre-glacial and interglacial (Newton et al., 2018). This produced surface debris, concentrated over relatively weaker strata, which was then

cleared by the later passage of ice while being used as abrading tools to further enhance groove profiles prior to fresh plucking (Krabbendam et al., 2016; Newton et al., 2018). Importantly, any changes in ice flow over time can initiate normal (i.e. non-lateral) plucking and hence widening of steps (grooves). Significantly, this type of bedrock control can be compared to the stepped, terraced profiles that occur in layered rocks in non-glaciated areas, where the debris resulting from the weathering of one layer ends up resting on the dip plane of the more resistant rock beneath (Aydin and Egeli, 2001; Nkpadobi et al., 2016).

The structure and lithology model depicted in Figure 5.4 is particularly applicable to layered rocks of varying lithology and resistance but is not directly applicable to settings like the Moine schists at Ullapool, Scotland, characterised by remarkable lithological uniformity (Peach et al., 1907). The formation of stepped slope profiles prior to and/or during the Quaternary glaciations in such settings is more likely to have been conditioned by other bedrock characteristics such as joint and fracture zone spacing (Krabbendam and Glasser 2011; Krabbendam and Bradwell, 2014). The low standard deviation (20 m) in the spacing of the Ullapool grooves (Table 3.3 in Chapter 3) supports this scenario, whereby the relatively consistent spacing of the BMGs could represent a perpetuation of the structural regularities in the bedrock at initiation time, which had previously been exposed and weakened by pre-glacial weathering (c.f. Turner, 1952; Wood, 1969; Fahey, 1981).

Examples of bedrock control through juxtaposition (Figure 5.4) include the BMGs of inner Scoresby Sund, in East Greenland (Funder, 1978; Newton et al., 2018), the Vikna continental shelf off Norway (Ottesen et al. 2002) and the Franklin Mountains in NWT, Canada (Smith, 1948; Newton et al. 2018). At Scoresby Sund and Vikna, more resistant gneissic or crystalline bedrock appears to have supplied the tools to groove the conglomerates or other sedimentary rocks, respectively, lying immediately down-ice flow, as suggested by the linear initiation zones situated a short distance down-flow from the lithological contact (Figures 3.2B and 3.11B in Chapter 3). The BMGs at Franklin Mountains initiate along a fault zone and are associated with crag-and-tails (Figure 3.7B in Chapter 3). It is plausible that a linear outcrop of dolostone may have supplied the bedrock blocks used by the westerly flowing ice to groove the softer limestones and Cretaceous sedimentary rocks located down flow. However, the rock outcrops that seed the crag-and-tails seem to be located on all rock types except those of Cretaceous age, suggesting that many grooves on Cretaceous lithologies might simply be the troughs between streamlined tails seeded at other lithological contacts up-flow. This complex juxtaposition of streamlined landforms is an example of an initiator scarp (Figure 5.4), a feature that is common in softer bedrock and

Quaternary materials in the Canadian plains region and may relate to scarps facing either down- or up-ice (Evans et al. 2021; see also Bukhari et al. 2021). Clear evidence for juxtaposition at a regional scale is presented by Bukhari et al. (2021), who illustrate the impacts of crystalline Shield lithologies in erodent layers that eroded BMGs in less resistant Palaeozoic limestones located down-ice.

5.4.2 BMGs related to antecedent conditions

Where the role of bedrock structure in BMG production is less convincing, it is likely that the pre-glacial landscape or antecedent conditions are critical to explaining BMG initiation. Here two models of antecedence are proposed that might explain BMG initiation in situations where they are likely of considerable age, namely, through bedrock structure removal, and through cannibalization and excavational deformation of regolith.

The model of bedrock structure removal implies that BMG initiation took place in bedrock that was characterised by strong linear structures and/or the juxtaposition of strata of variable resistance to erosion, in that this bedrock was subsequently removed through repeat glaciations (Figure 5.5). This hypothetical example depicts sub-horizontally bedded strata typically observed in Carboniferous cyclothems, whereby more coherent limestones and sandstones lie over mudstones in repeat sequences. When it is near surface, the regularly spaced joints within the limestone develop into widening karst systems and dry valleys between glaciations. The exploitation of these inherent weaknesses by subglacial quarrying, aided by displacement along mudstone decollement zones, leads to the production of mega-blocks, which are then dragged through the mudstone to form BMGs. The existence of such mega-blocks is well known in glacially streamlined bedrock terrain, prompting predictions that the appropriately-sized striators are consistent with the adjacent production of mega-striations (cf. Shulmeister, 1989; Dredge, 2000; Bukhari et al., 2021). The exploitation of linear structures, karst systems/collapsed caverns, and variably resistant strata on the pre-glacial land surface (stage 1 in Figure 5.5) may have led to the initiation of BMGs during early glaciations (e.g. stages 2 and 3 in Figure 5.5), whereby glacial erosion, and abrasion in particular, would have been increasingly more effective in incipient grooves. This would have been due to Nobles and Weertman-type heat fluxes (Figure 5.2A), concentrated meltwater erosion, and the development of debris-rich basal ice stripes or longitudinal “debris streams” (cf. Boulton 1975 and 1979; Bradwell et al. 2008; Catania et al. 2005). Additionally, the continued exposure of resistant strata during glacial erosion over time could have resulted in punctuated replenishment of erodents (mega-blocks) and thereby ensured the continuous deepening of multiple generations of BMGs through the

vertical stratigraphic sequence. Regularly spaced jointing, as might often occur in limestones, for example, would control the size and shape of both erodent mega-blocks and remnant crags, thus explaining the relative regularity in groove width and spacing with distance down-ice flow (see Section 5.2). The lowering of the land surface by glacial erosion over longer timescales (stage 4) eventually removed those rocks and structures that were critical to groove initiation, superimposing BMGs onto the underlying, basement bedrock. BMG development can then continue even within rock of homogeneous character, particularly during glaciations in which ice flow direction was similar to BMG orientation. This situation would be best satisfied in settings where BMGs occupy prominent topographic lows but elsewhere any discordant ice flow directions might result in groove edge plucking, and hence widening, or infilling and masking by till blanket.

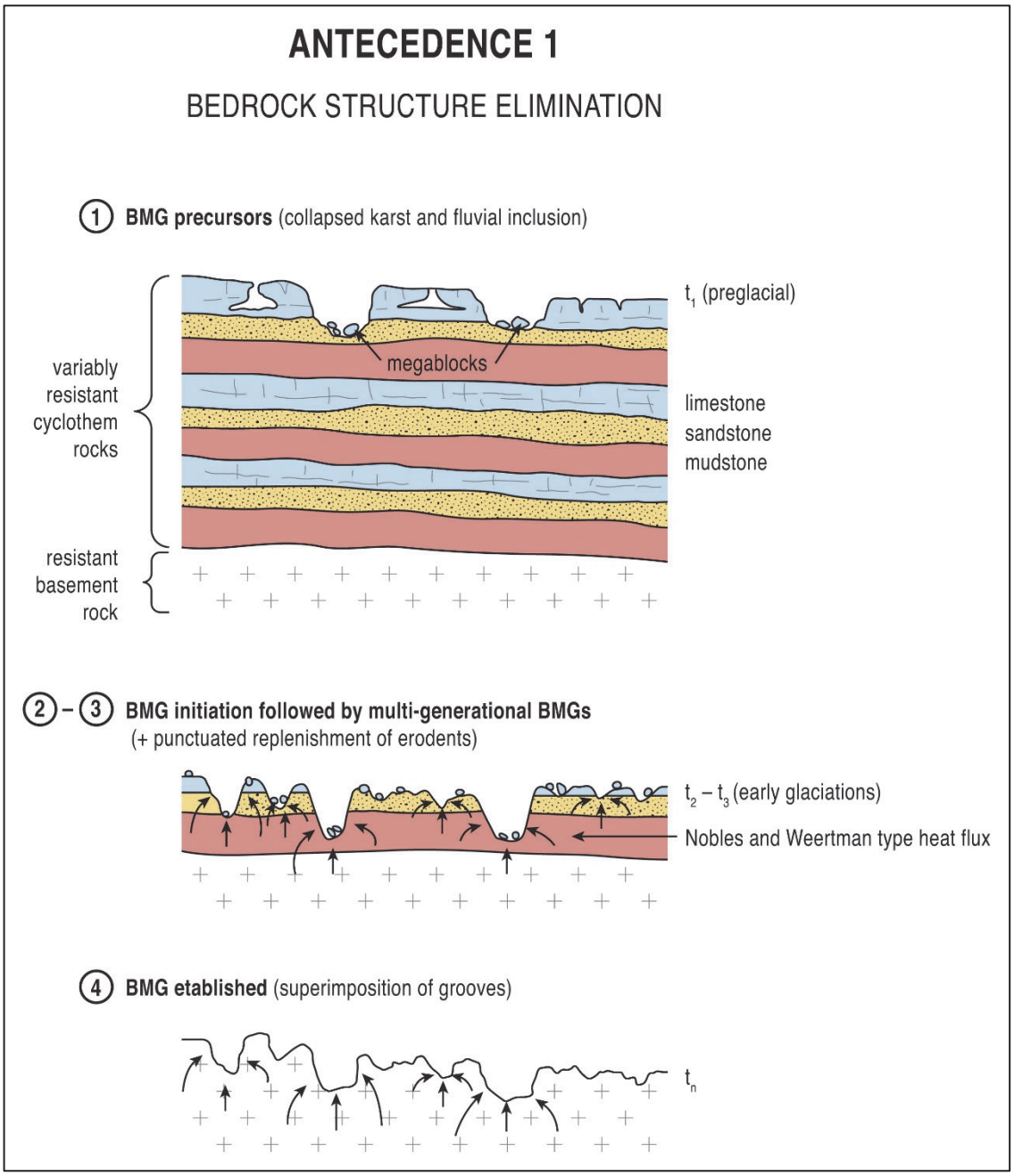

Figure 5.5. Hypothetical case for bedrock structure removal, based on strata with horizontally bedded sedimentary successions overlying more resistant basement rocks. Figure digitised by Chris Orton.

A similar form of bedrock structure removal can be hypothesized to explain the BMGs at Elphin, Scotland. These landforms occur in quartzite, which is a rock that is exceptionally resistant to abrasion (Krabbendam and Glasser, 2011) and to glacial erosion in general (Colgan et al., 2002; see Section 5.3.2). The rocks in the up-ice direction of the BMGs comprise mudstone, dolomite and limestone (Figure 5.6) and are therefore softer than the quartzite. Consequently, any abrading tools transported by glacier flow are unlikely to have been hard enough to initiate grooves. The solution to this problem may lie in the local geological stratigraphy in that the quartzite is positioned below a thinner and softer layer of sandstone, commonly referred to as the Fucoid beds, and these would have originally extended westwards over the quartzite (Figure 5.6). Hence, it is hypothesised that that the BMGs, which now occur exclusively in quartzite, could have been initiated in less resistant mudstone (Figure 5.7 part 1), by the agent(s) of erosion in operation at that time. Once established, the grooves continued to deepen until their floors reached the lithological boundary with the quartzite (Figure 5.7 part 2), superimposing the subglacial surface and its associated linear concentrations of glacial erosional processes onto the more resistant bedrock. The latest process of BMG erosion have been glacial, with plucking thought to have been particularly effective (Figure 3.4C and 3.4D in Chapter 3). As the BMg kept growing in depth and width, the Fucoid beds have gradually been removed by erosion (Figure 5.7 part 4). At present no in-situ Fuccoind bedrock has been observed in the field over the grooved area at Elphin. Furthermore, since the removal of the Fucoid beds, the geneal surface of the grooved terrain (i.e. the top of the ridges) has been lowered through erosion by several meters, as apparent in the stratigraphic sequence above the BMGs (Figure 5.6)

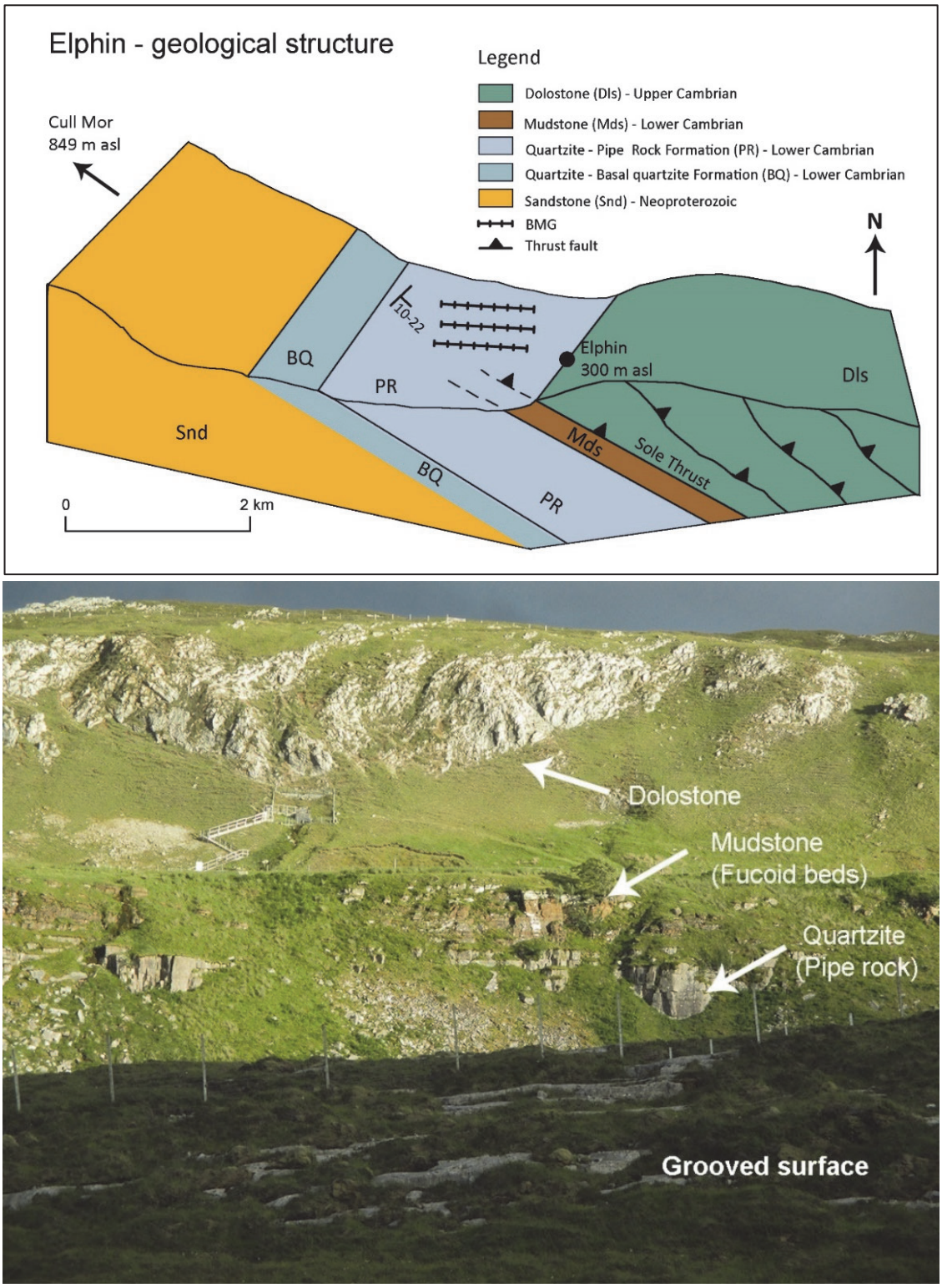

Figure 5.6. The bedrock structure and lithology in the area of the grooved terrain at Elphin; the diagram was redrawn and simplified from the geological map of the British Geological Survey (2008). Note the inferred extension of the mudstone layer (dark brown) over the Pipe Rock formation (PR) in which the BMGs currently occur. The photograph shows the geological stratigraphy above the grooved terrain. Note the present-day grooved surface of quartzite lying well below the mudstone layer (Fucoid beds) in which the BMGs may have been initiated.

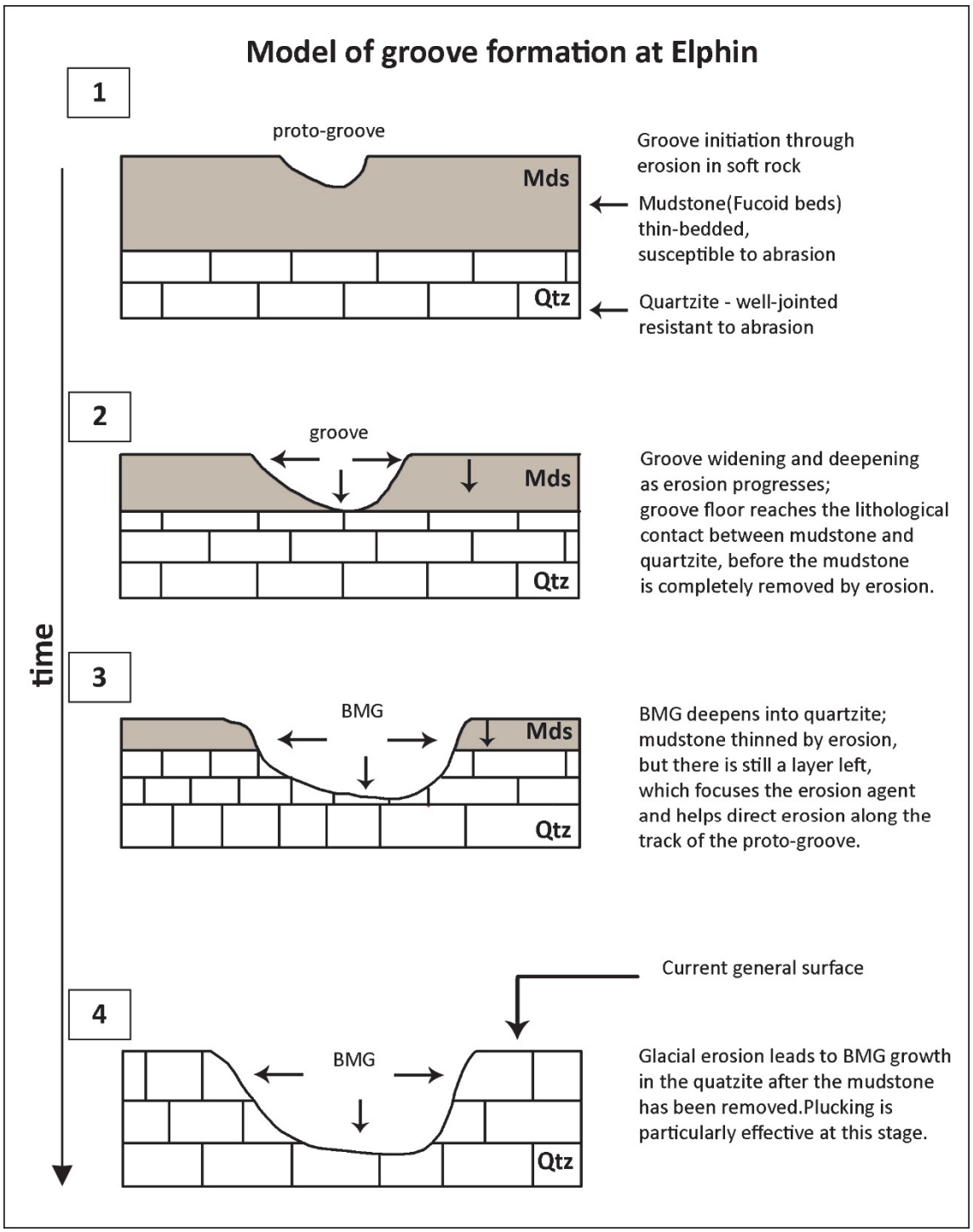

Figure 5.7. Schematic diagram of the antecedence hypothesis of BMG formation at Elphin, through bedrock structure removal.

5.4.3 The role of pre-Quaternary regolith in bedrock grooving

In order to appreciate the antecedent roles of cannibalization and excavational deformation of regolith, it is necessary to consider the first stages of erosion by an ice sheet advancing over a deeply weathered and regolith-covered terrain (Hall and Sugden, 1987; Lidmar-

Bergström, 1988; Nesbitt and Young, 1989; Patterson and Boerboom, 1999; Taylor and Eggleton, 2001; Bonow, 2005; Sugden and Jamieson, 2018; Jess et al., 2020; Figure 5.8). These have been summarised by Hall and Migoń (2010) as regolith stripping, tor demolition and block entrainment, and the removal of tor superstructures. Roches moutonnées then evolve from the glacial erosion and streamlining of exhumed tor stumps (Lindström, 1988) or through glacial adaptation of an etch surface. In areas that remained predominantly occupied by cold-based ice during the Quaternary glaciations, the remnants of the pre-glacial weathered regolith (saprolites) have survived (e.g. Setterholm and Morey, 1995; Hall and Sugden, 1987; Goodfellow, 2007; Figure 5.9), thus providing clear and valuable illustrations of the antecedent conditions for the development of early glacial erosional landforms.

The role of pre-Quaternary regolith/saprolites in the subglacial processes and dynamics of ice sheets has been demonstrated in an explanation of the mid-Pleistocene transition by Clark and Pollard (1998) and Roy et al. (2004). The mid-Pleistocene transition refers to a switch in ice sheet thicknesses at 0.8 Ma, at the time of change from 41 ka to 100 ka orbital forcing and is linked to the gradual stripping of saprolites and concomitant unroofing of unweathered bedrock. Applying this model of saprolite removal, Krabbendam and Bradwell (2014) propose that the regolith was stripped by early glaciations down to the pre-glacial weathering front, which presented an undulatory or rough subglacial surface because it was controlled by the pattern of fracture zones. This surface continued to reflect the undulatory nature of the weathering front even after numerous glaciations, because erosion was not particularly effective once the softer regolith had been removed (see also Sugden, 1976), with the exception of bedrock streamlining in areas of fast glacier flow (Bradwell, 2013; Krabbendam and Bradwell, 2014). Importantly, however, deep grooving would have been less likely in the more coherent bedrock than in the regolith/saprolite, so BMG initiation in the absence of bedrock structural and lithological control could conceivably have taken place in the regolith or lower saprolite (Figure 5.8).

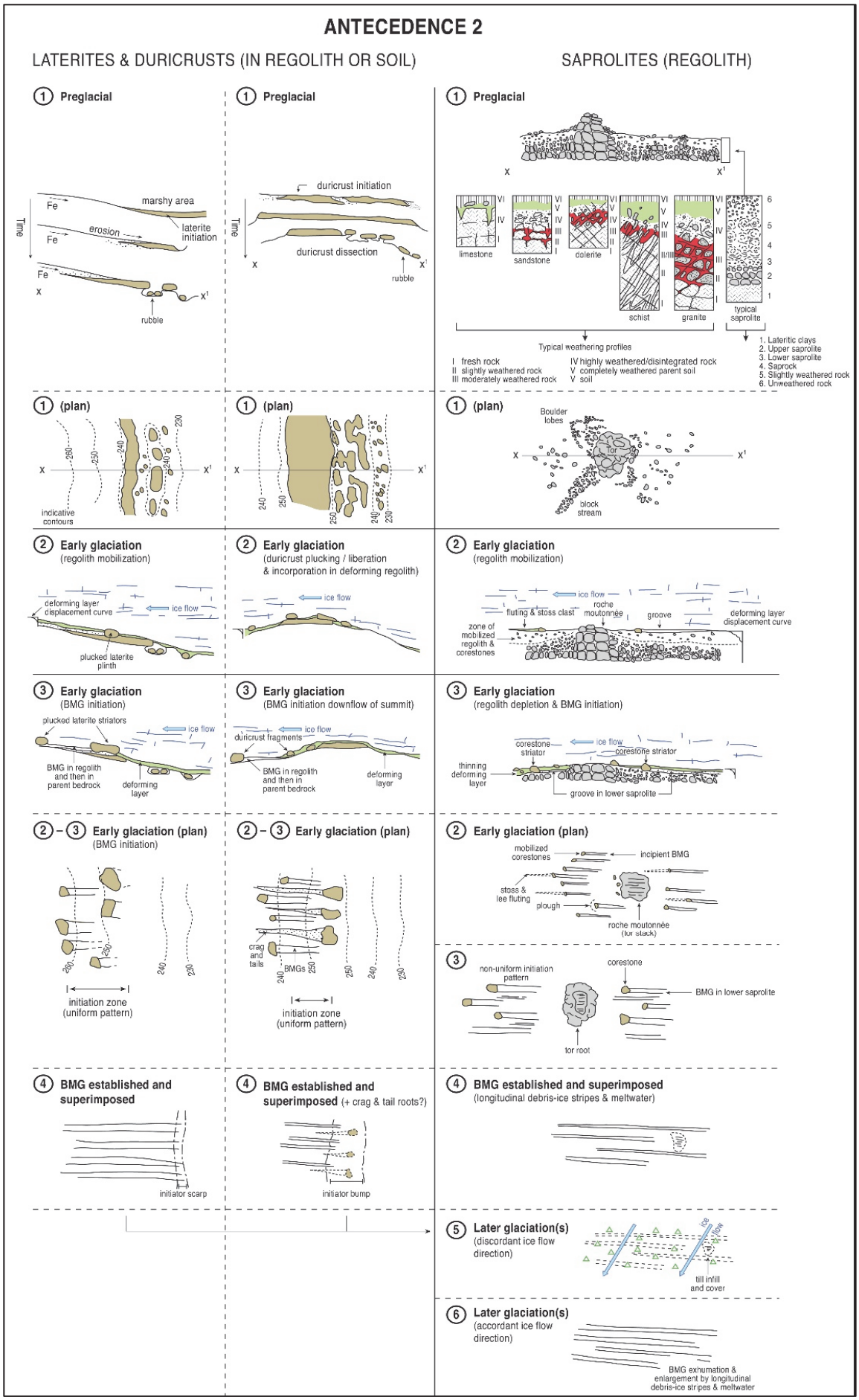
ANTECEDENCE 2
LATERITES & DURICRUSTS (IN REGOLITH OR SOIL)
SAPROLITES (REGOLITH)
1 Preglacial
marshy area
Fe
erosion
laterite initiation
Time
rubble
duricrust initiation
duricrust dissection
limestone
sandstone
dolerite
schist
granite
typical saprolite
Typical weathering profiles
I fresh rock
II slightly weathered rock
III moderately weathered rock
IV highly weathered/disintegrated rock
V completely weathered parent soil
VI soil
1. Lateritic clays
2. Upper saprolite
3. Lower saprolite
4. Saprock
5. Slightly weathered rock
6. Unweathered rock
1 (plan)
indicative contours
Boulder lobes
tor
block stream
2 Early glaciation
(regolith mobilization)
deforming layer displacement curve
ice flow
plucked laterite plinth
(duricrust plucking / liberation & incorporation in deforming regolith)
fluting & stoss clast
roche moutonnée
groove
deforming layer displacement curve
zone of mobilized regolith & corestones
3 Early glaciation
(BMG initiation)
plucked laterite striators
BMG in regolith and then in parent bedrock
deforming layer
(BMG initiation downflow of summit)
duricrust fragments
(regolith depletion & BMG initiation)
corestone striator
thinning deforming layer
groove in lower saprolite
2 – 3 Early glaciation (plan)
(BMG initiation)
initiation zone (uniform pattern)
crag and tails
BMGs
2 Early glaciation (plan)
mobilized corestones
incipient BMG
stoss & lee fluting
plough
roche moutonnée (lor stack)
non-uniform initiation pattern
corestone
BMG in lower saprolite
tor root
4 BMG established and superimposed
initiator scarp
(+ crag & tail roots?)
initiator bump
(longitudinal debris-ice stripes & meltwater)
5 Later glaciation(s)
(discordant ice flow direction)
till infill and cover
6 Later glaciation(s)
(accordant ice flow direction)
BMG exhumation & enlargement by longitudinal debris-ice stripes & meltwater

Figure 5.8. Hypothetical cases of antecedence in relation to pre-glacial land surfaces (after Thomas, 1974; Nesbitt and Young, 1989; Setterholm and Morey, 1995). Figure digitised by Chris Orton.

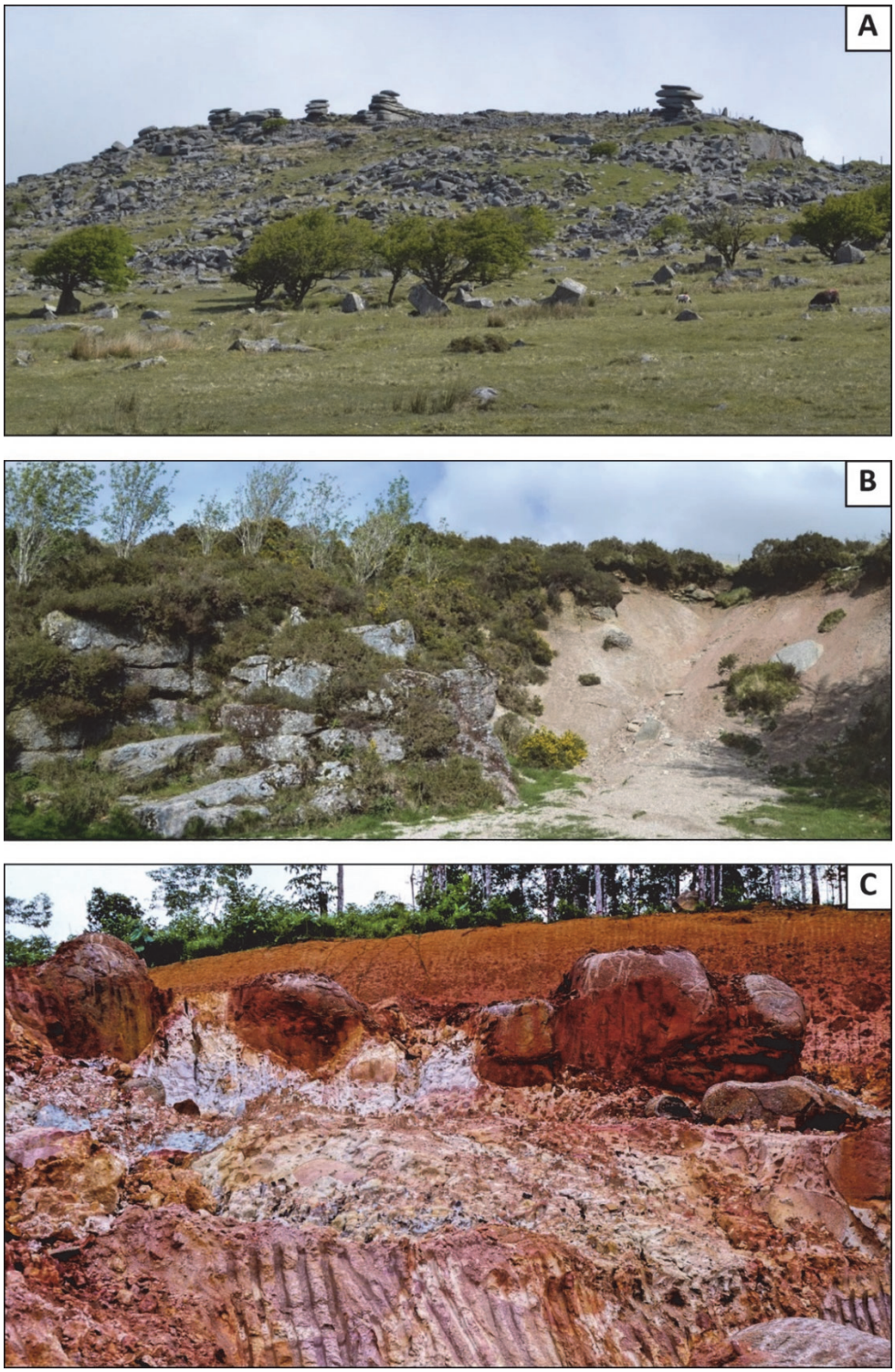

Figure 5.9. Examples representative of pre-glacial land surfaces. **A:** tor and blockfield-covered, etchplain-type land surface affected by Quaternary periglacial and permafrost processes, Rough Tor, Bodmin Moor (Photo: D.J.A. Evans); **B:** remnant granite saprolite with corestones and tor root, with upper stratigraphy recording Quaternary periglacial slope reworking, Two Bridges, Dartmoor (Photo: D.J.A. Evans); **C:** corestones in tropical saprolite, lateritic soil on granite, Malaysia (image used with permission from Fletcher and Baylis).

This mode of BMG production is conveyed in the new model (Figure 5.8) in four stages, the first of which presents the likely pre-glacial scenario for deeply weathered pre-Quaternary land surfaces. Depending on a combination of predominant climate, bedrock and near surface environmental conditions, the relatively hot climates of early Tertiary (early Palaeogene) times had created various types of regolith cover. Importantly, regolith comprise patchworks of coherent and incoherent materials characterised by either: a) relatively resistant cap rocks overlying less resistant parent soils (laterites and duricrusts); or b) saprolites developed by bedrock weathering profiles, in which relatively resistant corestones were distributed through a matrix of variably disaggregated and chemically weathered parent-rock material.

5.4.3.1 Laterites and duricrusts

Typical examples of the nature of pre-glacial laterites and duricrusts, both also known as cuirasse (Maignien 1966) and plinthites, are depicted in Figure 5.8 based upon modern exemplars summarised by Thomas (1974). They are lateritic soil horizons that become indurated once exposed by the stripping of soil and can occur on valley sides due to fluvial incision or over wide areas, to ultimately form mesas or tablelands. Plinthites, in particular, can become ironstone, a hard, iron-rich rock which can generate efficient striators once entrained into glacial flow. Fluvial dissection of laterite surfaces creates specific geomorphological features that ultimately constitute the Tertiary land surface inherited by Quaternary glacial processes. Thomas (1974) summarises the most significant of these as cliffs ('breakaways') that produce laterite rubble, bench or terrace-like features, and valley floor pavements of re-cemented laterite fragments.

The conceptual model in Figure 5.8 highlights the importance of laterite rubble and plucked fragments of plinthite within the precursor subglacial deforming layers created out of mobilized regolith during early glaciations. The importance of rubble terrain in subglacial mega-groove formation has been clearly illustrated by Bukhari et al. (2021) in relatively hard rocks and by Evans et al. (2021) in relatively soft lithologies (see Section 5.3.1). A similar origin for BMGs is envisaged in situations where laterite blocks were dragged through regolith and across underlying bedrock as deforming layers thinned due to excavational deformation (Hart et al., 1990; Eyles et al., 2016). This is effectively groove-ploughing *per se* (*sensu* Baligh, 1972; Boulton, 1975, 1976 and 1982; Boulton et al., 1979; Tulaczyk, 1999; Fischer et al., 2001; Evans et al., 2021), whereby the soft substratum is scored by erodent boulders (*sensu* Eyles et al., 2016). This is especially effective in settings where the parent bedrock is relatively soft, but BMGs could also be superimposed on

relatively resistant substrates via a similar process to that of bedrock structure removal outlined above (see Section 5.4.2). In plan view, the antecedent control of laterite landforms may be reflected in a uniform pattern of BMG emergence at a narrow initiation zone (Figure 5.8). Crag-and-tail features may also persist where tablelands were formerly located.

5.4.3.2 Saprolites

Pre-glacial saprolites, especially in crystalline lithologies, are typically associated with inselbergs (bornhardts and tors) that represent the more coherent areas within weathering bedrock profiles (Figure 5.9A). The various degrees of tor modification and preservation (Figure 5.9B) in glaciated terrain is widely acknowledged, as is the removal of surrounding regolith and the liberation of upper corestones by glacier ice (e.g. Johansson et al., 2001; André, 2004; Hall and Phillips, 2006; Phillips et al., 2006; Hall and Sugden, 2007; Hall and Migoń 2010). The model of saprolite control of BMG initiation proposed here (Figure 5.8) entertains the concept introduced above that upper regolith (saprolite) layers were mobilized by overriding ice during early glaciations to form precursor subglacial deforming layers. Importantly, it is also acknowledged that Pliocene/early Pleistocene environments were cold, and hence tor and saprolite landscapes were likely subject to periglacial and permafrost processes that would have arranged surface materials into patterned features such as boulder-fronted lobes and blockstreams (e.g. Clark, 1972; Evans et al., 2017; Ballantyne, 2018). This provides scope for pre-glacial alignment of the future striators, which may account for the relative regularity in the spacing of BMGs (see Section 5.2).

The vertical profiles of saprolites vary in depth depending on bedrock lithology but commonly display similar zonation, as depicted in stage 1 on Figure 5.8, based on the schemes of Nesbitt and Young (1989) and Setterholm and Morey (1995). Above the unaltered bedrock (Zone I) lie zones of slightly and moderately weathered bedrock (Zones II and III) or saprock. This passes upwards into highly weathered and disintegrated rock (Zone IV) and then completely weathered material (Zone V) capped by soil (Zone VI). The terms lower and upper saprolite are also used for Zones III to V, and regardless of bedrock type, contain vertically decreasing numbers and sizes of corestones, whose characteristics are related to the structures of the unweathered rock (Figure 5.9C). The soil and weathered material, and in some cases the upper saprolite, would be modified and re-arranged into periglacial and permafrost features during the onset of cold climate conditions. Later mobilization of this periglacially-altered zone as well as the upper saprolite by overriding ice would have created a subglacial deforming layer in which small corestones would act as typical till boulders, creating grooves, lodgement pavements and stoss-and-lee flutings

when they arrived at the ice–bedrock interface. Depletion of the deforming layer by excavational deformation would then have given rise to the liberation (effectively plucking) of larger corestones in the lower saprolite, turning tors into roches moutonnées (stages 2 and 3 in Figure 5.8). At this stage the large liberated corestones would plough through the lower saprolite, becoming erodents/mega-striators and thereby creating incipient BMGs. Because the erodents would be derived from tor superstructures, BMG initiation points would be relatively random in contrast to the initiator zones (scarps and bumps) created by disaggregating laterites and duricrusts (stages 3 and 4 in Figure 5.8).

This is consistent with descriptions of hard-bed landform assemblages in areas of palaeo-ice fast flow onset, often comprising a variety of forms in which BMGs occur interspersed with both positive, glacially-modified bedrock eminences (e.g. roches moutonnées, crag-and-tails, rock drumlins, ridges) as well as negative bedrock forms (e.g. bedrock channels, canyons, P-forms and depressions) (Evans, 1996; Lowe and Anderson, 2003; Roberts and Long, 2005; Roberts et al., 2010; Eyles, 2012; Bradwell, 2013; Krabbendam et al., 2016; Eyles et al., 2018). The lack of a coherent landsystem representative of fast-flow onset zones in bedrock terrain (see Sections 4.2.2 and 4.5.3 Chapter 4) could be due to the topographic variation derived from site-specific bedrock-weathering interactions, which are still reflected in the present-day landscape, despite general streamlining by repeat glaciations (Bonow et al., 2005). This presumed pre-glacial surface roughness is probably also reflected in the wide scatter of data on BMG length/width and length/depth relationships as derived from individual sites (see Figure 3.18 in Section 3.5.1, and Section 5.2). In the context of ice-stream landsystems, the often chaotic, non-standardised occurrence of hard-bed assemblages is a product of the inheritance of a weathered surface and partial, patchy subglacial erosion and contrasts with the more consistent, well-defined, and somewhat predictable, patterns of soft-bed landform assemblages of the middle and lower reaches of ice-stream landsystems, comprising long trains of MSGLs (Stokes and Clark, 2001; Spagnolo et al., 2014).

Important in the antecedent hypothesis, regardless of the exact mode of operation, is the persistence of BMGs once initiated (stages 4–6 in Figure 5.8). The presumption is that BMGs become superimposed and established on more coherent or resistant substrates, effectively becoming the focus of abrasion and meltwater drainage during later glaciations, especially when ice flow direction is accordant with BMG axes. Discordant ice flow would either pluck and thereby widen BMGs in cases of till depletion (excavational deformation) or infill and seal off BMGs in cases of till advection towards the site (constructional deformation). This

model of long-timescale evolution of BMGs implies that they are hybrid glacial erosional features.

A further long-timescale implication of the antecedent hypothesis is the likelihood that the optimum conditions for BMG initiation and development may migrate spatially over time. This concept was first introduced for the regional glaciation of North America by White (1972 and 1988) as the "arc of exhumation", or the westerly and southerly margin attained by the migration of the crystalline Shield–Palaeozoic boundary zone (S–PBz of Bukhari et al., 2021). This boundary represents the present position of repeated down-ice stripping of the Palaeozoic limestones from the crystalline basement, where over-deepened basins are presently located as well as most of the North American BMGs (see Figure 2 in Newton et al., 2018, and Figure 3.7B in Chapter 3). Migration of this boundary over time represents also the migration of an initiator zone for plucked mega-rafts (i.e. limestone blocks being dragged over fewer resistant strata) as well as the zone of increased grooving of Palaeozoic and younger rocks by crystalline blocks removed from the Shield to the north.

5.5 Conclusions

In order to explain the diagnostic physical characteristics and occurrences of BMGs, four hypothetical scenarios for BMG genesis are proposed that are consistent with the assumptions that BMGs are created by subglacial abrasion and, in situations where they are independent of bedrock controls, are of early-Quaternary age, possibly even pre-glacial. Also important are working assumptions that BMG initiation requires the impact of relatively soft substrates by harder mega-striators or mega-blocks that have been derived from nearby outcrops.

Two scenarios for BMG development relate to primary bedrock control. The first simply invokes subglacial abrasion in the accentuation of pre-existing, major bedrock structure and lithological changes, whereby steps in tilted layered rocks, flow-parallel folded strata of different resistance and multiple surface occurrence of intrusive dykes control the pattern of glacial erosion. In situations where such structural alignments are ice-flow parallel it is entirely conceivable that BMGs may be generated relatively quickly. The second relates to the juxtaposition of lithologies of contrasting resistance, especially at linear lithological boundaries or major faults. Here the passage of relatively hard striator blocks are plucked from fault scarps/fault zones, or derived from more resistant lithologies up-ice, and then

dragged across the softer bedrock located down-ice flow. Again, BMGs may be generated relatively quickly in such settings.

The occurrence of BMGs apparently unrelated to any structural control, warrants the consideration of precursor or antecedent conditions and the recognition that BMGs are likely of considerable antiquity. For these situations, two further scenarios are proposed that relate specifically to BMG initiation. The first is bedrock structure removal, which explains how BMGs were initiated in bedrock characterised by strong linear structures and/or the juxtaposition of strata of variable resistance to erosion, followed by removal of this bedrock by repeated glacial erosion. The second scenario invokes the cannibalization and excavational deformation of regolith, involving the mobilization of cemented cap rocks and corestones and their use as erodents in incipient and early subglacial deforming layers developed in pre-Quaternary regolith; this is effectively groove-ploughing *per se* (*sensu* Baligh, 1972; Boulton, 1975, 1976 and 1982; Boulton et al., 1979; Tulaczyk, 1999; Fischer et al., 2001; Evans et al., 2021). The involvement of pre-Quaternary regolith in BMG initiation addresses the second research question, related to an old, pre-glacial age for BMGs, in confirming a strong likelihood that at least some BMGs may date back to the beginning of the Quaternary.

Once grooves have been initiated, their accentuation and growth is ensured because they continue to be the focus of subglacial erosion processes, providing they are not sealed off from the ice–bed interface by accreting till. These processes include meltwater erosion as well as abrasion by flow-parallel, debris-rich basal ice stripes ("debris streams") controlled by alternating ice-bed interface conditions. Groove development could potentially be paused if sediment infill occurs as a result of changes in ice-flow direction. This would protect a BMG from removal by erosion and ensure a resumption of development once ice-flow once again became (sub-)parallel to the groove and the sediment infill was cleared. While erosion is operational, a groove will continue to deepen as long as the lowering of the intervening ridges takes place at a slower rate. In relation to the first research question (see Section 5.1), concerning the maintenance of consistent flow directions for long enough to allow a BMG to develop, this finding implies that, once established, BMGs may be difficult to erase, and also explains BMG preservation beneath ice sheets that underwent shifting flow directions.

The high preservation potential of individual BMGs is difficult to reconcile with their apparent scarcity relative to other subglacial landforms, the explanation of which forms the

subject of the third research question. If there was widespread scope for the existence of pre-cursor conditions necessary to BMG initiation, as the proposed genetic scenarios indicate, and the BMGs are able to survive shifting ice-flow directions throughout multiple glacial cycles, then why are there so few BMGs? The answer may lie in the expanding databases of geophysical evidence from the vast areas of streamlined glaciated terrain typically composed of unconsolidated sediment appearing to overlie grooved bedrock.

Finally, in terms of future research directions, a final question ought to be posed: how can antecedence be tested? Clearly in order for precursor mega-blocks/rafts, such as corestones and cemented cap rocks, to be viable as mega-striators they need to be observed *in situ*, preferably in positions related to stages 2 or 3 of the antecedence models. Some *in situ* exposures have been identified by Evans et al. (2021) in soft bedrock and sediment-cored MSGLs that have been grooved by bedrock mega-rafts, thereby demonstrating the groove-ploughing genesis of such landforms during the last glaciation. However, groove ploughing by the earliest subglacial deforming layers and erodents in pre-Quaternary regolith remains to be similarly verified and tested.

5.6 References

André, M.F., 2004. The geomorphic impact of glaciers as indicated by tors in North Sweden (Aurivaara, 68 N). *Geomorphology*, *57*(3-4), pp.403-421.

Alley, R.B., 2000. Continuity comes first: recent progress in understanding subglacial deformation. *Geological Society, London, Special Publications*, *176*(1), pp.171-179.

Aydin, A. and Egeli, I., 2001. Stability of slopes cut in metasedimentary saprolites in Hong Kong. *Bulletin of Engineering Geology and the Environment*, *60*(4), pp.315-319.

Baligh, M.M., 1972. *Applications of plasticity theory to selected problems in soil mechanics* (Doctoral dissertation, California Institute of Technology).

Ballantyne, C.K., 2018. *Periglacial geomorphology*. John Wiley & Sons, Chichester.

Benn, D.I. and Evans, D.J.A. 2006. Subglacial megafloods: outrageous hypothesis or just outrageous. In: Knight, P.G. (ed.), *Glacier Science and Environmental Change.* Blackwell, London, pp.42-46.

Bonow, J.M., 2005. Re-exposed basement landforms in the Disko region, West Greenland—disregarded data for estimation of glacial erosion and uplift modelling. *Geomorphology*, *72*(1-4), pp.106-127.

Bougamont, M., Tulaczyk, S. and Joughin, I., 2003a. Numerical investigations of the slow-down of Whillans Ice Stream, West Antarctica: is it shutting down like Ice Stream C?. *Annals of Glaciology*, *37*, pp.239-246.

Bougamont, M., Tulaczyk, S. and Joughin, I., 2003b. Response of subglacial sediments to basal freeze-on 2. Application in numerical modeling of the recent stoppage of Ice Stream C, West Antarctica. *Journal of Geophysical Research: Solid Earth*, *108*(B4).

Boulton, G.S., 1976. The origin of glacially fluted surfaces-observations and theory. *Journal of Glaciology*, *17*(76), pp.287-309.

Boulton, G.S., 1979. Processes of glacier erosion on different substrata. *Journal of glaciology*, *23*(89), pp.15-38.

Boulton, G.S., 1982. Subglacial processes and the development of glacial bedforms. In: Davidson-Arnott, R., Nickling, W. and Fahey, B.D. (eds.), *Research in Glacial, Glacio-fluvial and Glacio-lacustrine Systems*. Geobooks, Norwich, pp. 1-31.

Boulton, G.S. and Clark, C.D., 1990. A highly mobile Laurentide ice sheet revealed by satellite images of glacial lineations. *Nature*, *346*(6287), pp.813-817.

Boulton, G.S., Morris, E.M., Armstrong, A.A. and Thomas, A., 1979. Direct measurement of stress at the base of a glacier. *Journal of Glaciology*, *22*(86), pp.3-24.

Boulton, G.S., 1975. Processes and patterns of subglacial sedimentation: a theoretical approach. In: Wright, A.E. and Moseley, F. (eds.), *Ice ages: ancient and modern*. Seel House Press Liverpool, pp. 7-42.

British Geological Survey (BGS), 2008. Ullapool. Scotland Sheet 101E. Bedrock 1:50,000 Geology Series. British Geological Survey, Keyworth, Nottingham, UK

Bradwell, T., 2005. Bedrock megagrooves in Assynt, NW Scotland. *Geomorphology*, *65*(3-4), pp.195-204.

Bradwell, T., 2013. Identifying palaeo-ice-stream tributaries on hard beds: Mapping glacial bedforms and erosion zones in NW Scotland. *Geomorphology*, *201*, pp.397-414.

Bradwell, T., Stoker, M. and Krabbendam, M., 2008. Megagrooves and streamlined bedrock in NW Scotland: the role of ice streams in landscape evolution. *Geomorphology*, *97*(1-2), pp.135-156.

Bukhari, S., Eyles, N., Sookhan, S., Mulligan, R., Paulen, R., Krabbendam, M. and Putkinen, N., 2021. Regional subglacial quarrying and abrasion below hard-bedded palaeo-ice streams crossing the Shield–Palaeozoic boundary of central Canada: the importance of substrate control. *Boreas 50*(3), pp.781-805.

Carney, F., 1910. Glacial erosion on Kelleys Island, Ohio. *Geologica. Society of America Bulletin*, *46*, pp.241-283.

Catania, G.A., Conway, H., Raymond, C.F. and Scambos, T.A., 2005. Surface morphology and internal layer stratigraphy in the downstream end of Kamb Ice Stream, West Antarctica. *Journal of Glaciology*, *51*(174), pp.423-431.

Chamberlin, TC. 1888. The Rock-Scorings of the Great Ice Invasions. *US Geological Survey, 7th Annual Report*, 155–254.

Christoffersen, P. and Tulaczyk, S., 2003a. Response of subglacial sediments to basal freeze-on 1. Theory and comparison to observations from beneath the West Antarctic Ice Sheet. *Journal of Geophysical Research: Solid Earth*, *108*(B4), pp.2222

Christoffersen, P. and Tulaczyk, S., 2003b. Thermodynamics of basal freeze-on: predicting basal and subglacial signatures of stopped ice streams and interstream ridges. *Annals of Glaciology*, *36*, pp.233-243.

Christoffersen, P., Tulaczyk, S., Carsey, F.D. and Behar, A.E., 2006. A quantitative framework for interpretation of basal ice facies formed by ice accretion over subglacial sediment. *Journal of Geophysical Research: Earth Surface*, *111*(F1), F01017.

Clark, C.D., 1993. Mega-scale glacial lineations and cross-cutting ice-flow landforms. *Earth Surface Processes and Landforms*, *18*(1), pp.1-29.

Clark, C.D., 1994. Large-scale ice-moulding: a discussion of genesis and glaciological significance. *Sedimentary Geology*, *91*(1-4), pp.253-268.

Clark, C.D., 1999. Glaciodynamic context of subglacial bedform generation and preservation. *Annals of Glaciology*, *28*, pp.23-32.

Clark, P.U. and Pollard, D., 1998. Origin of the middle Pleistocene transition by ice sheet erosion of regolith. *Paleoceanography*, *13*(1), pp.1-9.

Clark, R., 1972. Periglacial landforms and landscapes in the Falkland Islands. *Biuletyn Peryglacjalny*, *21*, pp.33-50.

Clarke, G.K., Leverington, D.W., Teller, J.T., Dyke, A.S. and Marshall, S.J., 2005. Fresh arguments against the Shaw megaflood hypothesis. A reply to comments by David Sharpe on" Paleohydraulics of the last outburst flood from glacial Lake Agassiz and the 8200 BP cold event". *Quaternary Science Reviews, 24,* pp.1533-1541.

Colgan, P.M., Bierman, P.R., Mickelson, D.M. and Caffee, M., 2002. Variation in glacial erosion near the southern margin of the Laurentide Ice Sheet, south-central Wisconsin, USA: Implications for cosmogenic dating of glacial terrains. *Geological Society of America Bulletin*, *114*(12), pp.1581-1591.

Dahl, R., 1965. Plastically sculptured detail forms on rock surfaces in northern Nordland, Norway. *Geografiska Annaler 47*(2), pp.83-140.

Dowdeswell, J.A., Ottesen, D. and Rise, L., 2006. Flow switching and large-scale deposition by ice streams draining former ice sheets. *Geology*, *34*(4), pp.313-316.

Dredge, L.A., 2000. Carbonate dispersal trains, secondary till plumes, and ice streams in the west Foxe Sector, Laurentide Ice Sheet. *Boreas*, *29*(2), pp.144-156.

Drews, R., Schannwell, C., Ehlers, T.A., Gladstone, R., Pattyn, F. and Matsuoka, K., 2020. Atmospheric and oceanographic signatures in the ice shelf channel morphology of Roi Baudouin Ice Shelf, East Antarctica, inferred from radar data. *Journal of Geophysical Research: Earth Surface*, *125*(7), pp.2020JF005587.

Dühnforth, M., Anderson, R.S., Ward, D. and Stock, G.M., 2010. Bedrock fracture control of glacial erosion processes and rates. *Geology*, *38*(5), pp.423-426.

Evans, D.J.A., Rea, B.R. and Benn, D.I., 1998. Subglacial deformation and bedrock plucking in areas of hard bedrock. *Glacial Geology and Geomorphology*.

Evans, D.J.A., Atkinson, N. and Phillips, E., 2020. Glacial geomorphology of the Neutral Hills Uplands, southeast Alberta, Canada: The process-form imprints of dynamic ice streams and surging ice lobes. *Geomorphology*, *350*, p.106910.

Evans, D.J.A., Kalyan, R. and Orton, C., 2017. Periglacial geomorphology of summit tors on Bodmin Moor, Cornwall, SW England. *Journal of Maps*, *13*(2), pp.342-349.

Evans, D.J.A., Phillips, E.R. and Atkinson, N., 2021. Glacitectonic rafts and their role in the generation of Quaternary subglacial bedforms and deposits. *Quaternary Research*, pp.1-35.

Evans, I.S., 1996. Abraded rock landforms (whalebacks) developed under ice streams in mountain areas. *Annals of Glaciology*, *22*, pp.9-16.

Eyles, N., 2006. The role of meltwater in glacial processes. *Sedimentary Geology*, *190*(1-4), pp.257-268.

Eyles, N., 2012. Rock drumlins and megaflutes of the Niagara Escarpment, Ontario, Canada: a hard bed landform assemblage cut by the Saginaw–Huron Ice Stream. *Quaternary Science Reviews*, *55*, pp.34-49.

Eyles, N., Putkinen, N., Sookhan, S. and Arbelaez-Moreno, L., 2016. Erosional origin of drumlins and megaridges. *Sedimentary Geology*, *338*, pp.2-23.

Eyles, N., Moreno, L.A. and Sookhan, S., 2018. Ice streams of the Late Wisconsin Cordilleran Ice Sheet in western North America. *Quaternary Science Reviews*, *179*, pp.87-122.

Fahey, B.D., 1981. Origin and age of upland schist tors in Central Otago, New Zealand. *New Zealand Journal of Geology and Geophysics*, *24*(3), pp.399-413.

Finlayson, A., Fabel, D., Bradwell, T. and Sugden, D., 2014. Growth and decay of a marine terminating sector of the last British–Irish Ice Sheet: a geomorphological reconstruction. *Quaternary Science Reviews*, *83*, pp.28-45.

Fischer, U.H., Porter, P.R., Schuler, T., Evans, A.J. and Gudmundsson, G.H., 2001. Hydraulic and mechanical properties of glacial sediments beneath Unteraargletscher, Switzerland: implications for glacier basal motion. *Hydrological Processes*, *15*(18), pp.3525-3540.

Funder, S., 1978. Glacial flutings in bedrock, an observation in East Greenland. *Bulletin of the Geological Society of Denmark*, *27*, pp.9-13.

Geikie, J., 1894. *The Great Ice Age and its relation to the antiquity of man*. E. Stanford, London.

Gjessing J. 1965. On 'Plastic Scouring' and 'Subglacial Erosion. *Norsk Geografisk Tidsskrift* 20: 1-37

Goldthwait RP. 1979. Giant Grooves Made by Concentrated Basal Ice Streams. *Journal of Glaciology* 23: 29 - 307.

Goodfellow, B.W., 2007. Relict non-glacial surfaces in formerly glaciated landscapes. *Earth-Science Reviews*, *80*(1-2), pp.47-73.

Graham, A.G.C., Lonergan, L. and Stoker, M.S., 2007. Evidence for Late Pleistocene ice stream activity in the Witch Ground Basin, central North Sea, from 3D seismic reflection data. *Quaternary Science Reviews*, *26*(5-6), pp.627-643.

Gray, J.M., 1981. p-forms from the Isle of Mull. *Scottish Journal of Geology*, *17*(1), pp.39-47.

Glasser, N.F. and Hall, A.M., 1997. Calculating Quaternary glacial erosion rates in northeast Scotland. *Geomorphology*, *20*(1-2), pp.29-48.

Hall, A.M., Krabbendam, M., van Boeckel, M., Goodfellow, B.W., Hättestrand, C., Heyman, J., Palamakumbura, R.N., Stroeven, A.P. and Näslund, J.O., 2020. Glacial ripping: geomorphological evidence from Sweden for a new process of glacial erosion. *Geografiska Annaler: Series A, Physical Geography*, *102*(4), pp.333-353.

Hall, A.M. and Migoń, P., 2010. The first stages of erosion by ice sheets: evidence from central Europe. *Geomorphology*, *123*(3-4), pp.349-363.

Hall, A.M. and Phillips, W.M., 2006. Weathering pits as indicators of the relative age of granite surfaces in the Cairngorm Mountains, Scotland. *Geografiska Annaler: Series A, Physical Geography*, *88*(2), pp.135-150.

Hall, A.M. and Sugden, D.E., 1987. Limited modification of mid-latitude landscapes by ice sheets: The case of northeast Scotland. *Earth Surface Processes and Landforms*, *12*(5), pp.531-542.

Hall, A.M. and Sugden, D.E., 2007. The significance of tors in glaciated lands: a view from the British Isles. *Du continent au bassin versant: theories et practiques en géographie physique (Hommage au Professeur Alain Godard). Presses Universitaires Blaise-Pascal, Lyon, France*, pp.301-311.

Hall, A.M., Ebert, K. and Hättestrand, C., 2013. Pre-glacial landform inheritance in a glaciated shield landscape. *Geografiska Annaler: Series A, Physical Geography*, *95*(1), pp.33-49.

Hallet, B., 1996. Glacial quarrying: A simple theoretical model. *Annals of Glaciology*, *22*, pp.1-8.

Hart, J.K., Hindmarsh, R.C. and Boulton, G.S., 1990. Styles of subglacial glaciotectonic deformation within the context of the Anglian ice-sheet. *Earth Surface Processes and Landforms*, *15*(3), pp.227-241.

Heikkinen, O. and Tikkanen, M., 1989. Drumlins and flutings in Finland: their relationships to ice movement and to each other. *Sedimentary geology*, *62*(2-4), pp.349-355.

Iverson, N.R., 1990. Laboratory simulations of glacial abrasion: comparison with theory. *Journal of Glaciology*, *36*(124), pp.304-314.

Iverson, N.R., 1995. Processes of erosion. In: Menzies, J. (ed.), *Modern Glacial Environments: Processes, Dynamics and Sediments.* Butterworth-Heinemann, Oxford, pp.241-260.

Iverson, N.R., 2000. Sediment entrainment by a soft-bedded glacier: a model based on regelation into the bed. *Earth Surface Processes and Landforms 25*(8), pp.881-893.

Iverson, N.R., 2010. Shear resistance and continuity of subglacial till: hydrology rules. *Journal of Glaciology*, *56*(200), pp.1104-1114.

Jeofry, H., Ross, N., Le Brocq, A., Graham, A.G., Li, J., Gogineni, P., Morlighem, M., Jordan, T. and Siegert, M.J., 2018. Hard rock landforms generate 130 km ice shelf channels through water focusing in basal corrugations. *Nature communications*, *9*(1), pp.1-9.

Jess, S., Stephenson, R., Roberts, D.H. and Brown, R., 2019. Differential erosion of a Mesozoic rift flank: Establishing the source of topography across Karrat, central West Greenland. *Geomorphology*, *334*, pp.138-150.

Johansson, M., Olvmo, M. and Lidmar-Bergström, K., 2001. Inherited landforms and glacial impact of different palaeosurfaces in southwest Sweden. *Geografiska Annaler: Series A, Physical Geography*, *83*(1-2), pp.67-89.

Kor, P.S.G., Shaw, J. and Sharpe, D.R., 1991. Erosion of bedrock by subglacial meltwater, Georgian Bay, Ontario: a regional view. *Canadian Journal of Earth Sciences*, *28*(4), pp.623-642.

Krabbendam, M. and Bradwell, T., 2011. Lateral plucking as a mechanism for elongate erosional glacial bedforms: explaining megagrooves in Britain and Canada. *Earth Surface Processes and Landforms*, *36*(10), pp.1335-1349.

Krabbendam, M. and Bradwell, T., 2014. Quaternary evolution of glaciated gneiss terrains: pre-glacial weathering vs. glacial erosion. *Quaternary Science Reviews*, *95*, pp.20-42.

Krabbendam, M. and Glasser, N.F., 2011. Glacial erosion and bedrock properties in NW Scotland: abrasion and plucking, hardness and joint spacing. *Geomorphology*, *130*(3-4), pp.374-383.

Krabbendam, M., Eyles, N., Putkinen, N., Bradwell, T. and Arbelaez-Moreno, L., 2016. Streamlined hard beds formed by palaeo-ice streams: A review. *Sedimentary Geology*, *338*, pp.24-50.

Laverdière, C., Guimont, P. and Pharand, M., 1979. Marks and forms on glacier beds: formation and classification. *Journal of Glaciology*, *23*(89), pp.414-416.

Laverdière, C., Guimont, P. and Dionne, J.C., 1985. Les formes et les marques de l'érosion glaciaire du plancher rocheux: signification, terminologie, illustration. *Palaeogeography, Palaeoclimatology, Palaeoecology*, *51*(1-4), pp.365-387.

Le Brocq, A.M., Ross, N., Griggs, J.A., Bingham, R.G., Corr, H.F., Ferraccioli, F., Jenkins, A., Jordan, T.A., Payne, A.J., Rippin, D.M. and Siegert, M.J., 2013. Evidence from ice shelves for channelized meltwater flow beneath the Antarctic Ice Sheet. *Nature Geoscience*, *6*(11), pp.945-948.

Lidmar-Bergström, K., 1988. Denudation surfaces of a shield area in south Sweden. *Geografiska Annaler: Series A, Physical Geography*, *70*(4), pp.337-350.

Lidmar-Bergström, K., 1989. Exhumed Cretaceous landforms in south Sweden. *Zeitschrift für Geomorphologie. Supplementband*, *72*, pp.21-40.

Lidmar-Bergström, K., 1995. Relief and saprolites through time on the Baltic Shield. *Geomorphology*, *12*(1), pp.45-61.

Lidmar-Bergström, K., 1997. A long-term perspective on glacial erosion. *Earth Surface Processes and Landforms 22*(3), pp.297-306.

Lidmar-Bergström, K., Olsson, S. and Olvmo, M., 1997. Palaeosurfaces and associated saprolites in southern Sweden. *Geological Society, London, Special Publications*, *120*(1), pp.95-124.

Lindström, E., 1988. Are roches moutonnées mainly pre-glacial forms?. *Geografiska Annaler: Series A, Physical Geography*, *70*(4), pp.323-331.

Lister, H., Pendlington, A. and Chorlton, J., 1968. Laboratory experiments on abrasion of sandstones by ice. *Snow and Ice. Reports and Discussions*, pp.98-106.

Livingstone, S.J., Ó Cofaigh, C., Stokes, C.R., Hillenbrand, C.D., Vieli, A. and Jamieson, S.S.R., 2012. Antarctic palaeo-ice streams. *Earth-Science Reviews*, *111*(1-2), pp.90-128.

Lowe, A.L. and Anderson, J.B., 2003. Evidence for abundant subglacial meltwater beneath the paleo-ice sheet in Pine Island Bay, Antarctica. *Journal of Glaciology*, *49*(164), pp.125-138.

Maignien, R., 1966. Induration des horizons des sols ferrallitiques. *Cahiers ORSTOM. Série Pédologie*, *4*(4), pp.29-31.

Munro-Stasiuk, M.J., Fisher, T.G. and Nitzsche, C.R., 2005. The origin of the western Lake Erie grooves, Ohio: implications for reconstructing the subglacial hydrology of the Great Lakes sector of the Laurentide Ice Sheet. *Quaternary Science Reviews*, *24*(22), pp.2392-2409.

Nesbitt, H.W. and Young, G.M., 1989. Formation and diagenesis of weathering profiles. *The Journal of Geology*, *97*(2), pp.129-147.

Newton, M., Evans, D.J.A., Roberts, D.H. and Stokes, C.R., 2018. Bedrock mega-grooves in glaciated terrain: A review. *Earth-Science Reviews*, *185*, pp.57-79.

Nkpadobi, J.I., Raj, J.K. and Ng T.F., 2015. Influence of discontinuities on the stability of cut slopes in weathered meta-sedimentary rocks, *Geomechanics and Geoengineering*, *10*(4), 290–302.

Nobles, L.H., Weertman, J., 1971. Influence of irregularities of the bed of an ice sheet on deposition rate of till. In: Goldthwait, R.P. (Ed.), Till, a Symposium. Ohio State Univ.Press, Columbus, Ohio, pp. 117–126.

Ó Cofaigh, C., Pudsey, C.J., Dowdeswell, J.A. and Morris, P., 2002. Evolution of subglacial bedforms along a paleo-ice stream, Antarctic Peninsula continental shelf. *Geophysical Research Letters*, *29*(8), pp.41-1.

Ó Cofaigh, C., Evans, D.J.A. and Smith, I.R., 2010a. Large-scale reorganization and sedimentation of terrestrial ice streams during late Wisconsinan Laurentide Ice Sheet deglaciation. Geological Society of America *Bulletin*, *122*(5-6), pp.743-756.

Ó Cofaigh, C., Dowdeswell, J.A., King, E.C., Anderson, J.B., Clark, C.D., Evans, D.J.A., Evans, J., Hindmarsh, R.C., Larter, R.D. and Stokes, C.R., 2010b. Comment on Shaw J., Pugin, A. and Young, R. (2008): "A meltwater origin for Antarctic shelf bedforms with special attention to megalineations", Geomorphology 102, 364–375. *Geomorphology*, *117*(1), p.195.

Olvmo, M. and Johansson, M., 2002. The significance of rock structure, lithology and pre-glacial deep weathering for the shape of intermediate-scale glacial erosional landforms. *Earth Surface Processes and Landforms*, *27*(3), pp.251-268.

Olvmo, M., Lidmar-Bergström, K. and Lindberg, G., 1999. The glacial impact on an exhumed sub-Mesozoic etch surface in southwestern Sweden. *Annals of Glaciology*, *28*, pp.153-160.

Olvmo, M., Lidmar-Bergström, K., Ericson, K. and Bonow, J.M., 2005. Saprolite remnants as indicators of pre-glacial landform genesis in southeast sweden. *Geografiska Annaler: Series A, Physical Geography*, *87*(3), pp.447-460.

Ottesen, D., Dowdeswell, J.A., Rise, L., Rokoengen, K. and Henriksen, S., 2002. Large-scale morphological evidence for past ice-stream flow on the mid-Norwegian continental margin. *Geological Society, London, Special Publications 203*(1), pp.245-258.

Patterson, C.J. and Boerboom, T.J., 1999. The significance of pre-existing deeply weathered crystalline rock in interpreting the effects of glaciation in the Minnesota River valley, USA. *Annals of Glaciology*, *28*, pp.53-58.

Peach, B.N., Horne, J., Gunn, W., Clough, C.T., Hinxman, L.W., Teall, J.J.H., 1907. The Geological Structure of the North-West Highlands of Scotland. Memoir of the Geological Survey of Great Britain, HMSO, Glasgow. 668 pp.

Phillips, W.M., Hall, A.M., Mottram, R., Fifield, L.K. and Sugden, D.E., 2006. Cosmogenic 10Be and 26Al exposure ages of tors and erratics, Cairngorm Mountains, Scotland: timescales for the development of a classic landscape of selective linear glacial erosion. *Geomorphology*, *73*(3-4), pp.222-245.

Rafaelsen, B., Andreassen, K., Kuilman, L.W., Lebesbye, E., Hogstad, K. and Midtbø, M., 2002. Geomorphology of buried glacigenic horizons in the Barents Sea from three-dimensional seismic data. *Geological Society, London, Special Publications*, *203*(1), pp.259-276.

Rea, B.R., 1996. A note on the experimental production of a mechanically polished surface within striations. *Glacial Geology and Geomorphology*.

Rea, B.R., Evans, D.J.A., Dixon, T.S. and Whalley, W.B., 2000. Contemporaneous, localized, basal ice-flow variations: implications for bedrock erosion and the origin of p-forms. *Journal of Glaciology*, *46*(154), pp.470-476.

Riedel, M., Dallimore, S., Wamsteeker, M., Taylor, G., King, E.L., Rohr, K.M., Hong, J.K. and Jin, Y.K., 2021. Mega-scale glacial lineations formed by ice shelf grounding in the Canadian Beaufort Sea during multiple glaciations. *Earth Surface Processes and Landforms*, *46,* pp.1568-1585.

Roberts, D.H. and Long, A.J., 2005. Streamlined bedrock terrain and fast ice flow, Jakobshavns Isbrae, West Greenland: implications for ice stream and ice sheet dynamics. *Boreas*, *34*(1), pp.25-42.

Roberts, D.H., Long, A.J., Davies, B.J., Simpson, M.J. and Schnabel, C., 2010. Ice stream influence on west Greenland ice sheet dynamics during the last glacial maximum. *Journal of Quaternary Science*, *25*(6), pp.850-864.

Roy, M., Clark, P.U., Raisbeck, G.M. and Yiou, F., 2004. Geochemical constraints on the regolith hypothesis for the middle Pleistocene transition. *Earth and Planetary Science Letters*, *227*(3-4), pp.281-296.

Salzmann, U., Williams, M., Haywood, A.M., Johnson, A.L., Kender, S. and Zalasiewicz, J., 2011. Climate and environment of a Pliocene warm world. *Palaeogeography, Palaeoclimatology, Palaeoecology*, *309*(1-2), pp.1-8.

Setterholm, D.R. and Morey, G.B., 1995. *An extensive pre-Cretaceous weathering profile in east-central and southwestern Minnesota* (No. 1989). US Department of the Interior, US Geological Survey.

Sharpe, D.R. and Shaw, J., 1989. Erosion of bedrock by subglacial meltwater, Cantley, Quebec. *Geological Society of America Bulletin*, *101*(8), pp.1011-1020.

Shaw, J. and Sharpe, D.R., 1987. Drumlin formation by subglacial meltwater erosion. *Canadian Journal of Earth Sciences*, *24*(11), pp.2316-2322.

Shaw, J. and Gilbert, R., 1990. Evidence for large-scale subglacial meltwater flood events in southern Ontario and northern New York State. *Geology*, *18*(12), pp.1169-1172.

Shaw, J., 2002. The meltwater hypothesis for subglacial bedforms. *Quaternary International*, *90*(1), pp.5-22.

Shaw, J., Pugin, A. and Young, R.R., 2008. A meltwater origin for Antarctic shelf bedforms with special attention to megalineations. *Geomorphology*, *102*(3-4), pp.364-375.

Shulmeister, J., 1989. A conceptual model for the deposition of the Dummer Moraine, Southern Ontario. *Geomorphology*, *2*(4), pp.385-392.

Smith HTU. 1948. Giant Glacial Grooves in Northwest Canada. *American Journal of Science* 246 (8): 503–14.

Spagnolo, M., Clark, C.D., Ely, J.C., Stokes, C.R., Anderson, J.B., Andreassen, K., Graham, A.G. and King, E.C., 2014. Size, shape and spatial arrangement of mega-scale glacial lineations from a large and diverse dataset. *Earth Surface Processes and Landforms*, *39*(11), pp.1432-1448.

Stokes, C.R. and Clark, C.D., 2001. Palaeo-ice streams. *Quaternary Science Reviews*, *20*(13), pp.1437-1457.

Sugden, D.E., 1968. The selectivity of glacial erosion in the Cairngorm Mountains, Scotland. *Transactions of the Institute of British Geographers*, 45, pp.79-92.

Sugden, D.E., 1974. Landscapes of glacial erosion in Greenland and their relationship to ice, topographic and bedrock conditions. *Institute of British Geographers Special Publication*, *7*, pp.177-195.

Sugden, D.E., 1976. A case against deep erosion of shields by ice sheets. *Geology*, *4*(10), pp.580-582.

Sugden, D.E., 1978. Glacial erosion by the Laurentide ice sheet. *Journal of Glaciology*, *20*(83), pp.367-391.

Sugden, D.E. and Jamieson, S.S., 2018. The pre-glacial landscape of Antarctica. *Scottish Geographical Journal*, *134*(3-4), pp.203-223.

Taylor, G. and Eggleton, R.A., 2001. *Regolith Geology and Geomorphology*. John Wiley & Sons, Chichester.

Thomas, M.F., 1974. *Tropical Geomorphology*. Macmillan, London.

Tulaczyk, S., 1999. Ice sliding over weak, fine-grained tills: dependence of ice-till interactions on till granulometry. *Special Papers-Geological Society of America*, pp.159-178.

Turner, F.J., 1952. "Gefuegerelief" illustrated by "schist tor" topography in central Otago, New Zealand. *American Journal of Science*, *250*(11), pp.802-807.

Veillette, J.J., Dyke, A.S. and Roy, M., 1999. Ice-flow evolution of the Labrador Sector of the Laurentide Ice Sheet: a review, with new evidence from northern Quebec. *Quaternary Science Reviews*, *18*(8-9), pp.993-1019.

White, W.A., 1972. Deep erosion by continental ice sheets. *Geological Society of America Bulletin*, *83*(4), pp.1037-1056.

White, W.A., 1988. More on deep glacial erosion by continental ice sheets and their tongues of distributary ice. *Quaternary Research*, *30*(2), pp.137-150.

Witkind, I.J., 1978. Giant glacial grooves at the north end of the Mission Range, northwest Montana. *J. Res. US Geol. Surv*, *6*(4), pp.425-433.

Wood, B.L., 1969. Periglacial tor topography in southern New Zealand. *New Zealand Journal of Geology and Geophysics*, *12*(2-3), pp.361-375.

Zumberge, J.H., 1955. Glacial erosion in tilted rock layers. *The Journal of Geology*, *63*(2), pp.149-158.

Chapter 6. Conclusions and further research

6.1 Key conclusions

The overall aim of this thesis was to advance understanding of BMG formation. Several different approaches were involved, comprising literature review, statistical analysis and conceptual modelling of BMG development. Data were either newly derived through remote sensing and fieldwork, or were gathered from the scientific literature. The questions posed in Section 1.1 have been addressed throughout this thesis and conclusions are succinctly presented in the following sub-sections.

6.1.1 What are typical BMG dimensions?

In this study approximately 30 BMG sites spread across the world, most of them located in the northern hemisphere are reviewed (see Chapter 2). Of these, 10 sites have been systematically sampled for morphometric data (see Chapter 3). Landform measurements confirm that BMGs are large-scale elongate landforms with a high degree of parallelism to former regional ice-flow directions. BMGs have lengths of 224–2269 m, widths of 21–210 m, depths of 2–15 m, elongation ratios of 5:1 to 42:1, and a spacing between adjacent individuals of 35–315 m (based on the aggregated global population using data within the 10^{th} and 90^{th} percentiles). There is pronounced variability between the sampled sites, in terms of both the spatial and the statistical distribution of BMG metrics, likely due to the variability in geological characteristics that resulted in different susceptibility of rocks to erosion, and to differences in palaeoglaciological history. However, based on the aggregated global dataset, BMGs plot as a single landform population with a unimodal spatial distribution and overlapping value ranges for all metrics, which implies that they represent one landform type.

6.1.2 What are the relationships between BMG metrics?

There are weak linear relationships between BMG length and width or depth, based on mean values from each individual sampled landform. The weakness of these correlations is interpreted as being due to highly variable local control factors pertaining to small-scale structural features. Thus, regardless of length, grooves can be either wide or narrow, and deep or shallow when compared to others within the same population. This may also reflect the existence of BMGs of different ages within the same site, especially if it is assumed that new grooves appear in the system as older ones continue to develop. When the same

analyses are based on the overall mean value per site for each metric, the linear correlations between length and all the other metrics are consistently strong ($R^2 > 0.7$). Thus, at any stage of BMG development, the overall correlation between metrics representative for the whole groove population at any given site is predictable within a relatively narrow range. These strong correlations remain consistent regardless of the within-site variability between individuals, or differences in glaciological conditions or geological characteristics between sites. The strength of these relationships points to the existence of an overarching "law" of BMG development, likely inherent to the physics of subglacial bedrock erosion. In other words, while BMGs may be initiated in different ways (see Chapter 5), the subsequent erosional processes tend to produce very similar expression in the landscape. The linear correlations between width and depth are consistent across the spectrum of analysis, and are relatively strong within individual sites. The reduced within-site variability shows the tendency of BMGs to become wider as they deepen, which confirms their previously-assumed high survival potential (see Section 6.1.6).

6.1.3 What controls BMG formation?

The BMGs thought to have formed under the primary control of fast-flowing ice are the largest in the dataset and have the lowest elongation ratios (5:1 to 7:1). This is interpreted as being the result of enhanced lateral erosion induced by fast-flowing ice in contact with the flanks of the grooves, possibly over long periods of time. It also indicates that BMGs widen faster than they lengthen, thereby explaining the observed reduction in length:width (i.e. elongation) ratio during development (see Section 3.5.2). When bedrock geology is the primary control factor, the BMGs have smaller dimensions and higher elongation ratios (10:1 to 42:1), with grooves from plucking-dominated sites occupying mid-range positions in the metrics spectrum, and those from abrasion-dominated sites comprising the smallest BMGs in the dataset (see Section 3.5.2). There is independent evidence to suggest that the deepest BMGs may have formed with the added contribution of water erosion, whether through dissolution or mechanical processes. Albeit crude, the inferred difference between the dominance of plucking *versus* abrasion in BMG development is supported by an assessment of the response of different lithologies to each mechanism of erosion (see Section 3.2.2).

6.1.4 How do BMGs compare to MSGLs?

Morphometrically, BMGs and MSGLs plot as different populations. BMGs are on average approximately 4× shorter, 3.5× narrower, 3.5× more closely spaced and about 2× deeper (see Section 3.5.3), based on the global dataset. However, if one focuses on BMGs and MSGLs belonging to the same ice-stream landsystem the morphometric differences between the two landform types are somewhat smaller, with the BMGs being approximately 2.5× shorter, 1–1.6× narrower and 0.8–1.5× more closely spaced than their associated MSGLs. The low elongation ratios of BMGs in comparison to those for MSGLs are interpreted as the result of the different mechanisms of landform evolution, with the former widening though lateral erosion and the latter lengthening as soft sediment is mobilised and deposited downstream. Despite similarities in their morphology and occurrence within the same ice-stream landsystems, BMGs and MSGLs remain different landform types due to their different morphometry and formation mechanisms.

6.1.5 Are BMGs formed through ice streaming?

The link between BMG formation and fast-ice flow is not definitively confirmed here, but the case study at Ullapool, Scotland, UK shows that erosion beneath fast-flowing ice is not a necessary pre-condition for BMG development (see Chapter 4). The BMGs there represent only one structural landform assemblage, which occurs in conjunction with several others, and the high visibility of grooves in the landscape is due to their alignment parallel to ice flow and bedrock strike, which enabled enhanced subglacial erosion through lateral plucking and abrasion. This conclusion is supported by independent evidence from elsewhere in Scotland, where BMGs occur in an area with similar lithology and structural orientation relative to palaeo-ice flow, but they were affected by slower ice sheet flow. The Ullapool case study also reveals that the study area represents a groove-and-lochan landscape of areal scouring, characterised by the widespread occurrence of glacially-modified structural lineaments of medium-to-large scale. The landforms comprise cross-cutting linear landforms, with a geometrical regularity, and lakes are commonly present in the bedrock basins at the intersection of structural lines. Considering the inferred ancient origin of the structural features underpinning most linear landforms, apart from the BMGs, it is not unlikely that the grooved area represents a pre-Quaternary erosion surface, similar to an etchplain, subsequently modified by glacial erosion. If confirmed, this conclusion would support a pre-Quaternary origin for the BMGs. The current findings show that, although fast-flowing ice likely increased erosion rates and thus enhanced the BMGs at Ullapool, their formation did not require fast-flowing ice as a necessary pre-condition, as

long as BMGs can, theoretically, develop as a velocity–duration product. The wider implication is that BMGs may not be considered by default a diagnostic landform of erosion through fast-flowing ice; each hard-bed landform assemblage in fast-flow onset zones needs an assessment that considers all landforms, not just those aligned parallel to former ice-flow direction.

6.1.6 How were BMGs initiated?

Once initiated, it is relatively straightforward to explain how BMGs continue to grow, as their negative relief enables the focus of subglacial erosion processes, including those which involve the agency of meltwater. However, groove initiation remains poorly understood. In the absence of any unequivocal evidence for BMG initiation, four hypothetical scenarios are proposed here, which are capable of accounting for the main physical characteristics of grooves and their geological context of occurrence. The underlying assumptions are that BMGs were initiated through glacial abrasion, and they are of significant age, possibly pre-glacial. Two scenarios relate to primary geological control: one whereby BMGs develop along pre-existing structural lines aligned sub-parallel to former ice-flow directions, typically applicable to tilted layered rocks with strike (sub)parallel to ice flow; the other scenario invokes the passage of relatively hard striator blocks plucked from fault scarps, or derived from more resistant lithologies up-ice, and then dragged across the softer bedrock down-ice flow, which they incise through abrasion and thus create proto-grooves. In cases with no apparent structural control, antecedent conditions are invoked for BMG initiation. These comprise bedrock structure removal, whereby BMGs were first initiated along pre-existing structural lines, they continued to deepen into rock layers beneath and eventually into the (harder) present-day layer, and over time the initial (softer) layers were all removed by erosion. This would explain why some BMGs bear no connection with any present-day geological structure and also constitutes a plausible explanation of BMG development in bedrock which is remarkably resistant to abrasion. The second scenario invokes the cannibalization and excavational deformation of regolith, involving the mobilization of cemented cap rocks and corestones, and their use as erodents on the substrate once entrained in glacial flow. Initially, erosion would take place in incipient and early subglacial deforming layers developed in pre-Quaternary regoliths, eventually followed by abrasion of the unweathered bedrock down-flow, once the erodents originating from the regolith attained contact with the bedrock. The apparent scarcity of BMGs globally is likely due to the fact that undiscovered BMGs are currently masked by unconsolidated deposits, as an expanding body of geophysical evidence seems to indicate.

6.2 Further research

6.2.1 Geological control factors

To further validate the relationship between BMG morphometry and geological control factors, further field evidence pertaining to the interplay between erosion and geology would be instrumental to understanding groove development, because it is the most reliable way to assess the efficiency of individual erosion mechanisms. Once the dominance of one mechanism of erosion is established at a site, the morphometry of the BMGs there can be assessed more confidently in the wider global context and in relation to other sites with similar susceptibility to erosion. This may help consolidate conclusions related to links between geology and morphometry in BMG formation. Of key importance in this respect are sites where the grooves cross lithological boundaries, like Franklin, NT, Canada, because the palaeoglaciological conditions can be assumed constant, and any changes in groove morphometry would be likely due to differential erosion underpinned by geology.

6.2.2 Links between BMGs and MSGLs

Future research could attempt morphometric analyses of ice-stream landsystem bedforms at the transition between hard and soft beds. Specifically, mapping and sampling for BMGs and MSGLs done systematically, following consistent protocols, could help further explore links between bedrock forms and MSGLs, and also between streamlined bedrock and fast-flow initiation. Conversely, a detailed investigation of BMGs from areas where the geological conditions are similar but the palaeoglaciology differs has the potential to advance understanding of the influence of fast-ice flow over BMG formation. For example, a comparison between the BMGs at Ullapool and those at Invermoriston would address this question, as both sites are located in a similar geological context, but one is in a fast-flow onset zone and the other is in an area of slow, normal ice-sheet flow.

6.2.3 Age of BMGs

Valuable insights into the age of BMGs could be gained through numerical modelling experiments, following in the advances being made in soft sediment landforms, such as drumlins. For example if erosion at BMG scales could be simulated and their morphogenesis modelled, we could start to glean more information about likely rates of erosion and time-scales of formation. Cosmogenic nuclide dating, especially in quartz-rich rocks, might also reveal the age and erosion rates of BMGs. It also remains to be tested by future research

whether the groove-and-lochan landscape type is a common occurrence in fractured, faulted and folded metasedimentary rocks, and whether it has an overarching palaeoglacial significance. The result in Chapter 4 has been interpreted to represent long-term glacial erosion throughout repeat glacial cycles, indicative of a relatively old age for the BMGs, pre-dating the last glaciation.

6.2.4 Testing the hypotheses of BMG initiation

In order to test the antecedence hypothesis whereby BMGs were initiated through the agency of boulders derived from pre-glacial regolith, remnants of such erodents would need to be observed *in situ*, preferably within the BMGs, and pertaining to intermediary stages proposed in the antecedence models. Key sites for future research would be grooved areas spanning adjacent lithologies of different hardness, and particularly the lithological contacts at initiator fault scarps (e.g. Section 3.2.2.4). At such locations the displacement of large bedrock fragments could be assessed in relation to existing structural lines (e.g. joints and fractures), as could the role of striators of such rocks on the softer lithologies down-ice flow. In as much as detailed geological maps are a valuable resource, fieldwork remains invaluable, because relatively small-scale features responsible for bedrock plucking are rarely recorded on maps. Considering the difficulty in accessing the bedrock directly beneath ice sheets in Greenland and Antarctica, where BMGs have been identified and are thought to be undergoing active modification through erosion, geophysical means could potentially be used to investigate their evolution, especially in relation to rates of growth.

Chapter 7. Appendix

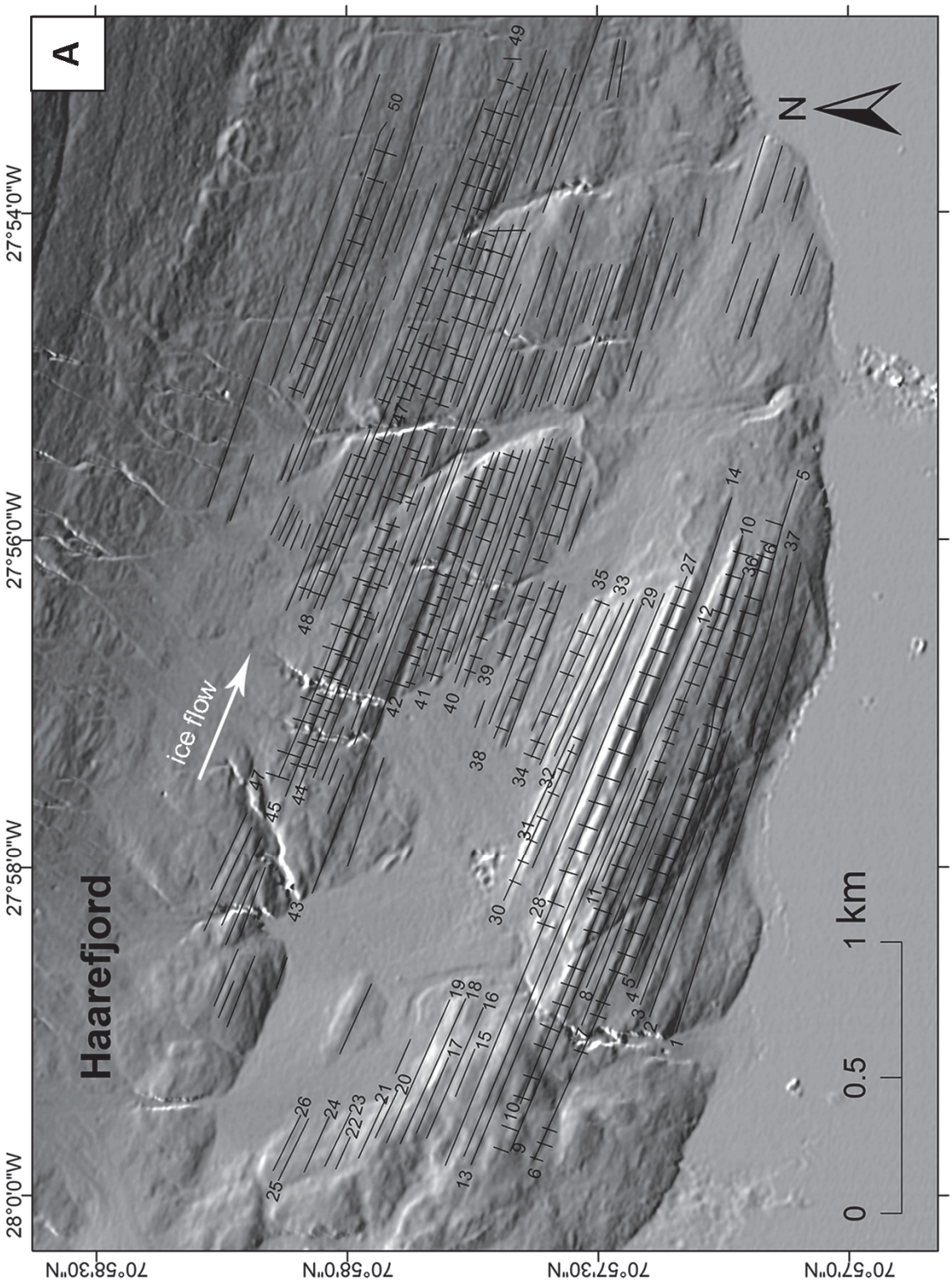

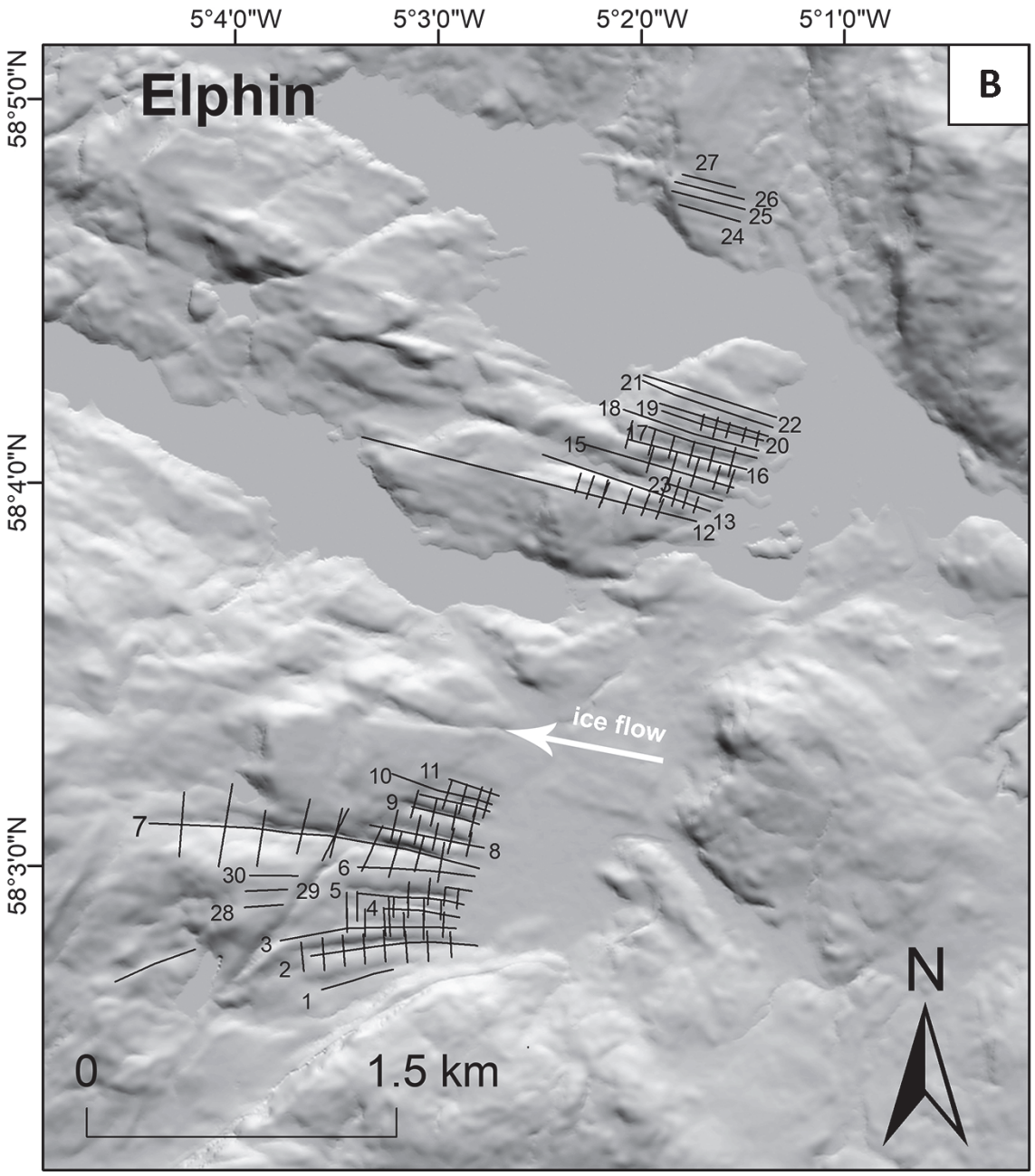
5°4'0"W
5°3'0"W
5°2'0"W
5°1'0"W
58°5'0"N
58°4'0"N
58°3'0"N
Elphin
B
27
26
25
24
21
18
19
22
17
20
15
16
23
12
13
ice flow
10
11
9
7
8
30
6
29
5
28
4
3
2
1
0
1.5 km
N

C
Ullapool
ice flow
N
0
1
2 km
4°58'0"W
5°0'0"W
5°2'0"W
5°4'0"W
5°6'0"W
57°58'0"N
57°57'0"N
57°56'0"N
57°55'0"N

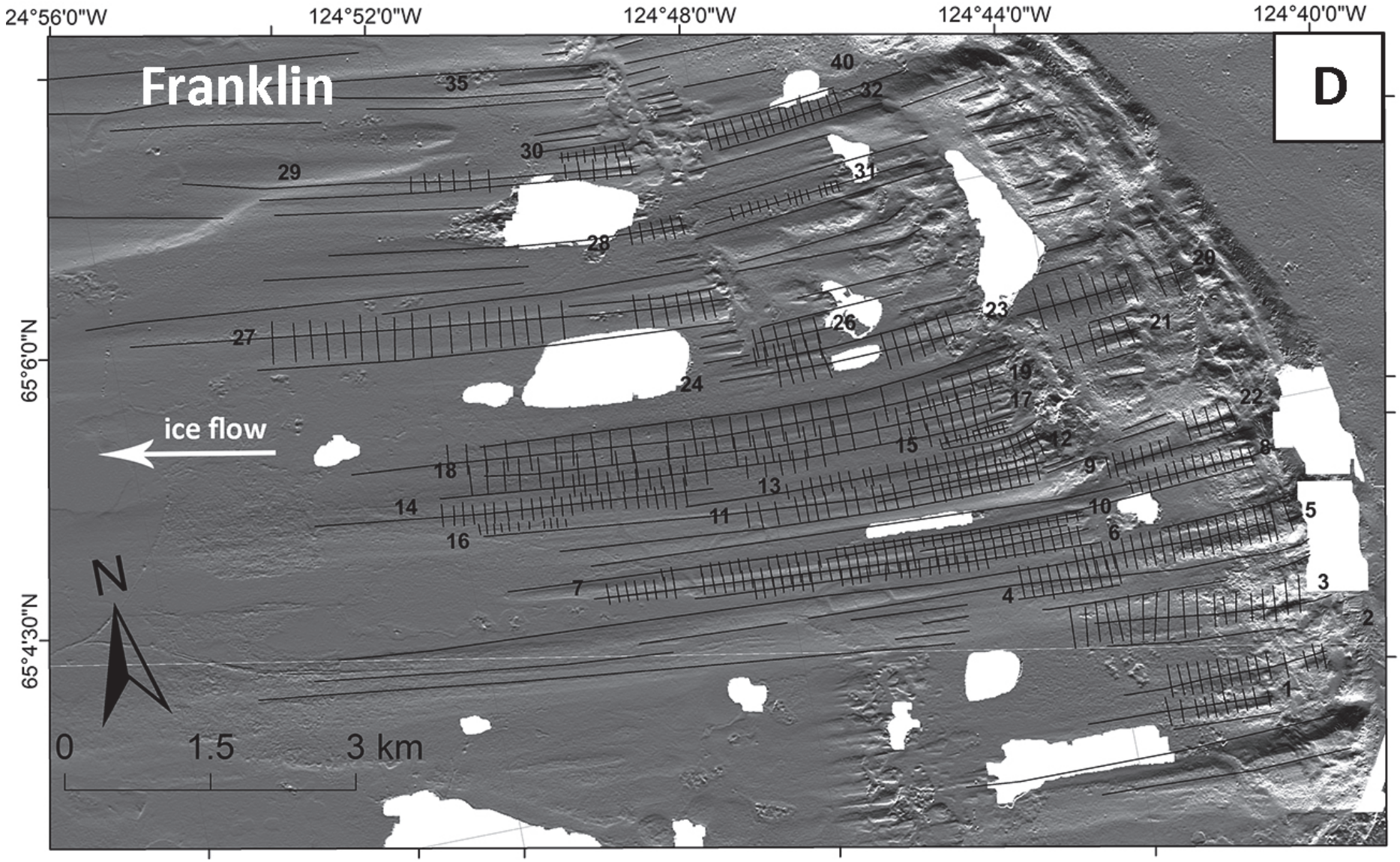
Franklin
D
24°56'0"W
124°52'0"W
124°48'0"W
124°44'0"W
124°40'0"W
65°6'0"N
65°4'30"N
ice flow
N
0
1.5
3 km
40
35
32
30
29
31
28
27
26
23
29
21
24
19
17
22
15
12
9
8
18
13
14
11
10
5
16
6
7
4
3
2
1

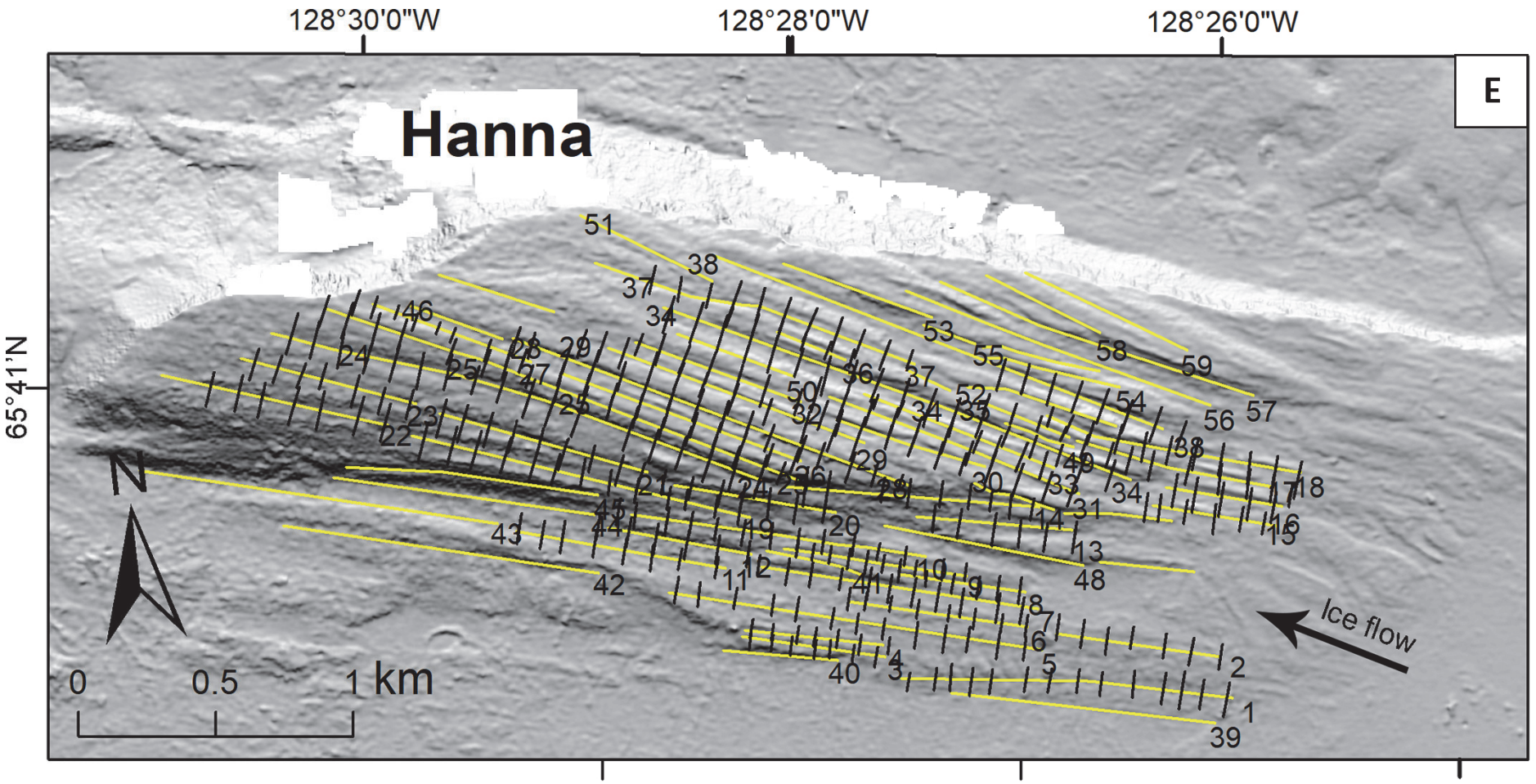
128°30'0"W
128°28'0"W
128°26'0"W
65°41'N
E
Hanna
N
0
0.5
1 km
Ice flow

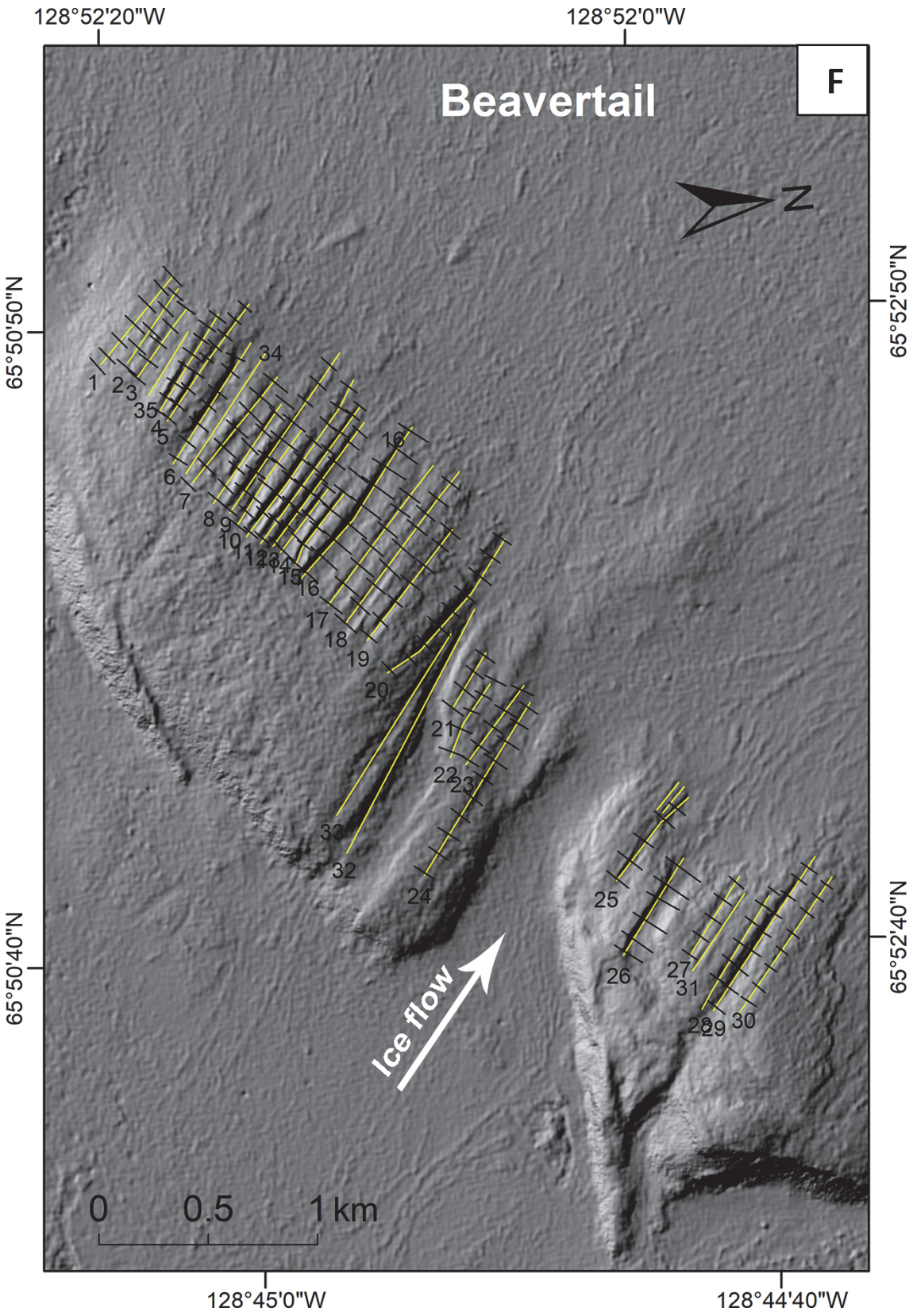
128°52'20"W
128°52'0"W
F
Beavertail
N
65°50'50"N
65°52'50"N
65°50'40"N
65°52'40"N
1
2
3
35
4
5
34
6
7
8
9
10
11
12
13
14
15
16
16
17
18
19
20
21
22
23
24
25
26
27
31
28
29
30
33
32
Ice flow
0
0.5
1 km
128°45'0"W
128°44'40"W

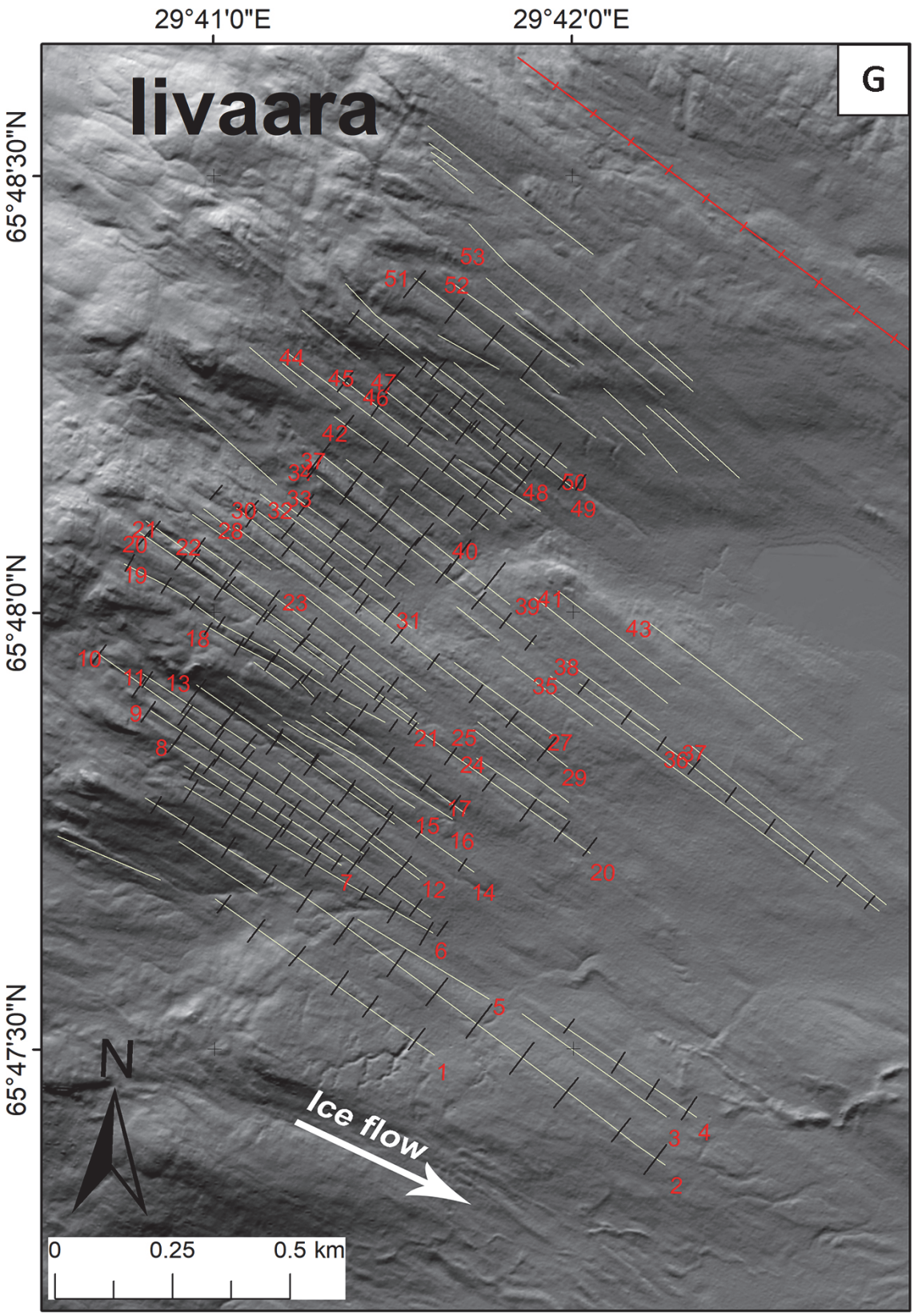
29°41'0"E
29°42'0"E
65°48'30"N
65°48'0"N
65°47'30"N
livaara
G
N
Ice flow
0
0.25
0.5 km

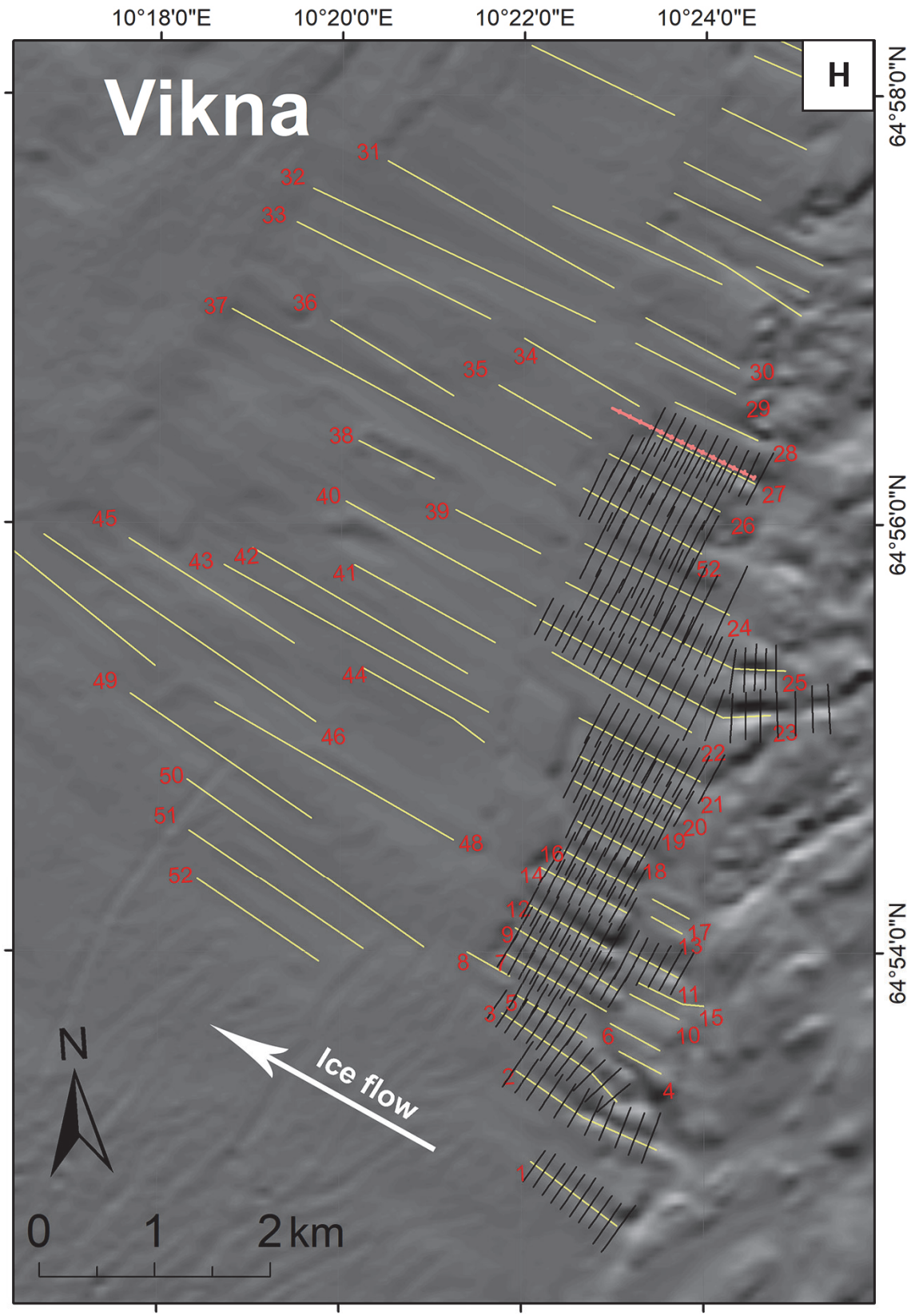
10°18'0"E
10°20'0"E
10°22'0"E
10°24'0"E
64°58'0"N
64°56'0"N
64°54'0"N
H
Vikna
31
32
33
37
36
35
34
30
29
38
28
40
27
39
45
26
43
42
41
52
24
49
44
25
46
23
22
50
21
51
20
19
48
16
14
18
52
12
17
9
13
8
7
11
3
5
15
6
10
2
4
1
N
Ice flow
0
1
2 km

N 55° 16' 22"
W 127° 49' 31"
W 127° 51' 14"
N
500 m
Hazelton
Ice flow
1
2
3
4
5
6
7
8
9
10
11
12
13
14
15
16
17
18
19
20
21
22
23
24
25
26
27
28
29
30
31
32
33
34
36
37

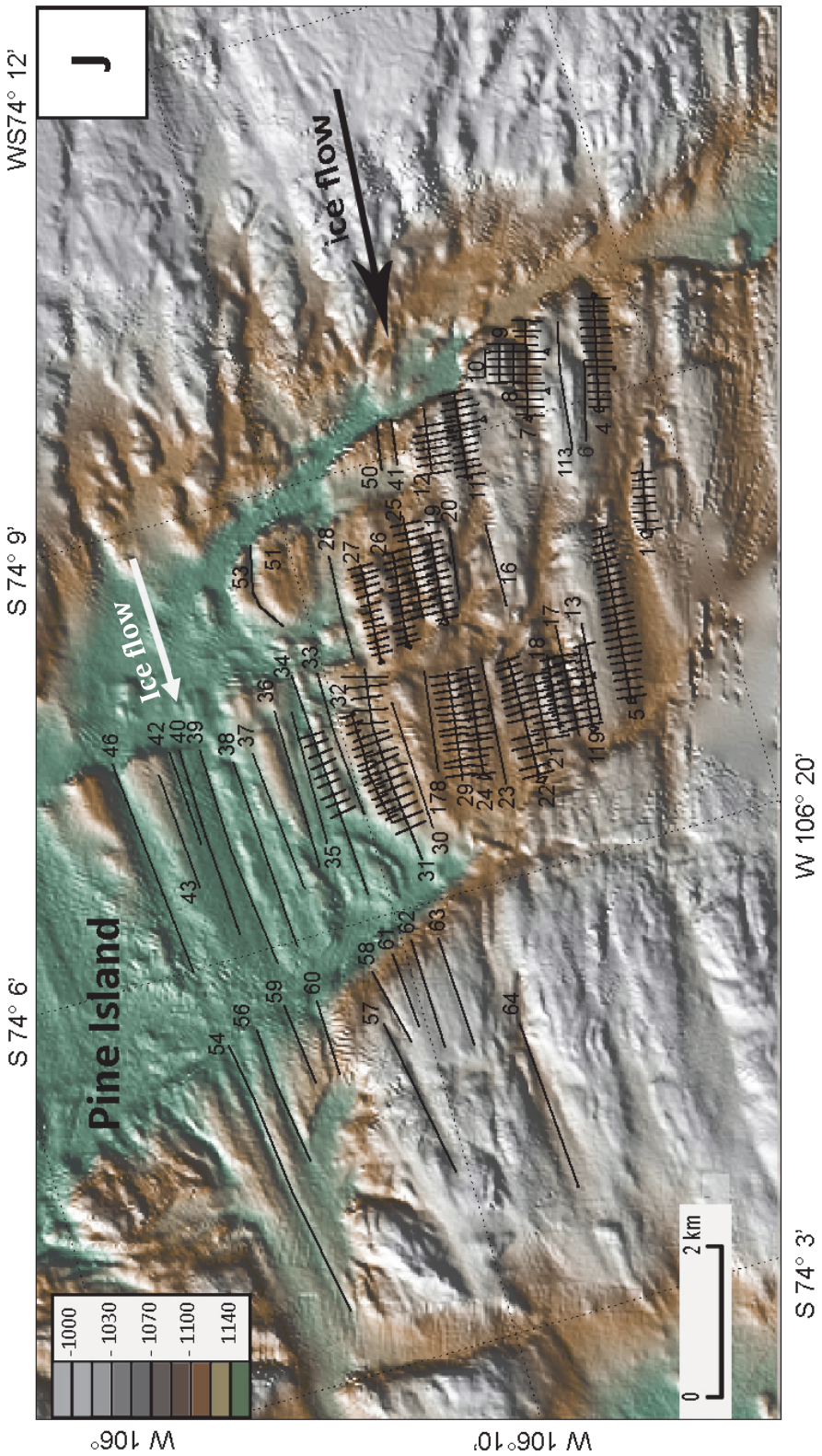

Figure 1. A-J: the sampled grooves in each study area showing the exact location of the cross-profiles based on which the depth and width were measured. All numbered grooves were sampled for lateral spacing, whereas width and depth were calculated at 100 m-intervals along minimum 10% of all mapped grooves (see also Section 3.3.2) in the ice-flow direction. Base image © NERC BGS UK for parts B and C; Arctic DEM provided by the Polar Geospatial Centre under NSF-OPP awards 1043681, 1559691, and 1542736 for part D, E and F; base image © National Land Survey of Finland for part G; base image © Norwegian Hydrographic Service for part H; base image © GoogleEarth Pro for part E; base image © GeoMapApp for Figure 1J

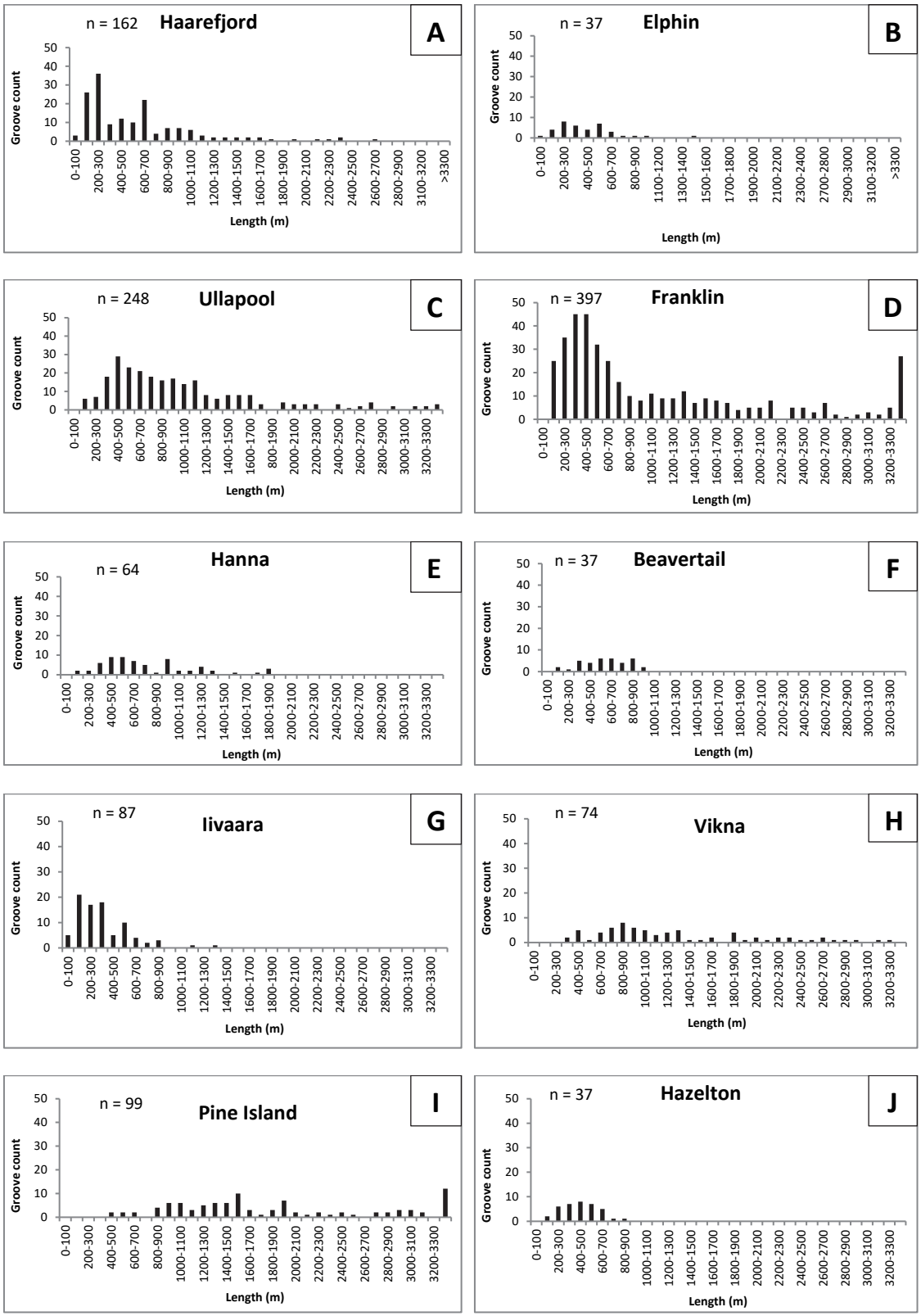

Figure 2. Frequency distribution histograms of length for individual study areas. The results for the aggregated BMG population are illustrated in Figure 3.17A in Chapter 3.

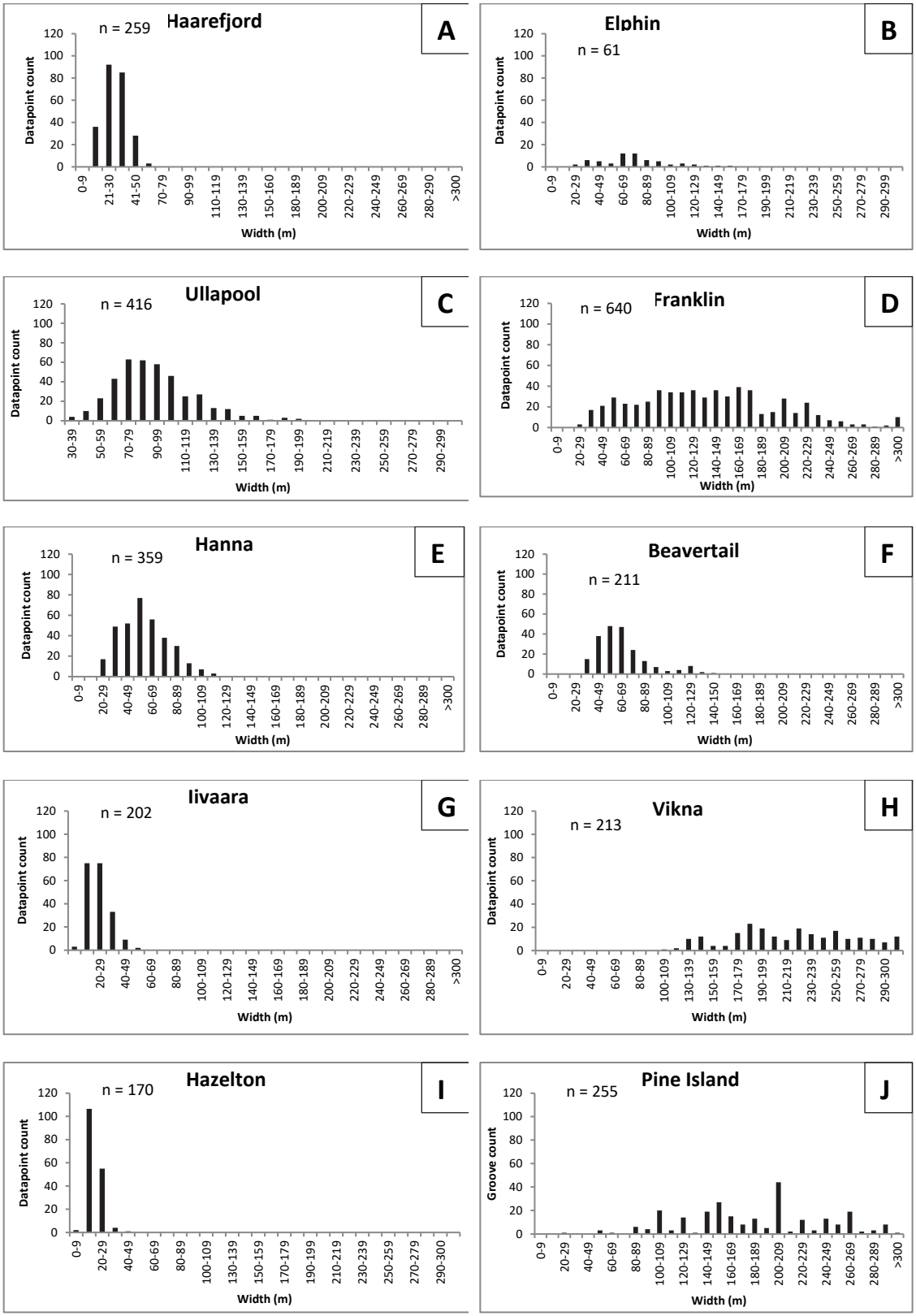

Figure 3. Frequency distribution histograms of width for individual study areas. The results for the aggregated BMG population are illustrated in Figure 3.17B in Chapter 3.

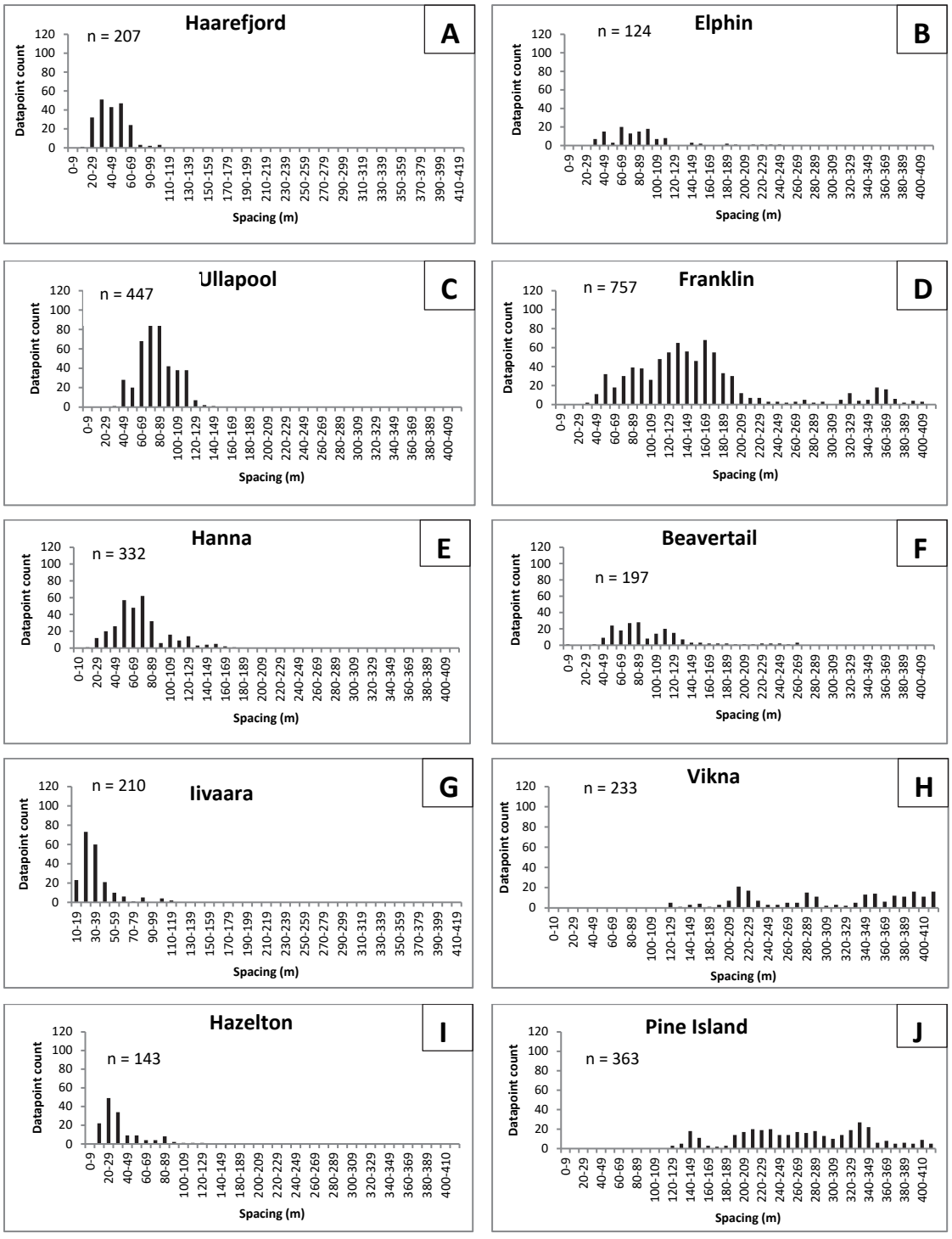

Figure 4. Frequency distribution histograms of spacing for individual study areas. The results for the aggregated BMG population are illustrated in Figure 3.17C in Chapter 3.

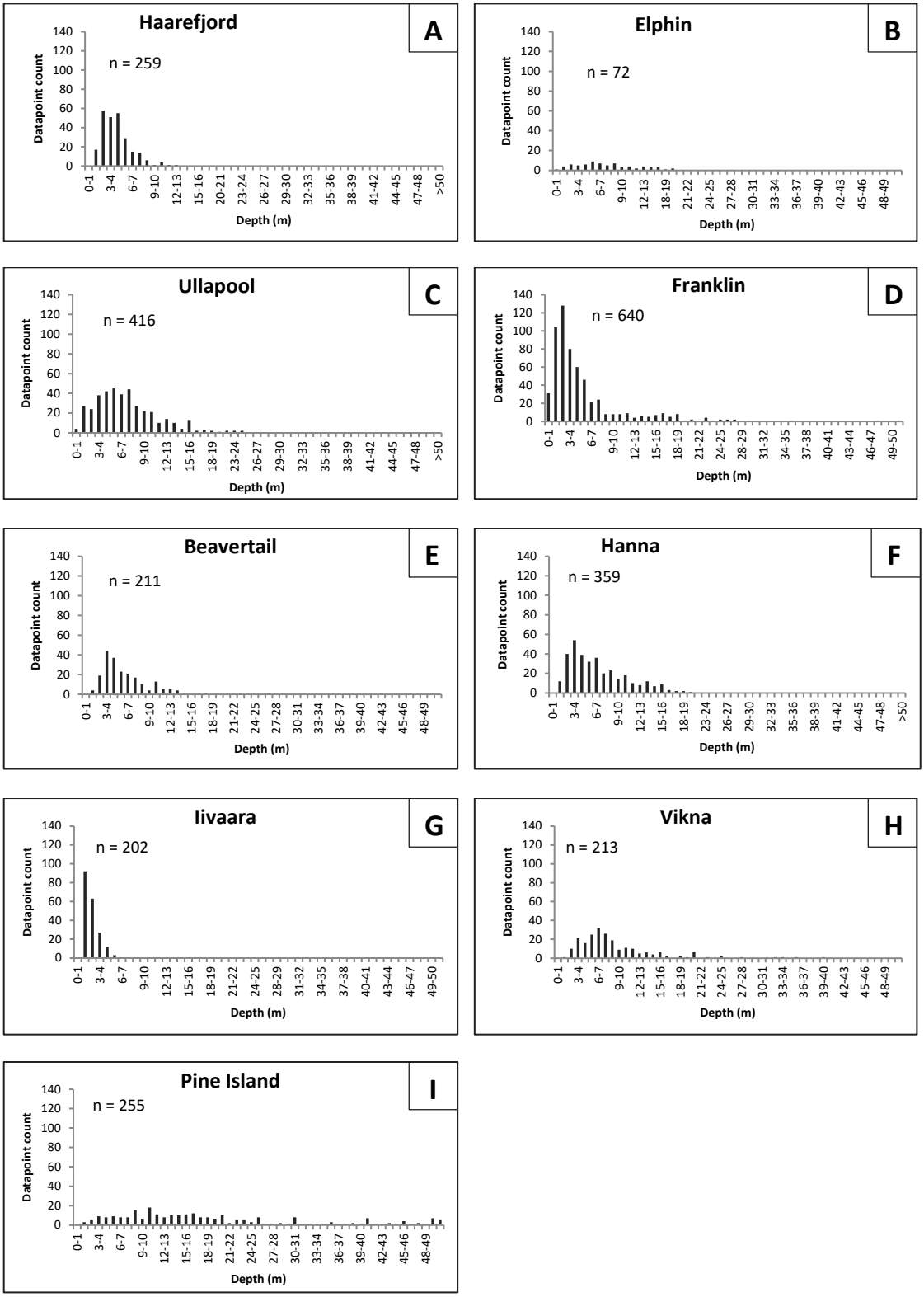

Figure 5. Frequency distribution histograms of depth for individual study areas. The results for the aggregated BMG population are illustrated in Figure 3.17D in Chapter 3.

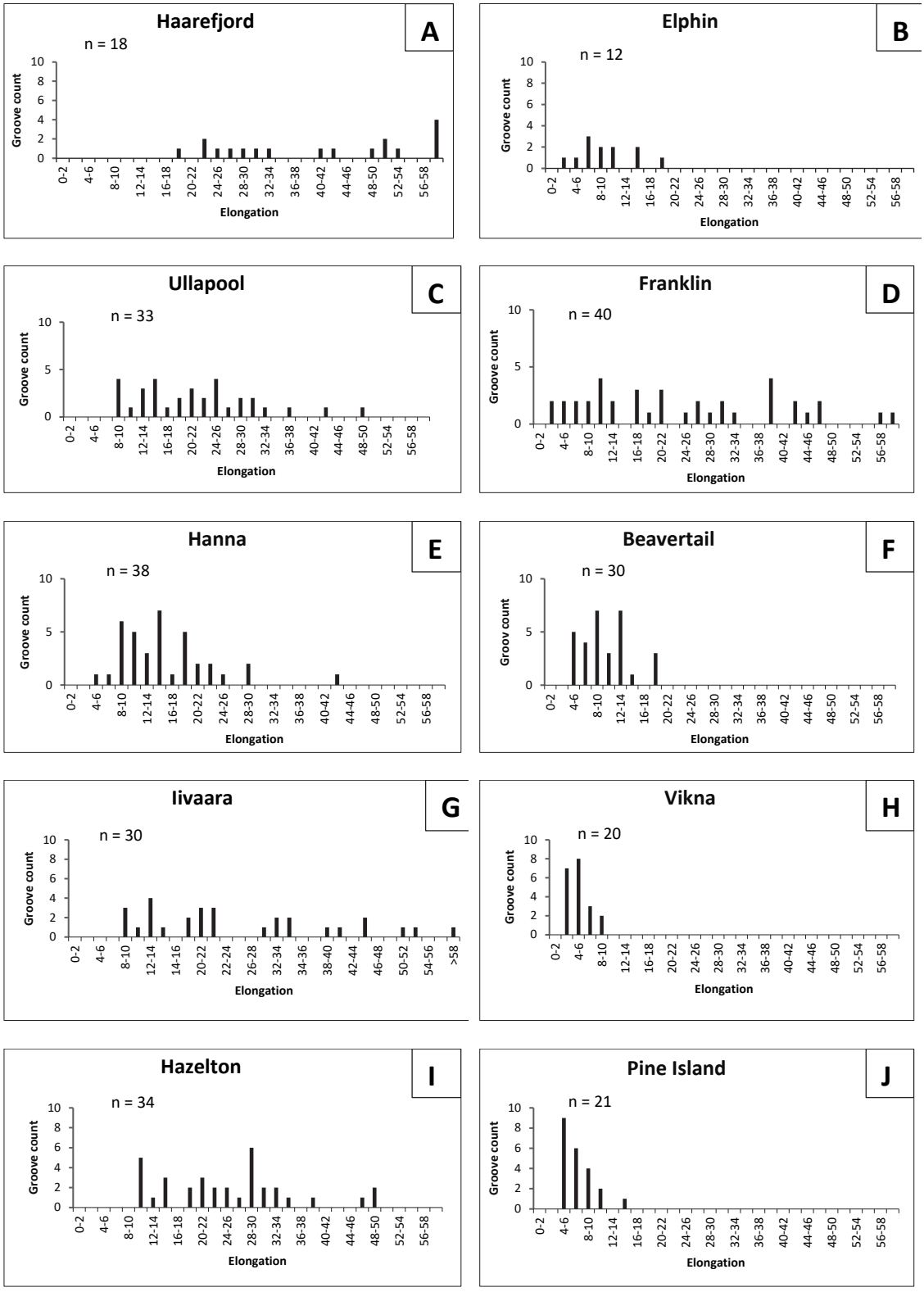

Figure 6. Frequency distribution histograms of elongation for individual study areas. The results for the aggregated BMG population are illustrated in Figure 3.17E in Chapter 3.

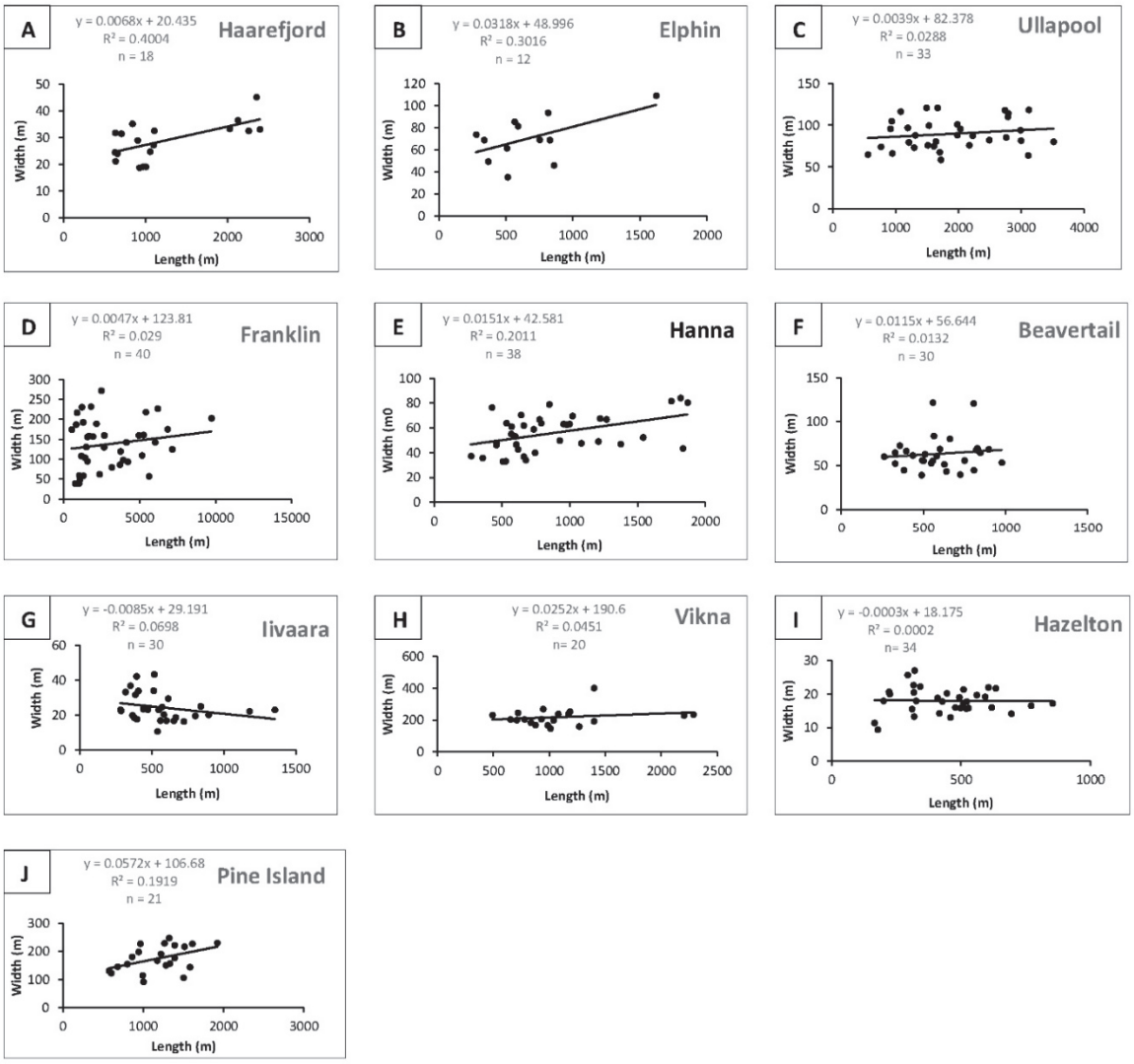

Figure 7. Groove length plotted against width for all sampled grooves in individual study areas. The figures represent mean values and each datapoint corresponds to a sampled groove. The results for the aggregated BMG population are illustrated in Figure 3.18 in Chapter 3.

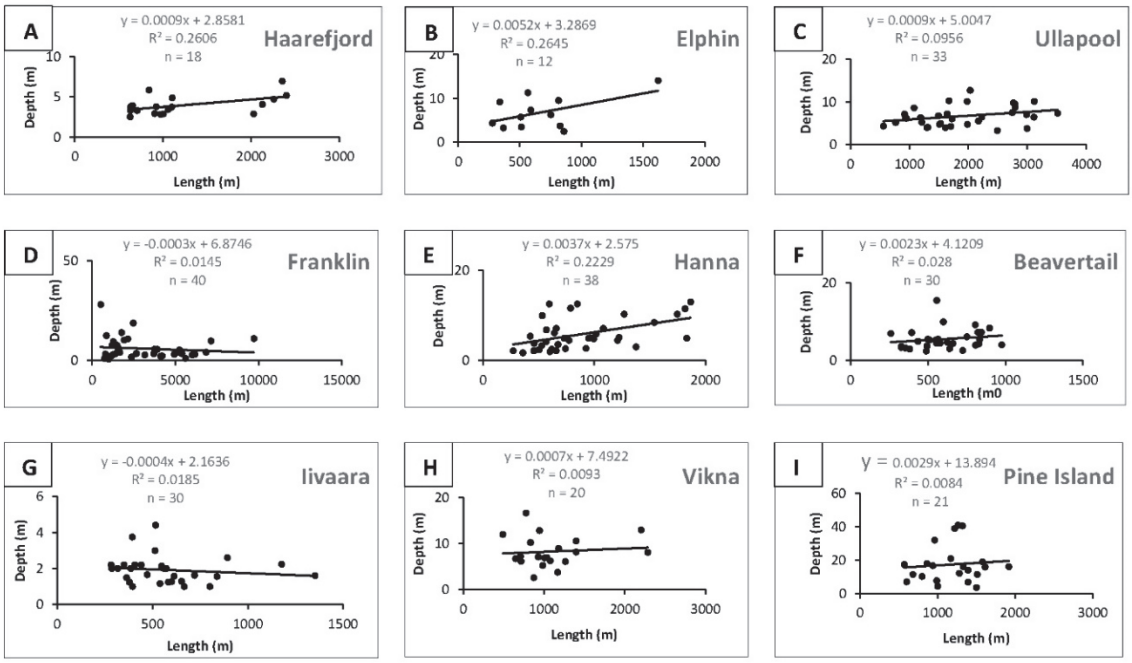

Figure 8. Groove length plotted against depth for all sampled grooves in individual study areas. The figures represent mean values and each datapoint corresponds to a sampled groove. The results for the aggregated BMG population are illustrated in Figure 3.18 in Chapter 3.

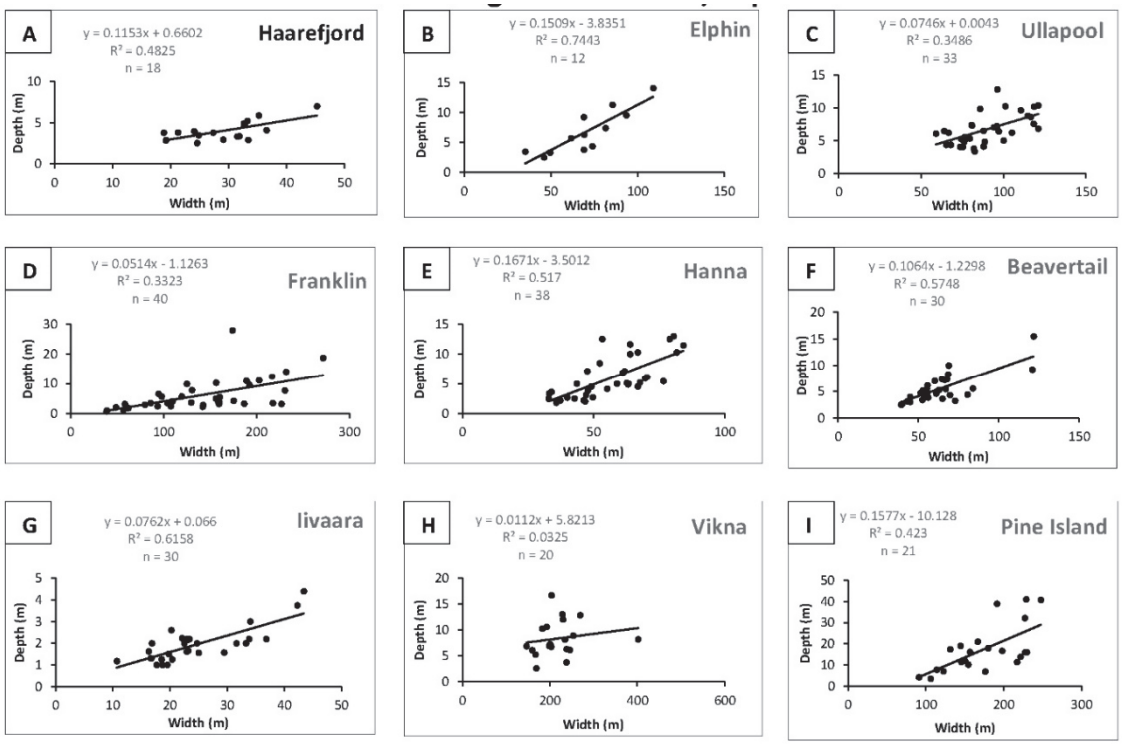

Figure 9. Groove width plotted against depth for all sampled grooves in individual study areas. The figures represent mean values and each datapoint corresponds to a sampled groove. The results for the aggregated BMG population are illustrated in Figure 3.18 in Chapter 3.